Exploring the roles of the Protein Kinase N family in breast cancer

Priththivika Baskaran

Submitted in partial fulfillment of the requirements of the Degree of Doctor of Philosophy

Centre for Tumour Biology
Barts Cancer Institute
Barts and The London School of Medicine and Dentistry
Queen Mary University of London
Charterhouse Square

Statement of originality

I, Priththivika Baskaran, confirm that the research included within this thesis is my own work or that where it has been carried out in collaboration with, or supported by others, that this is duly acknowledged and my contribution indicated. Previously published material is also acknowledged.

I attest that I have exercised reasonable care to ensure that the work is original, and does not to the best of my knowledge break any UK law, infringe any third party's copyright or other Intellectual Property Right, or contain any confidential material.

I accept that the College has the right to use plagiarism detection software to check the electronic version of the thesis.

I confirm that this thesis has not been previously submitted for the award of a degree by this or any other university.

Signature: Priththivika Baskaran

Date: 24.09.2018

Acknowledgement

This project was funded by the Medical Research Council (grant number: MR/K501372/1).

I would like to express my sincere gratitude to my primary supervisor, Dr. Angus Cameron, for his support, encouragement and patience throughout my project. Your dedication and enthusiasm has been a great inspiration to me. I am grateful to Dr. Ivan Quétier for his teaching and guidance as a mentor. I would also like to thank Ms. Elizabeth Murray and Dr. Lorena Alba Castellon, for all their help and motivation. Special thanks to Ms. Ami Desai, who has always been so helpful – particularly with *in vivo* experiments.

I am thankful to my secondary supervisor Prof. Kairbaan Hodivala-Dilke and members of the Cell Adhesion and Angiogenesis Lab for their advice and helpful feedbacks during presentations at lab meetings.

I would like to thank Prof. John Marshall and the Beta 6 group for their kindness, help and support during my PhD. Special thanks to Dr. Claire Reader and Dr. Zareen Khan for their teaching and guidance on mini-organotypic assays.

The lab and core facilities have been a great strength to my research experience at Barts Cancer Institute, for which I am thankful. I am grateful to Prof. Peter Parker and the staff at the Francis Crick Institute for their help with *in vivo* studies.

I would like to thank Dr. Kathryn Davidson for being a fantastic lab mentor during my master's degree. Your patience, kindness and trust in me has made my first experience in a working lab most memorable, which inspired and gave me confidence to do a PhD.

Thank you to my siblings who have kept me smiling during stressful times and have always taken great interest in asking for updates on my project. Finally, I am forever indebted to my parents (Mr. Baskaran Thambiaiah and Mrs. Sasivathany Baskaran) for all their sacrifices. You have given me the liberty and strength to be an independent woman and have always supported and trusted my decision to pursue further education.

Abstract

Solid tumours are composed of cancer cells and a variety of other cell types, forming the tumour microenvironment (TME). Cells within the TME promote cell survival, proliferation and epithelial-mesenchymal transition (EMT) of cancer cells. Among the key metastasis-inducing cellular components of the TME are cancer-associated fibroblasts (CAFs), which are activated by cancer cells through release of factors such as TGFβ.

Here we sought to delineate the role of the PKN kinases in breast cancer with a focus on mesenchymal-phenotype TNBC models and subsequently in CAFs. This study was motivated by the critical roles identified for PKN2 in mesenchymal cells during development, as well as in cell behaviours critically hijacked during breast cancer development and progression.

TNBC cells with mesenchymal-like morphologies (SUM159 and MDAMB231) showed reduced survival with PKN2 and PKN3 knockdown. This corroborated with previous finding where loss of PKN2 reduced proliferation of mice embryonic fibroblasts (MEFs) and systemic PKN2 knockout resulted in impaired development of the mesenchyme in mouse embryo. Therefore, subsequent studies in this project investigated the role of PKN2 in fibroblasts and their interaction with cancer cells.

The importance of the stroma in breast cancer has been demonstrated in several studies. The presence of stroma/desmoplasia in triple-negative breast cancer (TNBC) has been linked to bad prognosis, which is also contradicted in other studies. Our laboratory identified several cancer-associated roles for PKN2 in pancreatic fibroblasts, including activation and reciprocal signalling to cancer cells to promote proliferation and invasion. Data from this project indicate dependency on PKN2 for fibroblast activation. Subsequently, a panel of genes associated with PKN2-dependent fibroblast activation was selected to investigate the clinical relevance of PKN2 in breast cancer stroma. Furthermore, stromal deletion of PKN2 in a mouse orthotopic model resulted in tumours with reduced fibrotic stroma and decreased vasculature.

Table of contents

List of figures

List of tables

1. Introduction

1.1 Breast cancer

1.1.1 Background

In 2015 around 300,000 cases of new cancer diagnoses were registered in the UK, of which breast cancer was the highest contributor (15.4%) (Statistics 2017) and was the most common cancer in women. Although survival rates are improving, 1000 women die from breast cancer per month in the UK. Breast cancer causes 1 in 6 of all cancer deaths in women and thus represents the leading cause of cancer-related deaths after lung cancer (Dewis and Gribbin 2009).

1.1.2 Clinical & molecular classification of breast cancer

Conventional methods of classification involve histopathological methods, by using immunohistochemistry to identify oestrogen receptor (ER), progesterone receptor (PR) and HER2 expression, supplemented by clinicopathological factors such as tumour grade, size, lymph node and distant metastases. Studies using this method have demonstrated the prognostic and therapeutic relevance of this form of classification (Vallejos et al. 2010) (Cheang et al. 2009).

Furthermore, analysis of tumour gene expression in breast cancer has identified the implications of distinct molecular profiles in patients on treatment and outcome (Weigelt, Baehner, and Reis-Filho 2010). Perou *et al* classified breast cancer into five intrinsic subtypes (luminal A, luminal B, HER2 overexpression, basal and normal-like), based on gene expression, by using complementary DNA microarrays on tumour samples (Perou et al. 2000). Furthermore, the correlation between gene expression and clinical outcome was studied by Sørlie *et al* (Sørlie et al. 2001). Subsequently, studies using tissue microarrays

enabled protein expression profiling to validate the clinical relevance of classification by gene expression profiles (Abd El-Rehim et al. 2005). Overall, breast cancer is typically classified into three broad groups: luminal, HER2-enriched and triple-negative/basal tumours.

1.1.2.1 Luminal breast cancer

Luminal tumours express cytokeratin 8/18 and ER, components of normal mammary luminal epithelium. Luminal tumours can be further classified into two subtypes (luminal A and luminal B). Both luminal A and B express ER and/or PR. Patients with these tumours are responsive to hormonal therapy and have in general a good prognosis. Luminal B tumours are often more aggressive, with high Ki67 staining, expressing high levels of proliferative genes, with significantly worse prognosis than luminal A (Sorlie et al. 2003). A subset of luminal tumours also express HER2.

1.1.2.2 HER2-enriched breast cancer

These tumours lack ER and PR and are often grade 3 tumours, associated with poor prognosis (Sørlie et al. 2001). The enhanced expression of HER2 in these tumours act as a predictive factor of sensitivity to HER2-targeting therapy. Two key HER2-targeting agents are trastuzumab (Herceptin), a monoclonal antibody and lapatinib, a tyrosine kinase inhibitor (Abramson and Arteaga 2011). Furthermore, patients with this subtype of breast cancer have significantly higher pathological complete response due to better response to anthracyclines and taxanes (Brenton et al. 2005) than patients with luminal subtype.

1.1.2.3 TN/basal breast cancer (TNBC)

This subtype is the most invasive and heterogenous, characterised by absence of ER, PR and HER2 expression. Tumours of this subtype contribute to 10-20% of breast cancers, most common in younger patients, with poor outlook on survival and increased risk of relapse (Carey et al. 2006).

Gene expression profiles of this subtype of cancer share similarities with normal basal epithelial and breast myoepithelial cells, due to high expression of proliferative markers and basal markers (such as keratins 5, 6, 14, 17, EGFR) (Perou et al. 2000). TN/basal tumour have unique metastatic tropism of the visceral organs and rarely involves lymph node metastasis (Anders and Carey 2009).

1.1.2.4 TNBC subtypes

Gene expression analysis by Lehmann *et al* classified TN breast cancer (TNBC) into 6 subtypes: basal-like (BL1 and BL2), immunomodulatory (IM), mesenchymal (M), mesenchymal stem–like (MSL), and luminal androgen receptor (LAR) (Lehmann, Bauer, Chen, Sanders, Chakravarthy, Shyr, et al. 2011).

BL1 is associated with high expression of genes involved in the cell cycle, whereas BL2 tumours express genes involved in growth factor signalling such as EGF, IGF1R and MET pathway. Due to enhanced expression of proliferative markers, patients with BL1 and BL2 tumours treated with anti-mitotic drugs such as taxanes, as a neoadjuvant therapy, respond better than those with other subtypes (63% pathologic complete response) (Bauer et al. 2010). On the other hand, IM tumours express genes involved in immune responses.

Tumours of the M subtype are rich in motility-related genes, as well genes involved in cellular differentiation and ECM interaction pathways. This includes effectors in the Rho, Wnt, anaplastic lymphoma kinase (ALK) and TGFβ signalling pathways (Lehmann, Bauer, Chen, Sanders, Chakravarthy, Shyr, et al. 2011). MSL tumours are characterised by genes involving the growth signalling pathways such as EGFR, PDGF, G-protein coupled receptor and ERK1/2. This subtype is also known to have enhanced expression of genes related to angiogenesis (for example VEGFR and Tie2). Breast cancer of the LAR subtype express high number of androgen receptors, compared to other TNBC subtypes. These tumours express

genes involving hormonal regulation of androgen/estrogen metabolism and steroid synthesis. Compared to MSL and BL1, LAR has lower relapse-free survival (RFS).

1.1.3 Progression of breast cancer

Breast cancers confined to the mammary epithelium are known as in situ carcinoma, whereas tumours that have penetrated the surrounding tissues are known as invasive carcinoma. Tumours initiate from either the duct (ductal carcinoma) or the lobule (lobular carcinoma). Wellings *et al* first proposed the breast cancer progression model, starting with flat epithelial atypia (FEA), followed by atypical ductal hyperplasia (ADH) and ductal carcinoma in situ (DCIS) and finally invasive and metastatic ductal carcinoma (Wellings and Jensen 1973).

1.1.3.1 FEA

FEA involves proliferation of cells into benign lesions and changes in polarisation of columnar cells in the luminal epithelium (Aroner et al. 2010). This benign lesion is thought to precede low grade malignancy, although the link between FEA development and risk of progression to malignancy is not known for certain and was investigated by Said *et al* (Said et al. 2015). This study of more than 11,000 women with benign breast lesions reported a very low incidence of FEA (2.4%) and found no enhanced risk of progression to breast malignancies due to the presence of FEA. However, there is a correlation between presence of FEA and progression to ADH, which increases the risk of progressing to breast cancer.

1.1.3.2 ADH

ADH is often discovered during mammographic screenings in patients with microcalcification. ADH is a small focal benign lesion, formed by polygonal cells with hyperchromatic nuclei. ADH share some but not all characteristic features with DCIS. Unlike FEA, the increased risk of breast cancer in association with ADH is well established;

around four to five times increased risk in general, six-fold risk in pre-menopausal women and a ten-fold risk in those with a first-degree relative affected by breast cancer (Pinder and Ellis 2003).

1.1.3.3 DCIS

DCIS is a non-invasive malignant lesion, containing highly proliferative epithelial cells surrounded by myoepithelial cells and basement membrane within the luminal ducts (Pinder and Ellis 2003). Holland *et al*, proposed the classification of DCIS as high, low, or intermediate grade based on cellular features (Holland et al. 1994). Studies report an incidence of 50% for invasive breast cancer with the presence of microscopic DCIS at the same site, hence DCIS is a precursor lesion of invasive breast carcinoma (IBC).

1.1.3.4 Invasive Carcinoma

There are two arguments to explain the progression of DCIS to invasive carcinoma: acquired genetic changes and non-genetic changes. Evidence suggests a role for the tumour microenvironment (TME) as a non-genetic contributor to breast cancer progression. ECM remodelling, changes in non-malignant cell types of the TME such as fibroblasts and myoepithelial cells and epigenetic alterations in the stroma are thought to mediate disease progression (Cowell et al. 2013). This theory is supported by the characteristic loss of containment of malignant cells in invasive ductal carcinoma by the basement membrane, which is maintained in DCIS with the aid of tumour suppressive factors secreted by the surrounding myoepithelial cells. Changes in myoepithelial cells occurs in DCIS, where their role of tumour suppression is reversed to induce cancer progression. Work by Allen *et al* demonstrated that this change is driven by upregulation of the integrin αvβ6, leading to activation of TGFβ and MMP9 signalling (Allen et al. 2014).

Clinical studies demonstrated that 50% of patients with low-grade DCIS progress to breast cancer. This poses the need to identify the likelihood of developing breast cancer when

DCIS is detected during screening. Ma *et al* used samples from DCIS and matched invasive tumours using laser capture microdissection to compare the genetic expression profiles, to identify genes predictive of disease progression (Ma et al. 2003). This study demonstrated enriched expression of a set of 29 genes in invasive tumours, relative to the matched DCIS samples. This suggests these genes to be related to disease progression, though their significance in predicting progression is unknown.

1.1.4 Treatment options for breast cancer

1.1.4.1 Localised early breast cancer

Chemotherapy and targeted hormone therapy (depending on ER, PR and HER2 status) is given to patients with advanced but localised tumour prior to surgery (neoadjuvant therapy). Anthracycline- and taxane-based regimens are considered in the neoadjuvant setting.

Surgical options include breast-conserving lumpectomy or mastectomy with or without reconstruction, followed by regional or whole breast post-operative radiotherapy, depending on number of cancer-positive axillary nodes (Board 2017). According to the European Organization for Research and Treatment of Cancer's trial (EORTC-10801) (van Dongen et al. 2000) both surgical procedures carry low risks of local recurrences. Meta-analysis has shown the association between positive margins post-surgery with a two-fold increased risk of recurrence within the same site (Moran et al. 2014). Radiotherapy is essential in those with breast conserving surgery to eliminate residual disease and lower the chances of local recurrence. Adjuvant radiotherapy on the chest wall and regional lymph nodes is given to patients after mastectomy.

Post-operative treatment (adjuvant) includes chemotherapy, such as tamoxifen and aromatase inhibitors, depending on clinicopathological factors. Commonly anthracycline-based therapies, involving fluorouracil, epirubicin, and cyclophosphamide, are used as

adjuvants (Board 2017). Additional benefits were seen with the inclusion of taxanes, such as paclitaxel and docetaxel, to anthracycline-based regimens (De Laurentiis et al. 2008). In addition to systemic chemotherapy ER, PR and/or HER2 receptor expression are targets of endocrine therapy in hormone receptor-positive cancer. HER-2 receptor-positive patients can be treated with trastuzumab (Herceptin) and lapatinib, whereas ER and PR-positive cancers can be treated with tamoxifen. Absence of hormone receptors in TNBC therefore relies solely on chemotherapy.

1.1.4.2 Metastatic breast cancer

The aim of therapy at the metastatic stage is to extend and improve quality of life (referred to as palliative care). Patients with localised metastases can undergo surgery and radiotherapy. Otherwise, systemic chemotherapy and targeted or hormonal therapies are used. For hormone receptor-positive metastatic breast cancer, tamoxifen and aromatase inhibitors are mainly used in both pre- and post-menopausal women (Mauri et al. 2006). Furthermore, HER2-positive cancers can be targeted by HER2 directed monoclonal antibodies such as trastuzumab and pertuzumab (Perjeta) or by lapatinib (a tyrosine kinase inhibitor of HER2 receptor). Resistance to these endocrine therapies develop, requiring further targeted therapies such as rapamycin (mTOR inhibitor) and Palbociclib (CDK4/6 inhibitor).

Chemotherapy also plays a role in managing metastatic disease, particularly in hormone receptor-negative cancer and in advanced metastatic disease. Anthracycline (doxorubicin and epirubicin), taxanes (paclitaxel and docetaxel), cyclophosphamides, platinum-based agents (cisplatin and carboplatin) can be used alone or in various combinations (Johnston 2011).

1.1.5 Breast cancer genetics

Cancer genomics has revolutionised our understanding of the genetics underlying all malignancies. This work is being coordinated by large international consortia, pioneered in breast cancer by the Molecular Taxonomy of Breast Cancer International Consortium (METABRIC), the pan-cancer Cancer Genome Atlas program (TCGA), and extended through the International Cancer Genomes Consortium (ICGC).

1.1.5.1 METABRIC

The Molecular Taxonomy of Breast Cancer International Consortium (METABRIC), conducted a study using around 1000 primary tumours along with a validation set of around 1000 tumours with clinical follow-up (Curtis et al. 2012). This study demonstrated the relevance of inherited variants and acquired somatic copy number aberrations on expression of nearly 50% of genes. Novel subgroups with defined clinical outcomes were also identified in this study.

1.1.5.2 The cancer genome atlas (TCGA) project

TCGA has now characterised the molecular profiles of numerous cancer types, including Breast Cancer (Network 2012). This study incorporated six approaches to analyse gene expression in a large dataset of breast cancer: DNA copy number arrays, DNA methylation, exome sequencing, mRNA arrays, microRNA sequencing and reverse phase protein arrays.

Whole genome sequencing of samples considered by the TCGA identified just over 30,000 mutations. This included genes whose mutations were previously associated with breast cancer, such as PIK3CA, PTEN, AKT1, TP53, CDH1, RB1 and MAP3K1. Additionally, new genes, whose mutations had great significance in breast cancer were also identified. These included TBX3, RUNX1, CBFB, AFF2, PIK3R1 and PTPN22 that are involved the development of the mammary gland.

The study identified that ER-positive/luminal tumours had heterogenous spectrum of mutations, copy number changes and patient outcome. These tumours have a luminal gene expression signature and have a high frequency of PI3KCA, MAP3K1 and MAP2K4 mutations.

Furthermore, two subtypes of HER2-positive tumours were identified: HER2-Enriched (HER2E)-mRNA-subtype/HER2-positive and luminal-mRNA-subtype/HER2-positive tumours. The former subtype is characterised by DNA amplification of HER2 and overexpression of multiple HER2-amplicon associated genes that contribute to around 50% of clinically HER2-positive tumours. The remainder of HER2-positive tumours are classed as the luminal mRNA subtypes. Frequent mutations in the PI3-kinase pathway (PIK3CA, PTEN and PI3K1) have been identified and therefore offered new potential therapeutic targets in HER2-positive tumours.

Frequently mutated genes in luminal A subtype include MAP3K1, GATA3, TP53, CDH1, and MAP2K4. Mutations in luminal B were more diverse, with high frequency of mutations found in TP53 (missense mutations) and PIK3CA. In contrast, basal-like subtype of tumours did not harbour mutations in many of the genes commonly mutated in the luminal subtype. However, TP53 was most often mutated, present in 80% of cases (mostly nonsense and frame-shift mutations). As expected, HER2E subtypes had increased frequency of HER2 gene amplification. In addition, TP53 and PIK3CA were also frequently mutated in HER2E tumours.

Analysis of basal-like subtype of tumours, revealed high frequency of loss of function mutations in TP53, RB1, BRCA1 and PIK3CA. Furthermore, gene expression signatures show enrichment of keratins 5, 6, 7 and proliferative markers.

1.1.5.3 Use of genetics in the clinic to predict breast cancer prognosis

Predicting the outcome, once a diagnosis of breast cancer is made, was traditionally determined using histopathological factors. The accuracy of predicting outcome using this approach is limited in patients with smaller tumours that are of lower grade and in patients with negative lymph node status. Reflecting on the molecular tumour heterogeneity, demonstrated by DNA sequencing and gene expression profiling, molecular biomarkers have been considered as the way forward for personalised approach in predicting outcome. Microarray tests consisting of biomarkers, have been used in the clinic to predict recurrence in patients at the early stage of breast cancer. This has been applied to see which patients would benefit from chemotherapy.

A study conducted by van't Veer *et al*, is an example of using gene expression of tumour samples to determine predictive signatures for distant metastasis. Samples from over 100 primary breast tumours were used for DNA microarray analysis to see whether a gene expression signature predicting distant metastases in lymph node-negative patients can be identified (van 't Veer et al. 2002). Clustering, based on the expression of around 5,000 significant genes gave two main groups – predictive of good and bad prognosis. This predictive tool will aid in deciding the need for systemic adjuvant therapy, ensuring that patients undergo treatment if their genetic profile falls into the classification of bad prognosis. Furthermore, genes that were found to be overexpressed in the cluster for bad prognosis are also worth studying further as therapeutic targets.

Furthermore, three commercially available genomic biomarker assays include: Oncotype DX, (Genomic Health Inc., San Francisco) MammaPrint and PAM50 (Kittaneh, Montero, and Glück 2013).

The Oncotype DX assay was developed and validated in patients with hormone receptor-positive breast cancer, who were at the early stage of disease and were treated with

endocrine therapy (Paik et al. 2004). This assay is a real-time PCR-based assay, involving 21 genes. This assay calculates a recurrence score that predicts recurrence in patients with early stage hormone receptor-positive tumours, who were lymph node-negative and had 5 years of tamoxifen treatment. The recurrence score classifies patients as low-, intermediate-, or high-risk. Overall, reduced ER expression, together with increased expression of proliferative and invasive markers predicts high risk of recurrences. Meanwhile, increased expression of oestrogen-associated genes and GSTM1 and BAG1 predicts reduced risk of recurrences.

In contrast to Oncotype DX, MammaPrint and PAM50 have been developed from patients of all subtypes of breast cancer. MammaPrint is a 70-gene signature that consists of genes associated with tumour progression and metastasis (Tian et al. 2010). This signature predicts the risk of 10-year distant metastasis-free survival and classifies patients as low risk (>90%) and high risk (<90%).

PAM 50 (Prediction Analysis of Microarrays) involves a 50-gene microarray that classifies invasive breast cancers according to the intrinsic subtypes clinically: luminal A, luminal B, HER2-enriched, and basal-like (Parker et al. 2009). Additionally, this test gives values for proliferative markers and luminal markers such as ESR1, PGR, and ERBB2.

1.1.5.4 Overview of other breast cancer signatures

Comparison of gene signatures from similar studies of breast cancer samples shows that there is minimal overlap of genes. To investigate this observation further, Huang *et al* considered 33 breast cancer signatures from previous studies, to see whether genes from one signature overlapped with any other signatures. This study analysed 33 different breast cancer signatures to understand whether there are common functions that are associated with the genes across different signatures (Huang, Murphy, and Xu 2018). Out of 2239 genes, only 238 genes were commonly found in two different signatures. MKI67

was the most common gene, a marker of cell proliferation, found amongst 8 of the signatures.

Enrichment analysis of the 2239 genes for biological functions, resulted in 1979 function terms, of which 429 were common in at least 2 different signatures. The most common terms involved biological functions such as cell cycle, cell death, response to wounding, response to organic substance and intracellular signalling cascade. Common functional terms between ER-positive and ER-negative cancer included cell death, cell proliferation, intracellular signalling cascade, response to hormone stimulus, response to oxygen levels, bone development, DNA packaging and skeletal system development.

1.1.6 Breast cancer *in vivo* models

In vivo models are important research tools for breast cancer, as they aid the translation of in vitro findings to clinical practice. Pre-clinical studies involve the validation of results from *in vitro* studies in *in vivo* models that provide a physiologically relevant means of studying cancer initiation, invasion and metastasis. There are now many different mouse models of breast cancer, that each have their own advantages and flaws and address different aspects of breast cancer disease. These studies have contributed to the advancements in understanding cancer biology and therapy.

1.1.6.1. Cancer cell line derived xenografts (CDX)

Cancer cell-line xenografts are the most common and simplest type of model, in which cancer cell lines are engrafted in mice. Typically, human cell models are engrafted into immunocompromised mice to prevent immune rejection. The cells are engrafted via subcutaneous injection (ectopic), or by implanting cells in the mouse mammary gland (orthotopic). These models allow the study of cancer initiation, growth and progression to invasive and metastatic disease. However, as the cell lines used often derive from aggressive tumours, the early initiation of cancer cannot be easily modelled. Further,

tumours in CDX models are often homogeneous epithelial breast cancer cells, and as the mice are generally immunocompromised, the tumour microenvironment will not be truly representative.

In this project, several murine cell lines originate from mouse tumours. 4T1 cells were used that were derived from a spontaneous breast cancer in BALB/cfC3H mice (Dexter et al. 1978). Mouse breast cancer cell mBCC#4 were also used, originating from BlgCre $p53^{fl/fl}$ $Brca1^{fl/fl}$ mice (Molyneux et al. 2010). E0771 are derived from spontaneous mammary tumours in C57BL/6 mouse (Sugiura and Stock 1952). Both mBCC4 and E0771 cells are derived on a C57BL/6 background so can be xenografted to immune competent C57 mice. As our PKN2 knockout mouse models are also on a C57 background, this provides scope for modulating both the tumour cells and the tumour microenvironment.

1.1.6.2. Patient-derived xenografts (PDXs)

PDX models address some of the limitations of CDXs. PDXs involve primary human tumours or cells in immunocompromised mice. As the cancer cells have been hosted in a human, it is physiologically more relevant and not subjected to changes due to *in vitro* conditions. Tumours from PDXs show conserved histological and molecular features from the donor patients (Hidalgo et al. 2014). Therefore, this model is suited better to study the development of primary tumours, as well as metastatic disease (Hoffman 2015), and therapeutic efficacies.

1.1.6.3 Syngeneic models of breast cancer

In this model, cancer cells derived from mice are transplanted into strain-matched mice. This allows the study of cancer initiation and progression in immunocompetent mice. The intact immune system in this model, although murine, offers an optimal microenvironment to test cancer therapy, particularly immunotherapy (Coffelt and de Visser 2015). For example, Johnstone *et al* developed a syngeneic model of breast cancer

metastasis using EO771.LMB cancer cells, derived from a metastatic nodule in an orthotopic tumour model in a C57BL/6 mouse (Johnstone et al. 2015).

1.1.6.4. Genetically engineered mouse models (GEMMs) of breast cancer

GEMs allow the monitoring and study of early phases of tumour initiation and development. In this model, a tumour spontaneously forms in its native tumour microenvironment. The advantage of GEMMS is the ability to study the native tumour microenvironment, due to the intact immune system. Moreover, this model allows for the study of manipulating a specific gene in the host organism, leading to the validation of oncogenes and tumour suppressor genes. Additionally, this model can be used for knock-out and knock-in studies of the gene of interest.

Oncogenic-driven transgenic mice include the MMTV-PyMT model, which is also characterised by spontaneous metastatic disease in lymph nodes and lungs. The polyomavirus (PyV) middle T antigen is known to have the ability to induce transformation of cells and tumourigenesis (Guy, Cardiff, and Muller 1992a). This is mediated by its association with tyrosine kinases (such as c-src) and PI3K (Talmage et al. 1989). The expression of the middle T antigen in mammary epithelial cells of transgenic mice with the MMTV-PyV middle T antigen fusion gene was investigated. This resulted in the formation of tumours at multiple foci and frequently associated with metastases in the lung. In this project, PyMT-BO1 cells were used, which originate from the MMTV-PyMT breast cancer model, isolated from bone metastases (Su et al. 2016).

Blg-Cre $Brca1^{f/f}$ $p53^{-/+}$ mice were generated by Molyneux *et al* to investigate the origin of basal-like BRCA1 breast tumours (Molyneux et al. 2010). This model addressed the question whether the deletion of BRCA1 in the luminal mammary epithelium (where Blg promoter is most active) results in basal-like BRCA1 breast cancer. Tumours generated from Blg-Cre $Brca1^{f/f}$ $p53^{-/+}$ mice are generally invasive ductal carcinomas of no special

type, of histological grade 3. These tumours are positive for the K14 and the basal marker p63. Thus, histologically and immunohistochemically, these tumours closely resemble basal-like BRCA1 tumours in humans. Although genetic analysis of these tumours show enrichment for genes associated with ER-negative luminal cells, analysis based on two single sample predictor gene sets (SSPs) show that gene expression is typically common between ER-negative luminal mammary epithelium and basal-like breast cancer.

1.1.6.5 CDX in GEMMS

In this project, the effect of inducing systemic PKN2 (a serine/threonine kinase, see section 1.2) deletion in mice on the growth of breast cancer xenografts was investigated. Rosa26 Cre-ERT2 mice (iCre) were crossed with mice heterozygous for PKN2 knockout, allowing for systemic deletion of PKN2, induced by Cre recombinase upon tamoxifen treatment. In this model, BO.1 cells from MMTV-PyMT breast cancer model were orthotopically injected following treatment of mice with tamoxifen, for induction of PKN2 deletion. Systemic deletion of PKN2 in the embryo led to lethality at E9.5 (Quétier et al. 2016). Therefore, an inducible system for knocking out PKN2 was required to study tumour growth in adult mice.

1.2 PKN kinases

Protein Kinase N (PKN) is a family of serine/threonine protein kinases that bear high sequence homology with protein kinase C (PKC) and are therefore also known as the PKC-related kinases (PRKs). PKN kinases belong to the AGC superfamily of protein kinases, which also include protein kinase A (PKA; cAMP-dependent protein kinase), PKB/AKT, Rho-associated kinase (ROCK) and PKC.

PKN kinases include three isotypes in mammals: PKN1, PKN2 and PKN3. These isotypes show high homology within their C-terminal kinase domains but show more divergence in their N-terminal regulatory sequences (Palmer and Parker 1995). Thus, the three isotypes

are regulated differently, and are sensitive to distinct activators (Oishi et al. 1999). PKN1 and PKN2 are ubiquitously expressed (Palmer and Parker 1995) (Kitagawa et al. 1995), whereas PKN3 expression is restricted to cancer cells, as well as muscle, liver and endothelial cells (Oishi et al. 1999). PKN kinases are downstream effectors of Rho GTPases (Amano et al. 1996), which are associated with the regulation of actin cytoskeletal organisation (Vincent and Settleman 1997). However additional functions have also been ascribed to PKN: involvement in vesicular transport (Kawamata et al. 1998), glucose transport (Standaert et al. 1998) nuclear translocation (Mukai, Miyahara, et al. 1996) and regulation of meiotic maturation and embryonic cell cycle (Stapleton et al. 1998).

1.2.1 Structure of PKN kinases

The C-terminus contains the serine/threonine kinase domain that has high homology in sequence with PKC kinases. At the N-terminus there are three homologous regions (HR) consisting of approximately 70 aa that are rich in charged residues, named as HR1, HR2 and HR3 motifs (Palmer, Ridden, and Parker 1995). The first region forms an antiparallel coiled-coiled fold (ACC finger) by two alpha helices (Maesaki et al. 1999). Therefore, this region is also known as the ACC domain, which is the structure that binds the small GTPase RhoA. This domain also acts as a binding interface for other proteins such as anchoring protein CG-NAP (centrosome and Golgi localized PKN associated protein) (Takahashi et al. 1999).

Unlike mammalian PKC isoforms, PKN2 has HR1 domains that are conserved in yeast PKC isoforms (Roelants et al. 2017). The HR1 domain means PKN isoforms are regulated by Rho, as yeast PKC. Thus, PKN kinases are considered as the human orthologue of yeast PKC.

The HR2 domain consists of about 130 amino acids that precedes the catalytic domain. An auto-inhibitory region is found at the C-terminal end of the C2-like domain, which is

conserved amongst other PKN isoforms isolated form other organisms (Yoshinaga et al. 1999). Between the C2-like and the catalytic domain, there is a linker region. In PKN2 and PKN3 this linker contains one and two proline-rich regions respectively, which bind Src homology 2 (SH3) domains (Feng et al. 1994). This proline-rich region is not found in PKN1.

1.2.2 Regulation of PKN kinases

1.2.2.1 Activation of PKN Kinase Catalytic Activity

The regulation of kinase activity is commonly shared in members of the AGC kinase family, involving phosphorylation at the activation-loop sequence between the upper and lower lobe of the kinase domain, at the C-terminal hydrophobic motif (Frodin et al. 2002) and turn-motif (Hauge et al. 2007) (Parekh, Ziegler, and Parker 2000). Phosphorylation at the latter two sites is required for the interaction between the hydrophobic motif and a hydrophobic pocket at the upper lobe of the kinase domain, known as the PIF pocket (PDK1 Interacting Fragment) (Balendran et al. 2000). In the members of the PKC family, the activation loop, hydrophobic and turn motifs are often constitutively phosphorylated (see PDK1 and mTORC2 below), representing a 'primed' kinase domain. It has additionally been shown that the occupation of the nucleotide-binding pocket by ATP is required for the stability of the 'primed' conformation (Cameron et al. 2009).

In an inactive conformation, interaction between the primed PKC kinase domain and an autoinhibitory pseudosubstrate region within the regulatory domain blocks access to the active site. In order for the kinase to be activated, the active site needs to be relieved from its interaction with the regulatory domain at the N-terminus, which occurs allosterically. In the case of PKC, this allosteric activation typically occurs through biding of lipids to the regulatory domain C1 and C2 domains. PKN kinases share homology with PKC kinases at both the C-terminal kinase domain (Mukai and Ono 1994) and also share a homologous C2 domain within the regulatory domain (Mukai and Ono 1994). Therefore, similar

mechanisms of regulatory autoinhibition have been proposed for the PKN kinases. Binding of the C2 domain to lipids, and Rho binding to the HR1 domains (discussed above), are thought to relieve kinase domain auto-inhibition by the regulatory domain.

In support of this mechanism, partial hydrolysis of PKN to yield a liberated kinase domain results in increased kinase activity independent of unsaturated fatty acid (Mukai et al. 1994). This gave the first indication that the N-terminus of PKN kinases was required to regulate the activity of its kinase. Direct interaction between the C- and N-terminal regions of PKN kinases was demonstrated using yeast two-hybrid assay (Kitagawa et al. 1996). Furthermore, it was shown that the region between amino acids 39 to 53 in PKN kinases may represent an autoinhibitory pseudosubstrate-like region, although this remains an area of controversy (Kitagawa et al. 1995). Additionally, an autoinhibitory region between residues 455-511 of PKN kinases has also been identified, however dependent on arachidonic acid for relief from inhibition (Yoshinaga et al. 1999). This region is also involved in auto-inhibition of PKN via the dimerization of PKN2, discussed below.

1.2.2.2. Activation by Rho-family of GTPases

RhoA binds to PKN1 at the first two of three homologous motifs (HR1a and HR1b) of the HR1 domain. The homologous HR1 domain in PKN2, also binds GTP-RhoA. There are two contact sites for RhoA binding in the HR1 domain – one that requires the conformation of a nucleotide-bound state and the other that is nucleotide-independent. HR1a can only bind to GTP-bound RhoA, whilst HR1b can bind both GTP- and GDP-bound RhoA (Flynn et al. 1998). The N-terminus of PKN has activity to inhibit endogenous GTPase activity of RhoA and inhibits the interaction between GAP and RhoA – therefore also inhibiting GAP-stimulated GTPase activity of RhoA. Thus, the half-life of GTP-bound RhoA is increased when bound to PKN kinases (Mukai, Miyahara, et al. 1996).

1.2.2.3 Activation by Lipids and Secondary Messengers

PKN1 is activated in response to arachidonic acid cardiolipin, phospholipids and lysophospholipids (Mukai et al. 1994). Activators of PKC kinases such as calcium, phosphatidylserine, diacyglycerol and PMA do not have any effect on enhancing the kinase activity of PKN1 (Kitagawa et al. 1995). PKN2 and PKN3 on the other hand are considerably less sensitive to arachidonic acid (Oishi et al. 1999). Another study by Falk et al also demonstrated different sensitivity to lipids by the different PKN isoforms (Falk et al. 2014). PKN1 was activated by all lipids, except IP3 and DAG, whilst PKN2 was only responsive to arachidonic acid and PIP2. PKN3 on the other hand has very low sensitivity to arachidonic acid, with enhanced effect on its catalytic activity when levels of arachidonic acid are low.

1.2.2.4 Activation by PDK1 and mTORC2

Actin cytoskeleton rearrangement in response to growth factors is mediated by phosphatididylinositol-3-kinase (PI3K) activation (Kotani et al. 1994) (Wennström et al. 1994) (Martin et al. 1996). Phosphoinositide-dependent protein kinase-1 (PDK1) is a downstream effector of PI3K that can phosphorylate and activate proteins from the AGC kinase family, including PKN kinases (Le Good et al. 1998) (Kobayashi and Cohen 1999). The interaction between PKN kinases and PDK1 occurs between the C-terminus of PKN kinases and the kinase domain of PDK1. Thr774 in the activation loop of PKN kinases is phosphorylated by PDK1 to activate and increase the catalytic activity, causing actin cytoskeleton reorganisation in response to insulin (Dong et al. 2000).

A study on prostate cancer investigated the role of MTORC2 in regulating PKN1. PKN1 is overexpressed in prostate cancer, with increased expression in tumours of high Gleason score (Metzger et al. 2008) and in metastatic tumours, compared to primary tumours (Yu et al. 2004). It was demonstrated that phosphorylation of PKN1 at the turn motif is

mediated by MTORC2, downstream of PI3K (Yang et al. 2017). This allows PKN2 to elicit its effect on cancer cell migration, as discussed in 1.2.3.3.

1.2.2.5 PKN2 dimerisation

An alternative dimer-based autoinhibitory mechanism has also been proposed for PKN2. Here intramolecular interactions between two PKN2 molecules sequesters an inactive dimer in the cytoplasm prior to allosteric activation by Rho GTPases (Bauer et al. 2012). The interaction occurs at the catalytic site between the PKL sequence-binding site (residues 455-511) and the N-terminal binding site. The change in the conformation of the catalytic domain, inhibits the binding of the C-terminal to the HM/PIF pocket. Furthermore, the binding of Rho to the HR1 domain of PKN2 exposes the PIF domain, allowing for the activation of PKN2.

1.2.3 Functions of PKN kinases

PKN kinases are downstream effectors of Rho GTPases (Amano et al. 1996) which are strongly associated with regulation of the actin cytoskeleton (Vincent and Settleman 1997). However, many additional functions have also been ascribed to PKN, including involvement in vesicular transport (Kawamata et al. 1998), glucose transport (Standaert et al. 1998), nuclear translocation (Mukai, Miyahara, et al. 1996), regulation of meiotic maturation and embryonic cell cycle regulation (Stapleton et al. 1998) (Mukai 2003).

1.2.3.1 PKN is a Rho Effector

(i) Actin cytoskeletal organisation

Rho family GTPases are known regulators of actin cytoskeleton, through multiple effector pathways, including the ROCK, PAK, as well as the PKN kinases. However, the specific role of PKN in actin cytoskeleton regulation is not conclusive due to different results from various studies.

Studies in *Drosophila* suggests a role for PKN kinases in regulating actin-cytoskeleton during dorsal closure at the late stage of Drosophila development (Lu and Settleman 1999). The movement between actin and myosin is regulated by phosphorylation of their light chain (MLC), which regulates processes such as stress fibre formation (Katoh et al. 2001). PKN1 phosphorylates CPI-17, which enhances its inhibitory effect on myosin phosphatase (Hamaguchi et al. 2000); this increases sensitisation of smooth muscle cells to calcium ions. Calcium ions cause inhibition of myosin phosphatase, therefore increasing myosin phosphorylation that is required for contractility in smooth muscle cells.

Another way in which PKN1 is involved in regulating actin-cytoskeleton is by phosphorylating related proteins such as caldesmon and G-actin (Mukai et al. 1997). PKN kinases phosphorylate head-rod region of intermediate filament proteins, which in turn prevents polymerisation of neurofilaments (NFs) (Mukai, Toshimori, et al. 1996), vimentin and glial fibrillary acidic proteins (Matsuzawa et al. 1997) – required for regulating intermediate filaments. PKN kinases also phosphorylate microtubule-associated protein (MAP) tau (Taniguchi et al. 2001).

Furthermore, mass-spectrometry analysis of PKN2-deleted MEFs identified many phosphopeptide changes in proteins related to the cytoskeleton and intermediate filaments (Quétier et al. 2016). Examples include decreased phosphorylation of anillin, which is required for the scaffolding between RhoA, actin, and myosin during cytokinesis (Piekny and Glotzer 2008). Phosphorylation of nestin, an intermediate filament protein, was also reduced following PKN2 loss. In the normal mammary gland, nestin is expressed in basal and myoepithelial cells (Li et al. 2007). Furthermore, nestin is favourably expressed in basal-like and TNBC (Parry et al. 2008). TNBC progression and poor prognosis is also associated with nestin expression (Liu et al. 2010).

(ii) Role of PKN kinases in cell cycle regulation

To initiate mitosis, Cdc25C dephosphorylates Tyr-15 in Cdc2 to relieve its suppression, activating Cdc2/cyclin B histone H1 kinase. Therefore, Cdc25C needs to be tightly controlled to regulate mitotic entry. Addition of exogenous and active PKN kinases in *Xenopus* egg extracts, resulted in delayed mitosis. This was due to sustained inhibitory phosphorylation of Tyr-15 of Cdc2, mediated by inhibitory phosphorylation of Cdc25C by PKN (Misaki et al. 2001).

The role of PKN2 in mitosis was further investigated in HeLa cells (Schmidt et al. 2007). siRNA-mediated depletion of PKN2 in HeLa cells resulted in an increased number of binucleated cells after 72 hours, suggesting a role in cytokinesis. However, this effect was not observed when PKN1 or PKN3 were depleted. Analysing the localisation of PKN kinases during different cell cycle phases revealed accumulation of PKN1 and PKN2 at the cleavage furrow and the midbody during telophase and cytokinesis. This localisation of PKN2 was lost upon siRNA treatment, leading to the late cytokinesis defect. Further observation of PKN2-depleted cells showed delayed G2/M progression and apoptosis in nearly a third of binucleated cells. Finally, it was demonstrated that Ect2 mediated the phosphorylation of PKN2 by Rho GTPases, causing PKN2 localisation at the cleavage furrow. Furthermore, PKN2-depleted cells had reduced phosphorylation of Cdc25B family of protein phosphatases. Consequently, dephosphorylated Cdc25B proteins are inactive and unable to activate cyclin/Cdk complexes and initiate G2/M transition.

The role of the PKN in embryonic development was investigated in our recent paper (Quétier et al. 2016), which revealed a role for PKN2 in the regulation of mesenchymal cell growth. Inducible deletion of PKN2 in MEFS, using a conditional knockout model, decreased cell growth, and resulted in an increased proportion of cells at G1/G0 phase and loss of cells at S1 phase. This contrasts with the G2 mitotic arrest observed by

Schmidt et al described above (Schmidt et al. 2007). This observation was further supported by phosphoproteomic analysis in which deletion of PKN2 in MEFs caused decreased phosphorylation of numerous proteins involved in cell cycle (Quétier et al. 2016). Apoptosis was not affected in MEFs by PKN2 deletion. Further investigation revealed decreased proliferation of the pharyngeal mesoderm, upon PKN2 deletion, indicating that the *in vitro* function in mesenchymal cells in likely conserved *in vivo* (see mouse development section below).

(iii) Formation of apical junctions in epithelial cells

Apical junctions are crucial for polarity, permeability and cell-to-cell adhesion in epithelial cells. Rho is known to regulate the formation of apical junctions (Nusrat et al. 1995) (Smutny et al. 2010), with ROCK being the main downstream effector studied. Inhibiting ROCK in colon and breast carcinoma cell line disrupted or inhibited the formation of tight junctions (Walsh et al. 2001) (Shewan et al. 2005), but had no effect in other cells such as MDCK or HCT116 cells (Sahai and Marshall 2002). This led to the study of other downstream effectors of Rho that regulate the form of apical tight junctions.

A study by Wallace et al, involving an siRNA screen of 28 Rho effectors in human bronchial epithelial cells, identified PKN2 as a regulator of apical junctions (Wallace, Magalhaes, and Hall 2011). It is postulated the binding of Rho A to PKN2 at the N-terminal, relieves PKN2 from its auto-inhibitory conformation. Therefore, the activated kinase domain of PKN2 leads to its interaction with another protein, to allow for its localisation at apical junctions.

1.2.3.2 Physiological functions

(i) Drosophila and C.*Elegans*

The role of PKN kinases in normal development was studied in *Drosophila*, which has a single PKN orthologue. PKN kinase in *Drosophila* was shown to be necessary for dorsal closure during embryogenesis, downstream of Rho1 and Rac (Lu and Settleman 1999).

Specifically, PKN kinase is involved in a Rac-JNK pathway causing changes in cell shape and migration. This action is required to close the opening of the epidermal layer overlying the amnioserosa. In *Caenorhabditis elegans* PKN1 was shown to regulate muscle contraction, implying the functional versatility of PKN kinases as Rho effectors (Qadota et al. 2011).

(ii) Mouse Embryonic development

Our recent paper (Quétier et al. 2016), first demonstrated the role of PKN kinases on development, *in vivo*. Systemic deletion of each individual PKN kinase isoforms, demonstrated a PKN2-specific role in mouse embryonic development. PKN2 knockout was shown to be lethal in mouse embryos at embryonic day 10 (E10). PKN2 knockout embryos at E9.5 had deficient branchial arch formation, failed to undergo axial turning and had an underdeveloped mesenchymal compartment. Other abnormalities include cardiovascular defects and incomplete neural tube closure. Intriguingly, this study also revealed that PKN1 or PKN3 deleted mouse embryos showed normal development, implying a non-redundant role for the PKN2 isoform.

We have also demonstrated a role for PKN2 in MEFs in migration. Phosphoproteomic analysis, in PKN2-deleted MEFs, showed enrichment of phosphopeptides involved in cell cytoskeletal organisation. This corroborates with the finding that deletion of PKN2 in MEFs caused decreased migration, demonstrated in scratch wound assays and single cell migration assays. The failure of neural crest cells to migrate *in vivo* observed in PKN2-deleted embryos is likely to be due to the inability of neural crest cells to migrate through the mesoderm in the absence of PKN2. This provides *in vivo* evidence for a non-redundant role of PKN2 in migration suggested by this and other studies (Lachmann et al. 2011). Subsequent to our paper, Danno et al and Yang et al independently observed lethality between E9.5 and E10 in mice with systemic PKN2 deletion, as well as similar

abnormalities in branchial arch formation and neural tube closure (Danno et al. 2017) (Yang et al. 2017), confirming the validity of our work.

1.2.3.3 Function in cancer

(i) Prostate Cancer

Role of PKN1 in Prostate Cancer

PKN1 is overexpressed in prostate cancer, with increased expression in tumours of high Gleason score (Metzger et al. 2008). PKN1 was demonstrated to activate androgen receptor via the transactivation unit 5 (TAU-5) at the N-terminus (Metzger et al. 2003). Depleting PKN1 inhibits hormone-dependent proliferation of PCa cells. PKN1 interacts with the scaffold protein sperm-associated antigen 9 (SPAG-9/JIP4) to regulate migration-associated genes (Jilg et al. 2014). Co-localisation of PKN1 with DPA9 is required for the phosphorylation of p38 and cell migration. PKN1 knockdown resulted in a slight decrease in proliferation of PC-3M-luc2 androgen-independent prostate tumour cell lines, but this change was non-significant. However, the rate of apoptosis upon PKN1 depletion remained unaffected.

Role of PKN3 in Prostate Cancer

Constitutively active PI3K signalling is needed for the growth of invasive PC3 prostate cancer. Expression profiling has identified PKN3 to be dependent on this PI3K signalling. Furthermore, inhibiting PKN3 reduced the growth of prostate cancer cells in the same way as seen when p110b (the catalytic subunit of PI3K) was inhibited (Leenders et al. 2004). Moreover, conditional PKN3 knockout in a mouse prostate tumour model, published during the course of my studies, showed decreased tumour size and metastasis (Mukai et al. 2016).

(ii) Breast Cancer

PKN kinases and TNBC

Evidence for the role of protein kinase N (PKN) kinases in TNBC is found in the literature. Comparative genomic hybridisation and gene expression analysis of TNBCs has identified PKN1 to be overexpressed when this gene is amplified (Turner et al. 2010). Brough *et al* conducted a functional viability screen in over 30 breast cancer cells. PKN2 (Gene: PRKCL2) was identified as a candidate gene for cell viability dependence in TNBC cells, compared to non-TNBC cells (Brough et al. 2011). However, the mechanism by which PKN kinases are involved in TNBC is unknown.

Role of PKN3 in Breast cancer

The interaction of PKN3 with Rho-family GTPases and its role in breast cancer was investigated. PKN3 was reported to show preferential binding to Rho C, compared to Rho A and Rho B. Rho C has been proved to be a significant driver of breast cancer metastasis (Hakem et al. 2005) and its regulation has been associated with more invasive and aggressive breast cancers. Therefore, the role of Rho C-binding PKN3 in breast cancer was investigated. It was shown that the level of PKN3 expression and activity, as well as Rho C level, was highest in TNBC cell lines. Furthermore, TNBC with PKN3 knockdown showed reduced growth in 3-D cultures and in an orthotopic breast cancer model (Unsal-Kacmaz et al. 2012).

(iii) Migration

90% of deaths from solid tumours result from distant metastasis, illustrating the importance of cancer cell migration and invasion. The role of PKN kinases in cell migration has been demonstrated in various cancer cell line models.

Lachmann *et al* investigated the individual roles of each PKN kinases isoforms in migration. Using bladder tumour cells, with enriched PKN2 expression, the role of the different PKN

kinase isoforms was studied - via siRNA knock-down and rescue (Lachmann et al. 2011). It was demonstrated that depleting all three isoforms slowed wound healing in 2D scratch wound assays. Assessment of migration after depletion of individual isoforms showed the requirement of either of PKN1 or PKN2, whilst depletion of PKN3 had no migratory effect. In 3D, a 50% reduction in migration was observed with PKN2 depletion compared to 25% reduction with PKN1 depletion. Rescue experiments demonstrated the specific requirement of PKN2 for migration or chimeras with the regulatory domain of PKN2. Similarly, PKN2 deletion in mouse embryo resulted in reduced motility in mouse embryonic fibroblasts and disrupted migration of neural crest cells (Quétier et al. 2016).

(iv) Metastasis

Conditional PKN3 knockout in a mouse prostate tumour model showed decreased tumour size and metastasis (Mukai et al. 2016). Thereafter, the role of PKN3 in angiogenesis was studied by treating aortic rings from PKN3 knockout mice with fibronectin, vascular endothelial growth factors (VEGF), hepatic growth factor (HGF), etc in 3-dimensional culture *ex-vivo*. This resulted in reduced number of microvessel sprouting from the PKN3 knockout aortic rings, compared to the wild-type controls. *In-vivo* corneal pocket assay also demonstrated poor angiogenesis with PKN3 knockout. However, tumour growth in PKN3 knockout mice, compared to wild-type mice showed no significant reduction in tumour angiogenesis. Thus, PKN3 in the stroma was not significant for angiogenesis in the tumour. On the other hand, embryonic fibroblasts from PKN3 knockout mice showed decreased migration in response to various growth factors, such as fibronectin and lysophosphatidic acid (LPA). Furthermore, lung metastases after injection of melanoma cells in PKN3 knockout mice was reduced in size and number.

1.3 Importance of tumour microenvironment & the potential role of PKN2

1.3.1 Tumour microenvironment

Solid tumours are not only composed of cancer cells but also a variety of other cell types and an extracellular martrix together forming the tumour stroma or tumour microenvironment (TME). The TME is comprised of the extracellular matrix and non-malignant cells such as endothelial cells, pericytes, immune cells and fibroblasts. The TME harbours a variety of cells of mesenchymal origin such as fibroblasts, cancer-associated fibroblasts (CAFs), mesenchymal stem cells (MSCs), adipocytes, and endothelial cells. Other components of the TME include haematopoietic lineage cell such as lymphoid cells and myeloid cells. A major part of the TME is made up of non-cellular components such as collagens, proteoglycans, and glycoproteins that form the extracellular matrix (ECM). As we have identified roles for PKN2 in fibroblast like cells, this section will primarily focus on CAFs.

1.3.2 Role of fibroblasts and CAFs in TME

Fibroblasts are major contributors of the ECM, arising from different possible origins. CAFs can support cancer proliferation, drive tumour progression, invasion and metastasis (Tyan et al. 2012; Shekhar et al. 2001). These functions are mediated by their secretion of growth factors, ECM-modulating factors (Palmieri et al. 2003) (Orimo et al. 2005) (Dumont et al. 2013) and by their ability to migrate and invade through the ECM. CAFs are generally characterised by high expression of α-SMA, fibroblast activation protein (FAP), matrix metalloproteinases (MMPs), tenascin-C, and platelet-derived growth factor (PDGFRα/β) (Sappino et al. 1988) (Scanlan et al. 1994) (Ostman and Heldin 2007). High expression of α-SMA, the most widely used marker of activated fibroblasts (myofibroblasts and CAFs), has been associated with high grade tumours, lymph node metastasis and poor prognosis in

breast cancer. However, gene expression in CAFs show variation between different breast cancer subtypes (Surowiak et al. 2007) (Vallejos et al. 2012) (Yazhou et al. 2004).

1.3.2.1 CAF heterogeneity

A study by Costa et al investigated heterogeneity of CAFs in breast cancer and identified four distinct subtypes of CAFs called CAF-S1, CAF-S2, CAF-S3, and CAF-S4 (Costa et al. 2018). These subtypes are characterized by the expression of six fibroblast markers: FAP, integrin β1/CD29, αSMA, S100-A4/FSP1, PDGFRβ, and CAV1. CAF-S1 express all markers, except CV1. CAF-S2 generally have low expression of all the markers. CAF-S1 and CAF-S3 are considered as myofibroblast-like due to the expression of αSMA. CAF-S1 demonstrated immunosuppressive effect in breast cancer, by enhancing the inhibitory effect of regulatory T cell on T effector cell proliferation.

1.3.2.2 Origins of CAFs

The origins of CAFs within tumours remains inconclusive. One origin of CAFs is the fibroblasts that are resident within the TME and are activated by factors such as TGFβ and SDF (Kojima et al. 2010). This results in differentiation of fibroblasts into myofibroblasts (Rønnov-Jessen et al. 1995). Mesenchymal stem cells also have the capability to differentiate into CAFs (Mishra et al. 2008) (Weber et al. 2015).

Secondly, may derive from mesenchymal stem cells (MSCs). A study by Mishra *et al* demonstrated myofibroblast differentiation of bone marrow-derived MSCs, when treated with conditioned media from MDAMB231 cancer cells (Mishra et al. 2008). The gene expression profile of these differentiated MSCs were similar to CAFs. Furthermore, another study demonstrated the effect of osteopontin on MSCs differentiation into CAFs, mediated by the transcription factor MZF1 as well as TGFβ1.

Thirdly, CAFs have shown to arise from epithelial cells that have undergone epithelial-to-mesenchymal transition (EMT) (Zeisberg et al. 2007). Similarly, endothelial cells have also been demonstrated to differentiate into mesenchymal-like cells, via endothelial-to-mesenchymal transition (Zeisberg et al. 2007). These cells function as fibroblast in tissue remodelling, fibrosis and cancer.

1.3.3 Prognostic relevance of desmoplastic stroma in breast cancer

The importance of the stroma in breast cancer has been demonstrated in several studies. A gene analysis study identified a 50-gene stromal signature that can predict response to anthraxanes and taxane-based drugs in the neoadjuvant settings in breast cancer patients (Farmer et al. 2009). In general, a reactive stromal gene signature was associated with poor therapeutic response.

The presence of stroma/desmoplasia in triple-negative breast cancer (TNBC) has been linked to bad prognosis (Moorman *et al*, 2012; Downey *et al*, 2014; de Kruijf *et al*, 2011) but this is also contradicted in other studies (Kreike *et al*, 2007). Therefore, therapeutic approaches targeting the stromal compartment of tumours have become of interest.

1.3.4 Role of CAFs in the interaction between cancer and tumour microenvironment

1.3.4.1 Role of CAFs in tumour progression/metastasis

Metastasis requires ECM degradation, invasion/intravasation into lymph nodes or blood vessels, extravasation and the ability to proliferate and establish a secondary tumour at the new site. CAFs can play an important role in many of these aspects and here I will summarise some key known functions.

1.3.4.2 Effect of CAFs on ECM remodelling

A recent paper investigated the role of CAFs in ECM remodelling of breast tumours (Wang et al. 2017). CAFs were shown to affect the assembly and re-organisation of collagen I and

fibronectin, two important components of the ECM. First, CAFs lay down unfolded fibronectin fibres, that is followed by a denser matrix of collagen I after remodelling, resembling scar tissue after wound healing. Matrix metalloproteins (MMP-2, MMP-9 and MMP-12) secreted by CAFs also play an important role in ECM remodelling (Karagiannis et al. 2012). CAFs aid metastasis also by upregulating palladin expression and secreting proteolytic enzymes to degrade the ECM (Brentnall et al. 2012).

1.3.4.3 Effect of CAFs on cancer cell invasion

The collective invasion of cancer and fibroblasts were observed under 3D *in vitro* conditions, using organotypic culture model (Gaggioli et al. 2007) (Gaggioli 2008). This model involves the culture of cells on top of a gel matrix, composed of collagen I, as well as laminins and collagen IV. Cancer cells alone do not show any migration within the gel, unlike in the presence of fibroblasts, where invasion of cells down the gel is observed. Furthermore, the degree of invasion was dependent on the number of fibroblasts that were co-seeded with the epithelial cancer cells. A closer look at the invading cells revealed fibroblasts to be at the leading front, followed by cancer cells in tracks of degraded gel matrix.

1.3.4.4 Role of CAFs in EMT

EMT is a process whereby epithelial cells undergo morphological changes and become more mesenchymal-like. Cells undergoing EMT lose expression of epithelial marker E-cadherin and lose apico-basal polarity, whilst increasingly expression of mesenchymal markers such as vimentin, N-cadherin and Zeb1. This results in cells that are more motile, invasive and less polarised.

CAFs can trigger EMT in breast epithelial cells, which can that result in cancer stem cell-like aggressive behaviour, driving cancer metastasis (Soon et al. 2013). Factors such as TGF-β, CCL2 and IL-1β drive this process (Yu et al. 2014) (Tsuyada et al. 2012) (P et al.

2016). Moreover, CAFs also deposit their own ECM that has been shown to differ from the ECM laid down by normal fibroblasts. CAF-deposited ECM is more aligned in pattern (Dumont et al. 2013), induces EMT in tumour cells and contains high levels of fibronectin, biglycan and ECM-modulating enzyme lysyl oxidase.

1.3.4.5 Role of CAFs in altering metastatic tropism

Moreover, CAFs has shown to also pay a role in influencing metastatic tropism. For example, TNBC, that have a high tendency to metastasise to visceral organs, can alter their tropism to form bone metastases through exposure to CAF-secreted CXCL12 and IGF (Zhang et al. 2013). Another way in which CAFs may be involved in influencing the metastatic site, is by migrating together with the cancer cells to the metastatic site. This has been demonstrated, by Duda *et al,* in lung metastases *(Duda et al. 2010)*. The presence of stromal cells is thought to support the initiation and initial growth of secondary tumours in the lung.

1.3.4.6 Effect of CAFs on tumour drug response

A number of studies provide evidence to suggest the involvement of CAFs in drug resistance. Teicher *et al* observed different susceptibility of cancer cells to chemotherapy between *in vitro* and *in vivo* conditions (Teicher et al. 1990). Resistance demonstrated *in vivo* was absent when tested *in vitro*, indicating that factors present *in vivo* are required for developing resistance. In breast and colon cancer, the tumour-stroma ratio is predictive of the outcome of patients receiving adjuvant chemotherapy (Dekker et al. 2013) (Park et al. 2014). The gene expression profiles of the stroma of breast tumours have also shown to be able to predict outcome of patients undergoing neoadjuvant chemotherapy (Farmer et al. 2009).

The TME can affect response to therapy via intrinsic and acquired mechanisms (Klemm and Joyce 2015). Intrinsic mechanisms include reduced drug delivery, pro-survival

signalling and paracrine signalling loops. Acquired resistance can arise after exposure to therapy.

The ECM provides structural support to the TME, where collagen is a key player and contributes to mechanical properties that has implications for intrinsic drug resistance (Barocas and Tranquillo 1997). Studies have demonstrated that the amount and organisation of collagen affects interstitial diffusion and thereby delivery of drugs from the bloodstream. Eliminating collagen in tumours, using collagen-degrading enzyme collagenase, resulted in improved diffusion (Netti et al. 2000).

Tamoxifen resistance is an example that has been attributed to CAFs, mediated by upregulation of PI3K/AKT and MAPK/ERK pathways and phosphorylation of ER (Pontiggia et al. 2012). Metabolic changes in CAFs driven by cancer cells results in CAFs undergoing aerobic glycolysis, inducing oxidative stress and autophagy. This provides adjacent cancer cells with nutrients and mediates tamoxifen resistance; mimicked in co-culturing MCF7 with fibroblasts or supplementing with metabolic substrates such as ketone bodies. This mechanism of tamoxifen resistance was overcome by inhibiting the mitochondria in MCF7 cells. (Martinez-Outschoorn et al. 2011). Factors secreted by CAFs also contribute to drug resistance. For example, HGF that activates AKT and MAPK signalling pathways and chemokine CCL2 disable drug-induced apoptosis (Tsuyada et al. 2012).

Furthermore, a recent study identified two different sub-populations of CAFs in ER-positive breast tumours, that have varying effects on sensitivity to oestrogen (Brechbuhl et al. 2017). $CD146^{neg}$ CAFs decrease oestrogen sensitivity and thus induce resistance to tamoxifen, by diminishing the expression of ER in tumours. On the other hand, $CD146^{pos}$ population of CAFs maintain sensitivity to tamoxifen, due to unaffected levels of ER expression.

Non-malignant cells within the TME are genetically stable, unlike cancer cells, and are therefore stable therapeutic targets. The intrinsic roles of CAFs and their interaction with cancer and non-cancerous cells within the TME, makes them potential therapeutic targets.

Several studies have shown the potential of targeting CAFs directly and indirectly in cancer (Togo et al. 2013). Work by Loeffler *et al* (Loeffler et al. 2006) demonstrated that DNA vaccines generated for FAP (specifically overexpressed in fibroblasts within colon, breast, and lung carcinomas (Scanlan et al. 1994) can reduce tumour growth in combination with doxorubicin.

1.3.5 Role of TGFβ in tumour stroma and fibroblast activation.

CAFs are activated by factors secreted by cancer cells such as chemokines (e.g. CCL2) (Tsuyada et al. 2012), osteopontin (Mao et al. 2013), TGFβ and SDF (Kojima et al. 2010). Of these, TGFβ is best understood and further discussed in this project.

1.3.5.1 TGF signalling pathway

TGFβ1 is a ligand that binds to type II TGF-β receptor (TβRII) that consequently transactivates type I TGF-β receptor to initiate downstream signalling (Derynck and Feng 1997). The two main pathways downstream include canonical SMAD signalling and non-canonical signalling. SMADs are a family of transcription factors, of which SMAD2 and SMAD3 are activated by TGFβ via phosphorylation (Attisano and Wrana 2000). Activated SMAD 2 and 3 form complexes with SMAD4, mediating translocation of the active SMAD complexes to the nucleus to regulate transcriptional activity. Non-canonical activation pathways downstream TGFβ include Rho, Rac/Cdc42, Ras and PI3K (Derynck and Zhang 2003).

1.3.5.2 Effect of TGF on fibroblasts and tumour stroma

Enriched expression of TGFβ1 is associated with highly fibrotic tissue and ECM secretion (Brenmoehl et al. 2009). Work by Desmoulière *et al* demonstrated that treatment of

fibroblasts with TGFβ induced the expression of αSMA fibres, a marker of cellular differentiation into myofibroblasts (Desmoulière et al. 1993). Thus, in response to TGFβ, fibroblasts differentiate into myofibroblasts that are highly contractile and contribute to ECM and collagen deposition (hence fibrosis). Myofibroblasts are crucial during wound healing, however chronic activation of these fibroblasts results in excess collagen and ECM as in the case of CAFs in tumours.

Work by Kojima et al, studied the differentiation process of mammary fibroblasts into CAFs during tumour progression. CAFs promote invasive tumour growth through autocrine signalling loops such as SDF-1 and TGFβ (Kojima et al. 2010). Cancer cells within the TME secrete TGFβ, which stimulates additional TGFβ, as well as SDF-1, secreted by fibroblasts. These secretions are maintained, generating a positive feedback loop and lead to the activation of fibroblasts into pro-tumourigenic CAFs via auto-and co-stimulatory effects of these signalling loops.

In turn, activated fibroblasts (CAFs) promote tumour growth. For example, CAFs isolated from colon cancer secrete pro-invasive factors such as scatter factor/hepatocyte growth factor (HGF) and tenascin C, an ECM glycoprotein upregulated in response to TGFβ (De Wever et al. 2004).

Furthermore, a study by Orimo *et al* demonstrated that breast carcinoma-derived CAFs co-implanted with breast carcinoma cells significantly induce tumour growth than normal fibroblasts from the same patient, mediated by SDF-1 secretion (Orimo et al. 2005).

1.3.6 Role of PKN2 in fibroblast activation

Previous study in the lab, revealed that PKN2 deletion in MEFs resulted in their loss of ability to contract in collagen gels. Contractility is a phenotype of activated fibroblasts, hence indicating that PKN2 is important for this phenotype. Targeting PKN2 in this context

may have therapeutic potential of targeting fibroblasts and tumour stroma, to reduce their activation and desmoplastic reaction.

Furthermore, studies in a pulmonary smooth muscle cell line demonstrated disrupted TGF-mediated actin re-organisation and differentiation, following treatment with inhibitors that target downstream of RhoA, including PKN2 (Deaton et al. 2005). In this model, TGF-β1 induced activation of PKN, via phosphorylation, inducing expression of smooth muscle cell markers at transcript level. PKN2 depletion mediated by siRNA, also attenuated TGF-β1-mediated upregulation of smooth muscle cell markers. A similar phenotype was observed when MAPK activity was blocked by SB203580. Together with the positive correlation between MAP kinase activity and PKN2 kinase activity, it is postulated that p38 MAPK signalling regulating actin reorganisation via PKN2.

1.4 Project Aims

In vivo studies on mouse embryology in the lab demonstrated a physiological role of PKN2, in mouse development; PKN2 knockout in mice embryos showed developmental defects, growth retardation collapsed mesenchymal compartment and embryonic lethality at E9.5 (Quétier et al. 2016). *In vitro*, conditional PKN2 knockout in immortalised mouse embryonic fibroblasts (MEFs) also decreased cell growth and motility.

As PKN2 demonstrated a role for cell survival in a physiological model in MEFs, we wanted to investigate the relevance of PKN expression in breast cancer. Bioinformatic analysis of expression profiles from breast cancer datasets were used to study the expression patterns of PKN kinases between normal tissue and breast cancer tissue, as well as between different breast cancer types. We also wanted to investigate the role of PKN kinases in breast cancer cell survival, comparing luminal breast cancer cells with TNBC cells that are mesenchymal in phenotype.

The dependence on PKN2 in MEFs led us to expand the study to include fibroblasts and the tumour stroma, which are important non-cancerous compartments of tumours.

Work conducted in collaboration with John Marshall's group has demonstrated that PKN2 is required in MEFs to support pancreatic cancer cell (PCC) invasion. Knockout of PKN2 resulted in inhibition or reversal of the invasive phenotype and reversion to a polarised epithelial morphology. Interestingly, loss of PKN2 on day 8 after invasion converts invasive mesenchymal PCC to polarised epithelial PCC. This begged the question, whether the expression of PKN2 in fibroblasts had a significant effect on breast cancer survival and invasion, under 3D *in vitro* conditions.

Our recent paper demonstrated a role for PKN2 in the mesenchyme of embryos during development. Work in the lab also demonstrated that loss of PKN2, in a variety of mouse and human fibroblasts, reduced their contractility (a marker of activation) in collagen gels in response to TGFβ1. Furthermore, work by our collaborator (Claus Jorgensen, CRUK Manchester) identified PKN2 as a top hit from an RNAi screen to identify kinases important for TGFβ1-mediated activation of pancreatic fibroblasts. Here we sought to examine whether these roles for PKN2 are conserved in breast fibroblasts and primary breast CAFs. The clinical relevance of PKN2 in breast cancer stroma was investigated by analysing the expression of a panel of PKN2 surrogate markers (that are upregulated in activated MEFs upon TGFβ1 and/or BMP4 stimulation) in a stromal gene expression dataset (Finak et al. 2008) and whole tumour gene expression dataset from TCGA. Moreover, the effect of systemic deletion of PKN2 on tumour growth and stromal activity was studied using a mouse orthotopic model.

Summary:

The primary aims of this project are:

1. To investigate the relevance of PKN kinase expression on breast cancer survival and prognosis.
2. To study the role of PKN2 on TGFβ1-mediated fibroblast activation and investigate the clinical relevance of PKN2 surrogate markers in breast cancer stroma.
3. To examine the effect of fibroblasts and their expression of PKN2 on breast cancer cell viability, invasion and chemosensitivity.
4. To study the effect of global PKN2 deletion on tumour growth and stromal activation in a mouse orthotopic model.

2. Materials & Methods

2.1 Cell culture

Cells were cultured in sterile, uncoated T25, T75 or T175 flasks (Corning) in humidified conditions at 37°C, 10% CO_2. Most cells were cultured in Dulbecco's Modified Eagle's Medium (DMEM – Sigma, #D6429) and supplemented with Penicillin-Streptomycin (Sigma, P4333) and 10% fetal bovine serum (FBS). All cell lines were supplemented with FBS from one manufacturer (Sigma, #F9665), except for MEFs (Gibco, #10500-064) and CAFs (Lonza, #CC4101J, 2% v/v). The media conditions for the different cell lines are listed (Table 1).

MEFs were isolated from Rosa26$^{Cre/ERT2}$ PKN2$^{fl/fl}$ C57B/6J mouse embryo that were immortalised using the SV large T-antigen. Primary human breast CAFs were requested by the Breast Cancer Tissue Bank at BCI.

Cell in flasks are washed once in sterile phosphate buffered saline (PBS) and covered in 2ml of 1X trypsin-EDTA (Sigma, #59418C) and incubated at 37°C for 2-5 minutes. The flask is gently tapped to dislodge the detached cells and collected in fresh growth media. The number of cells is counted using a haemocytometer to seed for experiments and/or a proportion of the collected cell suspension is transferred to a new flask to continue the culture.

2.2 siRNA transfection

Cells were seeded at their appropriate seeding density and treated with siRNA (Dharmacon): siCtrl1: D-001210-01-20; siCtrl3: D-001210-03-20; siLuciferase: P-002099-01-50; sipkn2#3: D-004612-03-20; siPKN2#9: D-004612-09-20; siPKN2#10: D-004612-10-20; siPKN2#11: D-004612-11-20) the following day (target sequence in Table 2). The 20µM siRNA stock is diluted in 1X optiMEM (Gibco, #31985-62) and added to lipofectamine RNAiMax (Invitrogen, #13778-150) diluted in optiMEM. After incubation at room

temperature for 45 to 60 minutes, the diluted siRNA and transfection reagent is added to the cells in media, seeded at least the day before. The volumes of reagents for different vessel sizes per well are shown in Table 3.

Table 1. Cell media conditions for different cell lines

Cell line	Growth media	Additional Supplements
SUM159	F12 Ham (Sigma)	Insulin (Sigma, #I1882, 1µg/ml), hydrocortisone (1µg/ml)
MDA MB 231	DMEM (Sigma)	
MDA MB 468	DMEM - low glucose (Sigma, #D5921)	L-glutamine
MCF7	DMEM (Sigma)	
BT474	DMEM (Sigma)	
T47D	RPMI 1640 (Sigma)	Insulin (Sigma, #I1882)
4T1	DMEM (Sigma)	
E0771	RPMI (Sigma)	
MMTV	DMEM (Sigma)	
mBCC#4	DMEM (Sigma)	
MEFs	DMEM (Sigma)	
HMFU19	DMEM /F12H -1:1 (Sigma)	Amphotericin B (Sigma, #A2942, 2.5µg/ml)
CAFs	FGM™-2 Fibroblast Growth Medium (Lonza, #BE12-604F)	Insulin (Lonza, #CC-4021J, 5µg/ml), rhFGF-B (Lonza, #CC4065J, 1ng/ml), gentamicin and amphotericin (Lonza, #CC4126, 30µg/ml and 15ng/ml respectively)

Table 2. siRNA target sequence.

siRNA	Target sequence
siCtrl1	UAGCGACUAAACACAUCAA
siCtrl3	AUGUAUUGGCCUGUAUUAG
siLuciferase	CAUUCUAUCCUCUAGAGGAUG
siPKN2#9	GGAGCGCUCUGAUGGACAA
siPKN2#10	UAGACAGCCUGAUGUGUGA
siPKN2#11	GUACGCAUCCCUCAACUAG

Table 3. siRNA transfection.
Reagent volumes per well for different culture vessels.

Vessel	siRNA	RNAi Max	optiMEM	Media in wells
24-well plate	0.6µl	0.6µl	50µl	100µl
6-well plate	2.5µl	2.5µl	100µl	500µl

2.3 Inhibitors and cytotoxic assay

Cells are seeded onto 96-well plates at appropriate densities and incubated overnight. The next day, different concentrations of inhibitors were prepared by 1 in 3 serial dilution, of which 100µl is added per well after removing the culture media. Some wells are treated with fresh media or media containing dimethyl sulfoxide (DMSO – Sigma 276855), the vehicle of the drug, as control wells. Inhibitors used are bisindolylmaleimide I (Calbiochem, #203290), Go6976 (Calbiochem, #365250), PKC412 (Calbiochem, #539648) and Y27632 (Calbiochem, #688000). After three doubling times, cell viability was assayed using the MTT assay.

2.4 MTT assay

Cells were seeded on 96 well plates for treatment with inhibitors the next day. At endpoint, the appropriate volume of 5X Thiazolyl Blue Tetrazolium Bromide (MTT-Sigma M2128) solution is added to the media in wells to make a final concentration of 1x (1mg/ml). Plates are incubated at 37°C from 30 to 90 minutes until purple crystals are visible under the microscope. Thereafter, MTT-containing media is removed, whilst purple formazan crystals remain attached to the plate. These crystals are dissolved in dimethyl sulfoxide (DMSO-fisher D/4120PB08) for absorbance to be read at 550nm using a spectrophotometer.

2.5 Western blotting

2.5.1 Preparation of whole cell lysates

Cells in culture are washed once in PBS, and lysed in sample buffer (410mg sucrose in 3% SDS and 65mM Tris-HCl pH0.8) and sonicated to reduce viscosity. To quantify protein concentrations, standard solutions of BSA (Sigma Aldrich, UK) were prepared at 0, 0.1, 0.2, 0.4, 0.8, 1, 1.2, 1.6, 2mg/ml in sample buffer. The Bio-Rad DC protein assay kit (Bio-Rad

laboratories, Hercules, CA, USA) was used according to the manufacturer's guidelines to calculate the protein concentration for each sample. Lysates were diluted in sample buffer to adjust the protein concentration between samples. A volume of 4X LDS sample buffer (Novex, #NP008) with 10% dithiothreitol (DTT) is added to lysates to make the final concentration 1X. This was then heated for 5 minutes at 95˚C.

2.5.2 Sodium dodecyl sulphate polyacrylamide gel electrophoresis (SDS-PAGE) and transfer

Bis-Tris (4-12%) pre-cast gels (Nusep, #NG11-420) or 8% polyacrylamide gels were used to run the samples. Protein lysate samples were loaded per well along with PageRuler Pre-stained protein ladder (Thermo scientific, #26616) for separation by electrophoresis at 120V using 1X Tris-Glycine SDS PAGE running buffer (Severn Biotech, #20-6400-10). Proteins from the gel are transferred onto a nitrocellulose membrane (GE Healthcare, #10600008) by the wet transfer method. A sandwich, composed of 2 sponges, 2 Whatmann papers, gel, nitrocellulose membrane, 2 Whatmann papers and 2 sponges are placed in the transfer unit and placed in the tank. The transfer apparatus is filled with transfer buffer (1X Tris-Glycine-Severn Biotech, #20-6300-10), whilst the tank is filled with water. The transfer process takes place at 4°C at 35V for 2 hours or at 12V overnight.

2.5.3 Immunoblotting

After transfer, membranes are blocked in 5% w/v non-fat milk (Sigma, #70166) in 1% Tween-20 (Bio Chemica, #A1389,0500) and tris-buffered saline (TBS-Severn Biotech, #20-7301-10) for at least 30 minutes at room temperature and thereafter washed in TBST every 5 minutes thrice. Membranes are incubated in primary antibody, diluted in 5% w/v bovine serum albumin (BSA-Sigma, #A8022) and TBS-T overnight t 4°C under constant rolling motion. Next day, the membranes undergo three 10-minute TBST-T washes before incubating in HRP-conjugated secondary antibody (in 5% w/v non-fat milk) for 2 hours at

room temperature. Before chemi-luminescent detection, membranes undergo three 10-minute TBS-T washes. ECL Western blotting detection reagents (GE Healthcare, #RPN2106) was added to membranes and incubated for 1 minute before exposing to an autoradiographic film and developed in a film processor or exposed and developed in an automated chemiluminescent imager (Amersham Imager 600). For low-expressing proteins, Luminata Forte (Millipore, #WBLUF0100) or Crescendo (Millipore, #WBLUR0100) were used.

2.5.3.1 Primary Antibodies

Table 4. List of primary antibodies for western blotting

Antibody	Supplier	Catalogue nr	Species	Detects	Dilution
GAPDH	Santa Cruz	sc-25778	Rabbit	Human/Mouse/Rat	1:2000
HSC-70	Santa Cruz	sc-7298	Mouse	Human/Mouse/Rat	1:2000
Phospho-PRK1 (Thr774)/PRK2 (Thr816)	CST	2611	Rabbit	Human/Mouse/Rat	1:1000
Phospho-Smad2 (Ser465/467)/Smad 3 (Ser423/425) (D27F4)	CST	8828	Rabbit	Human/Mouse/Rat /Monkey	1:1000
PKN2	R&D Systems	MAB5686	Mouse	Human/Mouse/Rat	1:1000
SMAD2/3	BDT	610843	Mouse	Human/Mouse/Rat /Dog	1:1000

2.5.3.2 Secondary Antibodies

Table 5. List of secondary antibodies for western blotting.

Antibody	Supplier	Catalogue/reference number	Dilution
ECL Anti-Rabbit IgG HRP-linked whole antibody	GE Healthcare	NA934V	1:2000
ECL Anti-Mouse IgG HRP-linked whole antibody	GE Healthcare	NXA931	1:2000

2.6 Inducing PKN2 deletion in MEFs

MEFs to be treated are seeded in T75 flasks that should be 70-80% confluent on the day of treatment. 4-hydroxy tamoxifen (Sigma) is prepared under the hood in darkness, to avoid isomerisation in response to light. 4-hydroxy tamoxifen at 10mM stock is diluted in PBS to give a 20μM solution. An appropriate volume of this solution is added to the media in the flask, so that the final concentration of 4-hydroxy tamoxifen is 400nm. The flask is incubated at 37˚C for 60 to 90 minutes, after which the media in the flask is replaced with fresh media. Cells treated with 4-hydroxy tamoxifen can be trypsinised to seed for experiments or passaging 24 hours after treatment. PKN2 deletion is apparent by western blotting 72 hours after treatment.

2.7 TGFβ1 stimulation in fibroblasts

Recombinant human TGFβ1 (Peprotech, #100-21-10) is reconstituted in 10mM citric acid, pH3 to give a 10ng/ml stock solution. Cells to be treated with TGFβ1 are seeded directly on plastic tissue culture vessels (6-, 12-, 24-well plates) or on coverslips in the wells. For acute stimulation, cells are serum-starved overnight the following day. For both acute and long-term treatment, the final concentration was 5ng/ml. On the day of treatment a concentrated stock solution is prepared, of which a small volume is added to wells with media from the day before.

2.8 Mini-organotypic assay

2.8.1 Experimental set-up

This is a small-scale 3D assay that was used to study the interaction between fibroblasts and cancer cells (schematic of experimental set-up shown in Fig. 1). Transwell inserts (Costar, #3413) placed onto 24-well plates and the porous membrane (pore size 0.4um) is

coated with 300ul collagen (diluted 1:100 in PBS) and incubated at 37˚C for 45 minutes. The collagen-matrigel gel is prepared (reagents and amounts below) on ice. After removing excess collagen from transwells, 20ul of the gel mix was added onto the membranes and allowed to set at 37˚C for 1 hour. Cell suspensions are prepared in 200ul of culture media containing a total of 100,000 cells and added on top of the set gel. The slits on the transwell inserts are used to add 600ul of culture media to the bottom to the wells. The next day, the media at the bottom of the wells is replaced with 350ul of fresh culture media and serum-free media is added on top of the gels. The media is replaced every 2-3 days.

2.8.1.1 Reagents

Reagents required:

- 525µl collagen type I (Corning, #354236)
- 175µl Matrigel Basement Membrane Matrix (Corning, #356234)
- 100µl 10x DMEM (Sigma, #D2429)
- 100µl cell culture media (DMEM)
- 100µl filtered FBS (Gibco)
- Add 25µl per ml 1M NaOH to get bright pink/fuscia color

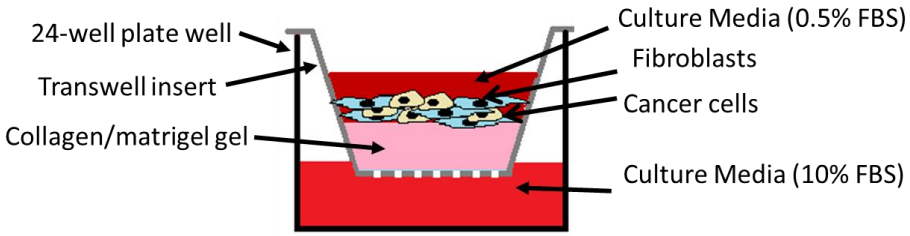

Figure 1. Mini-organotypic assay set-up

2.8.2 Harvesting gels

At endpoint gels are fixed in formalin by adding 200µl above and 600µl below the transwell inserts and left overnight. Thereafter the formalin is replaced with 70% v/v ethanol for at least 10 minutes. The gels are removed from the transwell inserts using a sterile scalpel and placed between two sponges within a cassette and stored in 70% v/v ethanol. This is handed in to be paraffinized, embedded, sectioned and H&E stained by the pathology services.

2.8.3 H&E staining quantification

H&E image of gels are converted to a binary image, where positively-stained area become black and the remainder white. The area occupied by black pixels can then be calculated. This method was used to measure the total cell density, which includes all cells within the gels. To count the number of invasive cells, the collective cell area is deleted before converting to a binary image. Rather than measuring total area, the individual cells are recognised as a particle and counted. The particle size was limited to an arbitrary range from 10 to infinity, to avoid small artefacts from the counts. For both total and invasive cell measures, gels 1cm in length were used.

2.9 Luciferase assay

2.9.1 Introducing luciferase reporter into cells.

HEK293T cells were used to generate plasmid-containing viral particles. 650,000 HEK293 cells were seeded per well of a 6-well plate. The next day, the cells are transfected with 2.5µg of plasmid in 250µl optiMEM, along with 0.6µg of pMD2.G (VSV-G envelope-expressing plasmid-Addgene) and 1.15µg pCMV (2nd generation lentiviral packaging plasmid - Addgene) and 15µl Fugene (Promega, #E2311). After 6-24 hours, fresh media

was added to well and left for 48 hours. Viral supernatants were collected, spun for 10 minutes at 4000rpm and passed through 0.45µm filter.

Cells seeded in 6-well plates the day before are transduced with the viral supernatant, which is replaced with fresh media after 24 hours. After 72 hours, plasmid-expressing cells are selected with antibiotics for the following 10 days before using in assays. Cancer cells transfected with firefly luciferase plasmids were selected in puromycin (Invivogen, #ant-pr-1) at 2µg/ml, whereas fibroblasts transfected with renilla luciferase plasmids were selected in blasticidin (Gibco, #A11139-03) at 20µg/ml.

2.9.2 Experimental set-up

2.9.2.1 Growth (2D & 3D)

Cells are seeded either directly on plastic 96-well clear bottom white plates (Corning, #3610) for 2D culture assays or for 3D culture on 40µl of collagen, matrigel or a mixture of the two gels (as combined in mini-organotypic assays) that was incubated at 37˚C for 45 to 60 minutes. Cancer cells and fibroblasts were seeded at various seeding densities (depending on cell lines) at 1:2 ratio and incubated for 72 hours, unless stated otherwise.

2.9.2.2 Drug assay

Cells were seeded as for 2D cultures described in 2.8.2.i, but at lower seeding densities, and incubated for 72hours. On the third day, the drugs (paclitaxel – Millipore, #580555; doxorubicin – Tocris, #2252) were prepared at 3X the desired final concentration by serial dilution of which 50µl is added to the cells in 100µl of media to make 1X solution. The experiment is terminated 72 hours after drug treatment.

2.9.3 Assaying for luciferase reporter activity

Cells seeded on white 96-well plate are washed in PBS and lysed with 20µl per well of Cell Culture Lysis Reagent or passive lysis buffer for single- and dual-luciferase assay respectively. For single luciferase assay, the lysates undergo once freeze-thaw cycle before adding 100µl per well of the luciferase assay substrate (Promega E1510 for single luciferase and E1910 for dual luciferase) to detect luminescence at 590nm from the firefly luciferase reporter activity. For dual-luciferase this is followed by adding 100µl per well of 1X Stop & Glo reagent, which quenches the firefly luminescence, to allow detection luminescence at 460nm from renilla luciferase activity. Luminescence was read using BMG plate reader.

2.10 *in vivo* experiments

2.10.1 Subcutaneous injections

Experiments were performed under the Personal Licence number ID I4F848D34 and the Project License PPL 70/7449 19b/2. Mice were anaesthetised with isofluorane.

Cancer cells (MMTV or 4T1) and untreated or 4-hydroxy tamoxifen-treated MEFs (wt or PKN2 ko) to be used for injection were harvested from T175 flasks by trypsinisation. Cells were washed in PBS twice and finally re-suspended 333,000 cancer cells in 100µl PBS alone or with 666,000 MEFs in 100µl PBS. 200µl of cell suspension was injected subcutaneously per flank in both flanks of mice. Recovery of mice was monitored. Tumour growth was monitored twice weekly by measuring tumour size using digital callipers. Mice weights were also monitored twice per week. Mice were maintained until they presented with health issues (such as skin ulcerations) or tumour sizes reached the 1440mm^3 limit set by Home Office and PPL limits. Tumours were excised and fixed in formalin for 24 hours

before replacing with 70% ethanol. Fixed tumours were paraffin embedded and sectioned by the Pathology department for further immunochemical analysis.

2.10.2 Orthotopic injections

Experiments were performed at the Francis Crick institute in collaboration with Peter Parker. Orthotopic injections were carried out by Marianthi Tatari (Barts Cancer Institute).

2.10.2.1 Tamoxifen formulation and treatment

Tamoxifen (Sigma, #H7904) is dissolved in ethanol to make 10x solution (165mg in 550µl) at 55°C in a thermomixer (800rpm) for 30 minutes (with occasional vortexing). This stock is diluted in sunflower oil to make a 1x solution and incubated at 37°C for at least 1-2h in a shaker. Mice were administered an appropriate volume of the prepared tamoxifen, at the dose of 3mg/20g mouse weight (via oral gavage), thrice within two weeks.

2.10.2.2 Surgical procedure

The procedure was carried out in a laminar airflow cabinet under sterile conditions. Mice were injected intraperitoneally with the analgesic Buprex™ prior to anaesthetising them. Mice were put under anaesthesia chamber, containing Isoflurane and oxygen, for up to 5 minutes. With the mouse on its back, the mid-lower part of the abdomen is shaved on both sides, cleaned with PBS and antiseptic spray. A 2cm-incision is made in the middle of the lower abdomen. One mammary gland from each side is injected with 300,000 PyMT BO.1 cells in 30µl of Matrigel. The outer skin was closed with surgical staples, after which mice were placed in recovery cages with a heater under red light. Mice were observed until they returned to normal mobility to be transferred back to normal cages. The weights and tumour volumes were measured and monitored every 2-3 days. The experiment was terminated two weeks post injection when the mice were culled and the tumours were harvested and processed.

2.10.2.3 PCR genotyping

Primer sequences:

Fw: 5'-GGAACTTCGTCGAGATAACTTCG-3'

Rv1: 3' – CCGCCTACTGCGACTATAGAGATATC-5'

Rv2: 3' – CCCTCAGATGAGAAACATAATGAACT-5'

2.11 Immunostaining

2.11.1 Immunofluorescence: cell on coverslips

Cell are seeded on coverslips in 6- or 24-well plates to test αSMA expression upon TGFβ1 treatment. At endpoint, culture media was removed and replaced with 4% PFA v/v (16% PFA w/v Alfa Aesar, #3368) diluted in PBS for 20 minutes to fix cells. After three PBS washes, cells are permeabilised with a solution of 1% Triton-X and NH_4Cl (50mM) for 20 minutes and thereafter washed in PBS three times. Cells were blocked in a solution of 10% FBS with 0.1% Tween for 1 hour. Next, cells were incubated in primary antibody (mouse SMA, Dako, #M0851, 1:250 dilution), diluted in the blocking solution, for 2 hours at room temperature. After three washes in PBS, cells were incubated with secondary antibody (Goat Anti-Mouse Alexa FLuor-488, Invitrogen, #A11001, 1:200 dilution) and DAPI (Sigma, #D9542 at 1µg/ml final concentration), diluted in the blocking solution, for 1 hour. Before mounting the coverslips onto glass slides with mowiol, coverslips were washed three times in PBS and once in distilled water. Coverslips were left to dry at room temperature overnight before imaging or stored at -20˚C.

2.11.2 Immunofluorescence: paraffin sections

Paraffin sections on glass slides are de-waxed in xylene for 5 minutes (x2) and hydrated through a series of graded ethanol solutions (100%, 80%, 70%, 50% v/v in water), followed

by PBS wash. For antigen retrieval, slides are placed in boiling citrate buffer (0.01M solution of tri-sodium citrate with pH adjusted to 6) for 8 minutes in the microwave. After cooling down and PBS wash, slides are placed in 0.2% triton/PBS for 5 minutes for permeabilisation and blocked in PBSABC (2% BSA and 10% FBS solution in PBS) for 1 hour. Primary antibody is diluted in blocking solution (PBSABC) and applied on required area and incubated overnight at 4°C. The next day, slides are washed in PBSABC for 2 minutes thrice before incubating in secondary antibody (diluted in PBSABC) for 1 hour at room temperature. Thereafter, after three 5-minute PBSABC washed and incubated in DAPI (1:5000 dilution) for 15 minutes at room temperature. Finally, after three PBS washes, slides are mounted onto coverslips using mowiol.

2.11.3 Immunohistochemistry

Paraffin sections on glass slides are de-waxed in xylene for 5 minutes, twice and hydrated through a series of graded ethanol solutions (100% twice, 80%, 70%, 50% v/v in water) for 2 minutes each, followed by a two-minute wash in distilled water. Slides are washed in 30% hydrogen peroxide solution in methanol for 15 minutes between the two 100% ethanol washes. Slides are then placed in pre-heated citrate buffer (0.01M, pH6) for 10 minutes. After cooling down the slides in water, followed by two PBS washes, slides are incubated in avidin and biotin (Vector laboratories SP-2001) for 10 minutes each and washed in PBS twice. Thereafter, the slides are placed in blocking buffer (3 drops of goat serum in 10ml PBS -Normal Goat Serum Blocking Solution, Vector Laboratories, #S-1000) for 10 minutes and washed in PBS twice. Primary antibody was prepared in PBS and added to slides for overnight incubation at 4˚C in humidified chambers.

The following day, ABC Reagent (Vector ELITE ABC Kit, Vector laboratories, #PK-6200) was prepared and incubated at 4˚C for 30 minutes – 2 drops of Reagent A and 2 drops of Reagent B in 5ml PBS. Meanwhile, primary antibody is washed off with PBS twice and

incubated with biotinylated anti-mouse or anti-rabbit secondary antibody (provided in the Vector ELITE ABC Kit) for 40 minutes at room temperature. Slides were washed in PBS twice, before incubating with the ABC reagent for 30 minutes. After two PBS washes, slides were incubated with DAB (Dako, #K3468) for 2-5 minutes until dark brown staining is visible to the naked eye. After washing off the DAB with PBS and then water, sections were counterstained with Mayer's haematoxylin (Dako, #S3309) for 2 minutes. Finally, slides were washed in water to wash off the haematoxylin and dehydrated through the series of graded ethanol in reverse from lowest to highest and cleared in xylene. Dehydrated sections were mounted onto glass coverslips with DPX (VWR, #360294H) and left to dry at room temperature overnight.

For anti-mouse primary antibody staining on mouse tissue, an additional blocking step is required between blocking with goat serum and incubating with the primary antibody. Two drops of the Mouse IgG Blocking Reagent (MOM kit, Vector Laboratories, BMK-2202) in 2.5ml PBS is added to the sections for 10 minutes and washed off with two PBS washes. Thereafter, a stock solution of protein concentrate (provided in the kit) is diluted in 7.5ml PBS (solution referred to as diluent and added to sections for 5 minutes. This is tapped off before adding the primary antibody for overnight incubation. The following day, after washing off the primary antibody, the sections are incubated in Biotinylated Anti-Mouse IgG Reagent (2 drops in 5ml of diluent) for 40 minutes. Slides are washed with PBS twice, before incubating in ABC reagent.

2.11.4 Primary antibodies for IHC and IF

Table 6. List of primary antibodies for IHC and IF

Antibody	Supplier	Catalogue nr	Reactivity	IF Conc	IHC Conc
Mouse SMA Clone 1A4	Dako	M0851	Human	1:250	1:500
Endomucin	Santa Cruz	SC-65495	Mouse, rat	-	1:200
Rabbit Ki67 Clone SP6	Abcam	AB16667	Human, Mouse	-	1:100

2.11.5 Quantifying Sirius red and α-SMA staining

Stained sections were scanned using the Pannormamic 250 High Throughput Scanner. The scanned sections can be viewed on the Pannoramic Viewer software. Per tumour, multiple 835µm by 450µm approximate sections that collectively covered approximately 80-90% of the whole tumour were selected. The DensitoQuant program under the image analysis module of Pannoramic Viewer was used to measure the pixel area and intensity of the stainings. After selecting the areas of tumours to be analysed, the threshold is set on the DensitoQuant program, to stratify weak-, moderate- and strong-positive staining. For analysing α-SMA staining, the blue tolerance level was adjusted to represent the area occupied by nuclei and cytoplasm. Once the thresholds are set, the parameters are measured for all the sections within a tumour, tumour after tumour.

2.12 Statistical analysis

Statistical analysis was determined using an unpaired t-test or one-way analysis of variance (ANOVA), followed by a Bonferroni post-hoc test where appropriate. All statistical analyses were performed using GraphPad Prism 4.0 software (San Diego, CA, USA). Significance was assessed in all experiments as a probability value of $P<0.05$ (*), $P<0.01$ (**) and $P<0.001$ (***).

3. Results

3.1 Role of PKN kinases in breast cancer

Breast cancer is the most common cause of cancer-related deaths, after lung cancer, in women. Therefore, novel therapeutic agents are required to improve patient survival. As discussed in 1.2.3.3, PKN kinases have been demonstrated to be involved in breast cancer proliferation, invasion and metastasis. Therefore, the potential of these kinases as novel therapeutic targets in breast cancer was investigated. Firstly, the expression of the PKN kinase isoforms (PKN1, 2 and 3) and their prognostic relevance in breast cancer patients was analysed.

3.1.1 Clinical implications of PKN kinase expression on breast cancer survival

3.1.1.1 PKN kinase expression profile in breast cancer

To understand the clinical implications of PKN kinase expression in breast cancer patients, the expression levels of PKN kinases were first investigated. Analysis of PKN kinase expression levels across all available breast cancer datasets showed no significant differences between the three PKN kinase isoforms in normal individuals and patients with different subtypes of breast cancer (Fig. 2). This comparison includes between patients with luminal A, luminal B, Her 2, basal and TNBC. The data was also divided to compare patients with TNBC and non-TNBC. Overall, there were no differences in PKN kinase expression across different breast cancer types nor in comparison to normal samples.

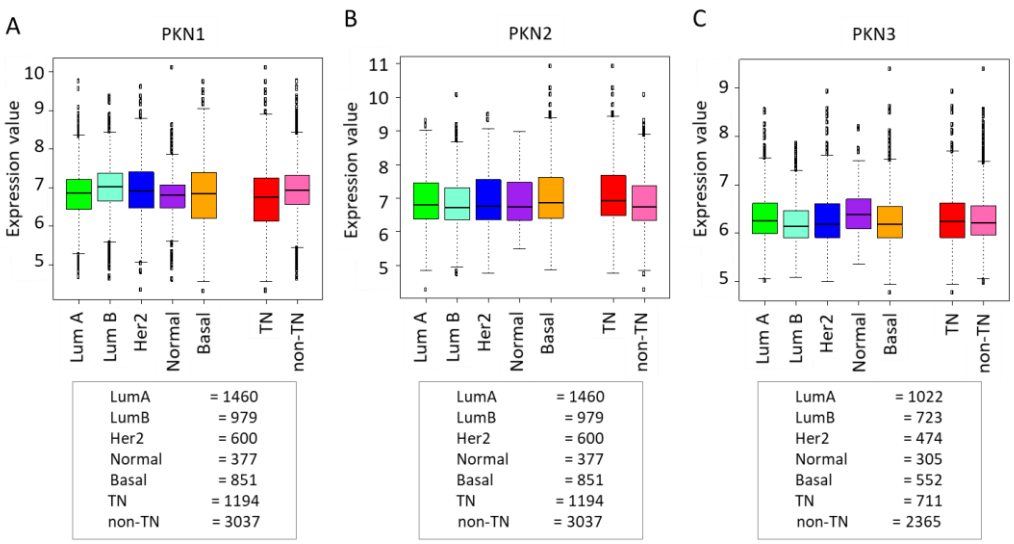

Figure 2. PKN kinase expression profile across different breast cancer subtypes

These plots show the expression values (log2 expression) of A) PKN1, B) PKN2 and C) PKN3 in different molecular subtypes of breast cancer and normal samples. The number of samples in each subtype is shown in the box below the plots. Each sample was assigned to a PAM50 molecular subtype based on the expression of the intrinsic gene list (Parker et al. 2009) - LumA, LumB, Basal-like, HER2-enriched, normal-like. The TN and non-TN definitions are also based on molecular classifications. The ER, PR and HER2 receptor status of each sample were defined by implementing functions within the MCLUST R library. The MCLUST algorithm was set to calculate the Bayesian Information Criterion (BIC) for a 2-component Gaussian distribution model. TN samples were isolated and the levels of gene expression compared to samples allocated to the non-TN group.

3.1.1.2 Analysing the effect of PKN kinase expression on breast cancer survival

Despite the lack of association between PKN kinase expression levels across different subtypes of breast cancer, the correlation between PKN kinase expression and survival was investigated using an online Kaplan-Meyer analysis tool (Győrffy et al. 2010). The correlation between PKN kinase expression and relapse-free survival was analysed, as this had the best number of patients for breast cancer. This analysis was automated for selecting the best performing threshold for defining low and high PKN kinase expression and involved only the best probe sets selected by JetSet algorithms. As multiple probes can detect a gene, Li *et al* developed this JetSet scoring system to assign one probe for a given

gene that scores best in three criteria: high specificity, ability to detect splice variants and unaffected by transcript degradation (Li et al. 2011).

The PAM50 single sample predictor (Parker et al. 2009) as applied to the breast cancer data to assign each sample to one of the five molecular subtypes (luminal A, luminal B, Her2+, normal breast-like or basal). Similarly, triple negative samples were also determined, as described by Lehmann *et al,* on the empirical expression distributions of ER, PR and Her2 (Lehmann, Bauer, Chen, Sanders, Chakravarthy, and JA 2011).

The expression levels of PKN kinase expression was plotted for each group (Fraley et al. 2012). Systematic comparisons were made between different combinations of PKN kinase isoforms and breast cancer classifications. The most intriguing comparisons are those involving comparisons between TNBC, non-TNBC, basal and mesenchymal-like breast cancer, due to the effect of PKN2 knockout in our inducible MEFs and the destructive effect on the mesodermal compartment of mice embryo upon systemic PKN2 deletion (Quétier et al. 2016).

Amongst all breast cancer datasets, high PKN1 expression has a significant ($P<0.001$) but modestly better RFS than patients with low PKN1 levels (Fig. 3A). This survival advantage is more apparent in patients with basal and ER-negative breast cancer (Fig. 3B, C), with no significant differences in ER-positive patients (Fig. 3D). Similar patterns were observed for the PKN3 isoform. Elevated PKN3 expression is associated with better RFS across all breast cancer data sets (Fig.5A). In basal, ER-negative and ER-positive breast cancer low PKN3 expression has a moderate but non-significant positive effect on RFS (Fig. 5B, C, D).

In contrast, PKN2 expression had no impact on RFS across all breast cancer datasets (Fig. 4A) and in basal breast cancer (Fig. 4B). However, this global analysis masks significant differences in behaviour between disease subtypes. There is significantly improved RFS in basal ($P=0.0067$) and ER-negative ($P=0.0028$) breast cancer patients with low PKN2

expression (Fig. 4C), whereas the converse is true for ER-positive patients (Fig.4D). As dependence on PKN2 in TNBC for cell survival has recently been demonstrated in several studies, the RFS for patients with low and high PKN2 expression was further investigated. Interestingly, analysis of overall TNBC data showed no difference in RFS between low and high PKN2-expressing patients (Fig.4E). We next analysed distinct subsets of TNBC using the Pietenpol classifications (Chen et al. 2012).

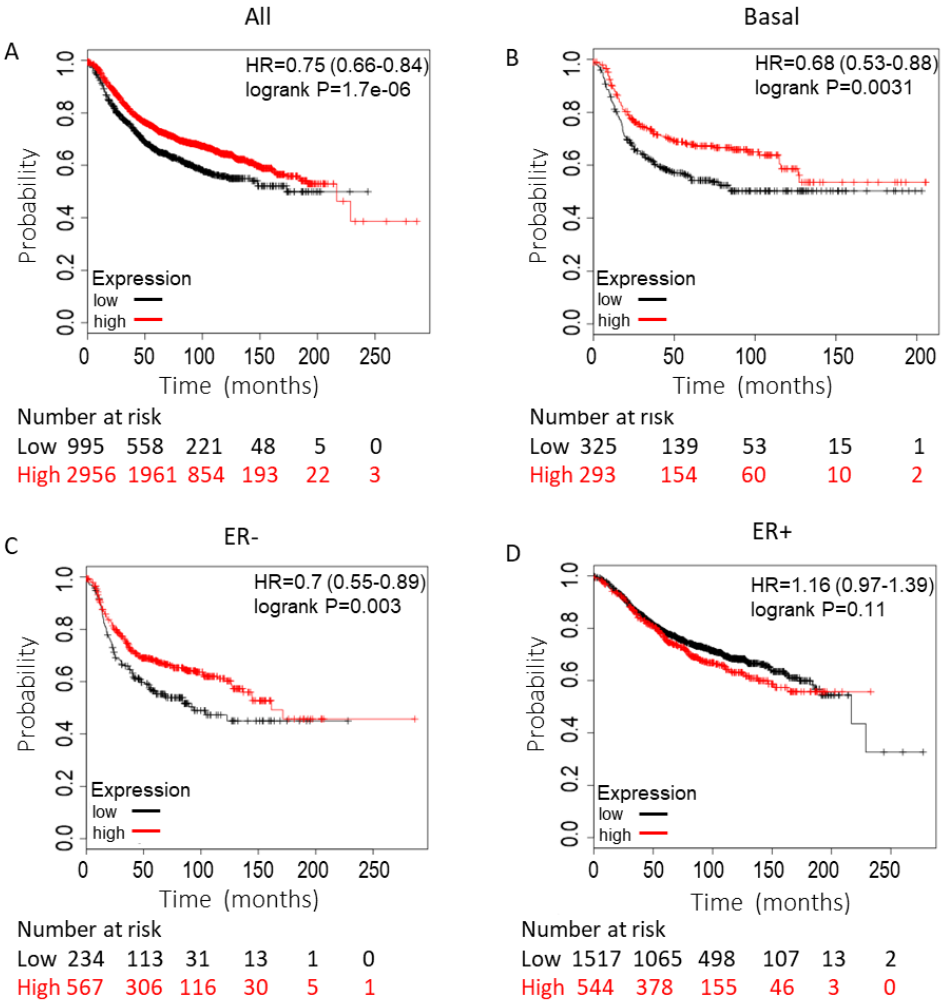

Figure 3. PKN1 expression analysis on breast cancer survival

Figure showing probability of relapse free survival (RFS) in patients with low and high PKN1 expression, generated using an online tool *(Györffy et al. 2010)*. PKN high and low expression threshold was selected at best cut-off for best performing threshold. PKN1 (affymetrix ID: 202161_at) was analysed for its prognostic relevance in **A.** all (n=3951), **B.** intrinsic basal (n=618), **C.** ER-negative (n=801) and **D.** ER-positive (n=2061) breast cancer.

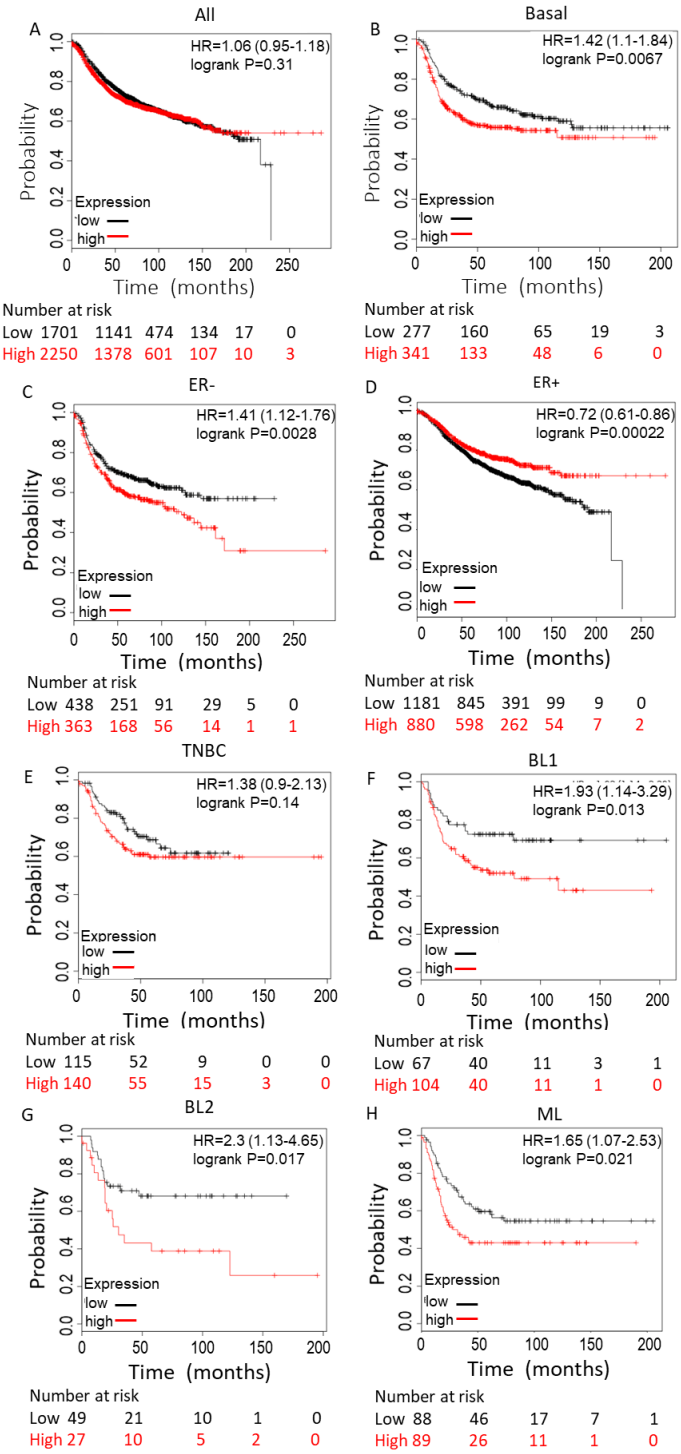

Figure 4. PKN2 expression analysis of breast cancer survival

Figure showing probability of relapse free survival (RFS) in patients with low and high PKN2 expression, generated using an online tool (Győrffy et al. 2010). High and low expression threshold was selected at best cut-off for best performing threshold. Out of three PKN2 probes, the one classed as the best probe by Jetset algorithm was chosen (affymetrix ID: 212628_at). **A.** All types of breast cancers, **B.** Intrinsic basal subtype **C.** ER-negative, **D.** ER-positive, **E.** TNBC – ER-negative, PR-negative and HER2-negative, and the Pietenpol subtypes: **F.** Basal-like 1 (BL1), **G.** Basal-like 2 (BL2) and **H.** Mesenchymal-like (ML). Number of patients at risk shown below the plots.

Those patients with TNBC classified as basal-like (BL1, BL2) or mesenchymal-like (ML), and with low PKN2 expression, have significantly improved RFS survival (Fig.4F, G, H). However, the low number of patients involved in this analysis must be considered (detailed in figure 4). Additionally, as mentioned above, intrinsic basal breast cancer classification shows the same pattern of behaviour (Fig. 4C). Together, these data suggest that high PKN2 expression is associated with poor survival in a subset of basal-like and mesenchymal-like breast cancer patients, in contrast to the PKN1 and PKN3 isoforms. This is particularly interesting as we have demonstrated that systemic deletion of PKN2 in mice embryo resulted in abnormal development of the mesodermal compartment (Quétier et al. 2016). Furthermore, MEFs from these embryos show dependence on PKN2 for proliferation *in vitro*.

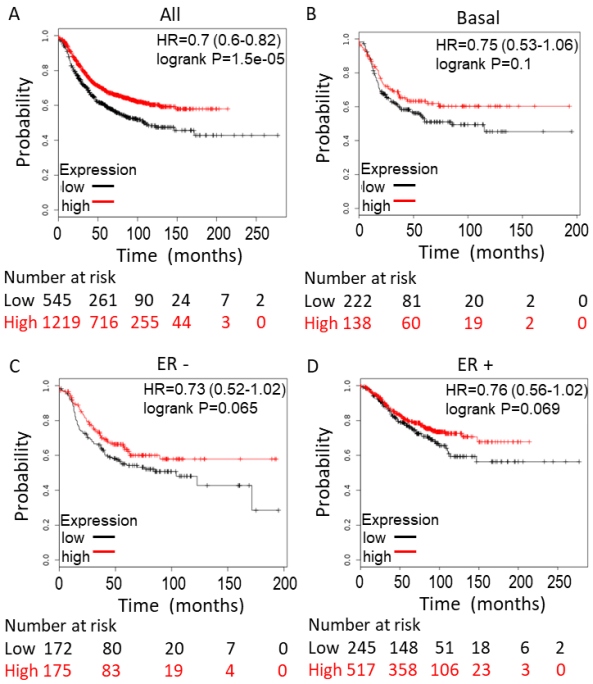

Figure 5. PKN3 breast cancer survival analysis.

Figure showing probability of relapse free survival (RFS) in patients with low and high PKN3 expression considering **A.** all breast cancer types, **B**. basal, **C.** ER-negative and **D.** ER-positive breast cancers. High and low expression threshold was selected at best cut-off for best performing threshold. Amongst three probes for PKN3, the one classed as the best probe set by Jetset algorithms was chosen (affymetrix ID: 226299_at). Plot generated using an online tool (Györffy et al. 2010). Number of patients at risk for each time point is indicated in numbers under the graphs.

In the following section, the effect of genetic and pharmacological inhibition of PKN kinases on viability of breast cancer cell lines *in vitro* will be discussed.

3.1.2 Effect of PKN kinases on breast cancer cell viability

The involvement of PKN kinases in cell cycle regulation has been demonstrated in physiological models, such as in *Xenopus* egg extracts (Misaki et al. 2001) and HeLa cells (Schmidt et al. 2007). Furthermore, our lab has demonstrated a role for PKN2 in the regulation of cell proliferation during development (Quétier et al. 2016). Induced conditional deletion of PKN2 at mid-gestation decreased proliferation of mesodermal cells *in vivo* and this growth defect was also observed in MEFs cell lines derived from this mouse model. Growth arrest resulted in an increased proportion of cells at G1/G0 phase and loss of cells in S phase, in PKN2-deleted MEFs. This observation was further supported by the finding of decreased phosphorylation of proteins involved in cell cycle regulation in PKN2-deleted MEFs from phospho-proteomic analysis (Quétier et al. 2016). These findings have subsequently been corroborated in another PKN2 mouse knockout mouse model (Danno et al. 2017).

Moreover, PKN kinases have also been implicated in cancer cell proliferation. Metzger *et al* demonstrated dependence of androgen-driven prostate cancer cells on PKN1 for proliferation (Metzger et al. 2008), whilst androgen-independent prostate cancer cell proliferation was unaffected by PKN1 expression (Jilg et al. 2014). Reduced PKN3 expression and activity downstream of PI3K resulted in reduced proliferation of PI3K-driven prostate cancer cells (Leenders et al. 2004).

Furthermore, the improved RFS in patients with basal breast cancer and basal/mesenchymal-like TNBC with low PKN2 expression was kept in mind and therefore, three TNBC and three non-TNBC cell lines were used for these studies. TNBC is the most

aggressive subtype of breast cancer and has poor prognosis due to unavailability of targeted therapy. PKN1 is overexpressed in TNBC (Turner et al. 2010). PKN2 was identified as a candidate gene for cell viability, selectively in TNBC cell lines, amongst a screen of 30 cell lines of various subtypes of breast cancer (Brough et al. 2011). These studies suggest that PKN kinases may play a role in TNBC cell proliferation.

3.1.2.1 Assessing the effect of targeting PKN kinases in breast cancer cell lines using siRNA

The effect of siRNA-mediated depletion of the three individual PKN kinase isoforms was tested on three TNBC cell lines (MDAMB231, SUM159 and MDAMB468) and three luminal breast cancer cell lines (MCF7, BT4T4 and T47D). Cells were transfected with a control siRNA (siCtrl or siLuciferase) or Dharmacon siRNA smart-pools, targeting the three PKN kinase isoforms individually. Cell viability was assayed using the MTT assay after three doubling times in 2D culture (Fig.6). The doubling times for each cell line was determined by recording cell counts over several days to calculate the approximate number of days required for the cell numbers to double.

SUM159 and MDAMB231 showed significantly decreased viability upon PKN2 or PKN3 depletion (Fig.6A, B), whilst MDAMB231 also showed reduced viability upon PKN1 loss. MDAMB468, MCF7, BT474 and T47D cell survival was unaffected by any PKN kinase isoform knockdown (Fig. 6C, D, E, F). Intriguingly, the two TNBC lines affected most by PKN deletion - MDAMB231 and SUM159 - are mesenchymal-like cell lines. This indicates a potential dependency on PKN kinases for cell viability in TNBC compared to luminal breast cancer cells, with most significant effect on viability in those with mesenchymal morphologies. Interestingly, we recently reported mesenchymal cell specific growth dependency on PKN2 during development (Quétier et al. 2016), perhaps suggesting a conserved function in mesenchymal phenotype cells.

3.1.2.2 siRNA deconvolution to validate the effect of PKN2 depletion in MDAMB231 and SUM159 on cell survival.

A role for PKN3 in the proliferation of TNBC has already been demonstrated *in-vitro* (3D culture) and *in vivo* (orthotopic tumours) (Unsal-Kacmaz *et al*. 2012). Therefore, we decided to focus on the novel role of PKN2 in breast cancer**.**

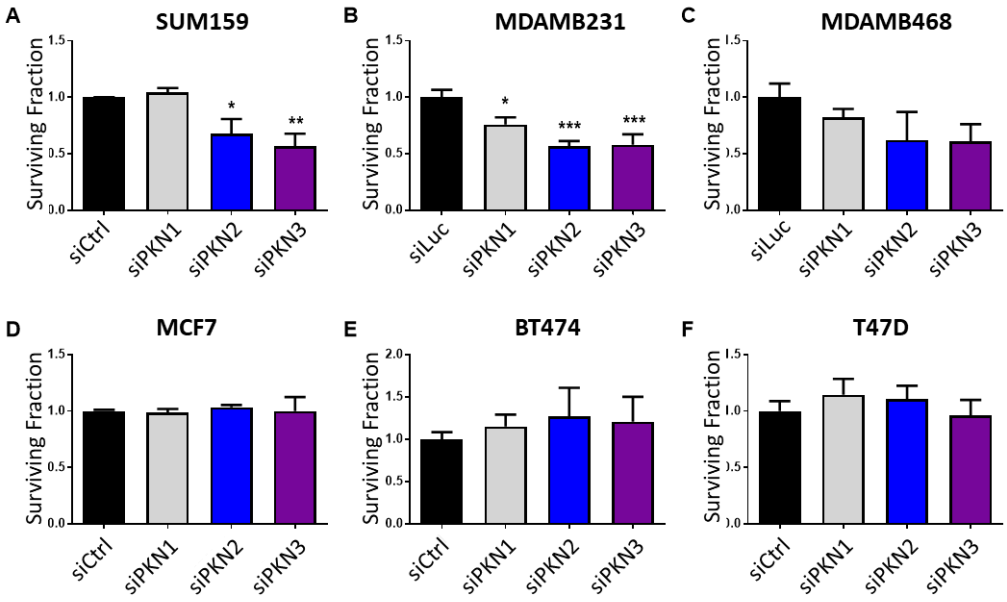

Figure 6. Effect of PKN2 loss in breast cancer cell viability in 2D culture.
Three TNBC cell lines: **A**. MDAMB231, **B**. SUM159, **C**. MDAMB468 and three non-TNBC cell lines: **D**. MCF7, **E**. BT474 and **F**. T47D were treated with control siRNAs (siCtrl1 or siLuciferase) or siRNA targeting the PKN kinases (siPKN1, siPKN2, siPKN3) for 3 doubling times. MTT assay was used to assess cell viability. Surviving fractions were normalised to control siRNA. ANOVA analysis was used to compare siCtrl or siLuciferase with surviving fractions of each siPKN isoforms. A, B, C, D: Collaboration with postdoctoral colleague Ivan Quétier. Data represents the mean +/- SD for n=3 biological repeats carried out in at least triplicates. Statistical analysis was carried out using ANOVA followed by Bonferroni post-hoc test: P<0.05 (*), P<0.01 (**), P<0.001 (***).

MDAMB231 and SUM159 showed significant reduction in cell survival upon PKN2 loss, mediated by the Dharmacon SMARTpool of four individual PKN2-targeting siRNAs (siPKN2#3, siPKN2#9, siPKN2 #10 and siPKN2 #11). To validate this effect, and control for

off-target effects, the siPKN2 pool was deconvoluted (four siRNAs used individually) and compared to the effect of two control siRNAs in MDAMB231 (Fig 7A) and SUM159 (Fig.7B). Three of four PKN2-targeting siRNAs resulted in reduced cell viability in both cell lines, of which two constructs (siPKN2#9 and siPKN2#11) reached statistical significance (P<0.01). Although this confirms dependence on PKN2 for viability, the effects were relatively modest. Subsequently, the effect of PKN2 depletion on cancer viability in 3D culture was investigated in MDAMB231 cell line to see whether there were similar or enhanced viability in more physiologically-relevant conditions.

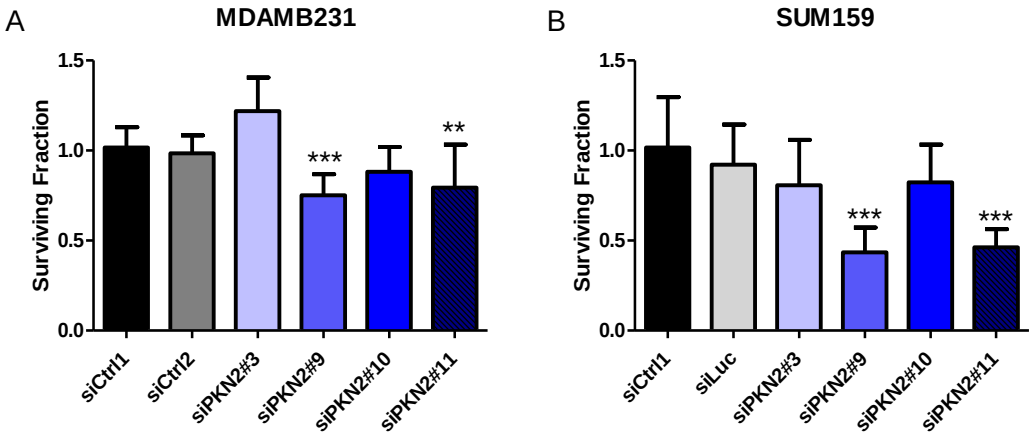

Figure 7. siPKN2 deconvolution in two PKN2-dependent cell lines for validation and testing for off-target effects

A. MDAMB231 and **B.** SUM159 were treated with control siRNAs (two of siCtrl1, siCtrl2 and siLuc) and four individual siPKN2 constructs (siPKN2#9, siPKN2#10, siPKN2#10) for three doubling times and assessed for cell viability by MTT assay. Surviving fractions were normalised to the average of control siCtrl1. Data represents the mean +/- SD for n=3 biological repeats carried out in at least triplicates. Statistical analysis was carried out using ANOVA followed by Bonferroni post-hoc test: P<0.05 (*), P<0.01 (**), P<0.001 (***).

3.1.2.3 Assessing the effect of PKN2 depletion on MDAMB231 cell viability and invasion in 3D culture.

Depletion of PKN3 was demonstrated to reduce proliferation and metastasis of breast orthotopic tumours *in vivo* and invasion in *in vitro* 3D models (Unsal-Kacmaz *et al*. 2012).

Focusing on MDMB231 cells, a common model to study metastatic breast cancer *in vivo*, the effect of PKN2 depletion on cell viability and invasion was studied in 3D culture.

MDAMB231, wild-type or treated with control- or PKN2-targeting siRNA for 24 hours, were seeded onto a gel composed of collagen and Matrigel. This gel composition aims to mimic the extracellular matrix compartment of tumours (Marshall 2011). The mixture of collagen and Matrigel is supplemented with serum and culture media and placed on a membrane with a pore size of 0.4µm of a transwell insert. These gels in transwells are placed in a 24-well plate containing media, where cells in media suspension are added on top of the solidified gel. Here, the cell viability, and invasion into the gel across a chemotactic gradient can be assessed in 3D.

The gels are fixed after 5 days, embedded in paraffin, sectioned and stained with H&E to visualise the cells within the gel (Fig.8A). Overall, the reduced number of PKN2-depleted cells (Fig.8A iv, v, vi) is visually apparent from the H&E stained sections, compared to control cell conditions. To assess the variability between replicates and between individual experiments, we wanted to describe the behaviour of these cells within the gels quantitatively.

Image J software was used to quantify the area occupied by all cells (total cell density) and invasion as described in chapter 2.5. We compared the effects between control and PKN2-targeting siRNA. Each quantitative parameter was normalised to siCtrl1-treated cells. Cells treated with siPKN2#9 and siPKN2#10 showed a small reduction in total cell density compared to siCtrl3 cells, however cell density was similar to that of siCtrl1 cells (Fig.8Bi). Further, differences in total cell density did not reach statistical significance between any conditions. In contrast to total cell density, both control siRNA–treated cells showed similarities in invasion parameters (Fig.8B ii, iii). In these cases, two of three PKN2-targeting siRNAs (#9, #10 and #11) significantly reduced invasive cell count and area compared to

siCtrl1 cells. These findings indicate that the total number of cells were unaffected by PKN2 depletion in 3D, whilst the number of invading cells were reduced upon PKN2 loss.

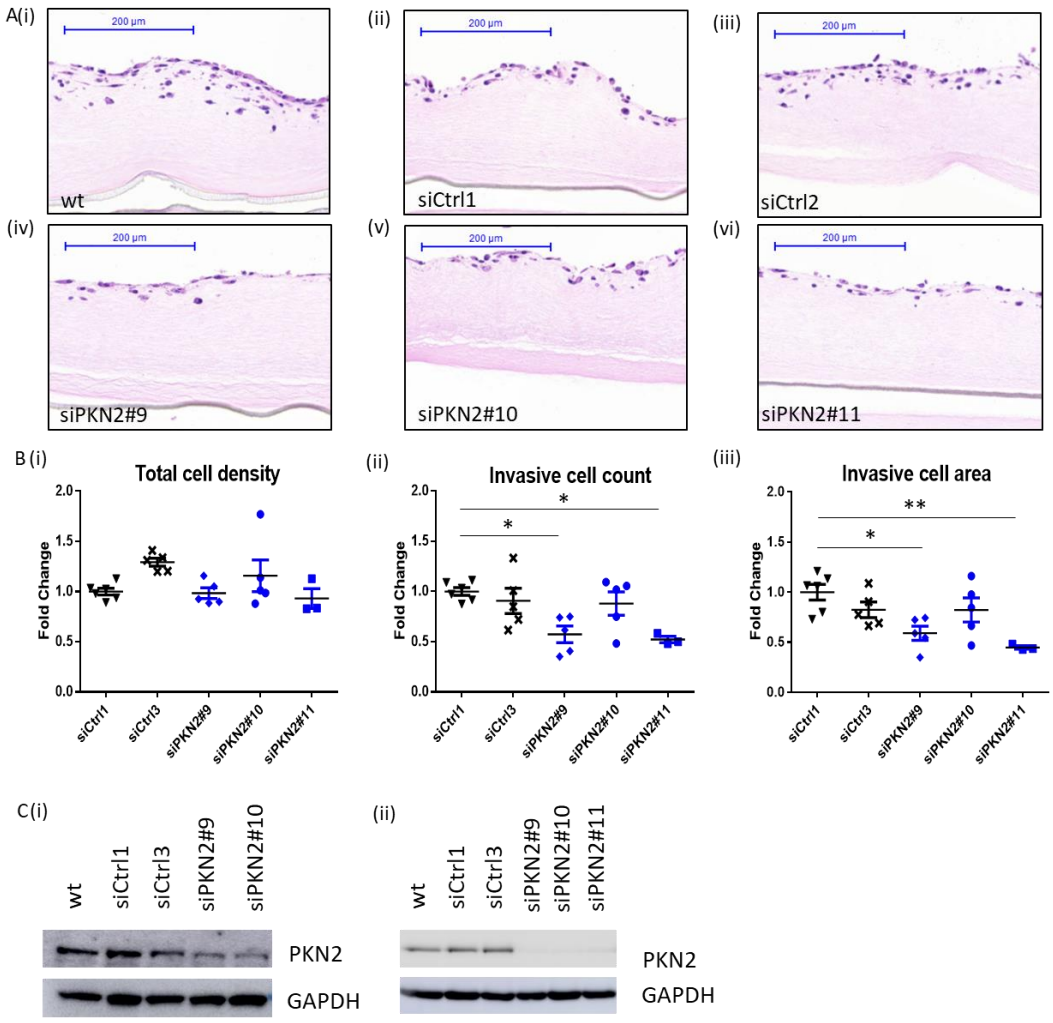

Figure 8. MDAMB231 growth and invasion in 3D mini-organotypic gels

MDAMB231 cells were seeded onto collagen/matrigel gels. After 5 days the gels were fixed and stained with H&E. Brightfield images of the gels show **Ai)** MDAMB231 cells untreated (wt) or pre-treated with control siRNA- **ii)** siCtrl1, **iii)** siCtrl2 or siPKN2 – **iv)** siPKN#9, **v)** siPKN2#10, **vi)**: siPKN2#11. These images are converted into a binary image; stained areas become black and the remaining background is white. **Bi)** The total area of black pixels was quantified to indicate total area occupied by cells (total cell density) **B(ii).** The number of single cells were counted using the particle analysis tool in Image J. **B(iii)** The area of black pixels occupied by invading cells was quantified. Values are normalised to siCtrl1 values to give relative fold change. **C(i)** and **C(ii)**: Western blots showing PKN2 expression of cells treated with control or PKN2-targeting siRNAs in MDAMB231 from two biological repeats. Data represents the mean +/- SD for n=2 biological repeats carried out in triplicates. Statistical analysis was carried out using ANOVA followed by Bonferroni post-hoc test: P<0.05 (*), P<0.01 (**), P<0.001 (***). n=2.

3.1.2.4 Assessing the effect of pharmacological inhibition of PKN2 kinases on breast cancer cell viability.

Targeting PKN isoforms by genetic means indicated a degree of dependency for viability in TNBC cell lines on PKN2 and PKN3. The effect of targeting PKN kinase activity pharmacologically resulted in similar differential effects between mesenchymal-like TNBC cells and luminal breast cancer cells. This study was conducted with two PKN-dependent TNBC cell lines (MDAMB231 and SUM159) and the two PKN-independent luminal breast cancer cell lines (MCF7 and T47D). As there are no specific inhibitors of PKN kinases, less selective inhibitors that have shown significant potency for PKN kinases have been used (Davies et al. 2000); (Falk et al. 2014); (Kohler et al. 2012).

Table 7 lists the potency of some of the inhibitors used against PKN isoforms and some of the significant off-target inhibitory activities on other kinases. Bisindolylmaleimide 1 (Bis 1) and PKC412 have high potency against PKN2, as well as other targets such as protein kinase C kinases (PKC kinases), fibroblast growth factor receptor 1 (FGFR1), 3-phosphoinositide dependent protein kinases (PDK kinases), and ribosomal protein S6 kinase B1 (p70S6K) (Table 7Ai, 1Bi). Bis 1 and PKC412 have higher binding affinity to PKN1, followed by PKN2 for Bis 1 and PKN3 for PKC412 (Table 1A ii, 1B ii). CEP701, also known as Lestaurtinib, has an IC_{50} value of 8.6nM against PKN1 (Kohler et al. 2012). Compared to PKN1 and PKN2, this drug has higher binding affinity to other kinases such as mitogen-activated protein kinase 3 (ERK1), insulin-like growth factor I receptor (IGFR1), mechanistic target of rapamycin kinase (MTOR) and epidermal growth factor receptor (EGFR1) (Table 7C). Go6976 has high potency against PKN2, as well as other kinases such as protein kinase C-alpha (PKCα), Janus kinase 2 (JAK2), cyclin dependent kinase 5 (CDK5), PDK1 and FGFR1 (Table 7D). Y27632 is primarily a Rho associated coiled-coil containing protein kinase (ROCK) inhibitor. It has a IC_{50} value of 0.6μM against PKN2 and 0.8μM against ROCK

II (Davies et al. 2000). Y27632 has higher potency against PKN2 than PKN1 (Table 7E i), which is reflected by the lower K_i binding affinity value for PKN2 than PKN1 (Table 7E ii).

Table 7. Inhibitory activity of Bis 1

Inhibitory activity of Bis I in (**Ai**), PKC412 **(Bi)**, Go6976 (**D**), and Y2732 (**Ei**) on PKN1 and/or PKN2, as well as some of the other off-targets. Ki values demonstrating differential PKN kinase isoform selectivity of (**A ii**) Bis 1, (**B ii**) PKC412 and (**Eii**) Y27632 [2] (Falk et al. 2014). **C**. Inhibitor binding affinity of CEP701 to PKN1 and PKN2 and some of the other off-targets. Inhibitory activity of drugs on kinases determined using [1] DiscoveRx KINOMEscan® platform (Anastassiadis et al. 2011); (Gao et al. 2013); (Wodicka et al. 2010). [3] (Davis et al. 2011).

A (i)

Bis 1 Targets	% Activity Loss (10μM) [1]
PKC kinases	99
p70S6K, CLK2	98
FGFR1, CDK9-cyclin T1,	97
PKN2	94
PDK1	85

B (i)

PKC412 Targets	% Activity Loss at (10uM) [1]
FGFR1	100
PKN2, PDK1, p70S6K	99
PKCγ	94
FGFR2	93
MLCK	90
PKCα, PKCβ, PKBγ	86

A ii)

Bis 1 [2]	PKN1	PKN2	PKN3
K_i (μM)	0.079	0.09	2.3

B ii)

PKC412 [2]	PKN1	PKN2	PKN3
K_i ($x10^{-5}$μM)	<10	<50	<20

C.

CEP701 Targets	Affinity ($-\log_{10}$ pKd) [1]
ERK1	5.0
CDK8	5.1
IGFR1, AKT1, MAP3K1	5.4
CDK11, ERBB2, MTOR	<5.5
EGFR	5.8
PKN1	8.3
PKN2	8.7

D.

Go6976 Targets	% Activity Loss (conc)
PKCα	99 (0.1μM) [3]
CDK5, JAK2	97 (10μM) [1]
PKN2	96 (0.1μM) [3]; 90 (10μM) [1]
PKCβ, PDK1, FGFR1	94 (10μM) [1]

E (i)

Y27632 Targets	% Activity Loss (10μM) [1]
ROCK II, PKN2	96
PKC ε	88
PKN1	58.3

E (ii)

Y27632 [2]	PKN1	PKN2	PKN3
K_i (μM)	0.7	0.22	0.013

These commercially available inhibitors, which also block other kinases, were tested for their effect on cell viability after three doubling times in 2D culture by MTT assay.

Effect of Bisindolylmaleimide I (Bis I) treatment on breast cancer survival

Bis I is a potent inhibitor of PKC kinases, as well as PKN1 and PKN2. Each cell line was initially tested with a range of different doses and thereafter treated with the chosen dose range for final analysis (Fig. 9). Calculations of IC_{50} values for the dose-response curves for each cell line (summarised in Table 8A) demonstrates increased sensitivity in PKN-dependent MDAMB231 and SUM159 cells than PKN-independent MCF7 and T47D.

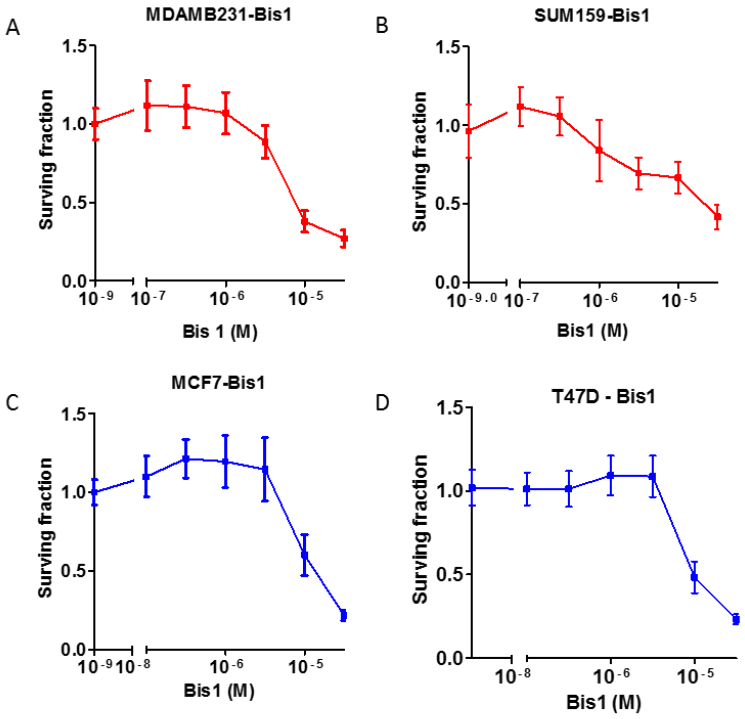

Figure 9. Dose-response curves of breast cancer cells treated with Bisindolylmaleimide I

A. MDAMB231 (n=3), **B**. SUM159 (n=3), **C**. MCF7 (n=3) and **D**. T47D (n=2) were treated with bisindolylmaleimide I (Bis I) 24h after seeding onto 96-well plates. Cell viability was assessed using MTT assay, after three doubling times. Cells were treated at the following concentrations: 0.1, 0.3, 1, 3, 10 and 30µM. Log_{10} of concentration (M) is plotted against values normalised to DMSO condition (plot before x-axis break) +/- SD for n=3 biological repeats carried out in at least triplicates. Statistical analysis was carried out using ANOVA followed by Bonferroni post-hoc test: $P<0.05$ (*), $P<0.01$ (**), $P<0.001$ (***).

Effect of PKC412 on breast cancer survival

PKC412, also known as midostaurin, is a staurosporine-derived PKC inhibitor (Gesher 1998) and subsequently recognised as a FLT3 inhibitor (Weisberg et al. 2002). This inhibitor is FDA

approved for AML treatment (Stone et al. 2017) in patients with FLT3 mutation, in addition to standard chemotherapy. Data from a kinase profiling screen indicates high potency for several other kinases such as FGFR1, FGFR2, PKC kinases and PKN2 (Table 2B i).

The dose-response curve for T47D cells showed a biphasic pattern at the tested dose range (Fig.10D). However, the other cell lines showed inhibitory response to the tested doses (Fig.10A, B and C). The IC_{50} values (Table 3B) suggests that the two PKN-dependent cell lines have higher sensitivity to PKC412 than MCF7, supported by the biphasic survival pattern shown by T47D cells.

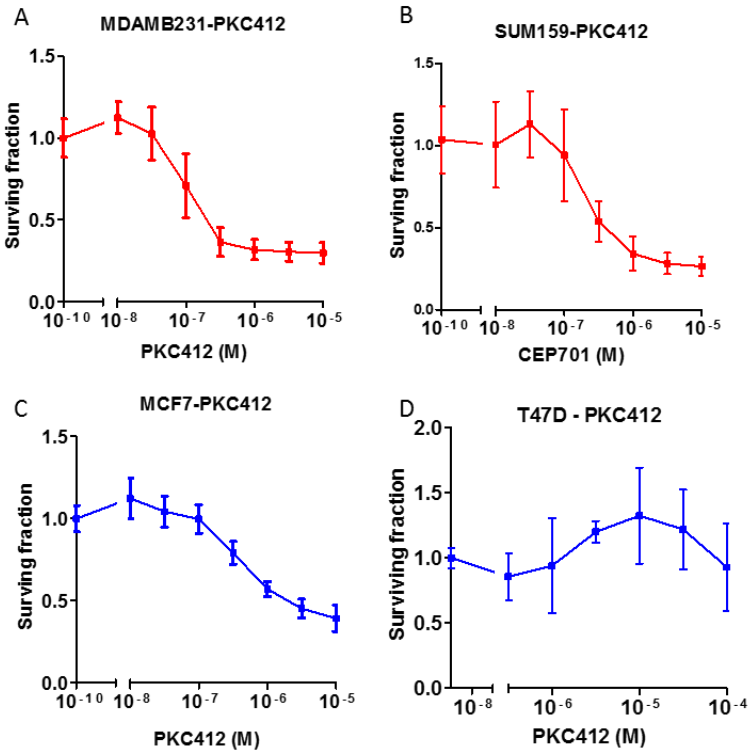

Figure 10. Dose-response curves of breast cancer cells treated with PKC412

A. MDAMB231 (n=3), **B**. SUM159 (n=3), **C**. MCF7 (n=3) and **D**. T47D (n=2) were treated with PKC412 the following day after seeding the cells onto 96-well plates. MDAMB231, SUSM159 and MCF7 were treated at the following concentrations: 0.01, 0.03, 0.1, 0.3, 1, 3, 10 and 30µM. T47D cells were treated at the following concentration: 0.3, 1, 3, 10, 30 and 100 µM. Cell viability was assessed using MTT assay, after three doubling times. Log_{10} of concentration (M) is plotted against values normalised to DMSO condition (plot before x-axis break) +/- SD for n=3 biological repeats carried out in at least triplicates. Statistical analysis was carried out using ANOVA followed by Bonferroni post-hoc test: P<0.05 (*), P<0.01 (**), P<0.001 (***).

Effect of CEP701 on breast cancer survival

CEP701, also known as lestaurtinib, has been involved in clinical trials as a JAK2 inhibitor to treat myeloproliferative neoplasms (Hexner et al. 2014) and as a FLT3 inhibitor to treat patients with acute myeloid leukemia (Knapper et al. 2006). Treating the four cell lines in question with this inhibitor (Fig.11) similarly showed increased sensitivity in SUM159 and MCF7 cells than MDAMB231 and T47D cells (IC_{50} values summarised in Table 3C).

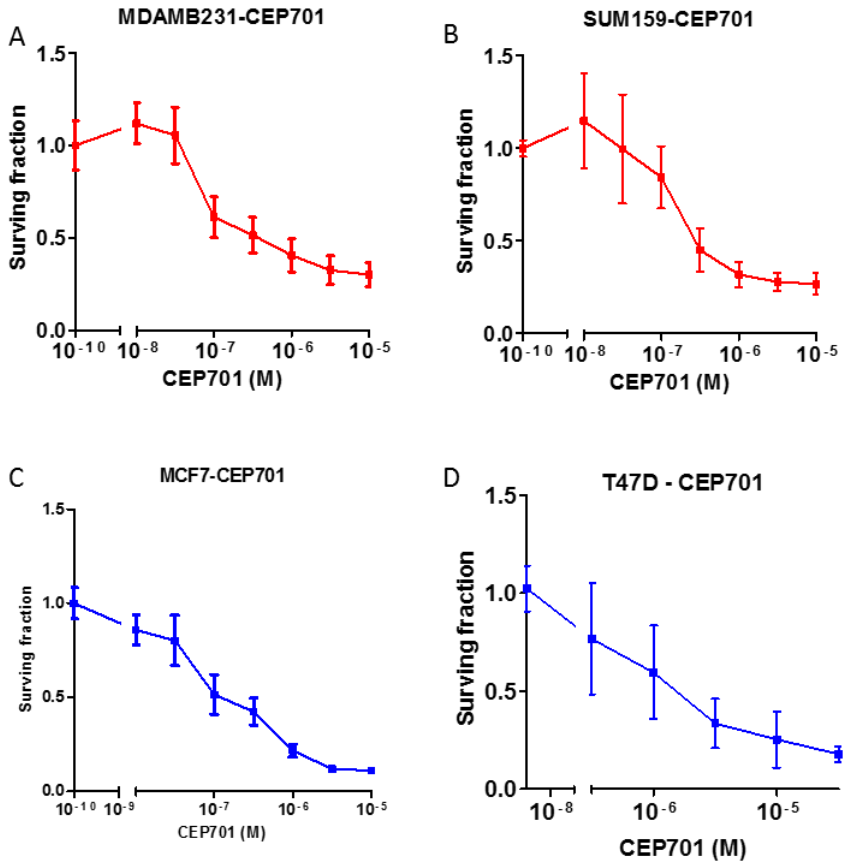

Figure 11. Dose-response curves of breast cancer cells treated with CEP701

A. MDAMB231 (n=3), **B**. SUM159 (n=3), **C**. MCF7 (n=3) and **D**. T47D (n=3) were treated with CEP701 the following day after seeding the cells onto 96-well plates. Cell viability was assessed using MTT assay, after three doubling times. MDAMB231, SUSM159 and MCF7 were treated at the following concentrations: 0.01, 0.03, 0.1, 0.3, 1, 3, 10 and 30µM. T47D cells were treated at the following concentration: 0.3, 1, 3, 10 and 30µM. Log_{10} of concentration (M) is plotted against values normalised to DMSO condition (plot before x-axis break) +/- SD for n=3 biological repeats carried out in at least triplicates. Statistical analysis was carried out using ANOVA followed by Bonferroni post-hoc test: P<0.05 (*), P<0.01 (**), P<0.001 (***).

Effect of Go67976 on breast cancer survival

An indolocarbazole with a similar structure to staurosporine, Go6976 is a potent inhibitor of FLT3 and JAK2 and is known to have anti-proliferative effects in AML cells (Grandage et al. 2006); (Yoshida et al. 2014). In addition, Go9676 has high potency against PKC kinases and PKN2 (Table 7D). Amongst the four tested cell lines MDAMB231 was the least sensitive, whereas T47D showed highest sensitivity (Fig.12A, D) (IC_{50} values summarised in Table 3D).

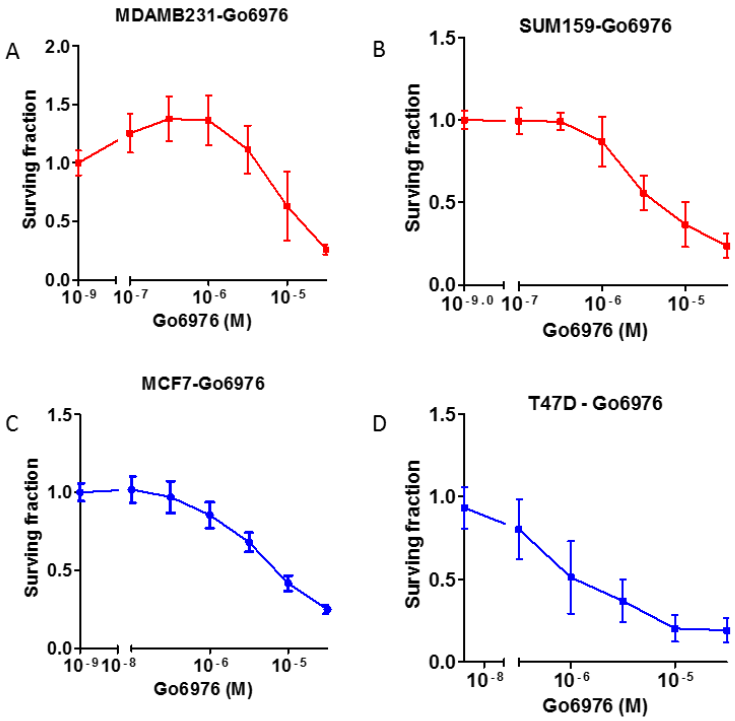

Figure 12. Dose-response curves of breast cancer cells treated with Go6976

A. MDAMB231 (n=3), **B**. SUM159 (n=3), **C**. MCF7 (n=3) and **D**. T47D (n=3) were treated with Go6976 the following day after seeding the cells onto 96-well plates. Cell viability was assessed using MTT assay, after three doubling times. MDAMB231, SUSM159 and MCF7 were treated at the following concentrations: 0.1, 0.3, 1, 3, 10 and 30µM. T47D cells were treated at the following concentration: 0.3, 1, 3, 10 and 30µM. Log_{10} of concentration (M) is plotted against values normalised to DMSO condition (plot before x-axis break) +/- SD for n=3 biological repeats carried out in at least triplicates. Statistical analysis was carried out using ANOVA followed by Bonferroni post-hoc test: P<0.05 (*), P<0.01 (**), P<0.001 (***).

Effect of Y27632 on breast cancer survival

This drug is widely used as a Rho kinase inhibitor (Ishizaki et al. 1996) and has been studied in neurodegenerative diseases (Bauer et al. 2009); (Liu et al. 2014) and in hypertension as a vasodilator (Uehata et al. 1997). Furthermore, treating prostate and breast cancer cells with Y27632, in addition to fibroblast cells, increases proliferation of cancer cells (Liu et al. 2012).

This inhibitor had no anti-proliferative effect on any of the cell lines at the tested dose range (Fig.13). This could be explained by the relatively low potency for PKN2 reported by Davies *et al* (IC_{50} =600nM) in a cell-based kinase inhibitor screen (Davies et al. 2000).

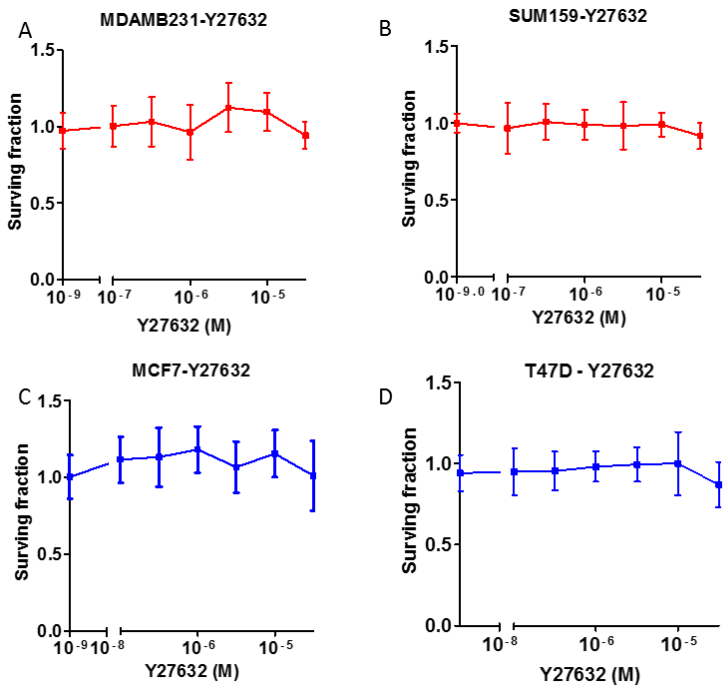

Figure 13. Dose-response curves of breast cancer cells treated with Y27632

A. MDAMB231 (n=3), **B**. SUM159 (n=3), **C**. MCF7 (n=3) and **D**. T47D (n=2) were treated with Y27632 the following day after seeding the cells onto 96-well plates. Cell viability was assessed using MTT assay, after three doubling times. All cells were treated at the following concentrations: 0.1, 0.3, 1, 3, 10 and 30µM. Log_{10} of concentration (M) is plotted against values normalised to DMSO condition (plot before x-axis break) +/- SD for n=3 biological repeats carried out in at least triplicates. Statistical analysis was carried out using ANOVA followed by Bonferroni post-hoc test: P<0.05 (*), P<0.01 (**), P<0.001 (***).

Overall, Bis I and PKC412 elicited enhanced anti-proliferative effects in PKN-dependent cell lines MDAMB231 and SUM159, when compared with PKN-independent MCF7 and T47D cells (Table 3A, B). CEP701 and Go6976 showed varying effects on the four different cell lines, which did not correlate with PKN expression dependence (Table 3C, D). No sensitivity was found in response to Y27632 at the tested range of doses. However, as these inhibitors target many other kinases, validating PKN2 as an anti-proliferative pharmacological target is limited. Therefore, genetic targeting of PKN currently remains a more desirable approach.

Table 8. Summary of PKN kinase inhibitor activities

IC_{50} values of **A**. Bis 1, **B.** PKC412 (IC50 values could not be calculated in T47D cells from the resulting dose-response curve), **C.** CEP701 and **D.** Go6976 in the tested TNBC (orange cells) or luminal (blue cells) breast cancer cell lines.

A. Bis1

Cell line	IC_{50} (μM)
MDAMB231	4.99
SUM159	3.860
MCF7	~ 9.833
T47D	~9.3

B. PKC412

Cell line	IC_{50} (μM)
MDAMB231	1.058e-007
SUM159	2.320e-007
MCF7	4.438e-007

C. CEP701

Cell line	IC_{50} (μM)
MDAMB231	8.329e-008
SUM159	1.633e-007
MCF7	1.266e-007
T47D	9.2e-7

D. Go6976

Cell line	IC_{50} (M)
MDAMB231	8.357e-006
SUM159	2.719e-006
MCF7	4.863e-006
T47D	9.6e-7

3.1.3 Summary

Ultimately the aim of our study was to examine whether targeting the PKN kinases might inhibit TNBC tumour growth and metastasis. To support this, results discussed in this chapter and other independent studies (Brough et al. 2011); (Lin et al. 2017) show a strong association between PKN2 and TNBC for cell survival.

The difference in viability with siRNA was however relatively moderate and replicating these results using shRNA presented with technical difficulties. Additionally, during the course of our work, a study on the role of PKN3 in breast tumour angiogenesis and metastasis was published (Mukai et al. 2016) and a separate study describing the role of PKN2 in TNBC cells (Lin et al. 2017).

Furthermore, a selective PKN kinase inhibitor is required to translate any findings from targeting this kinase to the clinic. A recent study (Lin et al. 2017) demonstrated potent selective inhibition of four TNBC cell line viability compared with four other non-TNBC cell lines using the PKC targeting inhibitor chelerythrine. Chelerythrine was then shown to induce apoptosis in the TNBC lines. They also demonstrated that knockdown of PKN2 in the four TNBC and four non-TNBC showed selective anti-proliferative effects specifically in TNBC cell line, corroborating our findings. They subsequently attribute Chelerythrine TNBC selectivity to its ability to inhibit of PKN2. The TNBC cell lines used in these studies are mesenchymal in phenotype (for e.g. MDAMB231 and SUM159) and/or classified as ML or BL TNBC cell lines (for e.g. MDAMB468, Cal-120 and BT549) (Lehmann, Bauer, Chen, Sanders, Chakravarthy, Shyr, et al. 2011).

However, this is questionable, as chelerythrine is not a PKN2-specific inhibitor. The MRC kinase profiling inhibitor database reports that chelerythrine is a very poor inhibitor of PKN2 (only 8% inhibition of PKN2 kinase activity at 10μM), whereas Tie2 activity is inhibited by 97% and FGFR1 by 56% (Anastassiadis et al. 2011); (Gao et al. 2013). Furthermore, chelerythrine also has high potency against PKC, with an IC_{50} value of 0.66μM against (Herbert et al. 1990).

Do mesenchymal cells depend on PKN2 to proliferate?

Several lines of evidence from independent studies suggest that we may have identified a mesenchymal cell-specific role for PKN2 in the regulation of cell growth. Firstly, systemic

deletion of only PKN2 but not PKN1 or PKN3 has detrimental effect on mesenchymal cell growth both *in vivo* and *in vitro* during embryonic development (Quétier et al. 2016). Secondly, genetic depletion of PKN kinases reduced cell viability of MDAMB231 and SUM159 breast cancer cells that have mesenchymal phenotypes. These cell lines had reduced viability when treated with two non-specific PKN kinase inhibitors Bis 1 and PKC412, compared to luminal breast cancer cell lines MCF7 and T47D. These data also agree with the findings from an independent functional viability screen in breast cancer cells (Brough et al. 2011), which identified PKN2 as a candidate gene for targeting cell viability in TNBC cells. Several other TNBC cell line hits identified in this screen, showing dependency on PKN2, also display mesenchymal phenotypes. Similarly, since conducting our study, Lin *et al* also reported the specific requirement of PKN2 exclusively in TNBC cells, compared to other breast cancer cells, for cell growth *in-vitro* and *in-vivo* (Lin *et al*. 2017), which corroborates our findings.

While the role of PKN2 mechanistically remains a focus in the lab, the relatively modest effect on TNBC growth, and the publication of competing studies, prompted us to change focus to examine a role for PKN2 in cancer-associated fibroblasts, one of the most significant mesenchymal phenotype cell types in many solid tumours, including those of the breast and pancreas. In breast cancer, fibroblast activation plays an important role in the tumour microenvironment and affects tumour progression, metastasis and drug response. Further, data from our lab has strongly implicated PKN2 in the regulation of pancreatic cancer associated fibroblasts. Therefore, the role of PKN2 in breast fibroblasts and how this affects their interaction with breast cancer cells was investigated.

3.2 Role of PKN2 in TGFβ1-mediated fibroblast activation

Fibroblasts within the TME become activated into CAFs in response to factors secreted by cancer cells, including TGFβ and PDGF (Ostman and Augsten 2009). Activated CAFs induce scar like fibrosis, through production of ECM proteins (desmoplasia), blocking entry of tumour-infiltrating immune cells and anti-cancer drugs (Orimo et al. 2005). Increased ECM deposition and tissue stiffness associated with many tumours further enhances CAF activation through mechanosensing pathways in a positive feedback loop. CAFs also secrete ECM remodelling enzymes, as well as growth factors and cytokines, which promote angiogenesis, inflammation, cell motility and invasion (Tyan et al. 2012); (Shekhar et al. 2001); (Soon et al. 2013). High expression of α-SMA, an important marker of activated fibroblasts (myofibroblasts and CAFs), which has been associated with high grade tumours, lymph node metastasis and poor prognosis in breast cancer (Yazhou et al. 2004); (Surowiak et al. 2006); (Surowiak et al. 2007). These findings suggest that studying the regulation of CAF activation in the stroma may provide important therapeutic targets.

Our recent report demonstrated a role for PKN2 in the mesenchyme of embryos during development (Quétier et al. 2016). Importantly, embryo morphogenesis defects indicate a loss of contractility within the mesenchymal compartment and this is accompanied by severe angiogenic defects. Work in the lab (in collaboration with John Marshall) further demonstrated that loss of PKN2, in a variety of mouse and human fibroblasts, reduced their contractility - a phenotypic marker of activation - in collagen gels, in response to TGFβ1 (Fig. 14). Together, these data suggest that PKN2 is critical for activation of fibroblasts both *in vitro* and *in vivo*, with potential implications for the activation of fibroblasts into CAFs in tumours.

Here we sought to examine whether PKN2 loss impacts on the activation of fibroblasts in breast cancer. As models, we used immortalised human breast fibroblasts (HMFU19) and

primary human breast cancer CAFs. We also used inducible conditional PKN2 knockout MEFs as a surrogate model, where we have previously identified a defect in TGFβ1-induced collagen contractility (Fig.14 - data not shown). We also focused on the induction of α-SMA fibres as a marker of fibroblast activation. Acute TGFβ1-mediated SMAD signalling was also investigated to probe for PKN2's mechanism of action.

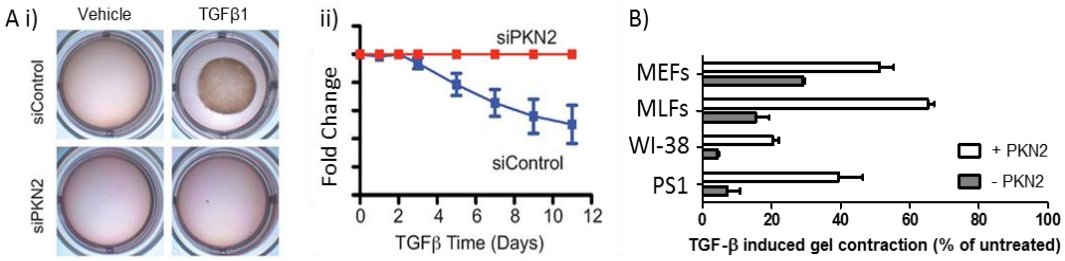

Figure 14. Collagen contraction assay to assess effect of PKN2 deletion in fibroblasts on activation

A. Human lung fibroblasts, treated with control or PKN2-targeting siRNA were seeded in collagen gels. The following day, normal culture media with or without TGFβ1 is added to gels. i) Images of gels. Gels with control siRNA treated cells, treated with TGFβ1, contracted compared to vehicle-treated gels. There was no contraction in response to TGFβ1 in gels with siPKN2 treated cells. ii) Over 11 days, the fold change in gels size decreased for siControl cells and remained unchanged for siPKN2 fibroblasts. B. Similar collagen contraction assays were done in other fibroblasts, comparing those that express PKN2 (+PKN2) and those without PKN2 (-PKN2). These fibroblasts include MEFs, mouse lung fibroblasts (MLFs), human fibroblast-like fetal lung cells (WI-38), and human pancreatic stellate cells (PS1). All fibroblasts show reduced gel contraction upon TGFβ1-induction with PKN2 loss.

3.2.1 Role of PKN2 in TGFβ-1 mediated induction of α-SMA fibres in fibroblasts

Work by Desmoulière *et al* demonstrated that treatment of fibroblasts with TGFβ induced the expression of α-SMA fibres, a marker of cellular differentiation (Desmoulière et al. 1993); (Chaponnier and Gabbiani 2004). Thus, fibroblasts differentiate into myofibroblasts in response to TGFβ, that are highly contractile and contribute to ECM and collagen deposition and consequent fibrosis. The presence of many α-SMA-expressing myofibroblasts has been associated with high grade tumours and low overall survival in

breast cancer (Surowiak et al. 2006); (Yang et al. 2017); targeting these myofibroblasts has been proposed as a potential therapeutic opportunity.

Previous work in the lab demonstrated reduced contractility in PKN2-depleted fibroblast models in response to TGFβ1, raising the possibility that targeting PKN2 may be beneficial for supressing CAF activation in tumours. Therefore, the ability of wt and PKN2 deleted/depleted MEFs and CAFs to express α-SMA fibres in response to TGFβ1 was tested.

MEFs (wt and PKN2 ko) were seeded onto glass coverslips in 24-well plates and treated the following day with TGFβ1 (5ng/ml) or vehicle control. Primary breast CAFs were treated with control siRNAs or a pool of PKN2-targeting siRNAs (siPKN2#9, siPKN2#10, siPKN2#11). After 72 hours, these CAFs were trypsinised and seeded onto coverslips and treated the following day with TGFβ1 (5ng/ml) or vehicle control. Fibroblasts were fixed 72 hours post TGFβ1 treatment. Three biological experiments were conducted per fibroblast model. The fixed cells on coverslips were immunostained for α-SMA, counterstained with DAPI and images were acquired on an LSM710 confocal microscope. Multiple images were acquired per condition to image cells that overlap minimally with neighbouring cells and to have a minimum of 20 cells per condition. Each image was analysed by counting the total number of cells, α-SMA-positive cells and grading the α-SMA brightness per cell (low, medium or high). The percentage of α-SMA-positive cells was scored, to quantify differences in the levels of α-SMA-positive cells, between untreated and TGFβ1-treated fibroblasts that do or do not express PKN2.

3.2.1.1 TGFβ1-mediated activation in MEFs is suppressed upon PKN2 deletion

More than 50 MEFs per condition were analysed for the expression of α-SMA fibres. Under basal conditions, approximately 40% of cells were found to express α-SMA (Fig. 15Ai, Ci – WT-TGF) and this was not significantly reduced upon deletion of PKN2 (Fig. 15Aii, 2Ci). There was a significant increase in α-SMA-positive cells in TGFβ1-treated compared to vehicle-

treated wt MEFs (Fig. 15A, B, Ci). This induction was not seen in PKN2-deleted MEFs and the percentage of α-SMA-positive cells was significantly lower in TGFβ1-treated PKN2 ko MEFs compared to TGFβ1-treated wt MEFs (Fig. 15Ci). Furthermore, α-SMA-positive cells were categorised according to the brightness of α-SMA immunostain as low, medium and high. There was a significant increase in wt MEFs, with medium-level α-SMA brightness, when stimulated with TGFβ1 (Fig. 15C iii). In contrast, there was no significant increase in TGFβ1-treated PKN2 ko MEFs, with medium brightness, when stimulated with TGFβ1. Further, the percentage of α-SMA medium brightness cells was significantly lower in the TGFβ1 stimulated PKN2 ko cells than in TGFβ1 stimulated wt cells. Due to high variation observed for some conditions, there were no statistically significant differences between untreated or TGFβ1-treated cells, graded as low or high brightness, regardless of PKN2 expression (Fig. 15C ii, iv). Overall, the percentage of α-SMA positive cells following TGFβ induction is reduced upon PKN2 loss. This helps explain the previous observation of reduced contractility of TGFβ1-stimulated MEFs in collagen gels, when PKN2 was deleted as α-SMA positivity has been directly correlated with cell contractility (Hinz et al. 2001).

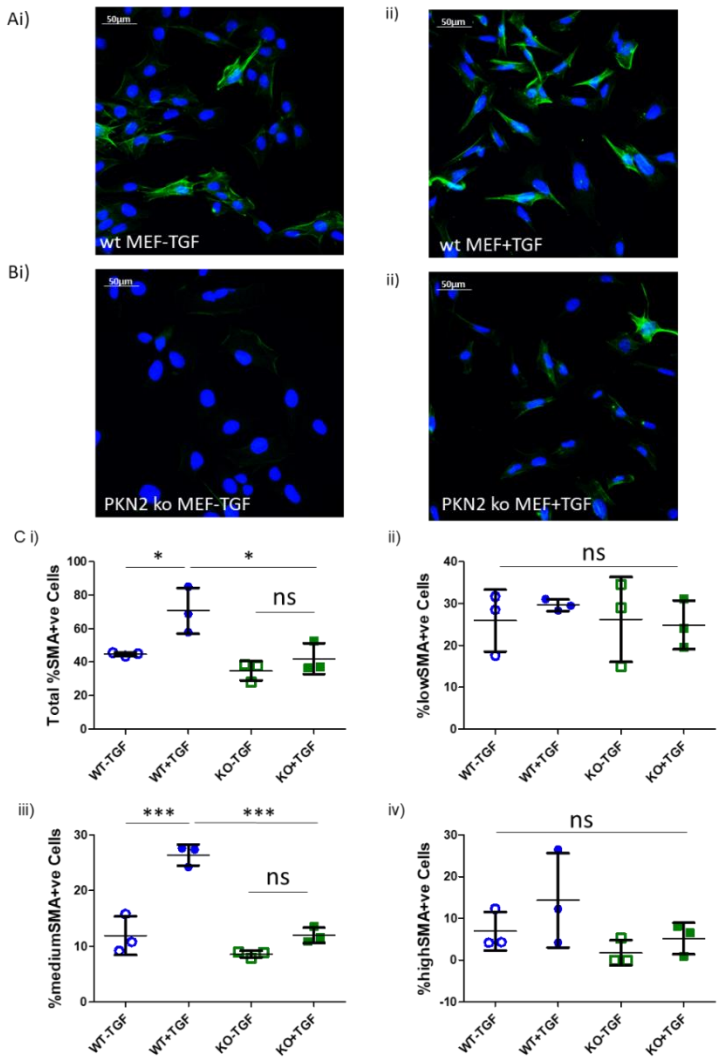

Figure 15. α-SMA fibre induction in TGFβ1-stimulated wt and PKN2 ko MEFs

MEFs (wt and PKN2 ko) seeded on coverslips were treated with 5ng/ml TGFβ1 or vehicle for 72h. At endpoint, cells were fixed and stained for α-SMA (green) and with DAPI (blue) for nuclei. In wt MEFs, there was an increased percentage of α-SMA-positive cells when stimulated with TGFβ1 (Aii) compared to untreated cells (Ai). In PKN2 ko cells treated with TGFβ1 (Bi), the increase in α-SMA was marginal compared to non-treated cells (Bii). Total number of α-SMA positive MEFs was counted and expressed as percentage of total cells (Ci). The brightness of α-SMA fibres for each cell was categorised as low, medium, high and expressed as percentage of total cells (Ci, ii, iii). Data represents the mean +/- SD for n=3 biological repeats carried out in duplicate coverslips. Statistical analysis was carried out using ANOVA followed by Bonferroni post-hoc test: P<0.05 (*), P<0.01 (**), P<0.001 (***).

3.2.1.2 TGFβ1-mediated activation of primary CAFs and the effect of PKN2 deletion

Primary cancer-associated fibroblasts (CAFs) from human patients were obtained from the Breast Cancer Tissue Bank, through collaboration with Prof. Louise Jones (Barts Cancer

Institute). CAFs are predominantly activated forms of resident fibroblasts in the tumour stroma and therefore often have high basal expression of α-SMA. Nevertheless, TGFβ1 was used to see whether the expression of α-SMA can be further stimulated and whether it will be affected by PKN2 expression.

Culturing primary CAFs presented with challenges due to their slow proliferation in culture and their propensity to arrest through senescence after very few cell passages. Furthermore, the number of cells seeded per condition was lower than that for MEFs, as CAFs have a larger surface area; at high densities, with overlapping cells, quantification of α-SMA was difficult. Therefore, the number of cells available for analysis ranged from 20 to 50 cells per condition. Surprisingly, the percentage of CAFs expressing α-SMA in basal conditions was quite low (10-40%). There was an overall increase in the percentage of α-SMA-positive cells upon TGFβ1 treatment in wt and control siRNA-treated CAFs in all three biological replicates (Fig. 16A, B, Di). However, there were no changes in siPKN2-treated CAFs in the percentage of α-SMA-positive cells upon TGFβ1 treatment (Fig. 16C, Di). There was significant variation in the base line percentage, which meant comparison of raw percentage differences did not reach statistical significance (Fig. 16Dii). To overcome this, the change in percentage of α-SMA-positive cells *for each experiment* was compared (Fig. 16D iii). The percentage change in α-SMA-expressing, PKN2-depleted CAFs between untreated and TGFβ1-treated cells was significantly lower compared to control cells (untreated and control siRNA-treated cells (Fig. 16D iii). Overall, these data show suppression of α-SMA induction in PKN2 depleted CAFs when stimulated with TGFβ1, consistent with the observations in MEFs.

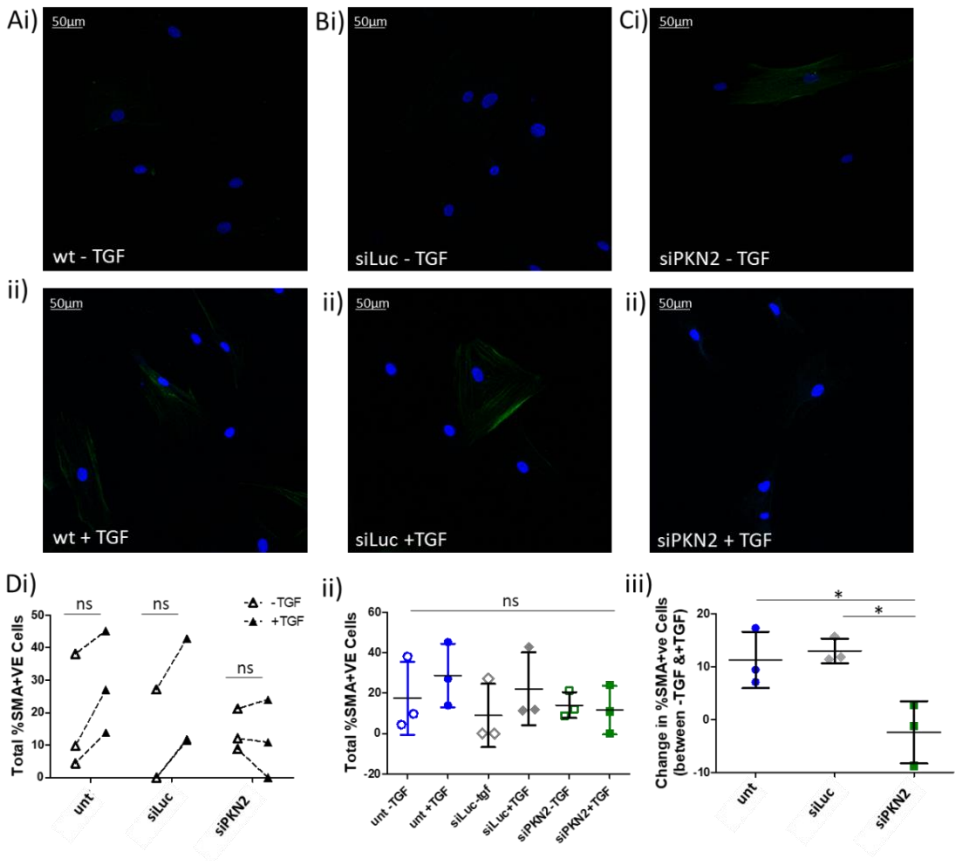

Figure 16. Induction of α-SMA fibres in CAFs and the effect upon PKN2 loss.

CAFs, wild-type(wt) or pre-treated with control siRNA (siLuc) or PKN2-targeting siRNA (siPKN2) were seeded onto coverslips and treated with 5ng/ml TGFβ1 or vehicle for 72h. Cells at endpoint were fixed and immunostained for α-SMA (green) and with DAPI (blue). Images were acquired using an LSM710 confocal microscope (A, B, C). The total number of α-SMA-expressing cells were counted and expressed as percentage of total cells and plotted on a matched dot plot to visualise the individual biological experiments (Di). For siLuc cells (non-targeting control) the values for two experiments are very similar and the plot overlaps, hence the solid line rather that the dashed lines, and apparent lack of a third experimental replicate. Total percentage of α-SMA-positive cells for the three biological experiments (Dii). The matched dot plot shows variation in basal levels of α-SMA-expressing cells between different cell conditions and experiments. Therefore, the changes in percentage of α-SMA-positive cells between untreated and TGFβ1-treated cells were plotted (Diii). Data represents the mean +/- SD for n=3 biological repeats carried out in duplicate coverslips. Statistical analysis was carried out using ANOVA followed by Bonferroni post-hoc test: P<0.05 (*), P<0.01 (**), P<0.001 (***).

3.2.2 Effect of PKN2 loss on acute signalling in fibroblasts upon TGFβ stimulation

Reduced α-SMA fibres in TGFβ1-activated, PKN2-deleted/depleted fibroblasts were observed in MEFs and CAFs. The role of PKN2 in suppressing α-SMA fibre formation might

lead to normalising an activated stroma. To exploit this pathway as a therapeutic target, the mechanism of PKN2's role in fibroblast activation needs to be investigated. Therefore, the immediate signalling pathway downstream of acute TGFβ1 stimulation was compared between wild-type and PKN2 deleted/depleted fibroblasts. Fibroblasts were deleted/depleted of PKN2 and serum-starved. The following day, stock TGFβ1 solution or culture media (for control cells) was spiked into the cell media. The addition of a small volume to the existing media reduces shear force on cells that is known to affect signalling downstream of TGFβ1 (Ahamed et al. 2008).

Protein lysates were collected across a time-course of stimulation and tested for canonical TGFβ-activated SMAD signalling, one of the main pathways responsible for TGFβ functions. In this pathway TGFβ binds to TGFβ type II serine/threonine kinase receptor (TβRII) and recruits type I receptor (TβRI) to form an oligomeric receptor complex (Yamashita et al. 1994). This complex results in phosphorylation and conformational change of TβRI by TβRII, leading to its activation. This leads to a signalling cascade involving the phosphorylation of SMAD2 and SMAD3, which form complexes with a transcription factor SMAD4. Finally, this complex translocates to the nucleus to mediate transcriptional activity.

3.2.2.1 PKN2 deletion and TGFβ1 stimulation across a timecourse in MEFs

MEFs (wt and PKN2 ko) were seeded onto 12-well plates in normal culture media and serum-starved the following day in 0.5% FBS media. The next day, TGFβ1 stock solution or normal culture media (vehicle) for control cells was added to the cells in media, to give a final concentration of 5ng/ml. Following stimulation for 5, 10, 30 and 60 minutes, cell were placed on ice, media was removed, cells were washed once in ice-cold PBS and lysed in lysis buffer.

MEFs were treated with TGFβ1 for 5, 10 30 and 60 minutes to study the kinetic of increasing phosphorylation of SMAD2/3. SMAD phosphorylation was detected after 5 minutes, which

increased up to 30 minutes after stimulation. Both wt and PKN2 ko MEFs showed near identical patterns and amplitude of SMAD2/3 phosphorylation (Fig. 17).

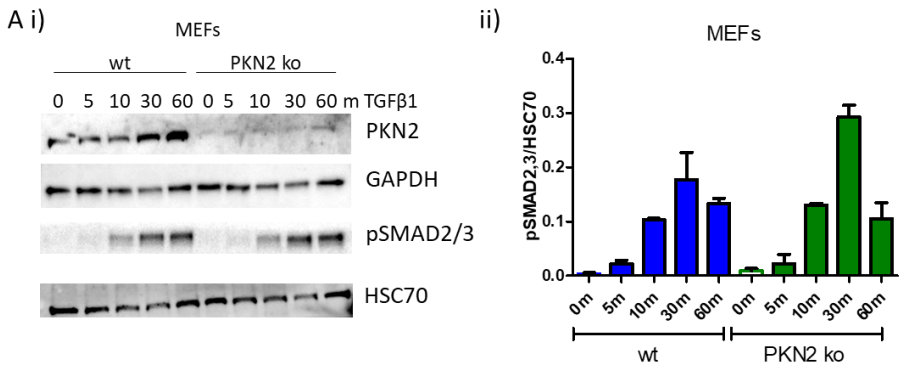

Figure 17. SMAD2/3 phosphorylation in wt & PKN2 ko MEFs after short-term TGFβ1 stimulation
MEFs were seeded, serum-starved overnight and treated the following day with 5ng/ml TGFβ1 for 0, 5,10, 30 and 60 minutes. Protein lysates were collected, separated by PAGE-SDS electrophoresis and blotted for the expression of PKN2, phosphorylation of SMAD2/3 (pSMAD2/3) and protein load controls GAPDH and HSC70 (Ai). Densitometry of bands was quantified using Image J tool to understand the changes in relative levels of pSMAD2/3 to the loading control HSC70 (ii). Data represents n=2 biological repeats. Statistical analysis was carried out using ANOVA followed by Bonferroni post-hoc test: P<0.05 (*), P<0.01 (**), P<0.001 (***).

3.2.2.2 PKN2 depletion and TGFβ1 stimulation in HMFU19 immortalised breast fibroblasts

Immortalised human mammary fibroblasts were obtained from Mike Allen (Barts Cancer Institute). These fibroblasts were immortalized by Professor Mike O'Hare, using hTERT and SV40 large tumour antigen (O'Hare et al. 2001). These cells were not included in our study of α-SMA fibres, as siRNA transfected cells expressed α-SMA fibres without stimulation and did not respond further to long-term TGFβ1 stimulation to induce increased α-SMA fibre formation. Nonetheless, the role of PKN2 on acute TGFβ1 stimulation was assessed in HMFU19, alongside MEFs and CAFs, to compare a range of fibroblast models.

HMFU19 were transfected with control siRNA (siLuc) and two individual PKN2-targeting siRNAs (siPKN2#9 and siPKN2#10). Transfected fibroblasts were seeded onto 12-well plates, three to four days post-transfection. The following day, TGFβ1 stock solution was added to

the cells in media to give a final concentration of 5ng/ml. Normal culture media was added to control cells. HMFU19 were seeded and stimulated with TGFβ1 in 0.5% FBS media. Protein lysates were collected at various timepoints: 0, 5, 10 and 30 minutes.

HMFU19 retained the ability to respond to TGFβ1 stimulation after 5, 10, and 30 minutes by inducing SMAD2/3 phosphorylation, regardless of PKN2 loss (Fig. 18). Control siRNA and PKN2 siRNA-treated cells showed increasing phosphorylation of SMAD2/ 3 with increasing time exposed to TGFβ1. There was a small reduction in SMAD2/3 phosphorylation at 30 minutes in siPKN2-treated HMU19, compared to control siRNA cells, though further replicates are required to assess statistical significance.

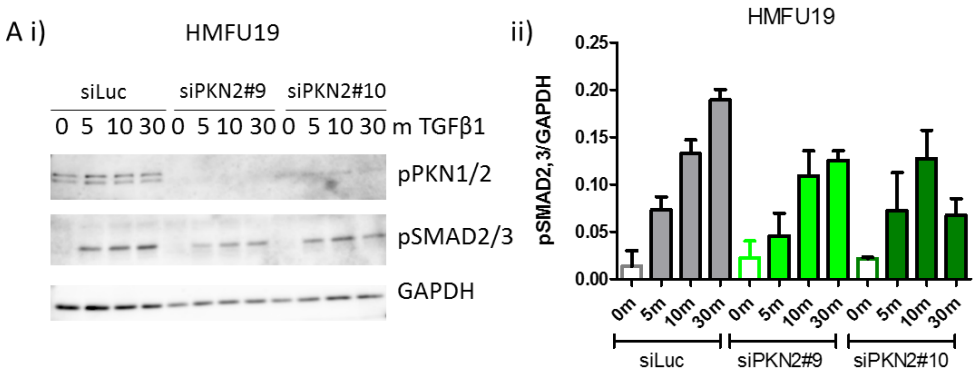

Figure 18. SMAD2/3 phosphorylation in HMFU19 fibroblasts upon acute TGFβ1 stimulation
HMFU19 cells were transfected with control siRNA (siLuc) or two PKN2-targeting siRNAs individually (siPKN2#9 and siPKN2#10) before seeding for TGFβ1 stimulation. Cells were starved overnight in reduced serum media and stimulated with 5ng/ml TGFβ1 for 0, 5, 10 and 30 minutes. Protein lysates were collected, separated by SDS-PAGE electrophoresis and blotted for the levels of phosho-PKN1 and phospho-PKN2 (pPKN1/2), phospho-SMAD2/3 (pSMAD2/3) and protein load control GAPDH (Ai). Densitometry of bands was quantified using Image J tool to understand the changes in relative levels of pSMAD2/3 to the loading control GAPDH (ii). Data represents the mean +/- SD for n=2 biological repeats.

3.2.2.3 Acute TGFβ1-mediated SMAD signalling in PKN2-deleted CAFs

CAFs were also transfected with siLuc but PKN2 was supressed using a pool of three PKN2-targeting siRNAs (siPKN2#9, siPKN2#10, and siPKN2 #11) as transfection efficiency was often poor with these cells and cell numbers were limited. As the culture of primary CAFs

presented with challenges, due to limited passaging and slow proliferation, the number of cells available for the experiment was limited. Thus, for PKN2 depletion a pool of PKN2-targeting siRNAs was used. Cells were seeded under the same culture conditions as for HMFU19, except that the culture media was supplemented with 2% FBS, as CAFs did not survive in 0.5% FBS media when previously tested. However, due to the low number of cells available, only one time-point of TGFβ1 stimulation (30 minutes) was tested.

The experiment in CAFs was consistent with MEFs and HMFU19, in that loss of PKN2 expression did not hinder SMAD2/3 phosphorylation following TGFβ1 stimulation for 30 minutes (Fig. 19). Further experiments are required to confirm these results in a panel of primary CAFs. Although repeats of this experiment were conducted, protein concentrations were too low to detect SMAD2/3 phosphorylation.

Together, the data from multiple fibroblast models, suggest that PKN2 is dispensable for canonical SMAD2/3 signalling downstream of acute TGFβ1 stimulation.

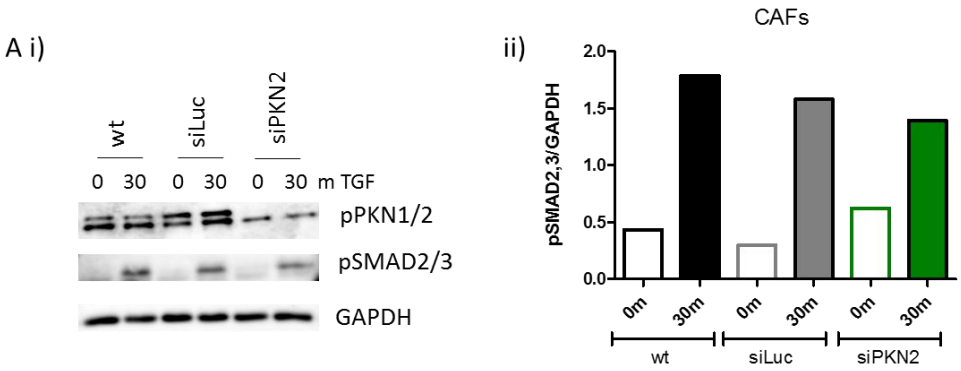

Figure 19. Assessing SMAD2/3 phosphorylation in CAFs after acute stimulation of CAFs with TGFβ1

Wild-type (wt) or CAFs transfected with control siRNA (siLuc) or PKN2-targeting siRNA (siPKN2) were seeded and starved in reduced serum media overnight. The following day, the CAFs were stimulated with 5ng/ml TGFβ1 or vehicle for 30 minutes. Levels of phosho-PKN1 and phospho-PKN2 (pPKN1/2), phospho-SMAD2/3 (pSMAD2/3) and protein load control GAPDH was assessed by western blotting **(i)**. Bands were quantified by densitometry using Image J tool to reveal changes in SMAD2/3 phosphorylation **(ii)**. Data represents one biological experiment carried.

3.2.3 Expression of PKN2 surrogate markers in breast cancer and their prognostic relevance

We next wished to assess whether the role of PKN2 in fibroblast activation has prognostic relevance in breast cancer. The expression of PKN2 may not itself be a useful biomarker for stromal activation, as it is known to be ubiquitously expressed in normal tissue and previous gene expression analysis showed no difference in PKN2 expression between normal tissue and breast tumours or between different breast cancer types (Section 3.1.1). Similarly, assessment of PKN2 protein expression across a panel of fibroblast lysates from breast cancer patients (provided by Iain Goulding, Breast Cancer Now Tissue Bank) showed no difference in PKN2 expression between matched protein lysates of normal and cancer-associated fibroblasts (Fig.20).

Table 9. Details of patients from which CAFs were obtained

Tissue type refers to whether the fibroblasts were obtained from normal surrounding tissue (S) or from the tumour (T). Patients had either invasive ductal carcinoma (IDC) or invasive lobular carcinoma (ILC).

Patient Number	Tissue type	Age	Tumour type	Grade	Her2	ER
1863	T	82	IDC	2	-	+
1863	S	82	IDC	2	-	
1902	T	47	IDC	3	-	+
1902	S	47	IDC	3	-	
1910	T	46	ILC	2	-	+
1910	S	46	ILC	2	-	
1939	T	79	IDC	3	-	+
1939	S	79	IDC	3	-	
1997	T	47	IDC	3	-	-
1997	S	47	IDC	3	-	

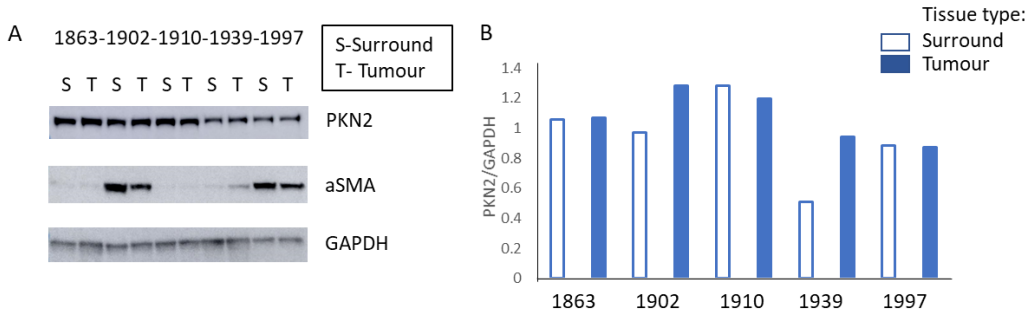

Figure 20. Protein expression of PKN2 in CAFs and normal fibroblasts from breast cancer patients

A. Western Blot showing level of PKN2, α-SMA and GAPDH protein levels. **B.** Densitometry of PKN2 bands, normalised against the loading control GAPDH to quantify the relative PKN2 expression between different patients from normal surrounding and tumour-associated fibroblasts.

Analysis of α-SMA fibres in several fibroblasts has shown reduced α-SMA fibres upon PKN2 depleted/deletion, when activated by TGFβ. However, expression of α-SMA was not detectable from the protein lysates of fibroblasts from some patients in the panel. Expression of α-SMA was detectable in fibroblasts from three of the patients, which showed different patterns between normal and cancer-associated fibroblasts. In patient 1902 and 1997, expression of α-SMA was in fact higher in fibroblasts from normal surrounding tissue compared to fibroblasts from tumour. Increased expression of α-SMA in tumour-associated fibroblasts, compared to normal fibroblasts, was shown by patient 1939. Significantly, high α-SMA did not correlate with enhanced PKN2 expression (Fig. 20). Overall, a-SMA expression appears to be variable between individual patient samples, and further, in cell lines, a-SMA was not enriched in tumour stroma, compared to surrounding stroma in individual cases. Together, this analysis indicates that PKN2 expression may not be a differential factor between normal and tumour-associated stroma.

Work on MEFs and pancreatic fibroblasts has shown similar protein expression of α-SMA in untreated and TGFβ-treated fibroblasts, despite increased α-SMA fibres in the TGFβ-treated fibroblasts, visible by immunostaining. This suggests that the amount of α-SMA may be similar between non-activated and activated fibroblasts in these models, but the amount of α-SMA that polymerise to form fibres changes. Hence, although PKN2 deletion

is associated with low α-SMA fibres, the expression levels of α-SMA may not be sufficient to differentiate normal and activated stroma.

While PKN2 expression alone does not correlate with myofibroblast phenotypes from patients, loss of PKN2 does result in a blockade in fibroblast activation in our experimental models. We therefore sought to develop a surrogate panel of markers to assess the potential effects of PKN2 suppression on the activation state of stromal fibroblasts. Examining how this surrogate panel relates to prognosis in breast cancer might then give some indication about the potential value of targeting PKN2.

3.2.3.1 Selecting surrogate markers of PKN2-related fibroblast activation

In collaboration with Ivan Quétier and Claus Jorgenson, changes in gene expression between non-activated and activated wild-type and PKN2-ko MEFs was analysed. From this, genes downregulated in stimulated PKN2 ko MEFs were selected as surrogate markers for the effect of PKN2 loss in suppressing stromal activation. MEFs were seeded on collagen gels for 3D culture and stimulated with TGFβ1 or BMP4 (another ligand of TGFβ receptors upstream of SMAD signalling) for 24, 48 and 72 h. At the end of stimulation, MEF RNA was extracted from the collagen gels using TRIzol and cDNA was generated using TaqMan (Applied Biosystems) reverse transcription. Expression levels of stromal genes was assessed using a custom Fluidigm expression assay panel in collaboration with Claus Jorgensen (Manchester CRUK).

From this data, 12 genes that showed reduced mRNA expression in PKN2 ko MEFs compared to wt MEFs, upon TGFβ1 or BMP4 stimulation, were selected as surrogate markers for PKN2 suppression and hence low activation status (Fig. 21, see appendix Fig.1, 2, 3 for excluded genes). These genes have various functions that have implications on cell survival, differentiation and interaction with ECM and are therefore relevant in cancer (Table 9).

The panel of genes was analysed for their relevance in breast cancer survival of patients. A similar study was conducted in breast cancer, using IGF-1 induced genes in primary breast fibroblasts, as the signature (Rajski et al. 2010). This IGF-1 study revealed increased likelihood of metastasis and low overall survival in patients at the early and advanced stage of breast cancer with high IGF-1 expression profile genes. Another study in pancreatic ductal adenocarcinoma (PDAC) generated two stromal signatures that distinguish between normal and activated stroma (Moffitt et al. 2015). The gene signature identified in this study for activated stroma also includes THBS2, COL1A1, FAP, CDH11, ITGA11 and POSTN in common with our signature.

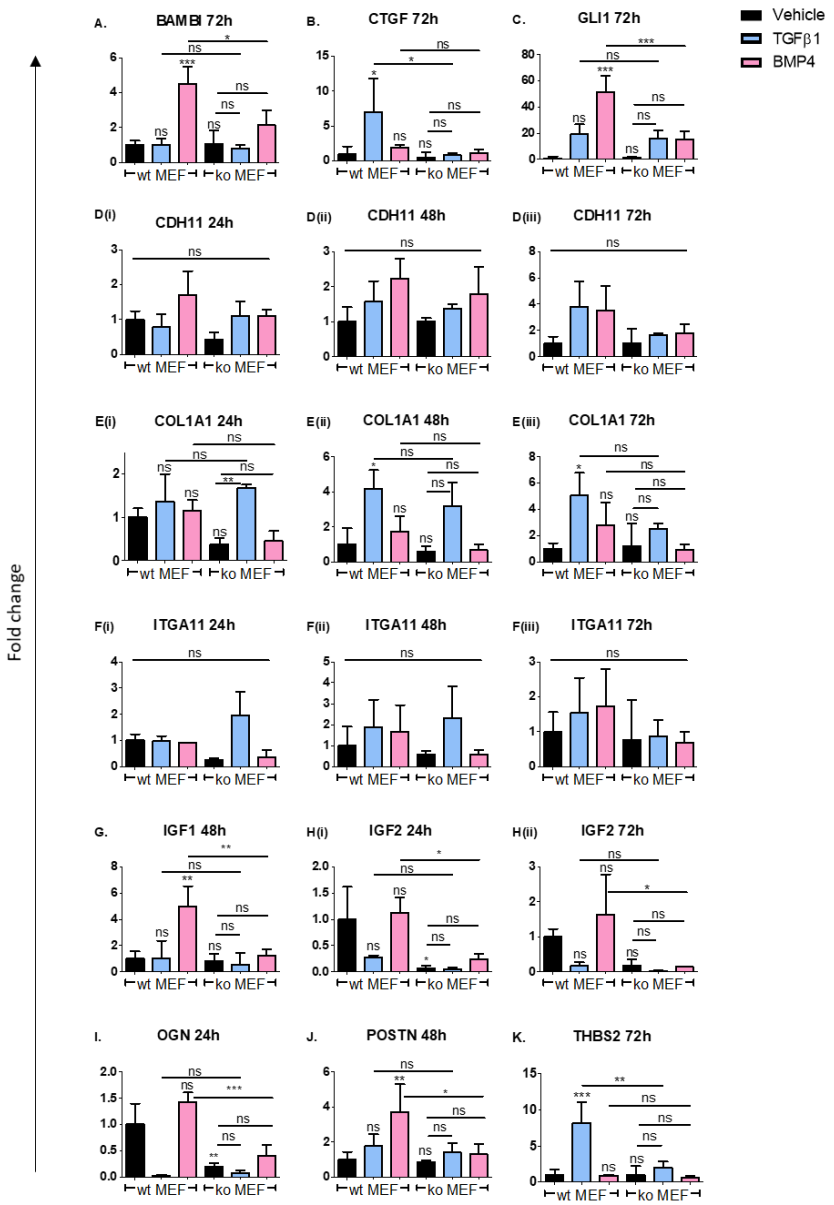

Figure 21. Changes in gene transcript levels upon stimulation in MEFs

Fold change represented is relative to wt MEFs treated with vehicle. CTGF and THBS2 showed significant reduction between wt and ko MEFs upon TGFβ stimulation (B, L). BAMBI, GLI1, IGF1, IGF2, OGN and POSTN were significantly downregulated in ko MEFs, compared to wt MEFs, when stimulated with BMP4 (A, C, G, H, J, K). CDH11 was downregulated in ko MEFs at 24h and 72h, compared to wt MEFs, when stimulated with BMP4 (Di, iii). At 24h, COL1A1 was downregulated in ko MEFs in response to BMP4 stimulation (Ei). At 48h and 72h, COL1A1 was reduced in ko MEFs in response to both TGFβ and BMP4 (Eii, iii). Gene expression of ITGA11 was reduced in ko MEFs consistently at 24, 48 and 72h in response to BMP4 (Fi, ii, iii). Although some of these markers did not reach statistical significance at specific timepoints, they were included as changes were consistent across the timecourse. Data represents the mean +/- SD for n=3 biological repeats. Statistical analysis was carried out using ANOVA followed by Bonferroni post-hoc test: P<0.05 (*), P<0.01 (**), P<0.001 (***).

Table 10. Functions of chosen surrogate markers of PKN2

Gene	Functions
Osteoglycin (OGN)	Expressed in normal breast connective tissue, compared to tumour stroma. (Bozoky et al. 2014); (Hu et al. 2018)
Insulin like growth factor 1, 2 (IGF1/2)	Produced by stromal cells in connective tissues of mammary gland. Switch from IGF1 to IGF2 synthesis seen in stromal cells of malignant mammary glands. Potential prognostic stromal marker in breast and lung cancer. (Marshman and Streuli 2002); (Yee et al. 1989); (Rajski et al. 2010)
GLI Family Zinc Finger 1 (GLI1)	Stem cell proliferation (Merchant et al. 2010). Stromal expression a prognostic predictor in breast cancer (O'Toole et al. 2011).
Cadherin 11 (CDH11)	Expressed in mesenchyme and epithelial cells that have undergone EMT. Mediates cancer invasion and metastasis (Tamura et al. 2008); (Huang et al. 2010)
Thrombospondin 2 (THBS2)	Cell-to-cell and cell-to-matrix interactions; anti-tumorigenic and anti-angiogenic (Lopes et al. 2003); (Good et al. 1990); (Streit et al. 2002)
Periostin (POSTN)	Tissue development, wound healing, epithelial cell adhesion and migration; cancer stem cell maintenance and metastasis. (Hamilton 2008); (Lambert et al. 2016)
Collagen, Type I, Alpha 1 (COL1A1)	Secreted factor in ECM. Induces EMT in hepatoma cells (Yang et al. 2014).
Integrin Subunit Alpha 11 (ITGA11)	Induces myofibroblast activation and differentiation, regulated by hedgehog signalling pathway. Highly expressed in fibrotic diseases. (Bansal et al. 2017)
Connective Tissue Growth Factor (CTGF)	Abundantly expressed in CAFs, therapeutic monoclonal antibodies developed (Xing, Saidou, and Watabe 2010). Secreted factor in TME that aids tumour infiltration (Emon et al. 2018).
BMP and activin membrane bound inhibitor (BAMBI)	Antagonizes TGF-β1 signalling (Onichtchouk et al. 1999). Effect on cancer progression differs according to cancer type (Tang et al. 2018).
Fibroblast activation protein (FAP)	Cell surface protein expressed specifically on activated fibroblasts. (Garin-Chesa, Old, and Rettig 1990)

3.2.3.2 Bioinformatic analysis to understand clinical relevance of PKN2 surrogate markers

Understanding expression patterns and correlations between the surrogate markers of PKN2 using stromal dataset from breast cancer patients.

Targeting PKN2 genetically in fibroblasts allowed us to define a panel of markers associated with PKN2 status in activated fibroblasts. We hypothesised that targeting PKN2 is likely to supress this signature and sought here to explore whether such an altered

signature might be desirable in a prognostic, or even therapeutic, setting; should low expression of these markers be associated with better disease outcome it would support efforts to target PKN2 as a potential therapy. Commonly, whole tumour samples are used to analyse gene expression for prognostic indications. This comprises both tumour cells and many other cell types found in the surrounding stroma. It is now known that the stroma in breast cancer impacts tumour progression and outcome (Finak et al. 2008); (Cleator et al. 2006); (Farmer et al. 2009). Therefore, the relevance of our surrogate PKN2 gene signature specifically in breast tumour stroma was investigated for any prognostic value.

Firstly, we examined the stromal gene expression dataset from breast cancer patients from Finak *et al* (Finak et al. 2008). Stromal tissue from patients with breast cancer with matched normal surrounding stroma was dissected using laser capture microscopy. The expression of the 12 genes in our stromal signature, in addition to PKN2, was compared between tumour-associated stroma and normal stroma. Expression of PKN2 and THBS2 did not differ between normal and tumour-associated stroma. All other genes, apart from CTGF and BAMBI, were expressed at much higher levels in tumour-associated stroma, compared to normal stroma (Fig.24). In contrast, BAMBI and CTGF are expressed at much lower levels in tumour stroma compared to normal stroma. The low expression of BAMBI, in comparison to the other genes that are activated upon TGFβ, could be explained by its inhibitory action on TGFβ signalling (Onichtchouk et al. 1999). The differential expression of the genes in the signature between normal and tumour-associated stroma indicates that the chosen genes are generally selective for activated tumour-associated stroma.

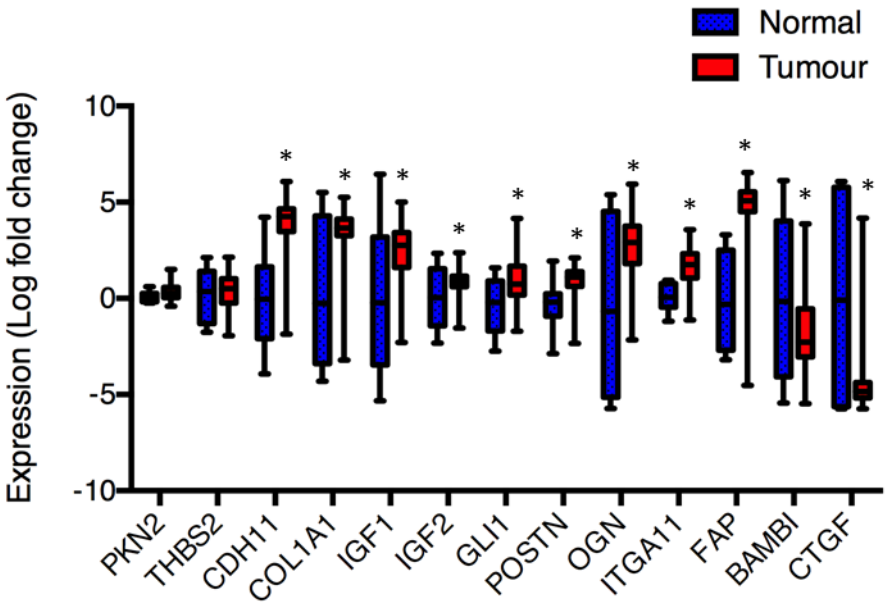

Figure 22. Expression of PKN2 surrogate markers in normal tissue and tumour stroma
Comparison of average gene expression between normal (blue bars) and matched tumour-associated stroma (red bars), using data from Finak *et al* (Finak et al. 2008). For expression statistics, GraphPad Prism's multiple t-test tool was used with false discovery rate (FDR) set at 1%. Significantly different expression between normal and tumour-associated stromal expression is indicated by * above the bar for tumour-associated stroma (red) in the compared pair P<0.05 (*).

Before investigating the prognostic relevance of our stromal gene signature in breast cancer, Pearson Product Moment Correlation Coefficient (PMCC) was applied to the Finak *et al* data to define the relationship between the genes in our signature.

In agreement with the average expression analysis, genes (except CTFG and BAMBI) in our signature mostly show positive correlation with each other in tumour-associated stroma, (Fig. 24A). In addition to CTGF and BAMBI, POSTN and THBS2 are negatively correlated with other genes in the signature in the stroma of normal tissue (Fig. 24B). However, the darker shades of red on the correlogram represent stronger correlation (higher correlation co-efficient) between the genes that are positively correlated in normal stroma. This could indicate reduced heterogeneity in normal stroma compared to tumour-associated stroma, where more genes are positively but weakly correlated. PKN2 expression, however, shows

little correlation with the signature, perhaps in line with our observation that PKN2 expression is not different between normal fibroblasts and CAFs.

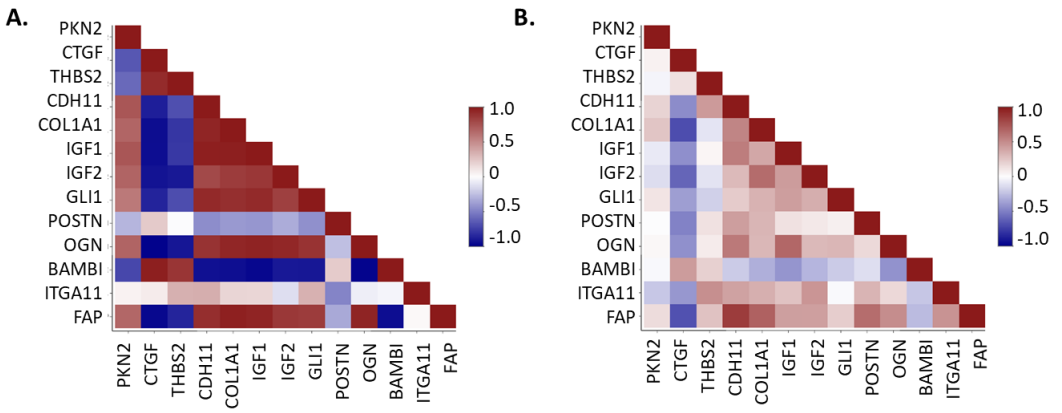

Figure 23. Correlogram demonstrating correlation between genes in the stromal signature

A. Normal stroma and **B.** Tumour-associated stromal gene expression correlogram. Key represents colour-coding according to the value of Pearson's correlation co-efficient. Data obtained from Finak *et al* (Finak et al. 2008).

The presence of stroma/desmoplasia in TNBC has been linked to bad prognosis in several studies (Moorman et al, 2012; de Kruijf et al, 2011). Interestingly, in luminal tumours, increased stromal content can predict better outcome (Downey et al. 2014) indicating that the stromal response can have both positive and negative prognostic value depending on disease type. The expression of our stromal markers in the stromal dataset from Finak *et al* was compared between TNBC and non-TNBC breast cancer stroma. More genes showed anti-correlation in the stroma of TNBC patients whilst more genes are positively correlated in the stroma of non-TNBC patients (Fig.24). This could be due to the known heterogeneity of TNBC. The anti-correlation in TNBC might suggest that expression of stroma in these patients does not follow the pattern of a PKN2 signature stroma. However, the major limitation of the dataset for TNBC cases is the low numbers (n=14).

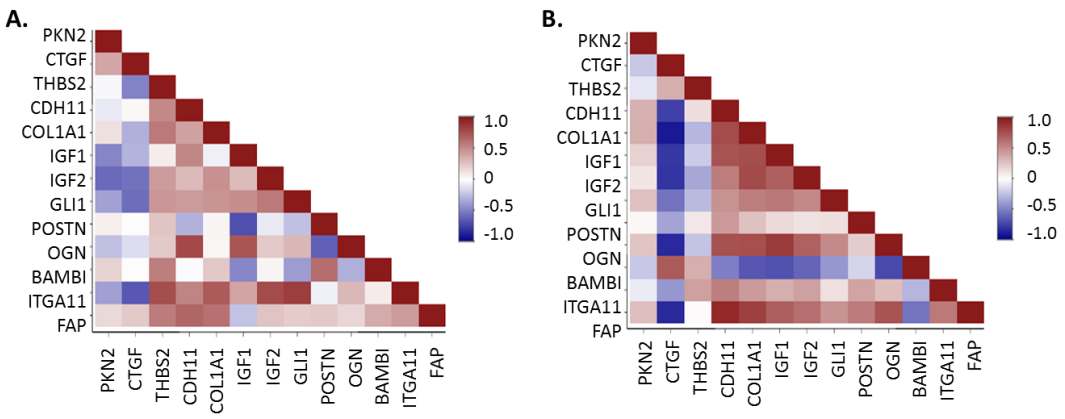

Figure 24. Correlation of PKN2 surrogate marker expression in TNBC and non-TNBC

Correlogram depicting association of genes in the signature in patients with **A.** TNBC and **B.** non-TNBC tumours. Data obtained from Finak et al (Finak et al. 2008).

Finak *et al* compared the gene expression profiles of tumour stroma with patient-matched normal tissue and identified a set of genes that were differentially expressed between the two types of tissue. Of these genes, 200 genes with the greatest difference in expression between normal and tumour stroma were used to perform cluster analysis. This resulted in three clusters, whose characteristics were related to disease outcome: good, poor and mixed outcomes (cluster 1, 2 and 3 respectively. The relevance of surrogate PKN2 marker expressions in patients in the three different clusters were investigated, alongside a comparison with the actual outcome data.

Comparing the stromal expression of genes in the signature between the different actual outcomes of patients showed significantly reduced expression of IGF1 and OGN in patients with poor outcome (Fig. 25A). These patterns of gene were also observed when considering the predicted outcome clustering by Finak *et al* (Fig. 25B), with the addition of reduced Gli1 expression in the poor outcome cluster. Interestingly, correlation analysis of the surrogate PKN2 marker genes in patients with predicted poor outcome compared with predicted good outcome shows significant differences regarding both CTGF and BAMBI; while BAMBI and CTGF anti-correlate with the signature in the good outcome cluster, BAMBI is positively

correlated, and CTGF show no correlation in the bad outcome cluster (Fig. 26). This indicates that the positive association of BAMBI with other genes in the stromal signature is linked to poor outcome. This suggests that the expression status of BAMBI relative to the other genes in the PKN2 signature may have clinical importance.

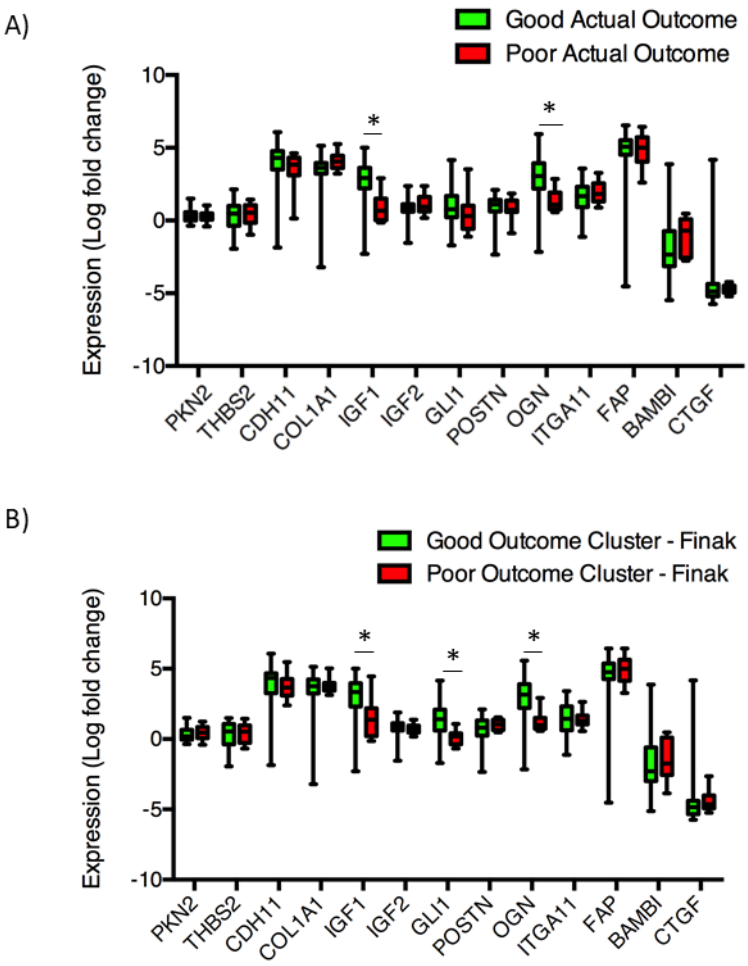

Figure 25. Gene expression in stroma of patients of different outcomes.

Comparison of stromal marker gene expression between patients according to A. actual outcome and B. Finak outcome cluster. Data obtained from Finak et al (Finak et al. 2008). For expression statistics, GraphPad Prism's multiple t-test tool was used with false discovery rate (FDR) set at 1%. Significantly different expression between good and poor outcome is indicate by *.

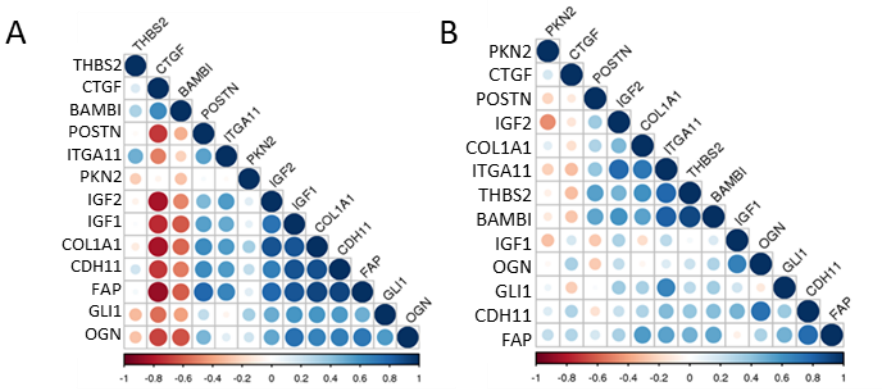

Figure 26. Correlation of PKN2 surrogate markers by predicted outcome

Correlogram depicted Pearson's correlation between genes in stromal signature. A. Patients with predicted good outcome and B. predicted poor outcome. Data obtained from Finak et al (Finak et al. 2008).

Expression profile heatmap and clustering of PKN2 surrogate markers from stromal samples of breast cancer patients

To look at the PKN2 signature genes in an unbiased way we next carry out hierarchical clustering of the Finak patient stromal samples according to their expression patterns of the 12 surrogate PKN2 genes and PKN2 (in collaboration with Professor Claude Chelala, analysis carried out by Dr Emanuela Gadaleta). This generated two clusters (here termed Cluster A and Cluster B), one of which (Cluster A) included all the patients with actual poor outcome (Fig. 27); this is a statistically significant enrichment (χ2-test -test; p=0.0003). Cluster A was moderately, but not significantly enriched for HER2-positive patients (χ2-test; p= 0.19) and - unsurprisingly given the outcome data - significantly enriched for grade 3 tumours (χ2-test -test; p=0.018). There was significant overlap with the poor outcome predicted by the clustering analysis generated by Finak et al, but importantly, our signature was significantly better at clustering the poor outcome patients from the stromal data set than the Finak panel.

We next compared the expression of the different signature genes to identify specific pattern changes. The poor outcome group was characterised by low expression of OGN

and IG1 and high expression of BAMBI (Fig. 28). Interestingly, these marker expression differences were not observed in the clustering conducted by Finak *et al.* This shows our clustering to be a powerful way of defining important prognostic differences in this dataset.

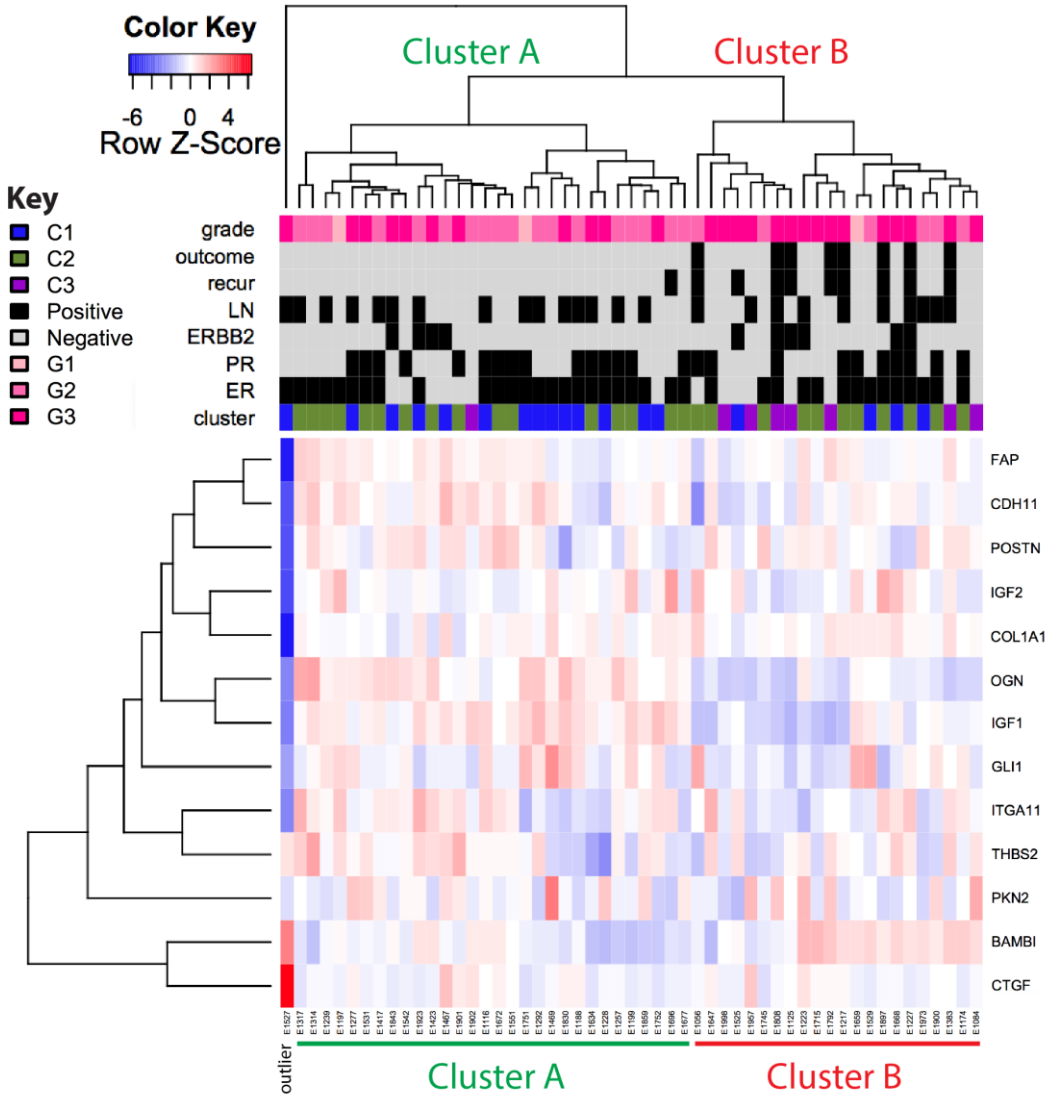

Figure 27. Expression heat map and clustering analysis of PKN2 surrogate markers in stromal dataset from Finak *et al*.

Hierarchical clustering of Finak patient stromal samples according to their expression patterns of the 12 surrogate PKN2 genes and PKN2. Patients, with the exception of a single outlier (E1527 – left most patient), cluster into two groups (A and B). Cluster B contains all patients with actual poor outcome. Abbreviations: recur (recurrence); LN (Lymph Node Spread). C1, C2 and C3 refer to clusters defined in Finak *et al* (Finak et al. 2008): C1(good); C2 (mixed); C3 (poor). G1, G2 and G3 refer to tumour grade.

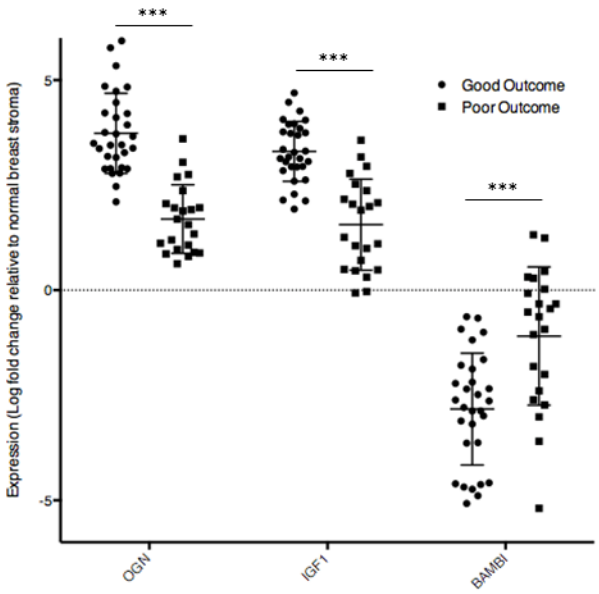

Figure 28. Comparison of protein expression between good and poor outcome.
This analysis revealed differences in OGN IGF1 and BAMBI. Expression of OGN and IGF1 is lower in patients with poor outcome. High expression of BAMBI is associated with poor outcome. Data obtained from Finak et al (Finak et al. 2008). GraphPad Prism's multiple t-test tool was used with false discovery rate (FDR) set at 5%. N=30 (good outcome), N=22 (poor outcome).

Survival analysis of OGF, IGF and BAMBI expression in the stroma of breast cancer patients

Together these data suggest that supressing OGN and IGF1 expression – potentially by targeting PKN2 - may be undesirable in breast cancer. The prognostic relevance (relapse-free survival - RFS) of these genes, as well as BAMBI - which was highly expressed in patients with poor outcome, was tested in whole tumour datasets using the online Km plot tool (Győrffy et al. 2010).

Low expression of OGN was associated with reduced RFS when considering all breast cancer data, as well as in basal and luminal A intrinsic subtypes (Fig. 29). There were no significant changes in RFS between TNBC patients with low and high expression of OGN, which was also observed in the different TNBC pietenpol classifications. These observations therefore corroborate with the finding of reduced expression of OGN in tumour stroma being clustered with patients with poor outcome.

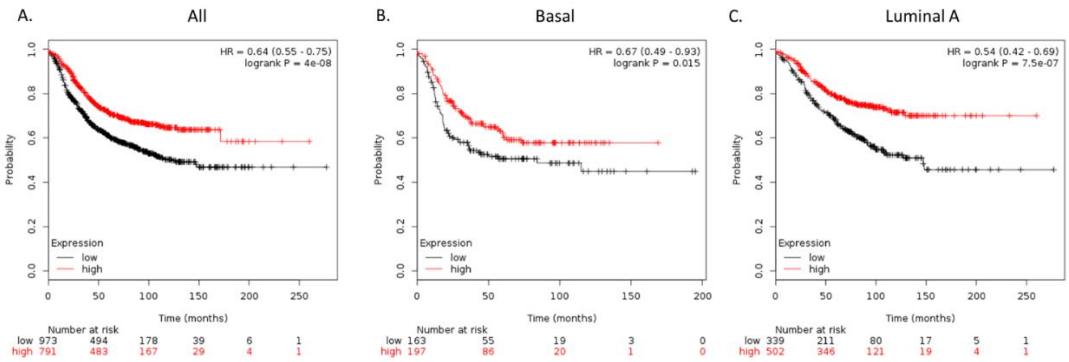

Figure 29. Effect of OGN expression on RFS

Figures show probability of relapse free survival (RFS) in patients with **A.** all, **B.** basal and **C.** luminal A subtype of breast cancer with low and high expression of OGN. Plots were generated using an online tool (Györffy et al. 2010). High and low expression threshold was selected at best cut-off for best performing threshold. Number of patients shown below plots.

IGF-1 expression is able to stratify patients into prognostic risk groups across multiple breast cancer groups (All, TN, Basal, Basal-like2 and Mesenchymal; Fig. 30). Considering all breast cancer data there is a slightly reduced RFS in patients with low IGF-1 expression up to 200 months, after which this differential is lost (Fig. 30A, $p<0.001$ HR 0.7). There is a clearer reduction in RFS in patients with basal subtype of breast cancer and low IGF-1 expression (Fig. 30C). Considering TNBC, overall patients with ER-, PR- and HER2-negative breast cancer and low IGF-1 expression had significantly reduced RFS (Fig. 30B), which was also seen when considering basal-like 2 and mesenchymal subtypes of TNBC (Fig. 30D and E). The negative effect of low IGF-1 expression on outcome seem to have more relevance in TNBC patients. Together, this analysis again correlates well with our clustering analysis of the Finak dataset on patient outcome.

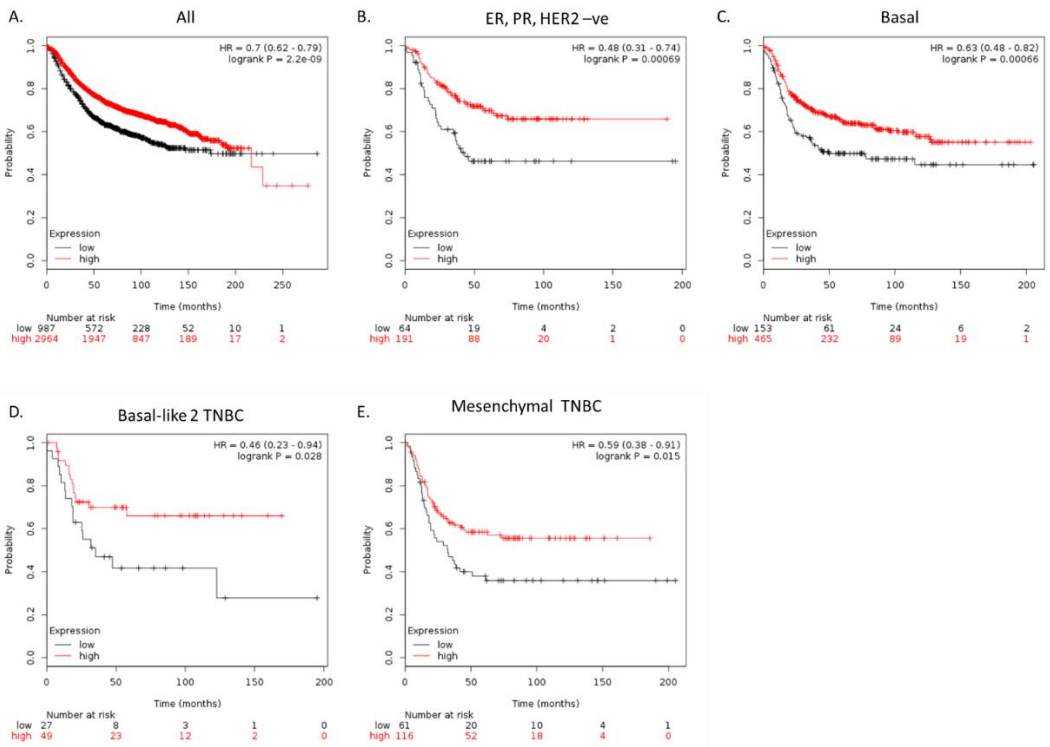

Figure 30. Effect of IGF-1 expression on breast cancer RFS
Figures show probability of relapse free survival (RFS) in patients with **A.** all, **B**. ER, PR and HER2 negative **C.** basal **D.** basal-like 2 TNBC and **E.** mesenchymal TNBC subtypes of breast cancer with low and high expression of IGF-1. Plots were generated using an online tool (Györffy et al. 2010). High and low expression threshold was selected at best cut-off for best performing threshold. Number of patients shown below plots.

Patients expressing high levels of BAMBI had reduced RFS, when considering all breast cancer patients (Fig. 31A). High expression of BAMBI is associated with improved RFS in the Her2+, Basal and the Basal-like 1 breast cancer (Fig. 31B, C and D). These observations support the finding from the stromal expression and clustering analysis. In contrast, in mesenchymal subtype of TNBC, high expression of BAMBI is related to increased RFS (Fig. 31E).

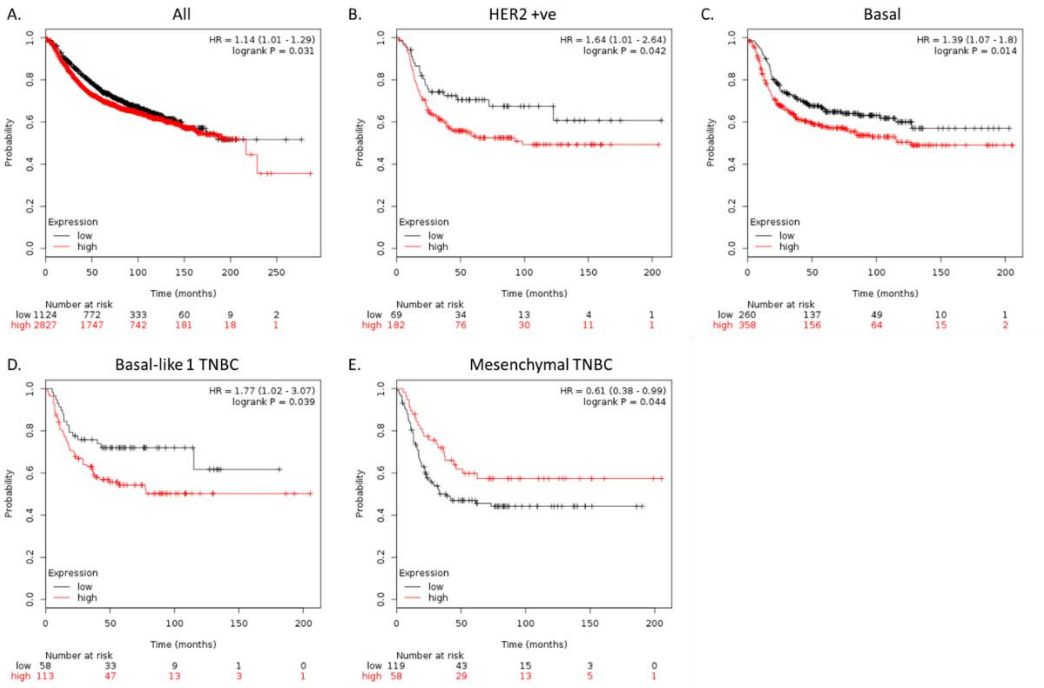

Figure 31. Effect of BAMBI expression on RFS

Figures show probability of relapse free survival (RFS) in patients with **A**. all, **B.** HER2-negative **C.** basal **D.** basal-like 1 TNBC and **E.** mesenchymal TNBC subtypes of breast cancer with low and high expression of BAMBI. Plots were generated using an online tool (Györffy et al. 2010). High and low expression threshold was selected at best cut-off for best performing threshold. Number of patients shown below plots.

In summary, clustering of stromal expression of PKN2 surrogate markers, which resulted in a cluster related to good outcome and another into poor outcome, suggests a potential importance of these genes in predicting outcome. In particular, OGN, IGF1 and BAMBI were differentially expressed between patients with poor and good outcome. Stromal OGN and IGF1 expression was lower in patients with poor outcome. This was reflected in reduced RFS when considering who breast tumour datasets, when comparing patients with low and high expression of OGN and IGF1. Expression of stromal BAMBI was higher in patients with poor outcome. This observation was reflected in RFS when considering whole tumour datasets of most breast cancer types in general. Thus, modulating OGN and IGF1 to induce expression and modulating BAMBI to suppress expression may be beneficial in breast cancer.

Expression analysis of PKN2 stromal markers in whole tumour TCGA dataset

A limitation of using the stromal dataset from Finak *et al* is the low number of samples. To address this issue and to widen the investigation of PKN2's relevance in breast cancer survival, whole tumour samples were also clustered using our surrogate signature. We acknowledge that this may be severely affected by the complex mix of cell types in these samples. We started with the TCGA dataset and studied the expression levels across different breast cancer types (in collaboration with Professor Clause Chelala, analysis carried out by Dr Emanuela Gadaleta and Dr Ai Nagano). The heat map indicates a weak association between basal breast cancer and low expression of the genes in the stromal signature (Figure 32A). Interestingly, amongst the different TNBC subtypes, BL2 and MSL tumours were associated with high expression of the surrogate markers (Figure 31B). This set of genes were also analysed for the effect on survival. There were no significant differences in breast cancer survival between patients expressing high or low levels of the PKN2 surrogate markers (Figure 33).

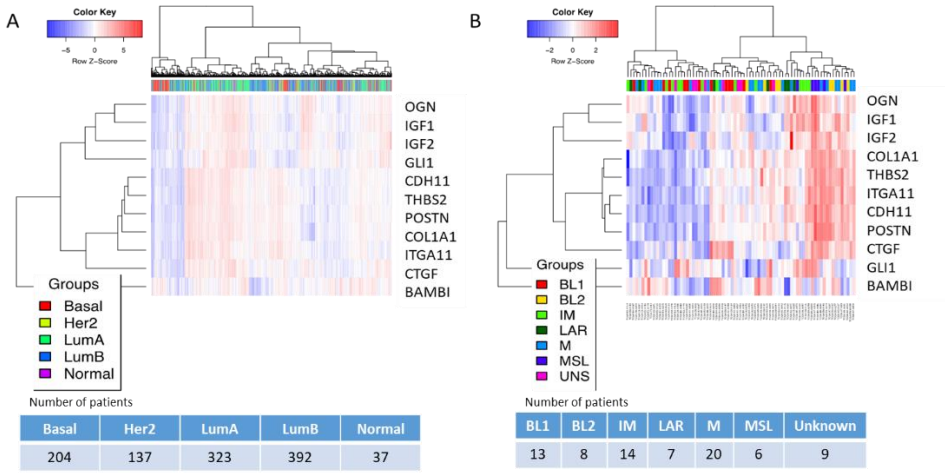

Figure 32. Hierarchical clustering of PKN2 surrogate markers' expression in whole breast tumour dataset.

Expression heat map of the 12 PKN2 surrogate markers and PKN2 analysed from whole tumour TCGA dataset in patients with **A.** basal, HER2, luminal A, luminal B breast cancer and normal tissue. **B.** The expressions of the surrogate markers were also analysed in patients with TNBC grouped by the difference TNBC subtypes.

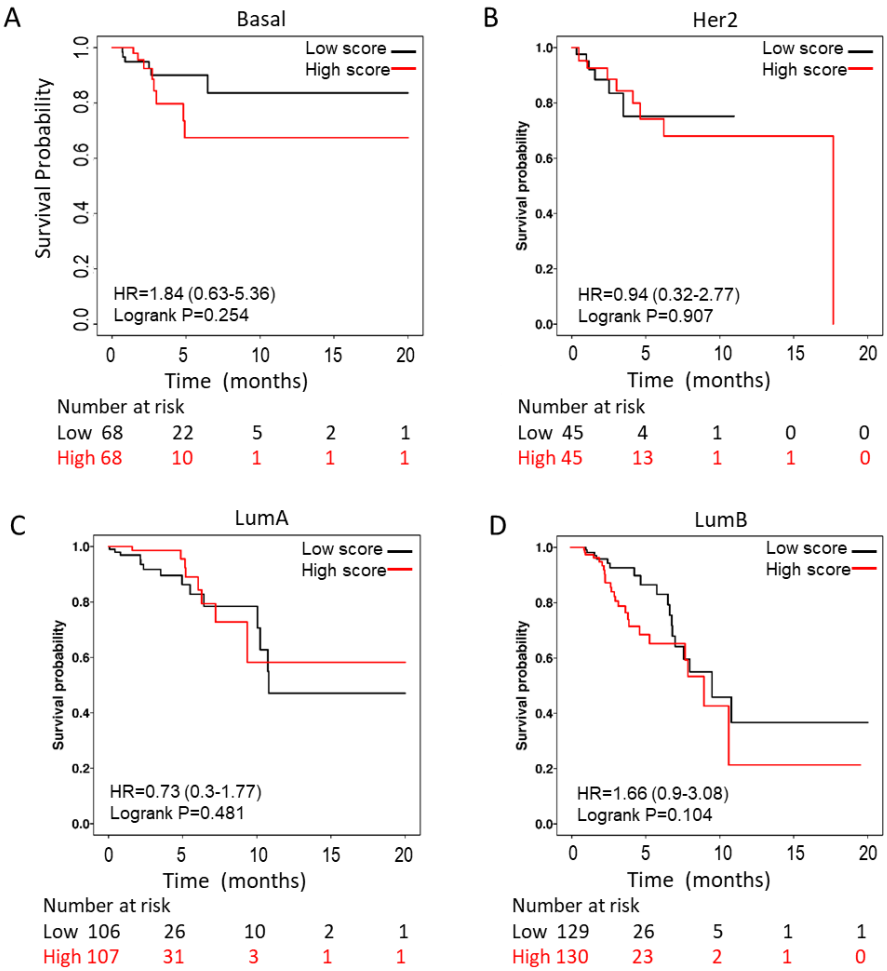

Figure 33. Survival analysis of breast cancer based on PKN2 surrogate marker expression

Based on low and high expression of PKN2 surrogate markers in A. basal, B. Her2, C. luminal A and D. luminal B breast cancers. Patients were assigned to risk groups based on the median dichotomisation of mRNA expression intensities. Number of patients shown below plots.

Thus, data from analysing the expression of surrogate PKN2 markers in whole tumour datasets, suggests enrichment in mesenchymal/basal-like subtypes of TNBC, that may be reflective of increased stromal activation in these subtypes. Survival analysis of this dataset showed no implication of global expressions of these surrogate markers on RFS. However, these surrogate markers are specific for stromal expression and therefore any potential effects on outcome may be diluted by other cancer cell types in whole tumour datasets.

3.2.4 Summary

The induction of α-SMA fibres upon long-term TGFβ1 stimulation in fibroblasts, a marker of activation, was assessed and compared between wt and PKN2 deleted or depleted fibroblasts. PKN2 loss in MEFs reduced the induction of α-SMA-expressing cells upon TGFβ1 treatment. There was also a reduction in the induction of α-SMA-expressing cells in PKN2-depleted CAFs upon TGFβ1 treatment. This indicates a role of PKN2 in fibroblast activation, which has an impact on several aspects of tumour biology including proliferation, invasion and progression.

Similar experiments in mouse pancreatic stellate cells (pancreatic fibroblasts), by Elizabeth Murray in our lab, showed reduced α-SMA fibres in PKN2 deleted cells (KO) upon TGFβ1 stimulation, compared to unstimulated and stimulated wt cells (figure 34). Furthermore, an RNAi screen by our collaborator (Claus Jorgensen, CRUK Manchester) identified PKN2 as a top hit kinase for TGFβ1-mediated activation of pancreatic fibroblasts. Together these data appear to indicate a conserved role for PKN2 in the activation of fibroblasts from multiple tissues, including the breast, pancreas and during embryo development.

We next sought to understand the mechanism that underlies the function of PKN2 in fibroblast activation. As a starting point, we examined acute signalling pathway downstream of TGFβ1 stimulation in several modes. Overall, MEFs, HMU19 fibroblasts and CAFs retained their canonical SMAD signalling in response to acute TGFβ1 stimulation. The phosphorylation of SMAD2 and SMAD3 was induced, in response to acute TGFβ1 treatment in these fibroblasts, regardless of their PKN2 expression levels. This implies that the defect in TGFβ1 responsiveness does not result from loss of TGFβ1 receptors or their proximal coupling to canonical signalling cascades.

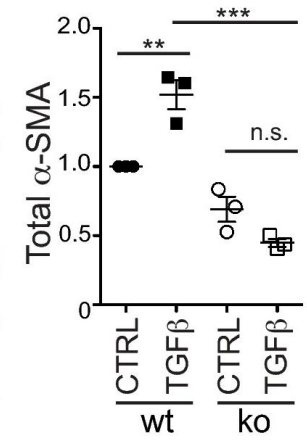

Figure 34. SMA fibre quantification in mouse pancreatic stellate cells.

Pancreatic stellate cells, wild-type (wt) or with PKN2 knockout (ko) were treated with TGFβ or untreated (CTRL) for 72h. Cells were fixed and stained for αSMA and quantified. Experiment and quantification done by Elizabeth Murray in collaboration with Nuria Gavaria. The values normalized to wt CTRL cells are shown for three biological cells carried out in duplicate coverslips. Data represents the mean +/- SD. Statistical analysis was carried out using ANOVA followed by Bonferroni post-hoc test: P<0.05 (*), P<0.01 (**), P<0.001 (***).

Although acute TGFβ1 was unaffected by PKN2 loss, other related signalling pathways may be affected. Quantitative mass spectrometry (MS) analysis and KSEA of serum-induced activation of MEFs revealed differences between wt and PKN2 ko MEFs in phosphorylation of proteins that have been associated downstream of TGFβ1 (Quétier et al. 2016). This includes downregulation of p70S6K (Fig. 35A) and upregulation of YAP (Fig. 35B). Therefore, the phosphorylation of these proteins can be assessed in response to TGFβ1 upon PKN2 loss.

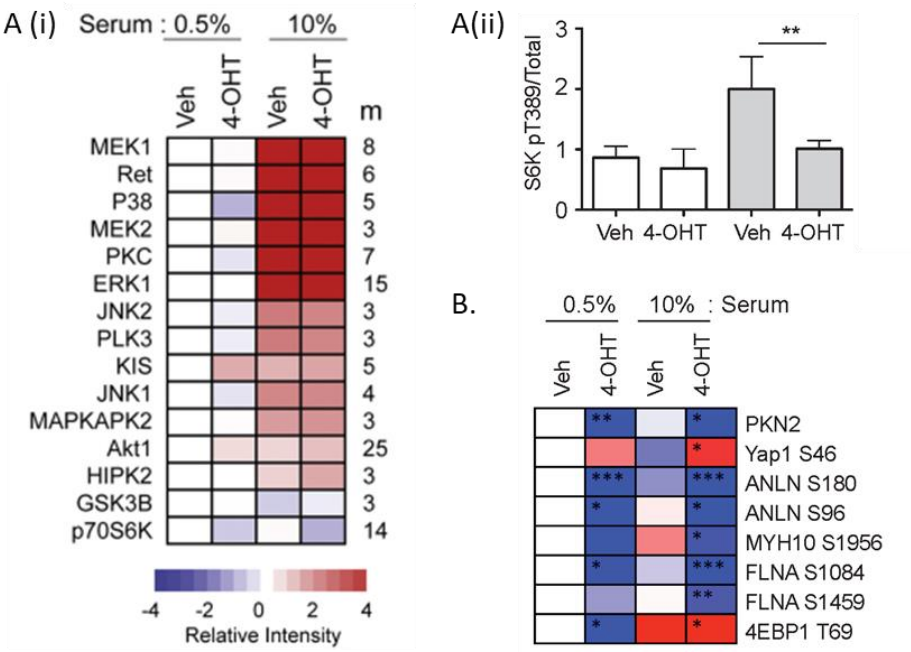

Figure 35. Quantitative mass spectrometry (MS) analysis and kinase substrate enrichment analysis (KSEA) following activated wt (Veh) and PKN2 ko (4-OHT) MEFs in response to serum. This experiment investigated the effect of PKN2 expression in stimulating MEFs. A, B (i) MEFs were serum starved (0.5% FBS) and re-stimulated (10% FBS) for 15 minutes prior to LC-MS/MS analysis (n = 4). m is the number of kinase substrate peptides quantified, relative to control extracts. *(Quétier et al. 2016)* . A(ii) Phosphorylation level of p70 S6K, relative to total protein in non-stimulated (white bars) and serum-stimulated (grey bars) wt (Veh) and PKN2-deleted (4-OHT) MEFs, determined by western blot (n=3) and quantified using densitometry.

Subsequently, the ability of PKN2-deleted MEFs to mediate translocation of the SMAD2/3/4 complex to the nucleus can be assessed. Furthermore, SMAD reporter cell lines have been generated in the lab to investigate the potential of transcriptional regulation and activation by the SMAD2/3/4 complex, in PKN2-deleted MEFs.

These studies suggest a role for PKN2 in fibroblast activation. Next, we wanted to see whether PKN2 in the stroma has any effect on breast cancer survival. PKN2 deletion was associated with reduced fibroblast activation, when assessing αSMA fibres in our fibroblast models. As PKN2 cannot solely be responsible in modulating stromal phenotypes, a panel of surrogate markers that accompany the phenotype of reduced stromal activation state upon PKN2 deletion was chosen. These genes were investigated for expression profiles and

prognostic relevance in breast cancer, considering both whole tumour datasets and stromal datasets only.

Expression of the surrogate markers of PKN2 were differentially expressed in normal and tumour stroma. Clustering analysis of the stromal dataset from Finak *et al*, based on the 12 surrogate PKN2 markers revealed two clusters, one of which (Cluster B) contained all the patients with actual poor outcome. This new cluster was also enriched for patients with predicted poor outcome, according to the gene signature used by Finak *et al*. Of the 13 genes, the expression of OGN, IGF-1 and BAMBI were differentially expressed between these two newly defined good and bad outcome clusters (Fig. 28)

The effect of OGN, IGF-1 and BAMBI expressions individually followed similar pattern that was observed with the clustering analysis, based on the predictive outcome clustered by Finak *et al*. This indicates that modulating the expression of these genes may have potential as therapeutic targets in breast cancer stroma.

Overall, data in this chapter support the fact that PKN2 suppression reduces fibroblast activation. The prognostic relevance of this phenotype was investigated by examining the expression of PKN2 and a panel of surrogate markers associated with reduced fibroblast activation upon PKN2 loss, in stromal and whole tumour breast cancer datasets. In the stroma, clustering identified two groups, defined by good and bad outcome - with differential expression of OGN, IGF and BAMBI between the two groups. In the stroma, low expression of OGN and IGF1, along with high expression of BAMBI, was associated with poor outcome. These observations were corroborated in survival analysis (RFS) of whole tumour datasets, in breast cancer overall. Thus, supressing PKN2 may normalise stroma to improve breast cancer survival, however the suppression of OGN and IGF1 may not be beneficial.

3.3 Exploring a role for PKN2 in stromal fibroblast regulation of breast cancer cell phenotypes

Studies in our laboratory on the role of PKN2 in embryogenesis suggest a role in the regulation of EMT and mesenchymal cell growth and contractility (Quétier et al. 2016). These roles appear to be conserved in various fibroblast lines and in mesenchymal TNBC cell lines. This prompted us to broaden our studies to examine the role of PKN2 in breast cancer stromal fibroblasts (CAFs) and to ask whether modulating PKN2 might alter interactions with breast cancer cells. CAFs play an important role in supporting breast cancer growth and invasion and have also been shown to affect chemotherapeutic drug sensitivity ((Cohen et al. 2017), (Orimo and Weinberg 2006), (Tao et al. 2017)). In a related project on pancreatic cancer, deletion of PKN2 from pancreatic fibroblasts (pancreatic stellate cells), reduced their ability to support pancreatic cancer cell invasion in 3D collagen-matrigel gels. Here we sought to see if similar mechanisms might occur in breast cancer.

3.3.1 Does PKN2 modulate fibroblasts to support breast cancer cell growth, migration and invasion in 3D cultures?

To mimic the physiological environment and interactions between different cell types, we co-cultured breast cancer cells lines with fibroblasts in 3D mini-organotypic assays. The effect of PKN2 depletion in fibroblasts on the interaction with breast cancer cells was initially studied using MEFs obtained from our inducible PKN2 conditional knockout mice (Rosa26 Cre ERT2 PKN2^{flox}). As described in section 2.5 and 3.1.1.3. these cells allow us to delete PKN2 expression completely and thus provide useful surrogate to explore effect of stromal PKN2 loss.

Untreated MEFs (wt MEFs) or MEFs induced for PKN2 deletion (PKN2 ko MEFs) were co-seeded with mouse breast cancer cell lines to study their interaction in mini-organotypic gels. At endpoint, the gels are fixed, paraffinized, sectioned and stained with H&E to

visualise the cells. H&E images can be used for quantification, by converting the H&E stained areas to black pixels. The quantification of the area occupied by black pixels therefore gives an unbiased indication of the area occupied by cells within the gel. In addition, the invading cells can be quantified individually to give invasive cell counts. Here, I will describe the interaction between MEFs and four different mouse cancer models: 4T1, mBBC#4 (BlgCre $p53^{fl/fl}$ $Brca1^{fl/fl}$ basal model), E0771 and PyMT.BO1 (MMTV-PyMT derived).

3.3.1.1 Effect of PKN2 expression in MEFs on 4T1 breast cancer cells in 3D mini-organotypic co-culture assays

4T1 breast cancer cell lines were originally derived from a spontaneous breast cancer model in BALB/cfC3H mice (Dexter et al. 1978). These cells are well known to metastasise to the liver, bone and lungs and are therefore used to study metastatic breast cancer progression (Heppner, Miller, and Shekhar 2000). 4T1 cells are considered as TNBC, express the epithelial markers E-cadherin and ZO-1 but also exhibit some mesenchymal cell characteristics, such as high invasive potential (Ferrari-Amorotti et al. 2014).

4T1 cells were cultured alone or co-cultured with wt or PKN2 ko MEFs, for four days in collagen-matrigel gels. H&E stains reveal that interaction between 4T1 and MEFs is required for efficient cell invasion (Fig.36 Aii, iii), whereas no cells have invaded the gel when 4T1 cell were seeded alone (Fig. 36Ai). This is supported by the cell counts of invading cells in each condition (Fig. 36B ii). Furthermore, there is a significant decrease in invading cells when 4T1 cells are co-cultured in PKN2-deleted MEFs, compared to co-culture in wt MEFs. This suggests that loss of PKN2 in MEFs affects cell invasion in this model.

Gels were fixed, sectioned and stained (by Elizabeth Murray) with cytokeratin to identify the proportion of cancer cells in the co-culture conditions. Staining indicated that the

majority of cell are invading epithelial cancer cells (Fig. 36C). Positive identification of fibroblasts was more difficult as mesenchymal markers are also expressed by subsets of cancer cells; 4T1 cells have been shown to exhibit mesenchymal phenotypes and can undergo EMT. We were unfortunately unable to conclusively stain the co-cultured fibroblasts unambiguously.

3.3.1.2 Effect of PKN2 expression in MEFs on mBCC#4 breast cancer cells in 3D mini-organotypic co-culture assays

Mouse breast cancer cell mBCC#4 (A kind gift from Prof. Matt Smalley, Cardiff University), originate from BlgCre $p53^{fl/fl}$ $Brca1^{fl/fl}$ mice described by Molyneux et al (Molyneux et al. 2010). This model was developed to investigate whether the deletion of BRCA1 in the luminal mammary epithelium (where Blg promoter is most active) results in basal-like BRCA1 breast cancer (Molyneux et al. 2010). Tumours generated from Blg-Cre Brca1f/f p53-/+ mice are generally invasive ductal carcinomas of no special type, of histological grade 3. These tumours are positive for the K14, K14 and the basal marker p63. Thus, histologically and immunohistochemically, these tumours closely resemble basal-like BRCA1 tumours in humans.

After 11 days of culture in organotypic gels, the addition of MEFs was once again found to enhance growth. Further, there was a small decrease in cell pixel area when mBCC#4 cells were co-cultured with PKN2 ko MEFs, compared to wt MEFs (Fig. 37Bi). Further examination is required to identify whether this phenotype is due to the reduced survival of PKN2-deleted MEFs or due to reduced cancer cell survival. However, there were no changes in the number of invading cells between the different conditions (Fig. 37 Bii).

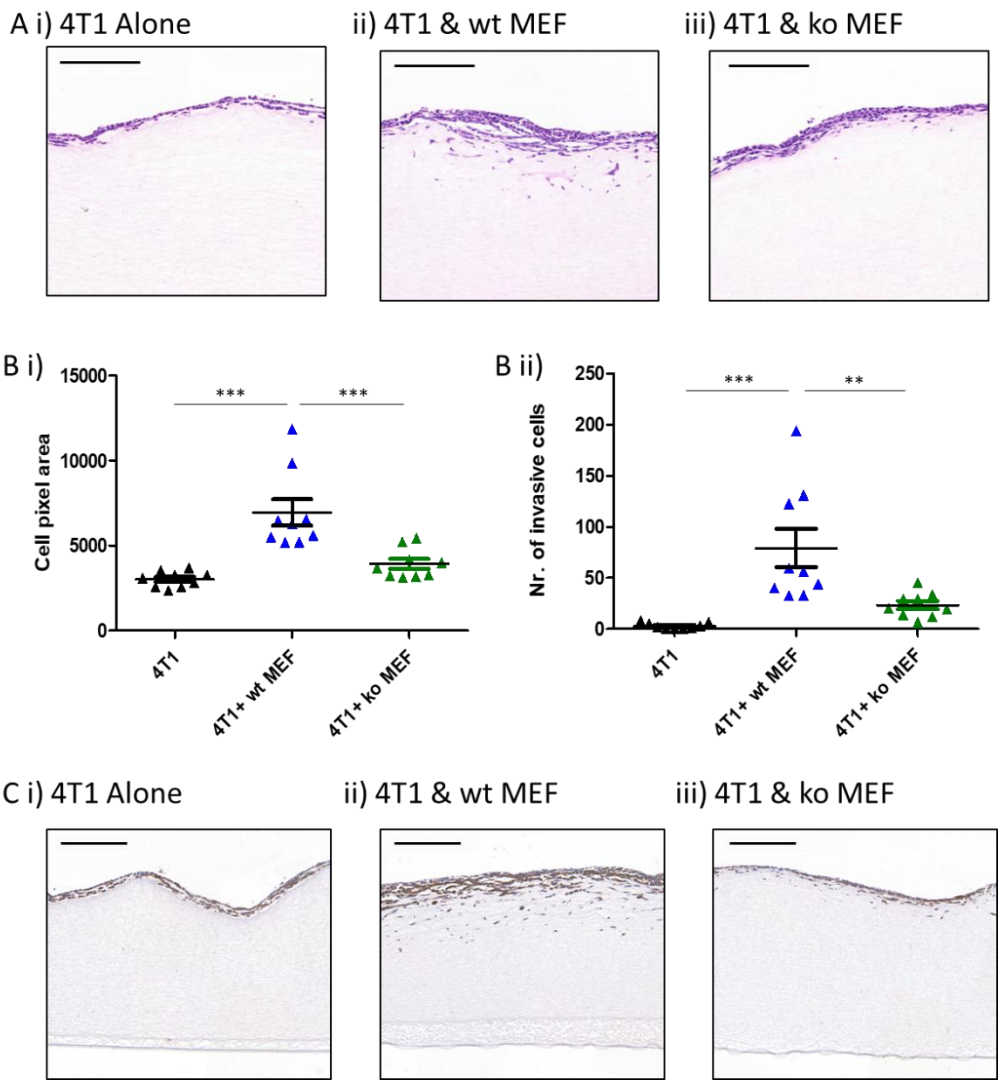

Figure 36. 4T1 & MEF 3D collagen-matrigel assay

A. H&E images of collagen/Matrigel gels seeded with i) 4T1 cells alone or co-cultured with ii) wild-type (wt) MEFs or iii) PKN2 ko MEFs. These images were converted to a binary image, to quantify Bi) total area occupied by black pixels (H&E stained area) and ii) number of invading cells using Image J software. Two to three replicate gels were seeded per condition, where two or three sections of gels (1cm in length) per replicate within a condition was quantified. C. IHC staining for pan-cytokeratin to identify 4T1 cancer cells (Elizabeth Murray). Scale bars represent 200 µm. Data represents the mean +/- SD for n=3 biological repeats carried out in triplicates. Statistical analysis was carried out using ANOVA followed by Bonferroni post-hoc test: $P<0.05$ (*), $P<0.01$ (**), $P<0.001$ (***).

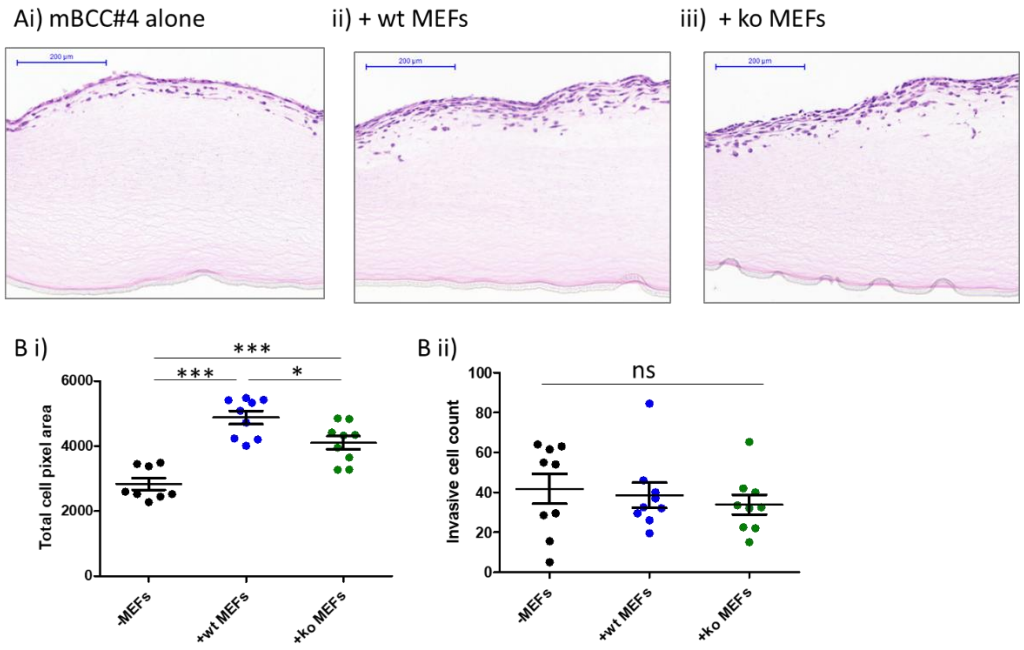

Figure 37. mBCC#4 & MEF 3D collagen-matrigel gels
A. H&E images of collagen/Matrigel gels seeded with **i)** *mBCC#4* cells alone or co-cultured with **ii)** wild-type (wt) MEFs or **iii)** PKN2 ko MEFs. These images were converted to a binary image, to quantify **Bi)** total area occupied by black pixels (H&E stained area) and **ii)** number of invading cells using Image J software. Three replicate gels were seeded per condition, where two or three sections of gels (1cm in length) per replicate within a condition was quantified. Data represents the mean +/- SD for n=3 biological repeats carried out in triplicates. Statistical analysis was carried out using ANOVA followed by Bonferroni post-hoc test: P<0.05 (*), P<0.01 (**), P<0.001 (***).

3.3.1.3 Effect of PKN2 expression in MEFs on E0771 breast cancer cells in 3D mini-organotypic co-culture assays

E0771 is a basal-like breast cancer cell line, derived from spontaneous mammary tumours in C57BL/6 mouse (Sugiura and Stock 1952). There were no differences in total cell pixels between co-cultures with wt MEFs and PKN2 ko MEFs (Fig. 38A and 38B), and growth of these cultures was not promoted significantly by the inclusion of MEFs. Further, under the tested conditions, cancer-fibroblasts interaction did not result in cell invasion. These cells did not penetrate and invade into the gels. This implies that the fibroblasts do not enhance growth or invasion of E0771 cells and that this interaction is also unaffected by loss of fibroblast PKN2 expression.

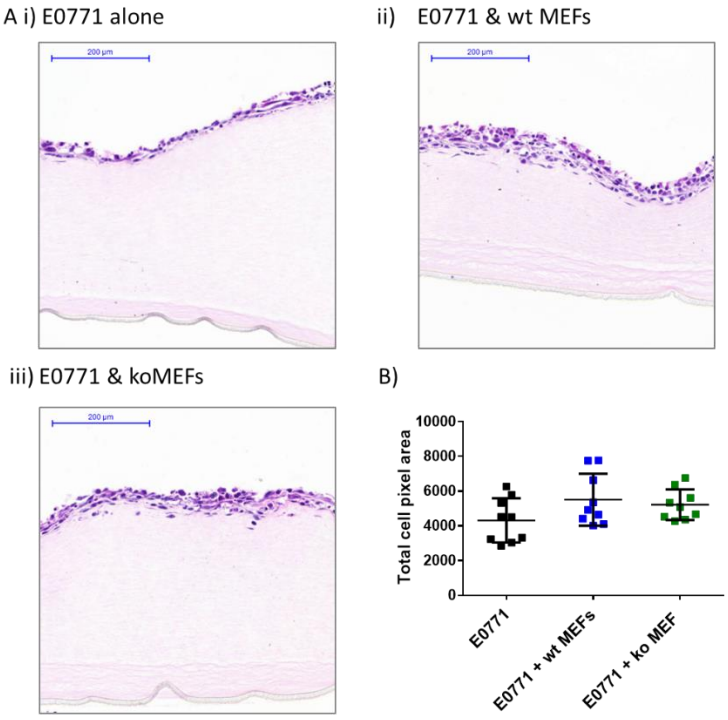

Figure 38. E077 & MEF 3D Collagen-matrigel assay.
A. H&E images of collagen/Matrigel gels seeded with **i)** *E0771* cells alone or co-cultured with **ii)** wild-type (wt) MEFs or **iii)** PKN2 ko MEFs. These images were converted to a binary image, to quantify **B.** total area occupied by black pixels (H&E stained area). Data represents the mean +/- SD for n=3 biological repeats carried out in triplicates. Statistical analysis was carried out using ANOVA followed by Bonferroni post-hoc test: P<0.05 (*), P<0.01 (**), P<0.001 (***).

3.3.1.4 Effect of PKN2 expression in MEFs on PyMT-BO1 breast cancer cells in 3D mini-organotypic co-culture assays.

PyMT-BO1 cells are a subline derived from the MMTV-PyMT breast cancer model, isolated from bone metastases (Su et al. 2016) (see section 1.1.6.4). MMTV-PyMT is a genetic mouse model where tumour formation is induced by MMTV promoter driven expression of the Polyoma Middle T-antigen (PyMT) specifically in breast epithelial cells. These cells originate from C57BL/6 mice and thus were subsequently employed in *in vivo* tumour study in this project, where syngeneic C57BL/6 lines were required. Female mice form multifocal tumours in their mammary glands, which progress to metastatic disease (Guy,

Cardiff, and Muller 1992b). PyMT-BO1 cells are characterised as luminal-like breast cancer cells.

Collagen-matrigel organotypic assays with these cells has shown large variation in behaviour. Overall, there no significant differences in total cell pixel area between wt MEFs and PKN2 ko MEFs (Fig. 39Bi). There were no differences upon PKN2 loss in MEFs in the number of invading cells into the gel (Fig. 39Bii).

Although mini-organotypic assays provide a 3D physiological setting to study cancer cell and fibroblast interaction, this assay also has its limitations. This assay has a high degree of variability (as observed with the PyMT-BO1 cell line), quantitation is complex and the protocol requires adaption for different cell models. Additionally, the assay is costly in terms of both reagents and time. Furthermore, differentiating between distinct cell populations by requires staining for epithelial and mesenchymal marker that presented with technical challenges in some cases. For this reason, we sought to develop more easily quantifiable models for measuring the heterotypic interactions between cancer cells and fibroblasts.

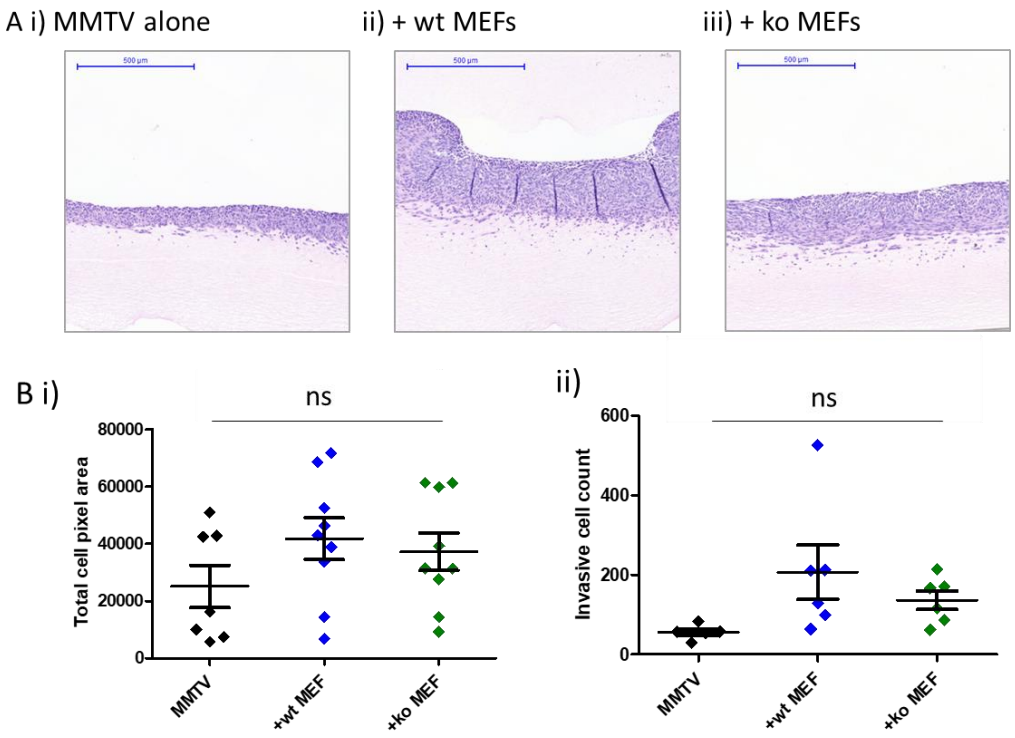

Figure 39 PyMT-BO1 & MEF 3D collagen-matrigel assay

A. H&E images of collagen/Matrigel gels seeded with **i)** PyMT-BO1 cells alone (MMTV) or co-cultured with **ii)** wild-type (wt) MEFs or **iii)** PKN2 ko MEFs. These images were converted to a binary image, to quantify **B.** total area occupied by black pixels (H&E stained area). Data represents the mean +/- SD for n=3 biological repeats carried out in triplicates. Statistical analysis was carried out using ANOVA followed by Bonferroni post-hoc test: P<0.05 (*), P<0.01 (**), P<0.001 (***).

3.3.2 Developing new *in vitro* models to explore cancer-fibroblast interaction

Due to the limitations of mini-organotypic assay mentioned above, we sought to develop a higher throughput luminescent system to study the interaction between cancer cells and fibroblasts in 2D and 3D cultures. To achieve this, a panel of cancer cell lines expressing firefly luciferase (FFL) reporter and fibroblast cell lines expressing Renilla luciferase (RL) reporter were generated. These cells were co-cultured, in 2D and 3D, and the cell viability of the cancer cells and fibroblasts was measured using a dual luciferase reporter system (Promega). Labelling the cancer and stromal components (fibroblasts) of these co-cultures allows the study of both compartments independently but simultaneously in co-culture.

Initial studies involved seeding firefly luciferase-expressing cancer cells with non-labelled MEFs from our inducible PKN2 conditional knockout mice. MEFs were untreated (wt MEFs) or pre-treated with 4-hydroxy tamoxifen (4-OHT) to induce PKN2 knockout (PKN2 ko MEFs) before co-culturing with labelled cancer cells. Cells were seeded on 96 well plates, as for standard 2D culture, or on top of small collagen and/or matrigel gels for 3D culturing. After 72h, cell viability of the labelled cancer cells (in mono-culture or within co-cultures with MEFs) was measured using the single luciferase assay (Fig. 40).

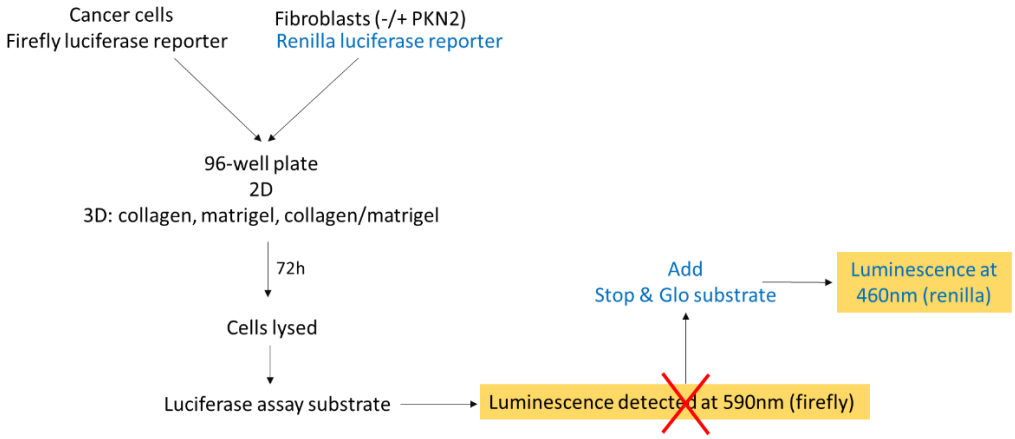

Figure 40. Schematic of single/dual luciferase assay protocol

Cancer cells, labelled with firefly luciferase reporter are cultured alone or with unlabelled/renilla luciferase reported-labelled fibroblasts (with/without PKN2 deletion). The cells are cultured in 96-well plates for 72hours, before lysing the cells to assay for the firefly luciferase activity (luminescence detected at 590nm. The viability of fibroblasts in co-culture with the cancer cell can be identified by adding a Stop & Glo substrate that quenched the firefly signal from cancer cells, allowing the activity of renilla luciferase to be detected by luminescence at 460nm.

3.3.2.1 Luciferase reporter assay to assess effect of PKN2 expression in fibroblasts on cancer cell viability

Two mouse breast cancer cell lines PyMT-BO1 and 4T1 were labelled with firefly luciferase reporter for the mouse co-culture models. Proliferation of PyMT-BO1 cells proved to benefit dramatically from the presence of either wt and PKN2 ko MEFs in 2D and 3D culture (Fig. 41). Interestingly, Matrigel provided significant support to PyMT-BO1 cell proliferation in mono-culture, and consequently limited the growth enhancing effect of co-culture with

fibroblasts (Fig. 41B). This is likely to be explained by the presence of extracellular matrix proteins and growth factors within Matrigel (Vukicevic et al. 1992), which in co-culture are provided by fibroblasts. These observations correlated with the behaviour seen in the organotypic assays.

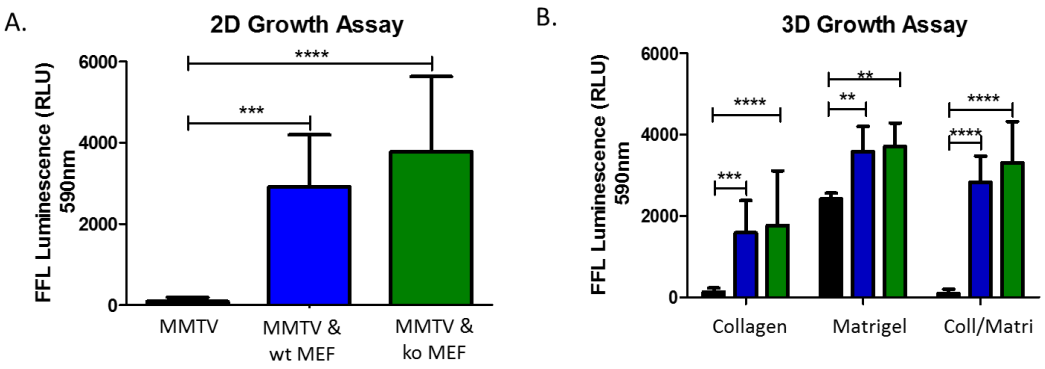

Figure 41. Effect of PKN2 expression in MEFs on PyMT BO1 cancer cells using luciferase reporter assays

PyMT-BO1 (MMTV) cells labelled with firefly luciferase (FFL) reporter were seeded **Ai)** under normal 2D conditions or **ii)** on top of gels for 3D conditions alone (black), co-cultured with wt MEFs (blue) or with ko MEFs (green). After three days, lysates were collected and assayed for the activity of the firefly luciferase reporter from the cancer cell using the Promega luciferase assay. Raw arbitrary values (RLU) are presented. Data represents the mean +/- SD for n=3 biological repeats carried out in triplicates. Statistical analysis was carried out using ANOVA followed by Bonferroni post-hoc test: $P<0.05$ (*), $P<0.01$ (**), $P<0.001$ (***).

In contrast, 4T1 cells showed no proliferative enhancement in the presence of MEFs and no difference with PKN2 ko MEFs (Fig. 42A, B). This result was surprising, as the increase in total cell number seen with mini-organotypic gels in the co-culture conditions was dramatic and significantly attenuated upon PKN2 loss in MEFs. The direct interaction of 4T1 cells with fibroblasts in mini-organotypics may result in pre-conditioning of MEFs by 4T1 cells, which are known to release TGFβ and other factors that activate fibroblasts (Nam et al. 2008). Therefore, we tested whether activating MEFs, prior to co-culture, might have a positive effect on 4T1 viability. MEFs were pre-activated with TGFβ1 for 72 hours before co-culturing with 4T1 cells for another 72h (Fig. 42C). However, activated MEFs also had no impact on

their interaction with 4T1 cells suggesting that the basal activation status of MEFs has no effect on 4T1 cell viability or proliferation. The effect of 4T1-MEF interaction on 4T1 survival was tested in 3D conditions. Cells were seeded on top of collagen (Fig. 42C), Matrigel (Fig. 42D) or a mixture of these gels (as used in mini-organotypic assays – Fig. 42E). The survival of 4T1 cells were also not affected by the co-culture of fibroblasts or PKN2 expression in MEFs under these 3D conditions. Matrigel closely mimics the ECM and is supplemented with growth factors (Vukicevic et al. 1992). The absence of enhanced cancer cell survival in the presence of fibroblasts, when seeded in Matrigel, suggests that 4T1 are self-sufficient for their survival, perhaps via autocrine secretion of growth factors.

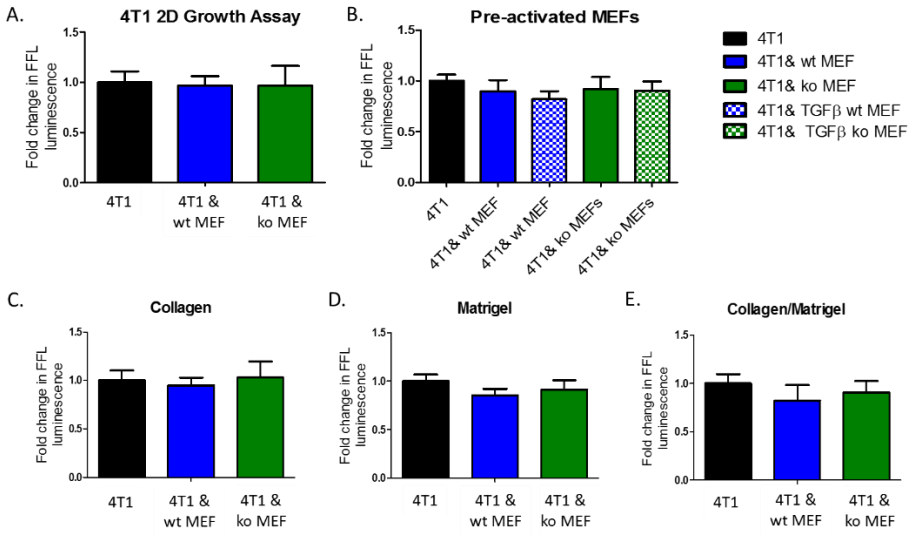

Figure 42. Effect of PKN2 expression in MEFs on 4T1 cancer cells using luciferase reporter assays
4T1 cells labelled with firefly luciferase (FFL) reporter were seeded **A.** under normal 2D conditions. **B.** wt and ko MEFs were pre-treated with 5ng/ml TGFβ1 for three days to activate them prior to seeding with 4T1 cells in 2D culture. The mono-culture of 4T1 and co-cultures with wt and ko MEFs were seeded on top of 40µl of **C.** collagen, **D.** matrigel and **E.** a mixture of collagen and matrigel as for mini-organotypic assays. After three days, lysates were collected and assayed for the activity of the firefly luciferase reporter from the cancer cell using the Promega luciferase assay. Data represents the mean +/- SD for n=3 biological repeats carried out in at least triplicates. Statistical analysis was carried out using ANOVA followed by Bonferroni post-hoc test: P<0.05 (*), P<0.01 (**), P<0.001 (***).

Subsequently, the viability of MEFs in these co-cultures was investigated. MEFs labelled with a renilla luciferase reporter were cultured alone or with firefly luciferase-labelled 4T1 for 72 hours before measuring cell viability. A dual luciferase assay kit (Promega) was used to obtain the differential signals from the two cell populations in the co-culture. Interestingly, 4T1 cells enhanced the proliferation of both wt and PKN2 ko MEFs, (Fig. 43). The small increase in wt MEF proliferation in the presence of 4T1, compared to the larger increase in PKN2 ko MEFs, could be due to the previously described basal difference in MEF proliferation upon PKN2 loss (Quétier et al. 2016). As PKN2 ko MEFs proliferate slower at basal level, after conditioning by 4T1 cells, there perhaps remains more capacity for growth enhancement in these cells. Interestingly, it suggests that the previously identified growth defect in PKN2 ko MEFs may be reversed by paracrine signals from the 4T1 cells. Identifying the growth enhancing factors is potentially an interesting future direction of research.

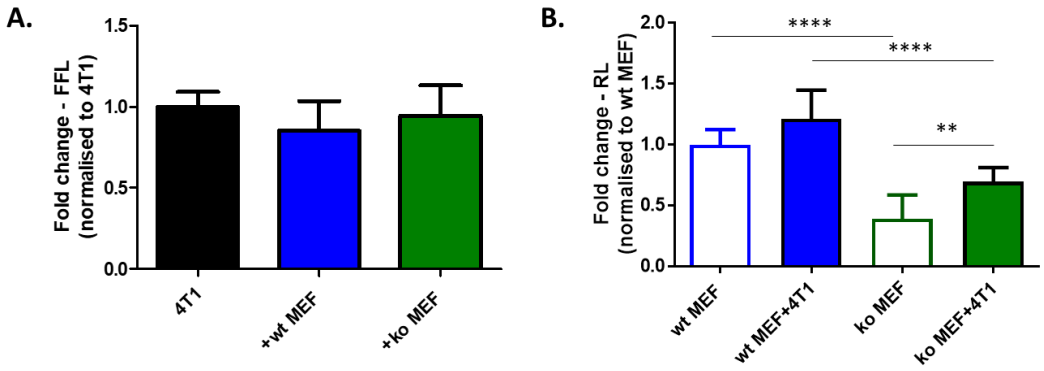

Figure 43. Effect of PKN2 expression in MEFs on PyMT BO1 cancer cells and MEFs using dual luciferase reporter assays

4T1 cells labelled with firefly luciferase reporter were seeded under normal 2D conditions alone (black), co-cultured with wt MEFs (blue) or with ko MEFs (green). wt MEFs (unfilled blue) and ko MEFs (unfilled green) were also seeded alone. After three days, lysates were collected and assayed for the activity of **A.** firefly luciferase (FFL) reporter from the cancer cell using the Promega dual luciferase assay and the activity of **B.** renilla luciferase (RL) reporter from the MEFs using the Stop & Glo reagent in the kit, which quenches the signal from the luciferase reporter at 590nm and gives a signal at 460nm. Data represents the mean +/- SD for n=3 biological repeats carried out in triplicates. Statistical analysis was carried out using ANOVA followed by Bonferroni post-hoc test: $P<0.05$ (*), $P<0.01$ (**), $P<0.001$ (***).

Having used our iPKN2 MEFs with mouse cancer cell lines as a tractable system for deleting PKN2 and optimising dual-luciferase assays, we next wished to translate findings to more

disease relevant human breast cancer models. We used human immortalised breast fibroblasts (HMFU19) and primary human CAFs, alongside MEFs to establish the role of PKN2 loss on the viability of human breast cancer cell lines.

Two human breast cancer cell lines, MCF7 and MDAMB231 were labelled with firefly luciferase and co-seeded with wt or PKN2 ko MEFs initially. These cancer cell lines were chosen to represent two different breast cancer types, luminal and TNBC respectively, where previously TNBC cells have shown direct PKN2-dependency for survival.

Viability of MCF7 was enhanced by the presence of both wt and ko MEFs (Fig.44 Ai). The viability of wt and PKN2 ko MEFs were unaffected when co-cultured with MCF7 (solid bars in Fig.44 Aii). As previously described, PKN2 ko MEFs have lower viability that wt MEFs in mono-culture. This was also observed here when co-cultured with MCF7 cells. Similarly, viability of MDAMB231 was enhanced by the presence of both wt and PKN2 ko MEFs (Fig.44Bi). However, there was a significant reduction in cancer cell viability when cultured with PKN2 ko MEFs when compared to culture with wt MEFs. The viability of MEFs in mono-culture and co-culture with MDAMB231 followed similar patterns to MCF7 co-cultures (Fig.44Bii). This suggests that PKN2 ko may affect paracrine signalling to MDAMB231 cells, either by altering the secretome or by reducing the absolute numbers of fibroblasts in the co-culture.

To assess the effect of fibroblasts on breast cancer viability, more relevant breast fibroblast models were used. A human mammary fibroblast cell line (HMFU19) was labelled with renilla luciferase reporter and two unlabelled human primary cancer-associated fibroblasts (CAFs) were used in 2D co-culture assays. MCF7 and MDAMB231 cell proliferation increased in co-culture with HMFU19 (Fig. 45Ai and Fig. 45Bi), whilst the proliferation of the fibroblasts was unaffected (Fig. 45Aii and Fig. 10Bii).

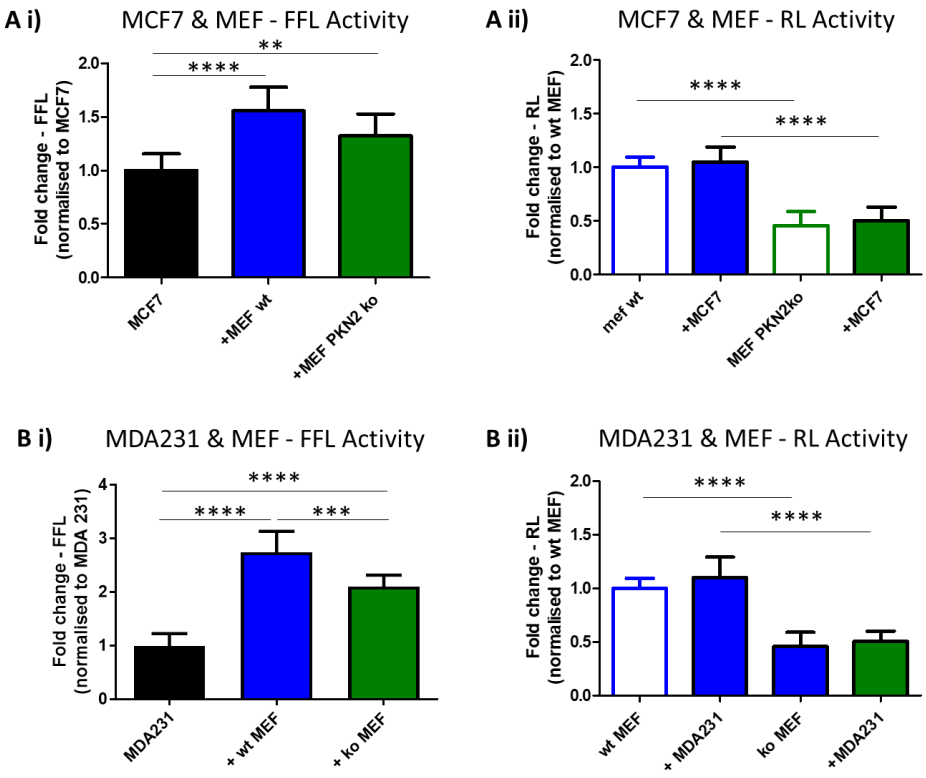

Figure 44. Effect of PKN2 deletion in MEFs on breast cancer cell viability

A) MCF7 cells and B) MDAMB231 (MDA231) cells were cultures alone (black bars) or co-cultured with wt MEFs (blue bars) or PKN2 ko MEFs (green bars) for 72h. At endpoint, cells were lysed and assayed for the activity of firefly luciferase from cancer cells, detected at 590nm (Ai, Bi). Stop & Glo substrate is added to quench this signal and luminescence at 460nm is detected from the renilla luciferase activity from MEFs (Aii and Bii). Raw arbitrary values (RLU) are normalised to the cancer mono-culture condition values to represent the fold change fold change. Data represents the mean +/- SD for n=3 biological repeats carried out in least triplicates. Statistical analysis was carried out using ANOVA followed by Bonferroni post-hoc test: P<0.05 (*), P<0.01 (**), P<0.001 (***).

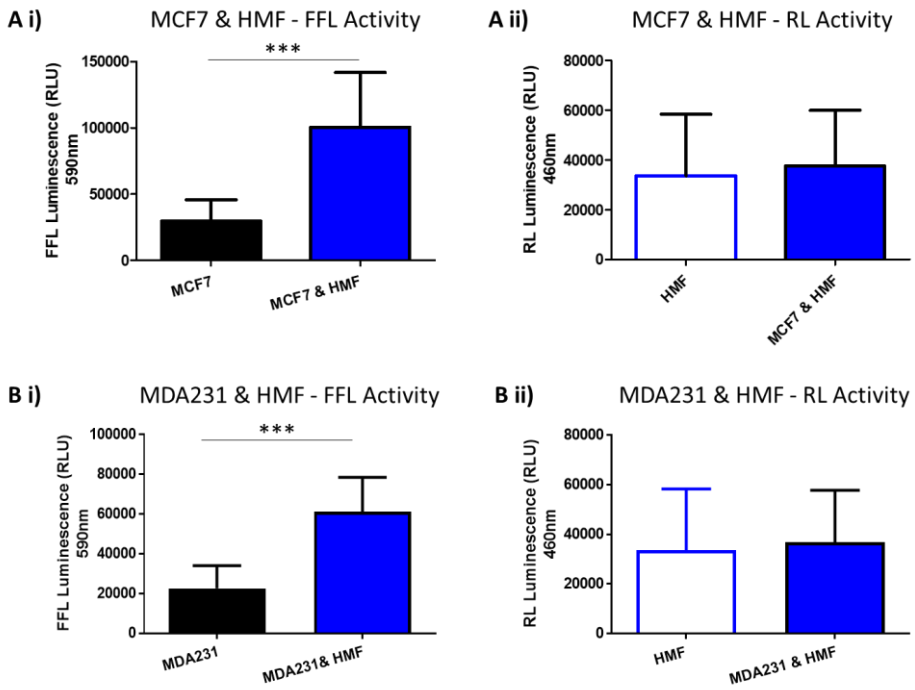

Figure 45. Effect of human mammary fibroblast on breast cancer viability

A) MCF and B) MDAMB231 (MDA231) were cultured alone (black bars) or co-cultured with Immortalised human breast fibroblast cell line HMFU19 (HMF – blue bars) for 72h. At end-point, cells were lysed to assay for the firefly luciferase activity from cancer cells (Ai and Bi: n=3) and thereafter for the renilla luciferase activity (Aii and Bii: n=2). Arbitrary raw values (RLU) are shown. Data represents the mean +/- SD for n=2 or 3 biological repeats carried out in triplicates. Statistical analysis was carried out using ANOVA followed by Bonferroni post-hoc test: $P<0.05$ (*), $P<0.01$ (**), $P<0.001$ (***).

Two different unlabelled CAF cell lines, 1997 and 1939, were tested for their effect on cancer cell proliferation or viability and for any changes upon PKN2 depletion in CAFs.

Unusual differences in proliferation levels of cancer cells in co-culture with CAFs, between different siRNA conditions, needed to be considered when interpreting the results. Untreated 1997 and 1939 CAFs both decreased MCF7 survival (compared to monocultures). However, control siRNA-treated CAFs did not have the same suppressive effect on MCF7 survival (Fig. 46A, B). This was consistent for both CAF lines used. Of potential interest, MCF7 survival was significantly lower when in co-culture with PKN2-depleted CAFs when compared to control siRNA treated CAFs. While the unusual

behaviour of the controls limits interpretation, it is tempting to speculate that PKN2 deletion may impact on the ability of CAFs to support MCF7 viability. Further control and PKN2 siRNAs could be used to clarify these results.

In initial experiments MDAMB231 and 1997 CAFS were seeded at 1:2 ratio and gave sufficient luminescence signal, there was increased MDAMB231 survival when in co-culture with control or PKN2-depleted 1997 (Fig. 46Ci). Similar enhancement of MDAMB231 survival was observed with control or PKN2-depleted 1939. In some experiments, MDAMB231 cells, when cultured alone did not give sufficient luminescence signal when assayed for luciferase activity at the end of some co-culture assays. This was under normal co-culture conditions, with cancer: fibroblast ratio of 1:2 and suggests that MDA231 cell proliferation is low when cultured alone at low cell densities, in the absence of growth supporting fibroblasts.

To increase the number of MDAMB231 cells for better signal, whilst seeding the same total number of cancer and fibroblast cells, the ratio of cancer to fibroblast was changed to 2:1. At this ratio, there were no significant differences in MDAMB231 survival between mono-cultures and co-cultures with control or PKN2-depleted 1997 or 1939 CAFs (Fig. 46 Cii, Dii). Overall, MDAMB231 survival was improved when cultured with 1939 and 1997 at the ratio of 1:2. At 2:1 ratio, there were no changes in MDAMB231 survival between mono- and co-culture conditions. These effects were unaffected by PKN2 depletion in CAFs.

MCF7 cells and 231 cells show contrasting behaviours when co-cultured with CAFs, as MDAMB231 benefit from the presence of CAFs, whilst survival of MCF7 was reduced when co-cultured with CAFs. This contrasts with the previous observation where MEFs enhanced survival of both cancer cell types. Furthermore, the survival advantage in MDAMB231 cells is also dependent on the ratio of co-cultured cells. Together, these data suggest that CAFs

may have both growth-enhancing and -suppressive effects, dependent on the cancer model. This perhaps relates to the conflicting data on the prognostic relevance of CAFs and fibrosis in distinct disease types. In TNBC, enhanced fibrosis gives a poor prognosis, whereas in luminal breast cancer this is not the case.

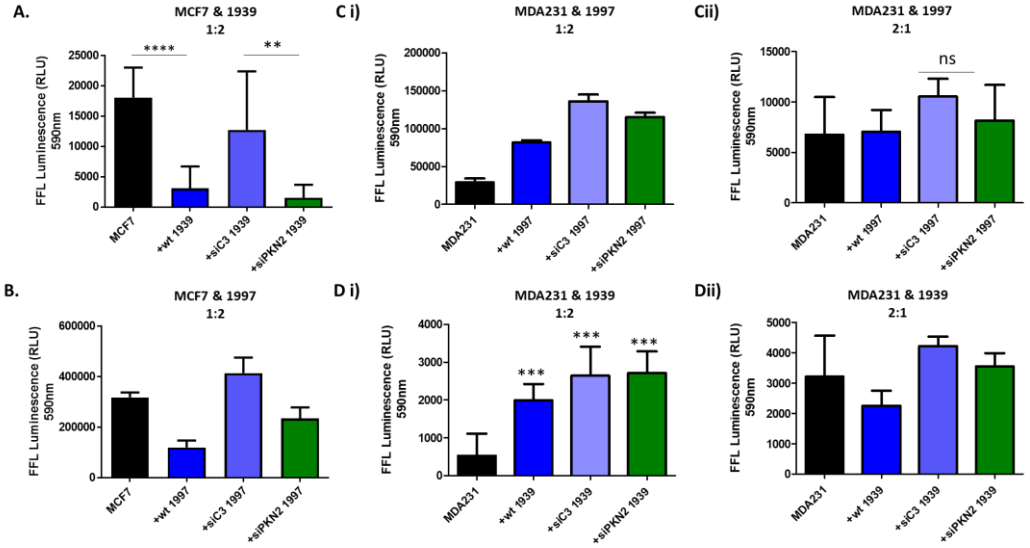

Figure 46. Effect of human primary CAFs on breast cancer cell viability

MCF7 and MDAMB231, labelled with firefly luciferase reporter, were cultured alone (black bars) or co-cultured with two different unlabelled CAFs: 1997 and 1939 (blue bars). After three days, lysates were collected and assayed for the activity of firefly luciferase (FFL) reporter from cancer cells. MCF7 co-culture assays were done under normal culture conditions with cancer to fibroblast ratio of 1:2 (A, B). Under these conditions, c-culture of MDAMB231 with 1997 only gave sufficient signal in one experiment (Ci) and all three experiments with 1939 (Di). Therefore, the cancer to fibroblast ratio was changed to 2:1 for MDAMB231 co-cultures with 1997 (Cii) and 1939 (Dii). Ci: n=1; A and Dii: n=2; B, Cii and Di: n=3. Data represents the mean +/- SD for experiments carried out in triplicates. Statistical analysis was carried out using ANOVA followed by Bonferroni post-hoc test: $P<0.05$ (*), $P<0.01$ (**), $P<0.001$ (***).

To summarise, in the mouse model, PyMT-BO1 cell lines showed increased viability of the cancer cells when in co-culture with MEFs (regardless of PKN2 loss). On the other hand, in co-cultures of 4T1 and MEFs, rather the MEFs have increased viability when in contact with 4T1, compared to when cultured alone.

In the human model, co-cultures of MCF7 & MDAMB231 with HMFU19, showed increased viability in the cancer cells, with no difference in HMFU19 viability. This observation was recapitulated when MEFs were co-cultured with these human cancer lines; encouragingly, deletion of PKN2 from MEFs appeared to attenuate the growth enhancement of both MCF7 and MDA231 cells. This suggests that modulating PKN2 in fibroblasts may provide a route for altering stromal support of tumour cells. CAFs did not support survival of MCF7 cancer cells, whilst supporting survival of MDAMB231 depending on the ratio of fibroblasts present.

3.3.2.2 Drug response of CAFs to doxorubicin and paclitaxel and the effect of PKN2 depletion

CAFs are known to decrease the sensitivity of cancer cells to chemotherapeutic drugs. For example, secretion of HGF by fibroblast has been described in resistance to BRAF kinase inhibitor in melanoma (Straussman et al. 2012) and resistance to lapatinib in $HER2^{+}$ breast cancer (Watson et al. 2018). Secretion of chemokines by CAF have also been related to chemoresistance. For example, studies in pancreatic cancer have demonstrated that secretion of chemokine CXCL12 results in resistance to gemcitabine (Singh et al. 2010). Furthermore, secretion of IL-6 by CAFs leads to resistance to erlotinib in lung cancer (Yao et al. 2010). Therefore, we wanted to investigate whether 1939 and 1997 CAFs have similar protective effects, and whether loss of PKN2 in these CAFs affects the sensitivity of breast cancer cells. The single or dual luciferase assays provide a great platform to study the response to drugs in both cell types simultaneously.

To study the effect of PKN2 loss in CAFs on drug sensitivity in cancer cells, CAFs were pre-treated with a control siRNA and a pool of three PKN2-targeting siRNAs and co-seeded with cancer cells for 72 hours before drug treatment and assayed for cell viability after 72 hours.

The effect of PKN2 deletion in CAFs on sensitivity to doxorubicin in MCF7 was tested. As previously described, MCF7 culture with CAFs suppressed their growth (Fig. 46A and 46B). Compared to wt CAFs (both 1939 and 1997), control siRNA-treated (siC3) CAFs had more positive effect on MCF7 survival. As the CAFs treated with control siRNA did not have similar effect on MCF7 survival as wt CAFs as expected, the reduced survival of MCF7 with PKN2-deleted CAFs is difficult to interpret conclusively. However, doxorubicin was found to have a dose dependent inhibitory effect on the growth of MCF7 cells and this sensitivity was only marginally affected by the inclusion of CAFs to the assay (Fig. 47). Perhaps importantly, PKN2 depleted 1997 cells and untreated wt 1997 CAFs show very similar patterns of sensitivity to doxorubicin. This does not support suppression of PKN2 in this model as a mechanism to increase drug sensitivity.

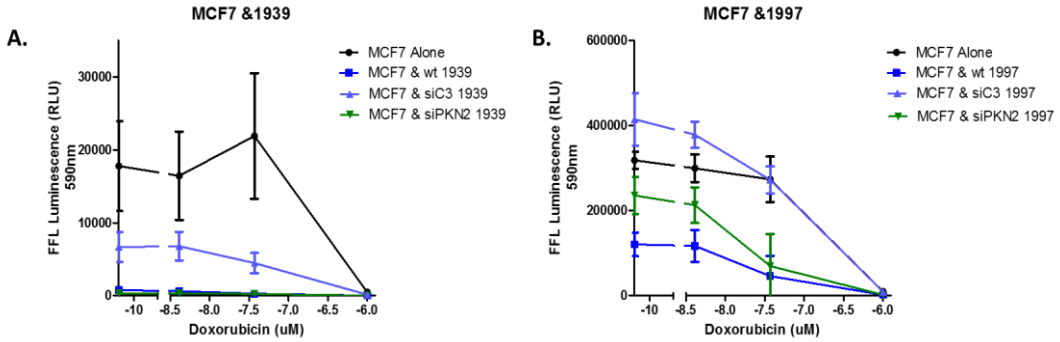

Figure 47. MCF7 sensitivity to doxorubicin and the effect from CAFs

MCF7, labelled with firefly luciferase, were seeded alone (black), with wt (blue), siC3-treated (light-blue) or siPKN2-treated (green) **A.** 1939 (n=3) or **B.** 1997 (n=2) CAFs. After 72h, these cells were treated with vehicle control or doxorubicin at 0.03, 0.3 and 1µM for another 72h. At endpoint, lysates were collected and assayed for the activity of firefly luciferase (FFL) reporter from MCF7 cancer cells. Raw arbitrary values (RLU) are presented. Data represents the mean +/- SD for n=2 or 3 biological repeats carried out in triplicates. Statistical analysis was carried out using ANOVA followed by Bonferroni post-hoc test: P<0.05 (*), P<0.01 (**), P<0.001 (***).

MDAMB231 were treated with two standard chemotherapy drugs used in breast cancer, doxorubicin and paclitaxel, in monoculture or in co-culture with two different CAFs (1997 and 1939). MDAMB231 were not sensitive to doxorubicin at the tested dose range in the

co-culture assay with 1939 (Fig. 48 Ai). The effect of CAFs and their expression of PKN2 on drug sensitivity is difficult to interpret from these results due to the large variation within technical and biological repeats and unusual kinetic of cell survival in some cell lines. Furthermore, CAFs treated with control siRNA did not behave comparably to wt CAFs. However, broadly there was no protection by CAFs (or PKN2 expression) from sensitivity to doxorubicin and paclitaxel in cancer cells.

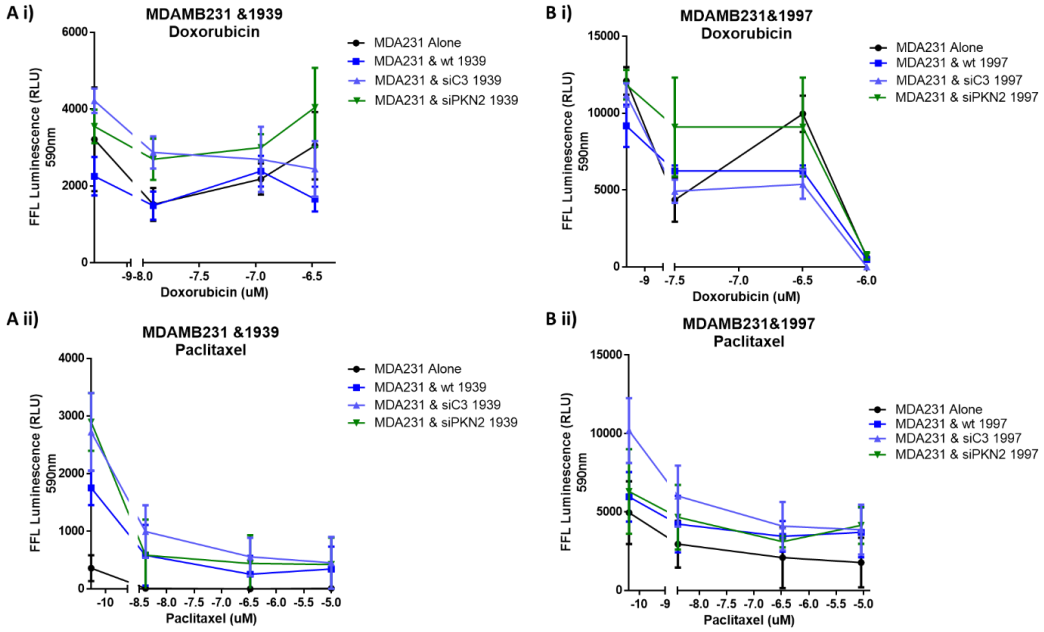

Figure 48. MDAMB231 & CAF sensitivity to doxorubicin and paclitaxel
MDAMB231 (MDA231) cells, labelled with firefly luciferase, were seeded alone (black), with wt (blue), siC3-treated (light-blue) or siPKN2-treated (green) **A.** 1939 or **B.** 1997 CAFs. After 72h, these cells were treated with vehicle control, doxorubicin (Ai, Bi) or paclitaxel (Aii, Bii) for another 72h. At endpoint, lysates were collected and assayed for the activity of firefly luciferase (FFL) reporter from MDAMB231 cancer cells. Raw arbitrary values (RLU) are presented. Data represents the mean +/- SD for n=2 biological repeats carried out in triplicates. Statistical analysis was carried out using ANOVA followed by Bonferroni post-hoc test: P<0.05 (*), P<0.01 (**), P<0.001 (***).

Optimisation of the dose range is also required, for example for MDAMB231 where doxorubicin had no anti-proliferative effect with 1939 CAFs and gave different results with 1997 CAFs across two experiments. Better tools to delete PKN2 in human fibroblasts are required to understand its role on cancer cells' drug response.

3.3.3 Assessing effect of PKN2 in MEFs in mixed cell breast cancer xenografts

Fibroblasts have been shown to support tumour growth *in vivo*, using mixed cell xenografts. Chatterjee et al examined the effect of fibroblasts of different origins on MDAMB231 proliferation, by co-injecting them into immunodeficient mice (Chatterjee et al. 2018). Tumours from cancer and fibroblast co-injections had increased growth compared with cancer cell alone. Another similar study demonstrated increased tumour growth when MDAMB231 cells were co-injected with fibroblasts, which was attributed to increased tumour vascularisation (Limoge et al. 2017). Furthermore, Olsen et al tested the effect of co-injecting mammary fibroblasts with a derivative of MCF7 cell lines on tumour growth, with and without oestrogen supplementation in *in vivo* mixed-cell xenografts (Olsen et al. 2010). This revealed increase tumour growth when fibroblasts were co-injected, which was unaffected by supplementation of oestrogen.

Given these published studies, we sought to examine the effect of fibroblasts, and their PKN2 status, on breast cancer growth, using mixed cell xenografts. Due to the *in vivo* setting, siRNA-mediated PKN2 suppression could not be employed, as the effect will only be transient. Therefore, MEFs from our inducible PKN2 conditional knockout mice (Rosa26 Cre ERT2 $PKN2^{flox}$) were used, as PKN2 deletion can be induced and the effect is long-term.

In mini-organotypic assays, co-culture of 4T1 cancer cells and MEFs resulted in increased cell proliferation and invasion, which was suppressed when MEF PKN2 was deleted. Therefore, this cancer cell line was tested *in vivo* to examine the effect of co-injecting fibroblasts (MEFs) - with or without PKN2 - on tumour growth. As 4T1 cells are derived from BALBc mice, these co-injection experiments were conducted in CD1 nu/nu immunosuppressed mice.

PyMT-BO1 cells (MMTV-PyMT derived) co-cultured with MEFs in the collagen/matrigel gels also showed increased growth compared with PyMT-BO1 cells alone, although no

differences were observed between wild-type and PKN2 ko MEFs. This cancer cell line was also tested *in vivo* and as it shares the same origin of mice as our MEFs (C57 BL/6 mice), this combination of cells could be injected in immune-competent C57BL/6 mice. We co-injected these combinations of cells subcutaneously into mice to study the role of PKN2 in fibroblasts *in vivo*.

MEFs from our conditional PKN2 knockout mouse model were untreated (wt MEFs) or pre-treated with 4-hydroxy tamoxifen (4-OHT) to induce PKN2 deletion (PKN2 ko MEFs) before co-injecting with cancer cells subcutaneously into the mice. 330000 cells per 100µl PBS were injected into both flanks or co-injected with wt MEFs in the left flank and PKN2 ko MEFs in the right flank (an additional 660,000 cells) of CD1 nu/nu mice (for 4T1 tumours) or C57BL6 mice (for PyMT-BO1 tumours).

At endpoint, tumours were harvested, fixed and sectioned. Tumours were stained with Sirius red to study whether loss of PKN2 in MEFs affected fibrous and desmoplastic composition of tumours. The stained sections were analysed to quantify the number of pixels with positively stained areas as a ratio to total pixels. PyMT-BO1 tumours were also stained for SMA, another marker of desmoplasia and fibrosis.

3.3.3.1 Effect of PKN2 expression in MEFs on tumour growth and desmoplasia when co-injected with 4T1 breast cancer cells in vivo

Tumour volume was measured from day 6 and thereafter every 2-3 days (Fig. 49A), and tumours weighed at endpoint (Fig. 49B). 4T1 tumours were harvested two weeks after injection. To our surprise, there were no changes in tumour volumes at any time point between the mono-culture and co-culture conditions. This was reflected in the tumour weights at endpoint. Although PKN2 loss in MEFs had no effect on tumour growth, fibroblast activation studies in the previous chapter suggest a possibility of reduced stromal activation and hence desmoplastic tissue upon PKN2 loss.

To investigate this, tumours were stained with Sirius Red to identify areas of collagen deposition. The stained sections were quantified for number of pixels positive for Sirius red staining (represented as RPT – ratio of positive to total pixels). This is to investigate differences in the desmoplastic nature of tumours and the level of activated stroma within the tumour. There were no significant differences between tumours from mice injected with cancer cells only, compared to mice co-injected with MEFs (Fig. 50).

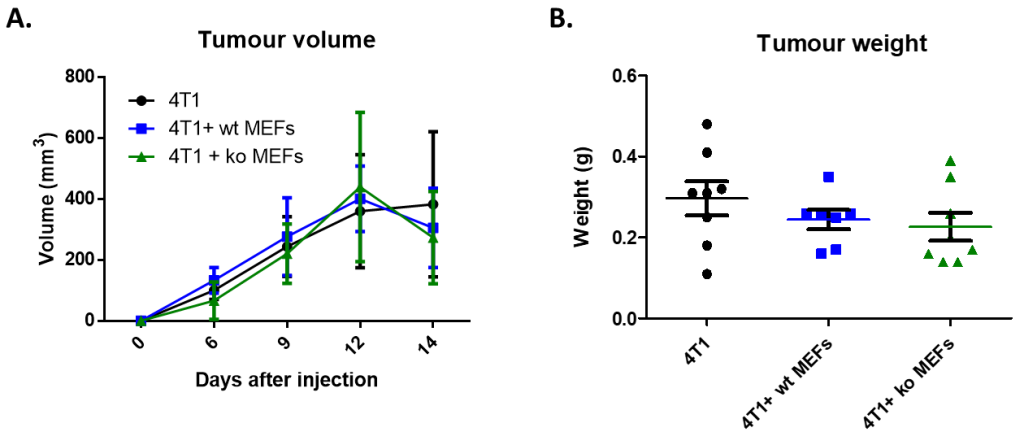

Figure 49. Volumes and weights of tumours in mice co-injected with wt or PKN2 ko MEFs and 4T1 breast cancer cells

CD1 nu/nu mice were injected with 4T1 cancer cells alone (black, n=8) or co-injected with wt MEFs (blue, n=7) or ko MEFs (green, n=8). **A.** Tumour volume was measured using a digital caliper from day 6 to day 14. Data represents the mean values +/- SD of biological repeats. **B.** Weights of excised tumours were measured after the mice were culled at endpoint. Data represents the raw values +/- SD. Statistical analysis was carried out using ANOVA followed by Bonferroni post-hoc test: $P<0.05$ (*), $P<0.01$ (**), $P<0.001$ (***).

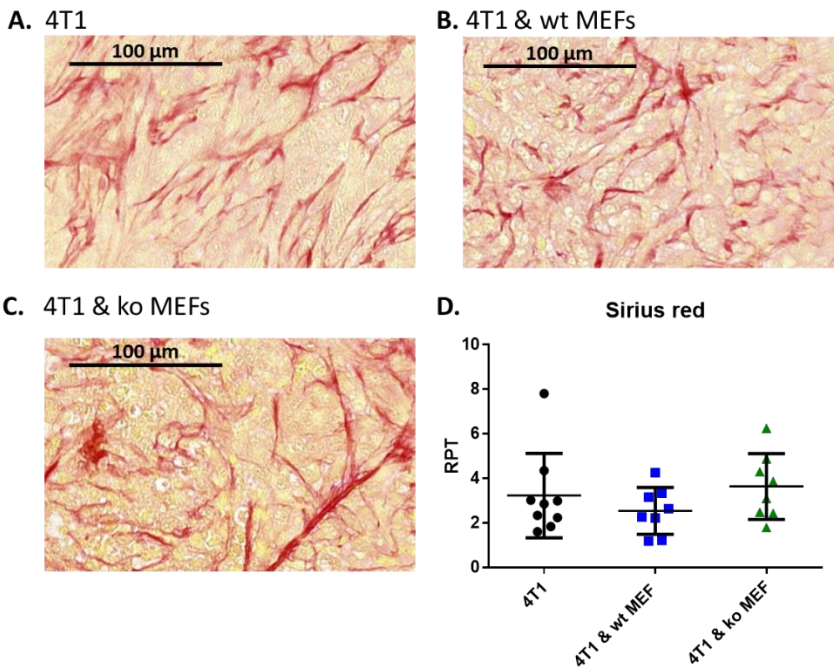

Figure 50. Sirius red staining of 4T1 and MEF tumours

Sections of the excised tumours were fixed in 4% PFA, paraffinised and sectioned. These sections were stained with Sirius red (**A**, **B** and **C**) and imaged using Pannoramic 250 High Throughput Scanner. The images can were viewed and the staining quantified using the Pannoramic Viewer software. At a fixed magnification, over 30 sections covering the inner part of the tumour of a tumour was selected (all with similar area) for quantification. The threshold was set to detect the pink/red areas of stained sections using the DensitoQuant tool in the Image Analysis modules. **D.** The ratio of number of pixels positive for Sirius red staining to total pixels (RPT) is presented. Data represents the mean +/- SD for biological repeats (4T1 only: n=9; 4T1 and wt MEFs: n=8; 4T1 and PKN2 ko MEFs: n=8). Statistical analysis was carried out using ANOVA followed by Bonferroni post-hoc test: P<0.05 (*), P<0.01 (**), P<0.001 (***).

3.3.3.2 Effect of PKN2 expression in MEFs on tumour growth and desmoplasia when co-injected with PyMT-BO1 breast cancer cells in vivo

PyMT-BO1 tumour volumes were measured from day 6 and monitored every three days (Fig. 51A), with tumours weighed at endpoint on day 12 (Fig. 51B). Over time, tumour volumes were higher when cancer cells and MEFs were co-injected, but PKN2 deletion in MEFs had no impact. Similarly, tumour weights at endpoint were higher in the co-injected mice, with no changes upon PKN2 deletion. Tumours from cancer and PKN2 ko MEFs co-injections had higher weights than MMTV cancer cell only tumours, but this did not reach

statistical significance. This data implies that tumour growth is enhanced in the presence of MEFs, but that this growth enhancement is unaffected by the deletion of PKN2. For this cell model, this concurs with the pattern of behaviour observed in organotypic assays.

Tumours were stained with Sirius red and α-SMA and quantified as for the 4T1 tumours. The RPT for α-SMA was similar between the different conditions (Fig. 52). The percentage of α-SMA-stained pixels out of total pixel was highest in tumours with wt MEFs, although differences were not statistically significant. Tumours of PyMT-BO1 co-injected with ko MEFs had an RPT for α-SMA similar to tumours from mice injected with PyMT-BO1 cells only. Compared to PyMT-BO1 & wt MEF tumours, RPT for Sirius red was also slightly lower in tumours with PKN2 ko MEFs (Fig.53). While these data show a trend towards wt MEFS inducing more a-SMA and Sirius red positive, no firm conclusions can be made due to the high variation in this data. Increased cohort size may have revealed more statistically robust data to support our *in vitro* studies.

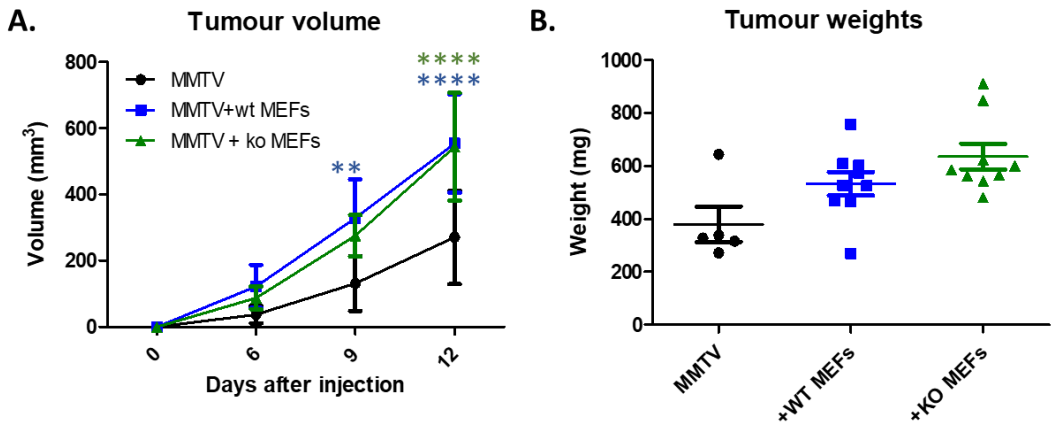

Figure 51. Volumes and weights of tumours in mice co-injected with wt or PKN2 ko MEFs and PyMT.BO1 breast cancer cells

C57/BL6 mice were injected with PyMT.BO1 (MMTV) cancer cells alone (black, n=5) or co-injected with wt MEFs (blue, n=9) or ko MEFs (green, n=9). **A.** Tumour volume was measured using a digital caliper from day 6 to day 12. Data represents the mean +/- SD of biological repeats. **B.** Weights of excised tumours were measured after the mice were culled at endpoint. Data represents the raw values +/- SD. Statistical analysis was carried out using ANOVA followed by Bonferroni post-hoc test: P<0.05 (*), P<0.01 (**), P<0.001 (***).

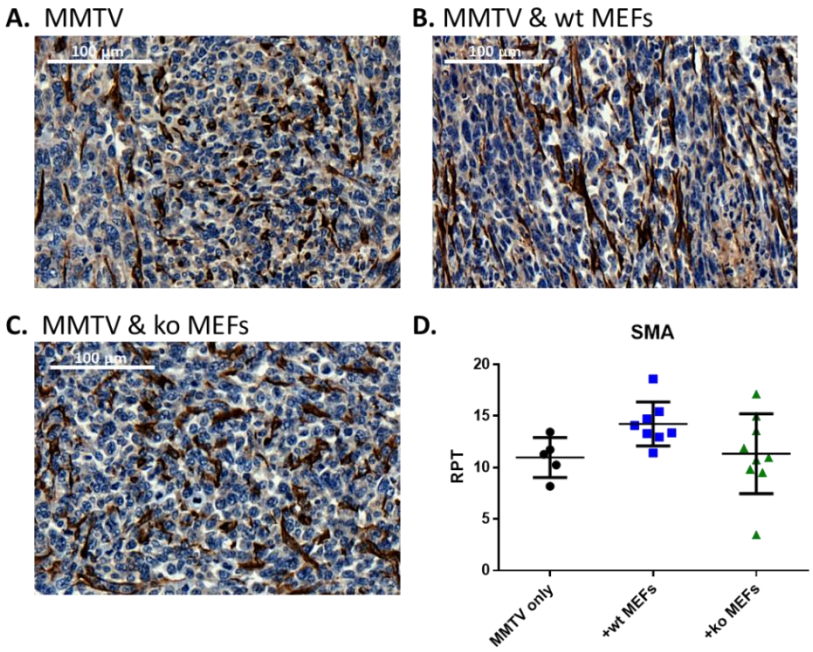

Figure 52. α-SMA staining of MMTV tumours

Sections of the excised tumours were fixed in 4% PFA, paraffinised and sectioned. These sections were stained with α-SMA (A, B and C) and imaged using Pannoramic 250 High Throughput Scanner. D) The images were viewed and the staining quantified using the Pannoramic Viewer software. At a fixed magnification, over 25 sections covering the inner part (to avoid the outer edge that is artificially intense in staining) of the tumour were selected (all with similar area) for quantification. The threshold was set to detect the areas of stained sections using the DensitoQuant tool in the Image Analysis modules. The ratio of number of pixels positive for α-SMA staining to total pixels (RPT) is presented. Data represents the mean +/- SD of biological repeats (MMTV only: n=5; MMTV & wt MEFs: n=9; MMTV & ko MEFs: n=9). Statistical analysis was carried out using ANOVA followed by Bonferroni post-hoc test: $P<0.05$ (*), $P<0.01$ (**), $P<0.001$ (***).

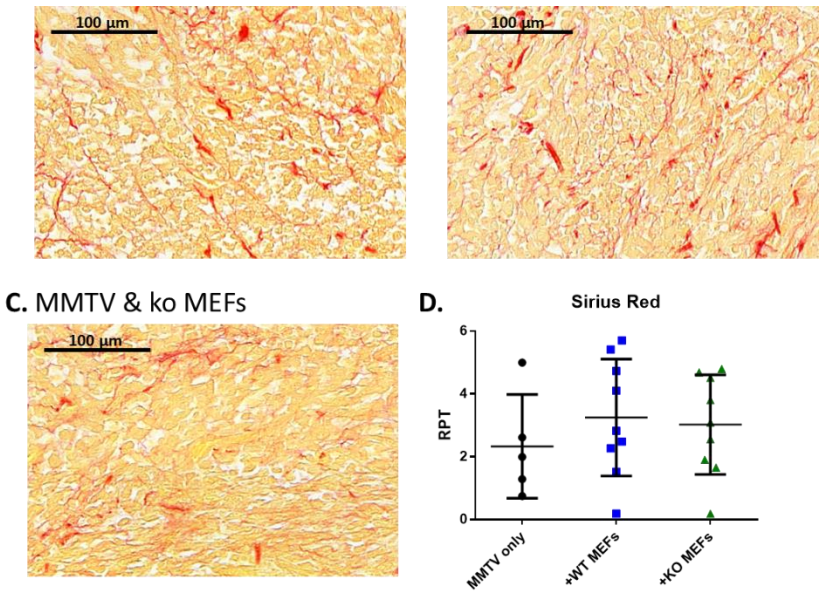

Figure 53. Sirius red staining of MMTV tumours

Fixed tumours MMTC subcutaneous tumours were stained with Sirius Red (A, B and C). D. At a fixed magnification, over 25 sections covering the inner part of the tumour, were selected for quantification. The threshold was set to detect the areas of stained sections using the DensitoQuant tool in the Image Analysis modules. The ratio of number of pixels positive for Sirius Red staining to total pixels (RPT) is presented. Data represents the mean +/- SD of biological repeats (MMTV only: n=5; MMTV & wt MEFs: n=9; MMTV & ko MEFs: n=9). Statistical analysis was carried out using ANOVA followed by Bonferroni post-hoc test: $P<0.05$ (*), $P<0.01$ (**), $P<0.001$ (***).

Unfortunately, despite significant efforts, we struggled to conclusively identify the origins of fibroblasts in tumours. Firstly, the tumours grown from cancer cells alone contained numerous α-SMA positive cells indicating recruitment of host fibroblasts to the tumours in the absence of co-injected MEFs. Secondly, we were unable to stain the GFP reporter expressed in our co-injected MEFs due to technical difficulties, perhaps associated with low GFP expression. Therefore, the proportion of injected MEFs versus recruited fibroblasts within the tumour remains unknown, making it difficult to attribute the observed phenotype to PKN2 loss in tumour fibroblasts. Recruitment of host fibroblasts to tumours may in fact explain the failure to recapitulate the enhancement of 4T1 cell

growth in vivo as recruitment of PKN2 wt host fibroblast could mask any effects of co-injected MEFs.

3.3.4 Summary

3.3.4.1 Assessing interaction between fibroblasts and cancer cells using mini-organotypic assays

Mini-organotypic assays provided a useful tool to study the interaction between wt and PKN2 ko MEFs with cancer cells in 3D culture, with the collagen/Matrigel mix mimicking the ECM of the tumour microenvironment. The presence of fibroblasts with 4T1 increased cell invasion in the gel, which was significantly reduced when PKN2 was deleted in MEFs.

3.3.4.2 Assessing interaction between fibroblasts and cancer cells using luciferase assays

We also developed a dual luciferase assay to provide a simple cost-effective method for examining the growth enhancing interaction between cancer cells and fibroblasts. Here, cancer cells were labelled with firefly luciferase reporter, whilst fibroblasts were labelled with renilla luciferase. Labelled cancer cells were seeded alone or co-cultured with labelled or unlabelled fibroblasts (wt or PKN2 deleted/depleted) in both 2D and 3D assays. At endpoint, the surviving cells can be quantified due to the differential expression of luciferase reporters between cancer cells and fibroblasts.

Luciferase assays of 4T1 and MEF co-cultures show enhanced MEF proliferation in the presence of 4T1 cells, whilst the proliferation of 4T1 was unaffected by MEFs. MEF proliferation was lower in the presence of 4T1 cancer cells when PKN2 was deleted in the MEFs. This suggests that deleting PKN2 may be a way of limiting CAF proliferation in response to signals from cancer cells. Suppressing CAF proliferation may be desirable in

some breast cancer cell types where desmoplasia and fibrosis contributes to poor disease outcome.

In contrast to the 4T1 cells, PyMT-BO1 assays show increased PyMT-BO1 proliferation in the presence of fibroblasts in 2D and 3D, which is unaffected by PKN2 loss on MEFs. This observation correlated with the mini-organotypic assays.

Both MCF7 and MDAMB231 showed enhanced viability in the presence of MEFs (unaffected by loss of PKN2) and HMU19. The CAF cell lines, 1997 and 1939, promoted proliferation of MDAMB231 cells, whilst reducing MCF7 proliferation. This demonstrates overlap between fibroblasts from different origins and supports MEFs as a useful surrogate model.

The use of siRNA to delete PKN2 in human fibroblasts cell line HMFU19 and particularly in primary CAF cells was challenging. As mentioned in chapter 3.1, we developed an inducible shRNA system to supress PKN2 expression in human breast cancer cell lines, which presented with technical difficulties. This system, once optimised, can be employed in human fibroblast models. Alternatively, CRISPR-Cas9 technology may provide a more robust and penetrant means of suppressing PKN2 expression.

Optimising methods of PKN2 deletion in fibroblasts can add value to this luciferase co-culture assay system, as the differential labelling of two cell types enables the study of cancer-fibroblast interaction with the ability to attribute any change to an individual cell type. This method can be employed on a large high-throughput screen, as cells can be co-

cultured in multi-well plates (reducing number of cells and reagents required) and the output can be quantified in an automated manner.

3.3.4.3 Interaction of MEFs (wt & PKN2 ko) with 4T1 and PyMT cells in vivo

After investigating the effect of PKN2 in fibroblasts on their interaction with cancer cells in *in-vitro* cultures, the effect *in-vivo* was investigated. Tumours with PKN2 ko MEFs had reduced areas of Sirius red staining and reduced proportion of area stained with α-SMA, compared to tumours with wt PKN2. These changes suggest reduced stromal activation in tumours where PKN2 was deleted in MEFs. This phenotype can influence tumour stiffness and sensitivity to chemotherapy, which are worth examining in future studies.

During the completion of my thesis write up, Lorena Alba-Castellon quantified blood vessel density in the 4T1 mixed cell xenografts and found that vessel density was significantly enhanced by the addition of MEFs, and further that this enhancement was reversed upon PKN2 deletion. This implies that stromal modulation of PKN2 may be a useful method for modulating tumour vascularisation, which will be discussed in more detail in Chapter 3.4.

Whilst mixed cell xenografts provide an opportunity to study the interaction between cancer cells and fibroblasts, interpretation was limited by recruitment of host stromal fibroblasts which will be wt for PKN2. Recruitment of endogenous fibroblasts may mask any effect of PKN2-deleted MEFs that are known to have lower survival that wt MEFs. Therefore, the effect of PKN2 deletion on tumour growth and pathology was investigated in the following chapter by targeting the entire stroma using a novel inducible conditional PKN2 knockout mouse.

3.4 Using a novel inducible PKN2 knockout mouse orthotopic model to explore stromal PKN2 function

Using *in vitro* co-culture models, we demonstrated that fibroblasts could enhance the growth of breast cancer cells in a PKN2 dependent fashion. These results were not recapitulated conclusively *in vivo* using mixed cell xenograft models. These models however suffer from some significant drawbacks. Firstly, as the injected mice are wild-type for PKN2, resident PKN2 expressing stromal cells, including fibroblasts, can be recruited to tumours. This was highlighted by the presence of large numbers of α-SMA positive mesenchymal cells in 4T1 tumours, even in the absence of any co-injected fibroblasts. This is likely to confound the effects of co-injecting PKN2 deleted fibroblasts. Added to this, we were unable to positively identify co-injected fibroblasts robustly in tumours, leading to ambiguity about the PKN2 status of fibroblast-like cells in the tumours. Finally, subcutaneous tumours are a poor substitute for orthotopic tumours where cells would be exposed to the breast microenvironment.

To overcome these limitations, we sought to develop a syngeneic orthotopic model using our inducible conditional PKN2 knockout mouse model (iPKN2: $PKN2^{fl/fl}$; $Rosa26\text{-}CreER^{T2}$). This would allow us to examine the effect of systemic PKN2 deletion on tumour pathology, with the added benefit of preserving an intact immune system. Orthotopic models are physiologically more relevant than subcutaneous models, particularly with regard to stromal responses (Fleming et al. 2010; Holen et al. 2017). Moreover, systemic deletion of PKN2 in this orthotopic model ensures that all resident and recruited fibroblasts should lack PKN2 expression. This will allow us to interpret any changes in fibroblast activation, due to PKN2 deletion, less ambiguously.

4T1 cells could not be used for orthotopic injections in mice, as these cells were isolated from a spontaneous tumour formed into BALB/c mouse, while our iPKN2 mice are of a C57Bl6 background; implantation of 4T1 will result in immune rejection. We are thus

limited to syngeneic C57BL/6 derived model, and here selected the BO.1 cell line, derived from an MMTV-PyMT model on a C57BL/6 background. Tumours which develop spontaneously in the MMTV-PyMT model contain abundant CAFs and exhibit fibrosis, further supporting use of xenografts from this model (Holen et al. 2017) (Takai et al. 2018).

We hypothesised that growth and activation of host fibroblasts within the orthotopic tumour may also be affected by PKN2 deletion resulting in changes in tumour growth, pathology, fibrosis and angiogenesis. Further, we envisaged that deletion of PKN2 might recapitulate some of the tissue phenotypes observed when PKN2 is deleted during mouse embryogenesis; induced deletion of PKN2 in embryos resulted in collapse of the mesenchymal compartment, a reduction of mesenchymal cell growth and contractility, and disruption of the developing vasculature (Quétier et al. 2016)

3.4.1 Experimental procedure of inducing PKN2 deletion and breast orthotopic injections in mice

We bred our conditional PKN2 mice to obtain littermate females to form the cohort for our 3 experimental groups (Fig. 54). $PKN2^{fl/fl}$; Rosa26-Cre/ERT2 mice were crossed with female $PKN2^{fl/+}$; Rosa26-Cre/ERT2 mice to give a 50:50 mix of $PKN2^{fl/fl}$; Rosa26-Cre/ERT2 and $PKN2^{fl/+}$; Rosa26-Cre/ERT2. These mice were divided into three experimental groups: (1) PKN2 Homo-KO: $PKN2^{fl/fl}$; Rosa26-Cre/ERT2 + Tamoxifen; (2) PKN2 Het-KO: $PKN2^{fl/+}$; Rosa26-Cre^{ERT2} + Tamoxifen; (3) PKN2 WT: Either genotype without Tamoxifen treatment (Vehicle).

Tamoxifen was administered, at the dose of 3mg per 20g mouse weight (dissolved in sunflower oil via oral gavage), thrice within two weeks to induce PKN2 deletion. This schedule has been demonstrated to induce penetrant systemic deletion of PKN2 in adult mice. Meanwhile control mice were treated with vehicle (Fig. 54). During embryogenesis,

heterozygous expression of PKN2 was sufficient to maintain PKN2 function, and it was envisaged that the tamoxifen treated heterozygous cohort would also control for the non-specific effects of tamoxifen administration.

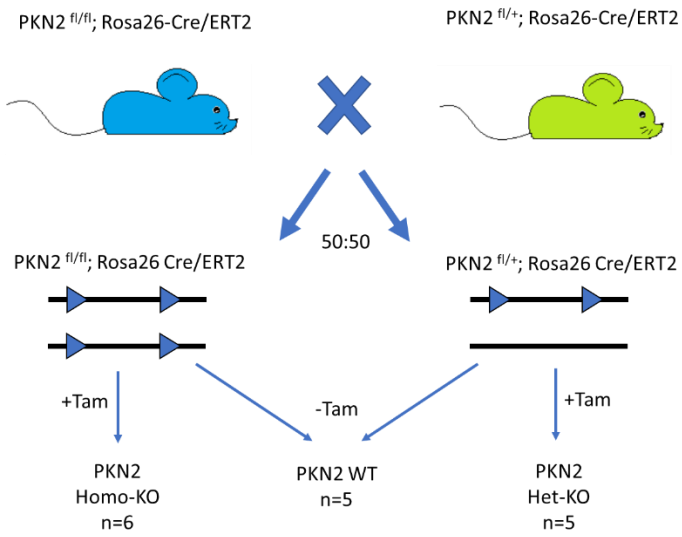

Figure 54. Breeding Schematic

Conditional PKN2 mice, homozygous (blue) for floxed PKN2 alleles and heterozygous (green) for floxed PKN2 with homozygous allele for CRE/ERT2 were bred to give littermates with heterozygous alleles for Cre/ERT2. Mice with homozygous floxed PKN2 were treated with tamoxifen to induce PKN2 deletion in both alleles (PKN2 homo-KO; n=6) Mice heterozygous for PKN2 floxed gene were also treated with tamoxifen to induce PKN2 deletion in one allele (PKN2 Het; n=5). Mice from both genotypes were untreated as control mice (WT; n=5).

Mice were injected with $3x10^5$ BO.1 cells in each (left and right) inguinal mammary fat pad. Cells were injected in 30uL Matrigel. The experiment was terminated two weeks post injection, when the mice were culled and the tumours were harvested. PCR analysis of extracted tumour DNA indicated robust recombination of the floxed allele in tamoxifen treated mice.

3.4.2 Systemic PKN2 deletion does not significantly affect breast orthotopic growth

Excised tumours were weighed and recorded at endpoint. When harvesting tumours from the mice at endpoint, it was apparent that there was sometimes additional tumour growth between the two injected sites, along the line of tumour engraftment. In some

mice, this resulted in additional subcutaneous tumours. We thus separately examined the total tumour burden and the size of the individual orthotopic tumours, remaining within the mammary fat pad.

There was a trend towards high total tumour burden when PKN2 was deleted, with no difference between het and homo PKN2 ko mice (Fig. 55). The orthotopic tumours were separated and weighed individually. There were no significant differences in the orthotopic tumour weights between the three groups (Fig. 56), indicating that loss of PKN2 in the surrounding tissue had no impact on net tumour growth within the mammary gland.

A.

Homo-WT	Het	Homo-KO
1.8	1.8	2.36
0.74	0.74	0.81
0.58	0.58	2.23
1.16	1.16	0.97
0.83	0.83	0.64
		2.53

B.

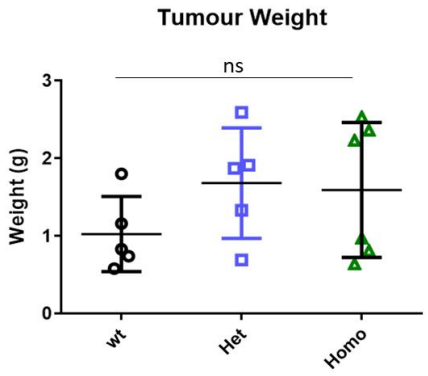

Figure 55. Total tumour weight (g) per mouse

A. Weights of tumours from left and right inguinal mammary fat pad sites as well as any additional subcutaneous tumours were added to give total tumour weights. B. Scatter plot representing weights per mouse in each experimental group – wt: n= 5; het: n=5, homo: n=6 mice). Data represents the raw values +/- SD of biological repeats. Statistical analysis was carried out using ANOVA followed by Bonferroni post-hoc test: P<0.05 (*), P<0.01 (**), P<0.001 (***).

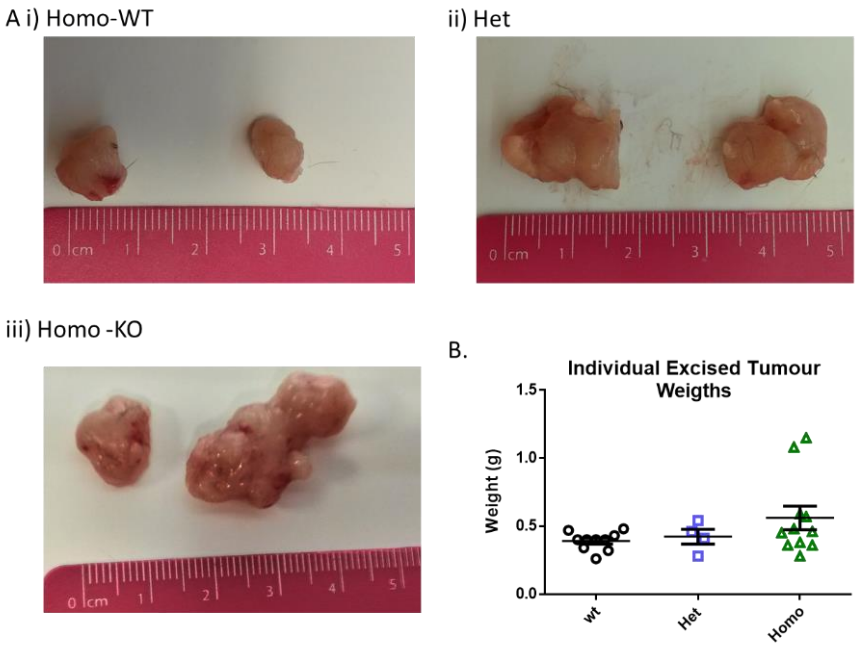

Figure 56. Excised orthotopic tumours and weights

A. Images of examples of tumours excised from i) wt, ii) het and iii) homo-KO mice at end-point. B. Plot of weights of excised tumours that could be separated as individual tumours from left and right inguinal mammary fat pads at endpoint in each cohort group of mice - wt: n= 10; het: n=4, homo: n=11 tumours). Data represents the raw values +/- SD of biological repeats. Statistical analysis was carried out using ANOVA followed by Bonferroni post-hoc test: P<0.05 (*), P<0.01 (**), P<0.001 (***).

3.4.3 Systemic PKN2 deletion in mice reduces fibrosis in orthotopic tumours

The potential role of PKN2 in the activation of fibroblasts was discussed in the previous chapter. Here, the effect of PKN2 ablation on activation of the tumour stroma was investigated *in vivo* using the orthotopic tumours. Tumours were fixed and embedded in paraffin. Sections were cut and mounted on slides to stain for α-SMA to give an indication of the activation state of mesenchymal cells within the tumour stroma (Fig. 57). Tumour sections were also stained for Sirius Red (Fig. 58), to give an indication of the collagen deposition from desmoplastic reaction within the tumour (Lattouf et al. 2014).

The ratio of Sirius Red or α-SMA-positive pixels to total number of pixels (RPT) was calculated by the DensitoQuant tool in Pannoramic Viewer. The average RPT from multiple

fields of views within a tumour (covering most of the inner tumour and avoiding the very outer edge of the tumour, where there is commonly darker artificial staining) was used to analyse for differences upon PKN2 loss. There were no significant differences in the ratio of α-SMA-positive pixels to total pixels in WT, het-KO or homo-KO groups (Fig. 57B). On the other hand, tumours from homozygous PKN2 KO mice had significantly lower RPT of Sirius Red than the WT and het group tumours (Fig. 58B). Whilst there were no differences in α-SMA positive pixel ratio upon PKN2 loss, reduced Sirius Red staining in PKN2-deleted tumours is an indication of reduced fibrosis and activated stromal activity. The lack of difference between WT and het mice suggests that one allele of PKN2 is sufficient to drive the fibrosis. Furthermore, the similarity between the tumours from WT and het PKN2-deleted mice controls for any potential effects of the tamoxifen administration used to induce recombination.

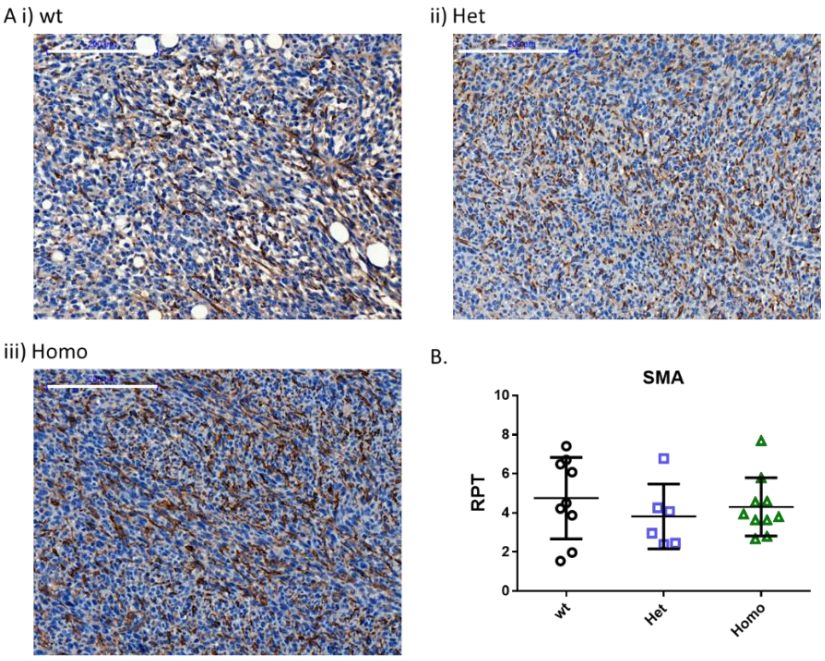

Figure 57. α-SMA staining of orthotopic breast tumours

A. Brightfield images of α-SMA stained tumours from i) wt: n= 9, ii) het: n=6 and iii) homo mice: n=10 tumours. Scale bar represents 200μm. **B.** Ratio of positive to total pixels (RPT) of α-SMA. Average RPT per tumour from several fields of view is plotted. Data represents the mean values +/- SD of biological repeats. Statistical analysis was carried out using ANOVA followed by Bonferroni post-hoc test: P<0.05 (*), P<0.01 (**), P<0.001 (***).

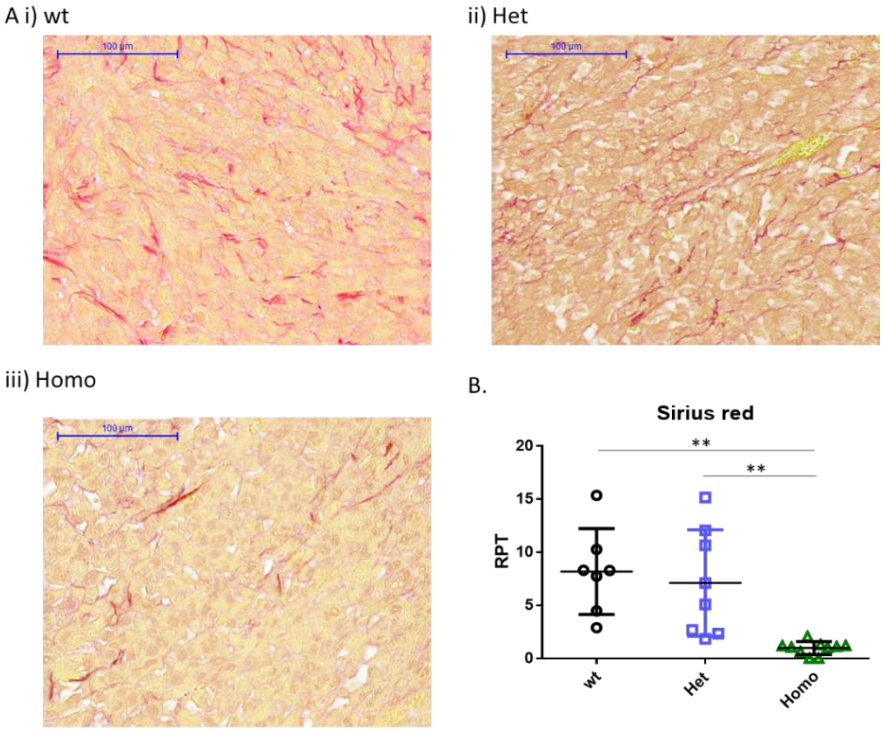

Figure 58. Sirius Red staining of orthotopic breast tumours

A. Brightfield images of Sirius red stained tumours from i) wt: n= 7, ii) het: n=8 and iii) homo mice: n= 10 tumours. B. Ratio of positive to total pixels (RPT) of Sirius red staining. Average RPT per tumour from several fields of view is plotted. Data represents the mean values +/- SD of biological repeats. Statistical analysis was carried out using ANOVA followed by Bonferroni post-hoc test: P<0.05 (*), P<0.01 (**), P<0.001 (***).

3.4.4 Systemic PKN2 deletion reduces blood vessel density in orthotopic tumours

Systemic deletion of PKN2 in mouse embryos presented with abnormal vasculature and an absence of vitelline vessels in the yolk-sacs, seemingly contributing to lethality at E10 (Quétier et al. 2016). Furthermore, the related PKN3 isoform has been shown to regulate tumour angiogenesis in a breast cancer model (Mukai et al. 2016). Therefore, tumours were stained for endomucin (Fig. 59A) to study differences in tumour vascularisation upon stromal PKN2 deletion (collaboration with postdoctoral colleague Dr Lorena Alba Castellon). The number of vessels were counted from several fields of view within the inner tumour, and the averages were compared. There was a significant reduction in the number of blood vessels in tumours from the homo KO group compared to wt and het

group (Fig. 59B). Thus, further investigation of PKN2 as a potential target for regulating angiogenesis and fibrosis in tumours may reveal clinical relevance with respect to tumour growth and metastasis.

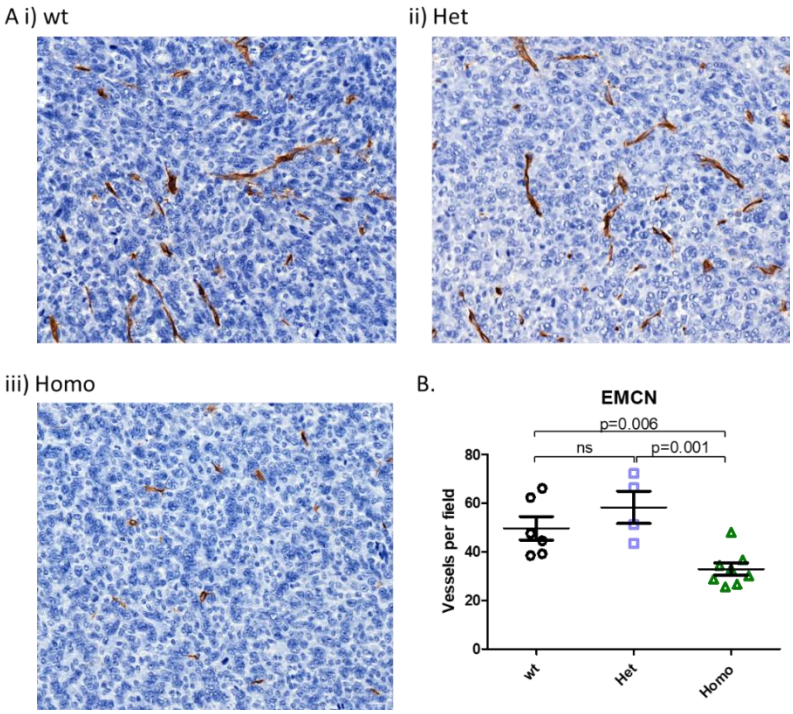

Figure 59. Endomucin staining of breast orthotopic tumours

A. Brightfield images of endomucin-stained tumours from i) wt, ii) het and iii) homo mice. **B.** Number of blood vessels. Multiple sections per tumour section was counted. Data represents the mean number of blood vessels per field +/- SD of biological repeats (wt: n= 6; het: n=4; homo: n=8 tumours). Statistical analysis was carried out using unpaired t-test to compare the differences between two cohort groups.

3.4.5 Summary

Here we used an orthotopic model to investigate the effect of deleting PKN2 throughout the tumour stroma, focusing on the fibrotic nature of the tumour and vascularisation. We acknowledge that this model does not delete PKN2 in fibroblasts alone, and phenotypes may therefore be attributed to loss from other stromal cells. As previously demonstrated in mouse embryos (Quétier et al. 2016), homozygous loss of PKN2 is required to see any overt phenotypic differences, whilst 50% PKN2 expression (heterozygous mice) is sufficient to mimic the WT mice. This behaviour appears to be the same for the fibrosis

and vascular phenotypes in tumours. Overall, these data indicate a potentially important role for PKN2 in tumour fibrosis and vascularisation.

Increased fibrosis and stromal activation has been associated with affecting drug entry (Orimo et al. 2005) and poor prognosis in breast cancer (Yazhou et al. 2004; Surowiak et al. 2006), and therefore further investigation of PKN2 in light of this phenotype can have important clinical relevance. In our study, tumours in mice with systemic PKN2 deletion in the surrounding stroma had reduced Sirius red staining. This suggests PKN2 as a potential target in stromal fibroblasts, as desmoplasia is a phenotype mediated by activated fibroblasts, which can affect disease prognosis and response to therapy (Pearce et al. 2018b); (Lovitt, Shelper, and Avery 2018).

Another factor related to stromal desmoplasia that can be examined in relation to PKN2 expression is tumour stiffness. In breast cancer, tumour stiffness is associated with promotion of cancer cell invasion and metastasis (Cavo et al. 2016), where stromal cells secrete factors that contribute to ECM re-modelling (Kharaishvili et al. 2014; McLane and Ligon 2016). Since evidence in this chapter and chapter 3.2 suggest modulation of stromal activation by PKN2, assessing tumour stiffness may provide interesting results of clinical significance.

Reduced numbers of endomucin stained vessels in tumours from PKN2 homo-KO mice has potential therapeutic implications. In mouse embryos, vascular defects were not caused by loss of PKN2 from endothelial cells; two independent endothelial specific PKN2 knockout models indicated normal vascular development and no lethality or overt phenotype in adult mice (Quétier et al. 2016). Rather, vascular defects in the mouse were attributed to collapse of the underlying mesenchyme, with defects in the cell biology of mesenchymal fibroblasts observed both *in vitro* and *in vivo* (Quétier et al. 2016). It

remains to be determined whether similar mechanisms play a part in the reduced blood vessel density we see with stromal knockout of PKN2 in tumours.

Tumour vasculature has many important roles, such as maintenance of tumour survival at the primary site as well as intravasation, dissemination and metastasis to secondary sites. Whilst anti-angiogenic therapies have positive effects on disease-free survival, no improvements in overall survival is observed (Bergers and Hanahan 2008). This failure has been attributed to acquired resistance as well as side effects, such as spontaneous internal bleeding (Elice and Rodeghiero 2012). Furthermore, reduced vascularisation causes increased intra-tumoural hypoxia, hindering delivery of chemotherapeutic drugs (Wong, Bodrug, and Hodivala-Dilke 2016) and potentially promoting metastatic spread. Therefore, in terms of therapy, vascular perfusion can have significant effects on drug delivery and it remains controversial whether reducing vasculature will be of benefit in tumour therapy.

3.4.5.1 Concluding remarks

Global deletion of PKN2 in mice resulted in tumours that are less fibrotic, with reduced vasculature. These characteristics have impacts on tumour stiffness, invasion, metastasis and chemosensitivity. Therefore, it will be valuable to examine these phenotypes and the relevance of PKN2 in future studies. Differences in other phenotypes, such as levels of immune cell infiltrates and degree of inflammation may provide insights into other functions related to PKN2. Additionally, comparisons can be made between global PKN2 deletion and stromal cell-specific PKN2 deletion, as well as exploiting genetic and pharmacological means of targeting PKN2.

Further study in the role of PKN2 in the regulation of the tumour fibrosis and vasculature, particularly with regard to mechanism, is clearly warranted and may reveal important and therapeutically exploitable avenues.

4. Discussion

PKN kinases are an enigmatic group of kinases that have received little attention to date, compared to their close PKC family relatives and the Rho effector kinases, ROCK1 and ROCK2. However, domain and sequence homology suggest that PKN kinases are the closest mammalian orthologues of yeast PKC (Mukai 2003; Roelants et al. 2017). The roles of yeast PKC include regulation of cell wall integrity, cytoskeletal dynamics and cell cycle progression downstream of yeast Rho1 (Heinisch et al. 1999) (Marini et al. 1996). In mammals, the PKC kinase family is broad and functionally diverged; the PKN kinases represent as a subgroup within this family which have retained the ability to regulate cell biology downstream of the Rho family (Amano et al. 1996). As downstream effectors of Rho, PKN kinases have demonstrated roles in regulating the cell cytoskeleton and motility (Vincent and Settleman 1997). Furthermore, studies using xenograft tumour models suggests similar functions to affect cancer invasion and metastasis (Mukai et al. 2016; Lachmann et al. 2011). Recent studies in genetically engineered mouse models, where PKN isoforms have been knocked out, have helped to delineate *in vivo* roles of PKN kinases in both normal physiology and in cancer (Quétier et al. 2016; Danno et al. 2017; Yang et al. 2017; Yasui et al. 2012; zur Nedden et al. 2018).

4.1 Role of PKN2 in breast cancer survival

Several studies suggested a role for PKN kinases in cell survival under normal physiological conditions and in cancer. Schmidt *et al* showed that PKN2-depleted HeLa cells showed delayed G2/M progression and increased apoptosis (Schmidt et al. 2007). Furthermore, the work in our lab on the role of PKN kinases in mouse embryonic development indicated selective dependency of mouse embryonic fibroblasts (MEFs) on PKN2 for cell growth both *in vitro* and *in vivo* (Quétier et al. 2016). In prostate cancer cells, depletion of PKN1 results in reduced hormone-induced proliferation (Metzger et al. 2008). Meanwhile,

depletion of PKN3, whose expression is driven by PI3K signalling, in prostate cancer causes reduced tumour cell proliferation (Leenders et al. 2004). Therefore, the project started with the aim to investigate the significance of PKN kinase expression on survival and proliferation of breast cancer cell models *in vitro*.

Bioinformatic analysis of the TGCA dataset was conducted to study the expression of PKN kinases in normal tissue and breast cancer tissue of different subtypes. This analysis revealed no significant changes in expression between normal and breast cancer tissues or across the different breast cancer subtypes. This finding contrasts with data from a recent study by Lin et al, that suggested high expression of PKN1 and PKN2 selectively in TNBC, in comparison to non-TNBC (Lin et al. 2017). However, their study was limited to cell line data from the CCLE database and moreover, the differences observed were minimal. Therefore, the unclear biological relevance in a disease setting needs to be noted when considering this study.

Perhaps more importantly, analysis of PKN kinase expression and relapse-free survival (RFS), using an online tool to generate Km plots (Győrffy et al. 2010), indicated a correlation between low PKN2 expression and high RFS in patients with ER-negative and basal breast cancer. This pattern was not seen when considering TNBC patients overall, however improved RFS with low PKN2 expression was observed when refining the analysis to patients with basal-like and mesenchymal-like TNBC using the Pietenpol subtype classification (Lehmann, Bauer, Chen, Sanders, Chakravarthy, and JA 2011). These subtypes of TNBC are mesenchymal in phenotype, perhaps further supporting a cell differentiation state dependent reliance on the PKN2 pathway. The limitation of the data set is the comparatively small sample size representing TNBC subtypes available for analysis (e.g. Mesenchymal subtype with PKN2 data; 171 patients).

The dependency on PKN2 in mesenchymal-like TNBC for survival corroborated with a study by Brough *et al,* whereby PKN2 was identified as a candidate gene for cell viability dependence in an siRNA screen (Brough et al. 2011). Cell viability upon PKN2 depletion was markedly reduced in TNBC that are known to have a mesenchymal phenotype, such as MDAMB231 and CAL120.

The dependency for PKN kinases in TNBC was investigated *in vitro*, comparing three TNBC and three non-TNBC cell lines. Moderate reduction in cell viability was observed upon siRNA-mediated PKN2 and PKN3 depletion in SUM159, MDAMB231 and MDAMB468, with no effect on non-TNBC cell lines. However, validating this effect with pharmacological agents was limited by non-specific PKN kinase-targeting inhibitors.

Since I started my research, Mukai *et al* published their work on a study involving knockout of PKN3 in a mouse prostate tumour model, that demonstrated decreased tumour size and reduced metastasis (Mukai et al. 2016). Furthermore, Lin *et* al published their work demonstrating the selective dependency of TNBC for PKN2 *in vitro* and *in vivo* (Lin et al. 2017). In this study PKN2 knockdown resulted in reduced colony formation and xenograft tumour growth.

Further investigation into the role of PKN kinases in TNBC was halted due to the relatively modest reduction in TNBC survival observed with PKN2/PKN3 depletion, the limited ability to target PKN2 pharmacologically and the publication of the aforementioned competing studies. However, the dependency on PKN2 for mesenchymal TNBC and in MEFs from our conditional PKN2 knockout model gave a new focus to the project, focusing on how PKN2 regulates fibroblast cell biology. Cancer-associated fibroblasts (CAFs), are important components of the tumour microenvironment, and PKN2 may this represent and interesting regulator of the tumour microenvironment, with implications on tumour progression and therapy response.

4.2 Role of PKN2 in stromal activation

Fibroblasts within the tumour environment can promote tumour progression. This requires the differentiation of fibroblasts in myofibroblast-like cells, otherwise described as activation into cancer-associated fibroblasts. Work by Kojima *et al* demonstrates an autocrine loop, whereby fibroblast activation and tumour progression are mediated by secreted factors SDF-1 and TGFβ (Kojima et al. 2010). Furthermore, enriched expression of TGFβ1 is associated with highly fibrotic tissue and ECM secretion (Brenmoehl et al. 2009). Work by Desmoulière *et al* demonstrated that treatment of fibroblasts with TGFβ induced the expression of α-SMA fibres, a marker of cellular differentiation into myofibroblasts (Desmoulière et al. 1993), and also a key biomarker for labelling CAFs in tumours.

Our work in mouse embryos indicated a potential requirement for PKN2 in the EMT of neural crest cells and mesenchymal contractility *in vivo* (Quétier et al. 2016); in the absence of PKN2, neural crest cells fail to migrate away from the neural tube and embryos fail to undergo axial turning, which is driven by coordinated contraction and elongation of mesenchymal cells within the mesoderm. The effect of PKN2 deletion on MEF activation in response to TGFβ was therefore examined.

A common characteristic of activated fibroblasts is their increased contractility within the ECM. Encouragingly, we showed that PKN2-deleted MEFs, treated with TGFβ, had reduced contractile ability in collagen gels. Based on this finding, the effect of PKN2 expression on the induction of α-SMA fibres in response to TGFβ, another marker of fibroblast activation, was tested. Overall, induction of α-SMA expression was reduced in both MEFs and primary breast cancer derived CAFs with loss of PKN2. This supports the idea that PKN2 has an effect on fibroblast activation and that this phenotype is conserved in both mouse and human fibroblast models. As CAF activation plays an important role in cancer progression and

metastasis, the mechanism behind the reduction in α–SMA fibres upon PKN2 loss was investigated.

The mechanism behind the reduced activation in PKN2-deleted fibroblasts will aid in targeting this pathway therapeutically. Therefore, the immediate signalling pathway downstream of TGFβ1 was tested in MEFs, HMFU19 normal breast fibroblasts and CAFs. This revealed no changes in the amplitude or time-course of SMAD2/3 phosphorylation when comparing wt and PKN2-deleted fibroblasts.

Work is in progress to study other related signalling pathways that may be affected, such as the non-canonical TGF signalling, through mechanosensory pathways including YAP and MRTF. Quantitative mass spectrometry (MS) analysis and KSEA of serum-induced activation of MEFs revealed differences between wt and PKN2 ko MEFs in phosphorylation of proteins such as YAP, MRTF, MEK1, ERK1, Akt and p70SK. These proteins have been associated with signalling pathways downstream of TGFβ1 (Piersma, Bank, and Boersema 2015), (Stratton et al. 2002), (Deaton et al. 2005), (Liu et al. 2016) (Gao et al. 2013). Therefore, the phosphorylation of these proteins can be assessed in response to TGFβ1 or other fibroblast activating signals upon PKN2 loss.

Additionally, it will be important to measure functional outputs of the TGFβ pathway, such as transcriptional activation. The ability of PKN2-deleted MEFs to mediate translocation of the SMAD2/3/4 complex to the nucleus can be assessed. SMAD reporter cell lines have been generated in the lab to investigate the potential of transcriptional regulation and activation by the SMAD2/3/4 complex, in PKN2-deleted cell models. Reporters for the mechanosensory regulated transcription factors YAP (TEAD-luciferase) and MRTF (SRF-luciferase) are also being used to ask whether PKN2 regulates mechanotransduction, which is known to depend on Rho (Provenzano and Keely 2011; Dupont et al. 2011; Small 2012).

In summary, these studies have provided preliminary evidence that suggest the importance of PKN2 in TGFβ-mediated fibroblast activation. In order to understand this phenotype better and identify intermediate targets that regulate this phenotype, the mechanism needs to be defined. Subsequently, the significance of stromal PKN2 expression on prognosis was investigated using data from patient's tumour samples.

4.2.1 Prognostic relevance of PKN2 expression and stromal activation

Understanding the cell biology of the TME is of both therapeutic and prognostic interest. Activation of the stroma can be a predictor of patient outcome and modulating the stroma has been proposed as a therapeutic opportunity to block tumour progression or enhance response to established therapies. Therefore, the potential of PKN2 as a modulator of tumours via the TME was investigated.

The prognostic relevance of PKN2-directed fibroblast activation in response to TGFβ was explored. As PKN2 is ubiquitously expressed, differences in expression of PKN alone cannot be solely considered when studying its function in normal and activated stroma. This was also supported by previous gene expression analysis that showed no difference in PKN2 expression between normal tissue and breast tumours or between different breast cancer types (3.1.1). Furthermore, protein lysates from a panel of CAF cells revealed no difference in PKN2 expression, when compared to the matched normal fibroblasts.

Hence, we sought to define a signature for fibroblasts depleted for PKN2, to act as a surrogate readout for PKN2 suppression or loss. A panel of surrogate markers for PKN2 was chosen from an experiment where wt and PKN2 ko MEFs were stimulated with TGFβ in collagen gels to measure changes in mRNA levels. Genes that were upregulated upon TGFβ stimulation in wt PKN2, but not in PKN2 ko MEFs were chosen as PKN2-related markers for stromal activation (Section 3.2, Table 10). The panel identified comprised the

following genes: IGF1, IGF2, CTGF, THBS2, COL1A1, CDH11, GLI1, POSTN, OGN, ITGA11, FAP and BAMBI. A similar study was conducted in breast cancer, using IGF-1 induced genes in primary breast fibroblasts, as the signature (Rajski et al. 2010). Genes in this panel that are in common with our PKN2 stromal panel include THBS2, COL1A1, FAP, CDH11, ITGA11 and POSTN.

Several other studies consider the gene expression profile of tumour stroma to identify prognostic markers. For example, a study identified 16 different stromal gene signatures, by comparing gene expression between cancer cells and stromal cells in TNBC tumours (Winslow et al. 2015). The set of genes in one of those signatures was ECM-related and was associated with increased risk of recurrence. This signature included genes in common with our signature: COL1A1, POSTN, THBS2 and CDH11. Heatmap clustering of TCGA data on the expression of this stromal gene signature shows clustering of basal breast cancer with low expression of signature 1, compared to all other subtypes and normal controls.

Furthermore, a study in PDAC cancer generated two stromal signatures that distinguish between normal and activated stroma (Moffitt et al. 2015). The gene signature for activated stroma includes THBS2, COL1A1, FAP, CDH11, ITGA11 and POSTN that is in common with our signature, suggesting that a number of PKN2 upregulated genes may correlate with a poor prognostic signature in the tumour stroma.

The clinical relevance of the TME has recently been explored in ovarian cancer by Pearce et al. Multiple genomic, proteomic, transcriptomic and functional analyses were conducted on ovarian cancer samples at various stages of the metastatic process (Pearce et al. 2018a). Profiling of genes and proteins in the ECM of TME identified a molecular signature that is predictive of outcome and tumour stiffness, not only in ovarian cancer

but also applicable in other cancer types (including TNBC). This paper essentially defined a common activated stromal signature, associated with poor outcome.

4.2.2 Prognostic relevance of PKN2 surrogate markers in breast cancer

Sources of stromal samples to investigate the clinical relevance of genes in the TME is often limited. Alternatively, whole tumour section scan be employed to conduct studies on changes in genes specific to the stroma, such as the study by Moffit et al. This study addressed the issue of bulk tumour analysis, which was overcome by using non-negative matrix factorization (NMF – a source separation technique) for microdissecting PDAC samples virtually, on the basis of tumour, stroma, and normal gene expression (Moffitt et al. 2015). A number of genes in our stromal signature are specifically increased in tumour-associated stroma. Therefore, a similar approach can be used to dissect the role of PKN2-regulated genes in activated stroma, using data from whole tumour samples, by focussing on those genes which are restricted in their expression to activated fibroblasts.
Gene expression of whole tumour samples from the TCGA dataset was analysed, considering the expression of PKN2 surrogate markers. Amongst the different TNBC subtypes, BL2 and MSL tumours were associated with high expression of the surrogate markers. However, there were no difference in survival outcomes between patients with low or high PKN2 expression. The major limitation of this dataset, for the purpose of studying the prognostic relevance of PKN2 in the tumour microenvironment, is that the sample is not specifically stromal tissue but includes cancer cells.

To address this limitation, the prognostic relevance of the twelve chosen surrogate markers of PKN2, associated with activated stroma, was interrogated in the stromal gene expression dataset from breast cancer patients from Finak *et al* (Finak et al. 2008). This data includes gene expression of stromal tissue from patients with breast cancer matched with normal surrounding stroma, dissected by laser capture microscopy. 10 (out of 12)

surrogate markers for PKN2 were differentially expressed between tumour-associated stroma, in comparison to matched normal stroma. This validated the specificity of most of the genes in our stromal signature to tumour-associated stromal tissue.

Furthermore, clustering analysis on the expression of genes in our stromal signature and Finak et al data on patient stromal samples revealed two clusters. One of these clusters encompassed patients that presented with poor outcome. This data strongly supports the validity of our stromal gene signature to study its potential as a predictor of patient outcome. Patients with poor outcome had low expression of IGF1 and OGN, in contrast to high expression of BAMBI - considered to be a negative regulator of TGFβ signalling.

4.3 Effect of PKN2 loss on the interaction between fibroblasts and cancer cells

Cancer-associated fibroblasts (CAFs) are activated fibroblasts found within the tumour microenvironment and studies have begun to unpick the reciprocal signalling between fibroblasts and cancer cells. This has been extensively studied in other common solid cancers such as those of the lung (Eberlein et al. 2015) and pancreas (Tape et al. 2016). *In vitro* co-culture studies demonstrated TGFβ- and αvβ6-mediated fibroblast activation by non-small cell lung cancer cells (NSCLCs), identified by induction of α-SMA fibres (Eberlein et al. 2015). This led to upregulation of genes that mediate mesenchymal phenotypes and invasive behaviours. Additionally, reduced sensitivity to anti-cancer agents was also observed in NSCLC in the presence of activated fibroblasts. Moreover, heterocellular multivariate phosphoproteomics using pancreatic ductal adenocarcinoma (PDA) and stromal cells, demonstrated that oncogenic signalling is also influenced by fibroblasts, which adds to the cell-autonomous oncogenic signalling in tumour cells ((Tape et al. 2016)). Furthermore, studies on fibroblasts and their interaction with breast cancer cells revealed implications on growth, invasion and chemo-sensitivity of breast cancer cells (Tao et al. 2017).

4.3.1 *In vitro* studies investigating the role of stromal PKN2 expression in breast cancer cell survival

In a related project in our lab on pancreatic cancer, deletion of PKN2 from either MEFs or pancreatic fibroblasts (pancreatic stellate cells), dramatically reduced their ability to support pancreatic cancer cell invasion in 3D collagen-matrigel gels. In my studies we sought to examine whether such interaction extended to breast cancer models. Fibroblasts that do or do not express PKN2 was investigated in *in vitro* and *in vivo* co-cultures.

Mini-organotypic assays were used as an *in vitro* model, where the 3D conditions and the Matrigel-collagen mix attempts to model the ECM that cancer and stromal cells reside in. Different mouse mammary cancer cell lines were cultured alone or co-cultured with wt or PKN2 ko MEFs. This demonstrated the dependence for stromal PKN2 in 4T1 cells for invasion.

To generate a simple system for assessing the growth of two different cell types in co-culture, cells were engineered for firefly (cancer cells) and renilla (fibroblasts) luciferase reporters were used. In general, increased cell viability of cancer cells was observed when in co-culture with fibroblasts. Co-cultures with MEFs resulted in increased proliferation of PMT.BO1, MDAMB231 and MCF7 cancer cells, which was unaffected by the expression level of PKN2 in MEFs. Similarly, MDAMB21 and MCF7 cell lines in co-culture with human mammary fibroblast cell line HMFU19, resulted in increased cancer cell proliferation. The CAF cell lines, 1997 and 1939, promoted proliferation of MDAMB231 cells, whilst reducing MCF7 proliferation.

The inducible system of conditional PKN2 knockout in MEFs provided a robust means of studying the effect of PKN2 loss on the interaction with cancer cells. However, the use of siRNA to delete PKN2 in human fibroblasts cell line HMFU19 and particularly in primary

CAF cells was challenging. Therefore, the results regarding the effect of PKN2 loss in HMU19 and CAFs on cancer cell proliferation could not be conclusively interpreted.

As well as affecting tumour growth, CAFs have also been demonstrated to mediate chemo-resistance. Tamoxifen resistance is an example that has been attributed to CAFs, mediated by upregulation of PI3K/AKT and MAPK/ERK pathways and phosphorylation of ER (Pontiggia et al. 2012). As part of the luciferase co-culture assays of human cancer cells and fibroblasts, the effect on drug sensitivity was also tested. Although the use of siRNA for PKN2 depletion caused experimental difficulties, preliminary results suggest that cell viability of MCF7 and MDAMB231 were largely unaffected when treated with doxorubicin or paclitaxel, in coculture with wild type CAFs. However, in order to assess the effect of PKN2 deletion in CAFs on cancer cell chemosensitivity better, more robust methods of depleting or deleting PKN2 are required, such as using shRNA or CRISPR/Cas9 system. The apparently senescent nature of many of the primary CAF lines used in the study, in addition to unknown toxicity caused by siRNA transfection affected basal survival of these cells.

4.3.2 *In vivo* studies investigating the effect of PKN2 deletion in the stroma on breast tumours

The interaction between cancer cells and fibroblasts was also investigated *in vivo*, using mixed cell xenografts. The significance of PKN2 expression in MEFs on cancer cells in contact, was investigated by monitoring tumour volumes. Differences in the level of stromal activation and tumour fibrosis, factors that can affect tumour progression, were also determined by α-SMA and Sirius Red staining. Two different syngeneic mixed-cell xenograft models were conducted tested with 4T1 and PyMT.BO1 cell lines. We used MEFs as a surrogate model for CAFs, as PKN2 deletion can be induced in these fibroblasts robustly.

4T1 tumour volumes and Sirius red staining were unaffected either by the presence of MEFs or their PKN2 status. On the other hand, co-injection of MEFs with PyMT.BO1 cells resulted in slightly larger tumours (statistically insignificant), although once again PKN2 status had little effect. Intriguingly however, tumours with PKN2 ko MEFs had reduced areas of strong Sirius red staining and reduced proportion of area stained with α-SMA, compared to tumours with wt PKN2. These results indicate that loss of PKN2 expression may result in reduced stromal activation in tumours.

A major drawback with this experiment was the technical difficulty with identifying injected MEFs despite cells being engineered to express GFP. This was in part attributed to diminished GFP-expression in cultured cells but may also indicate that injected fibroblasts are lost from the tumour or die. Additionally, large numbers of α-SMA positive cells were recruited to tumours, even in the absence of co-injected MEFs, making definitive interpretation of results difficult.

To address these limitations, the significance of stromal PKN2 expression on tumour pathology was investigated in a syngeneic orthotopic model using our inducible conditional PKN2 knockout mouse model (iPKN2: $PKN2^{fl/fl}$; $Rosa26^{Cre/ERT2}$). Hereby, tumour growth and biology can be studied in mice with systemic deletion of PKN2 and an intact immune system. Mice were injected with $3x10^5$ BO.1 cells in each (left and right) inguinal mammary fat pad. The experiment was terminated two weeks post-injection, where tumours showed no differences in size, regardless of stromal PKN2 expression status. Despite no differences in immunohistochemical staining for α-SMA, tumours from PKN2-deleted mice had dramatically reduced staining for Sirius Red, indicating reduced desmoplasia and suggesting reduced stromal activation. Furthermore, there was a significantly reduced number of blood vessels detected by endomucin staining in tumours from PKN2-deleted mice.

Exploring the mechanism of reduced vasculature upon PKN2 loss will provide useful insights into potential targets for anti-angiogenic therapy in tumours. This phenotype was also observed in mouse embryos with global deletion of PKN2, which resulted in abnormal vasculature and a lack of angiogenic remodelling (Quétier et al. 2016).Endothelial-specific deletion of PKN2 in embryos did not however replicate this phenotype, indicating that the reduced expression of PKN2 in other cells mediates the effect of reduced blood vessels.

Several studies indicate that CAFs in the TME play a major role in tumour angiogenesis (Bussard et al. 2016; Luo et al. 2015; Mao et al. 2013). One proposed mechanism is through the secretion of pro-angiogenic factors by CAFs themselves or by promoting secretion from cancer cells. *In vivo* studies by Hu *et al* in a DCIS mixed cell xenograft model showed increased expression of cyclooxygenase-2 (COX-2) in tumours that were co-injected with CAFs, compared to those with no or normal fibroblast co-injections (Hu et al. 2009). This was accompanied by increased expression of the pro-angiogenic factor VEGF. Orimo *et al* observed increased growth and tumour vascularisation when breast cancer cells were co-cultured with CAFs but not with normal fibroblasts (Orimo et al. 2005). These effects were demonstrated to be mediated by secretion of stromal cell-derived level factor 1 (SDF1) by CAFs.

Sewell-Loftin et al describe changes in mechanical properties of CAFs to promote tumour vascularisation (Sewell-Loftin et al. 2017). Employing a 3D *in vitro* model of blood vessel formation, it was observed that co-culture of endothelial cells with CAFs from breast tumours, rather than normal mammary fibroblasts, resulted in establishment of vascular network. Partial disruption of the vascular network via VEGF receptor inhibition demonstrated that other signalling pathways are involved. Further investigation revealed mechanotransductive pathways to be involved, where inhibition of YAP, ROCK2 and SN1 in CAFs suppressed vascularisation.

Lack of ER, PR and HER expression limits treatment of TNBC to chemotherapy and therefore gene candidate for targeted therapy has significant value. The raised microvessel density (Mohammed et al. 2011), VEGF gene amplification (Andre et al. 2009) and overexpression (Linderholm et al. 2009) suggests that blood vessels play an important role in TNBC tumours. These characteristics therefore indicate that TNBC may be susceptible and benefit from anti-angiogenic therapy. For example, Di Mauro *et al* recently identified the hedgehog signalling pathway, particularly Gli1 protein, as a potential target for anti-angiogenic therapy for TNBC (Di Mauro et al. 2017). This gene is one of the 12 genes in our stromal signature, as it was downregulated upon PKN2 deletion in MEFs. Therefore, studying the hedgehog signalling pathway and the relevance of PKN2 in tumours may provide mechanistic indications for the reduced blood vessels observed in our *in vivo* tumour model.

4.4 Concluding remarks

Data from this project strongly indicate a role for PKN2 in fibroblast activation. Investigating the molecular mechanism of this phenotype may provide therapeutic targets, as modulating fibroblast activation can have significant implications on tumour progression and disease outcome. Tumour models employing fibroblast-specific PKN2 deletion will provide insights into the relevance of PKN2 expression in fibroblasts, which can be compared to the phenotypes observed with global PKN2 knockout. Furthermore, the reduced blood vessels in tumours upon PKN2 deletion is worth further exploration as tumour angiogenesis is also a very important characteristic of cancer that has implications on tumour growth, invasion and metastasis.

Appendix

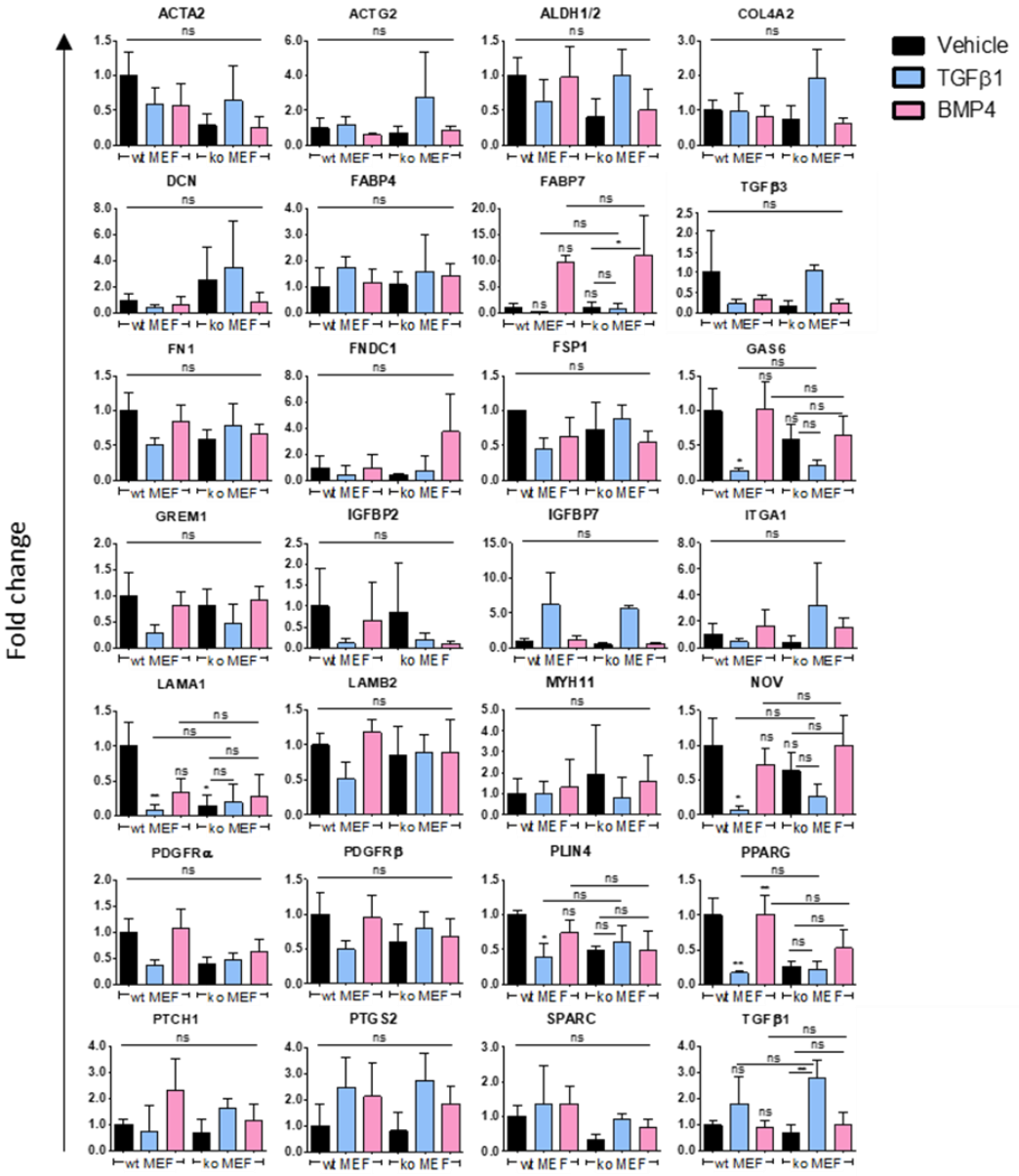

Figure 60. Fold change in gene transcript levels after 24h stimulation with TGFβ1 and BMP4 in MEFs

Fold change, relative to wt MEFs treated with vehicle, of genes that were not selected as PKN2 surrogate markers upon TGFβ1 and BMP4 stimulation. These genes along with the 12 genes chosen as PKN2 surrogate markers, were part of the custom Fluidigm expression assay panel in collaboration with Ivan Quétier and Claus Jorgensen (Manchester CRUK). Data represents the mean +/- SD for n=3 biological repeats. Statistical analysis was carried out using ANOVA followed by Bonferroni post-hoc test: $P<0.05$ (*), $P<0.01$ (**), $P<0.001$ (***).

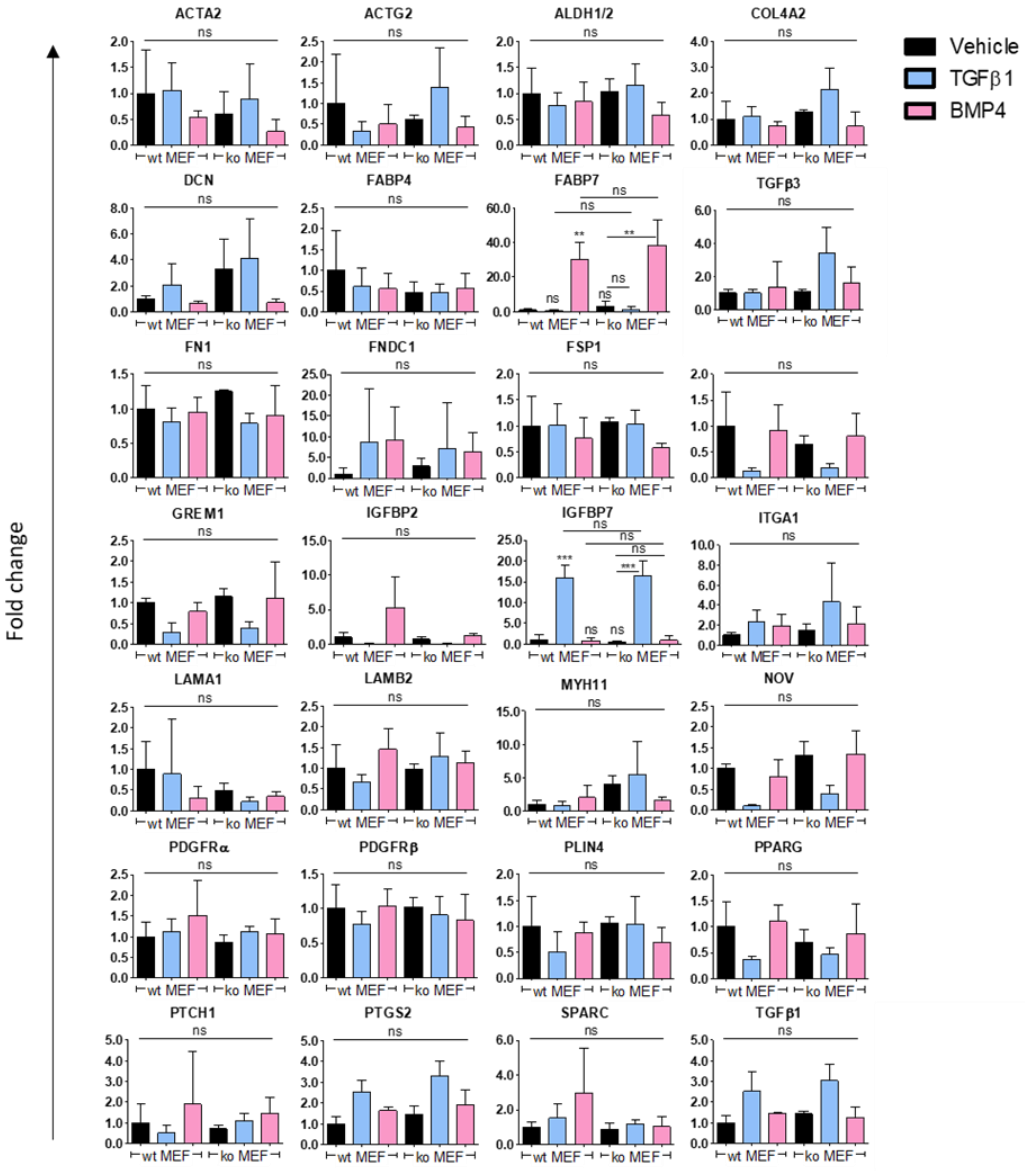

Figure 61. Fold change in gene transcript levels after 48h stimulation with TGFβ1 and BMP4 in MEFs

Fold change, relative to wt MEFs treated with vehicle, of genes that were not selected as PKN2 surrogate markers upon TGFβ1 and BMP4 stimulation. These genes along with the 12 genes chosen as PKN2 surrogate markers, were part of the custom Fluidigm expression assay panel in collaboration with Ivan Quétier and Claus Jorgensen (Manchester CRUK). Data represents the mean +/- SD for n=3 biological repeats. Statistical analysis was carried out using ANOVA followed by Bonferroni post-hoc test: P<0.05 (*), P<0.01 (**), P<0.001 (***).

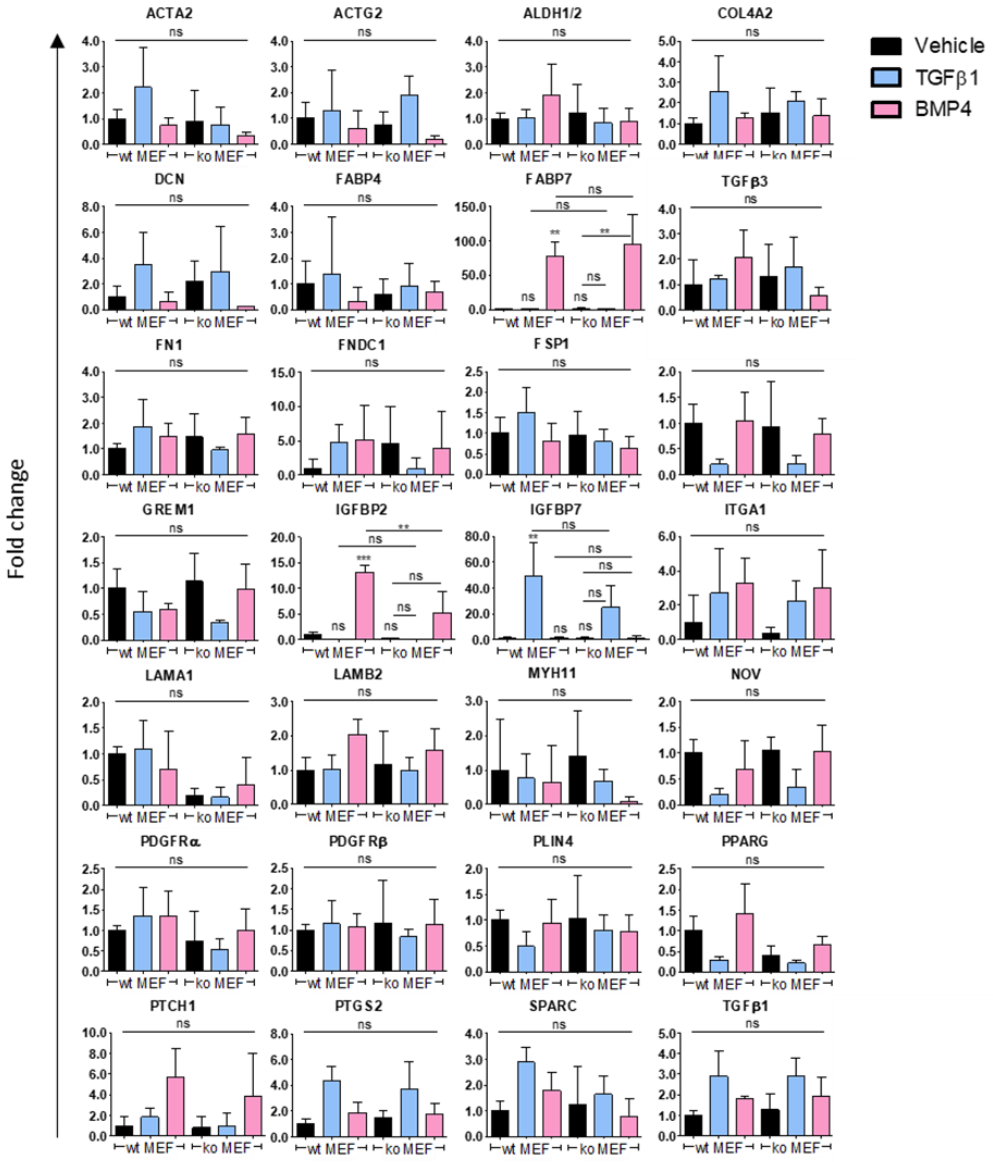

Figure 62. Fold change in gene transcript levels after 72h stimulation with TGFβ1 and BMP4 in MEFs

Fold change, relative to wt MEFs treated with vehicle, of genes that were not selected as PKN2 surrogate markers upon TGFβ1 and BMP4 stimulation. These genes along with the 12 genes chosen as PKN2 surrogate markers, were part of the custom Fluidigm expression assay panel in collaboration with Ivan Quétier and Claus Jorgensen (Manchester CRUK). Data represents the mean +/- SD for n=3 biological repeats. Statistical analysis was carried out using ANOVA followed by Bonferroni post-hoc test: P<0.05 (*), P<0.01 (**), P<0.001 (***).

References

Abd El-Rehim, DM, G Ball, SE Pinder, E Rakha, C Paish, JF Robertson, D Macmillan, RW Blamey, and IO Ellis. 2005. 'High-throughput protein expression analysis using tissue microarray technology of a large well-characterised series identifies biologically distinct classes of breast cancer confirming recent cDNA expression analyses', *Int J Cancer*, 116: 340-50.

Abramson, V, and CL Arteaga. 2011. 'New strategies in HER2-overexpressing breast cancer: many combinations of targeted drugs available.', *Clin Cancer Res*, 17: 952-8.

Ahamed, J, N Burg, K Yoshinaga, CA Janczak, DB Rifkin, and BS Coller. 2008. 'In vitro and in vivo evidence for shear-induced activation of latent transforming growth factor-beta1', *Blood*, 112: 3650-60.

Allen, MD, GJ Thomas, S Clark, MM Dawoud, S Vallath, SJ Payne, JJ Gomm, SA Dreger, S Dickinson, DR Edwards, CJ Pennington, I Sestak, J Cuzick, JF Marshall, IR Hart, and JL Jones. 2014. 'Altered microenvironment promotes progression of preinvasive breast cancer: myoepithelial expression of αvβ6 integrin in DCIS identifies high-risk patients and predicts recurrence.', *Clin Cancer Res*, 20: 344-57.

Amano, M, H Mukai, Y Ono, K Chihara, T Matsui, Y Hamajima, K Okawa, A Iwamatsu, and K Kaibuchi. 1996. 'Identification of a putative target for Rho as the serine-threonine kinase protein kinase N.', *Science*, 271: 648-50.

Anastassiadis, T, SW Deacon, K Devarajan, H Ma, and JR Peterson. 2011. 'Comprehensive assay of kinase catalytic activity reveals features of kinase inhibitor selectivity.', *Nat Biotechnol*, 29: 1039-45.

Anders, CK, and LA Carey. 2009. 'Biology, Metastatic Patterns, and Treatment of Patients with Triple-Negative Breast Cancer', *Clin Breast Cancer*, 9: 73-81.

Andre, F, B Job, P Dessen, A Tordai, S Michiels, C Liedtke, C Richon, K Yan, B Wang, G Vassal, S Delaloge, GN Hortobagyi, WF Symmans, V Lazar, and L Pusztai. 2009. 'Molecular characterization of breast cancer with high-resolution oligonucleotide comparative genomic hybridization array.', *Clin Cancer Res*, 15: 441-51.

Aroner, SA, LC Collins, SJ Schnitt, JL Connolly, GA Colditz, and RM Tamim. 2010. 'Columnar cell lesions and subsequent breast cancer risk: a nested case-control study', *Breast Cancer Res*, 12: 61.

Attisano, L, and JL Wrana. 2000. 'Smads as transcriptional co-modulators', *Curr Opin Cell Biol*, 12: 235-43.

Balendran, A., R. M. Biondi, P. C. Cheung, A. Casamayor, M. Deak, and D. R. Alessi. 2000. 'A 3-phosphoinositide-dependent protein kinase-1 (PDK1) docking site is required for the phosphorylation of protein kinase Czeta (PKCzeta) and PKC-related kinase 2 by PDK1', *J Biol Chem*, 275: 20806-13.

Bansal, R, S Nakagawa, S Yazdani, J van Baarlen, A Venkatesh, AP Koh, WM Song, N Goossens, H Watanabe, MB Beasley, CA Powell, G Storm, N Kaminski, H van Goor, SL Friedman, Y Hoshida, and J Prakash. 2017. 'Integrin alpha 11 in the regulation of the myofibroblast phenotype: implications for fibrotic diseases.', *Exp Mol Med*, 49: 396.

Barocas, VH, and RT Tranquillo. 1997. 'An anisotropic biphasic theory of tissue-equivalent mechanics: the interplay among cell traction, fibrillar network deformation, fibril alignment, and cell contact guidance.', *J Biomech Eng*, 119: 137-45.

Bauer, AF, S Sonzogni, L Meyer, S Zeuzem, A Piiper, RM Biondi, and S Neimanis. 2012. 'Regulation of protein kinase C-related protein kinase 2 (PRK2) by an intermolecular PRK2-PRK2 interaction mediated by Its N-terminal domain', *J Biol Chem*, 287: 20590-602.

Bauer, JA, AB Chakravarthy, JM Rosenbluth, D Mi, EH Seeley, N De Matos Granja-Ingram, MG Olivares, MC Kelley, IA Mayer, IM Meszoely, JA Means-Powell, KN Johnson, CJ Tsai, GD Ayers, ME Sanders, RJ Schneider, SC Formenti, RM Caprioli, and JA Pietenpol. 2010. 'Identification of markers of taxane sensitivity using proteomic and genomic analyses of breast tumors from patients receiving neoadjuvant paclitaxel and radiation.', *Clin Cancer Res*, 16: 681-90.

Bauer, PO, HK Wong, F Oyama, A Goswami, M Okuno, Y Kino, H Miyazaki, and N Nukina. 2009. 'Inhibition of Rho Kinases Enhances the Degradation of Mutant Huntingtin', *J Biol Chem*, 284: 13153-64.

Bergers, G, and D Hanahan. 2008. 'Modes of resistance to anti-angiogenic therapy', *Nat Rev Cancer*, 8: 592-603.

Board, PDQ Adult Treatment Editorial. 2017. 'Breast Cancer Treatment (PDQ®): Health Professional Version.', *PDQ Cancer Information Summaries*.

Bozoky, B, A Savchenko, H Guven, F Ponten, G Klein, and L Szekely. 2014. 'Decreased decorin expression in the tumor microenvironment.', *Cancer Med*, 3: 485-91.

Brechbuhl, HM, J Finlay-Schultz, TM Yamamoto, AE Gillen, DM Cittelly, AC Tan, SB Sams, MM Pillai, AD Elias, WA Robinson, CA Sartorius, and P Kabos. 2017. 'Fibroblast Subtypes Regulate Responsiveness of Luminal Breast Cancer to Estrogen.', *Clin Cancer Res*, 23: 1710-21.

Brenmoehl, J, SN Miller, C Hofmann, D Vogl, W Falk, J Schölmerich, and G Rogler. 2009. 'Transforming growth factor-beta 1 induces intestinal myofibroblast differentiation and modulates their migration', *World J Gastroenterol*, 15: 1431-42.

Brentnall, TA, LA Lai, J Coleman, MP Bronner, S Pan, and R Chen. 2012. 'Arousal of cancer-associated stroma: overexpression of palladin activates fibroblasts to promote tumor invasion.', *PLoS One*, 7: e30219.

Brenton, JD, LA Carey, AA Ahmed, and C Caldas. 2005. 'Molecular classification and molecular forecasting of breast cancer: ready for clinical application?', *J Clin Oncol*, 23: 7350-60.

Brough, R., J. R. Frankum, D. Sims, A. Mackay, A. M. Mendes-Pereira, I. Bajrami, S. Costa-Cabral, R. Rafiq, A. S. Ahmad, M. A. Cerone, R. Natrajan, R. Sharpe, K. K. Shiu, D. Wetterskog, K. J. Dedes, M. B. Lambros, T. Rawjee, S. Linardopoulos, J. S. Reis-Filho, N. C. Turner, C. J. Lord, and A. Ashworth. 2011. 'Functional viability profiles of breast cancer', *Cancer Discov*, 1: 260-73.

Bussard, KM, L Mutkus, K Stumpf, C Gomez-Manzano, and FC Marini. 2016. 'Tumor-associated stromal cells as key contributors to the tumor microenvironment', *Breast Cancer Res*, 18: 84.

Cameron, A. J., C. Escribano, A. T. Saurin, B. Kostelecky, and P. J. Parker. 2009. 'PKC maturation is promoted by nucleotide pocket occupation independently of intrinsic kinase activity', *Nat Struct Mol Biol*, 16: 624-30.

Carey, LA, CM Perou, CA Livasy, LG Dressler, D Cowan, K Conway, G Karaca, MA Troester, CK Tse, S Edmiston, SL Deming, J Geradts, MC Cheang, TO Nielsen, PG Moorman, HS Earp, and RC Millikan. 2006. 'Race, breast cancer subtypes, and survival in the Carolina Breast Cancer Study', *JAMA*, 295: 2492-502.

Cavo, M, M Fato, L Peñuela, F Beltrame, R Raiteri, and S Scaglione. 2016. 'Microenvironment complexity and matrix stiffness regulate breast cancer cell activity in a 3D in vitro model', *Sci Rep*, 6: 35367.

Chaponnier, C, and G Gabbiani. 2004. 'Pathological situations characterized by altered actin isoform expression', *J Pathol*, 204: 386-95.

Chatterjee, S, P Basak, E Buchel, J Safneck, LC Murphy, M Mowat, SK Kung, P Eirew, CJ Eaves, and A Raouf. 2018. 'Breast Cancers Activate Stromal Fibroblast-Induced

Suppression of Progenitors in Adjacent Normal Tissue', *Stem Cell Reports*, 10: 196-211.

Cheang, MC, SK Chia, D Voduc, D Gao, S Leung, J Snider, M Watson, S Davies, PS Bernard, JS Parker, CM Perou, MJ Ellis, and TO Nielsen. 2009. 'Ki67 index, HER2 status, and prognosis of patients with luminal B breast cancer', *J Natl Cancer Inst*, 101: 736-50.

Chen, X., J. Li, W. H. Gray, B. D. Lehmann, J. A. Bauer, Y. Shyr, and J. A. Pietenpol. 2012. 'TNBCtype: A Subtyping Tool for Triple-Negative Breast Cancer', *Cancer Inform*, 11: 147-56.

Cleator, SJ, TJ Powles, T Dexter, L Fulford, A Mackay, IE Smith, H Valgeirsson, A Ashworth, and M Dowsett. 2006. 'The effect of the stromal component of breast tumours on prediction of clinical outcome using gene expression microarray analysis', *Breast Cancer Res*, 8: R32.

Coffelt, SB, and KE de Visser. 2015. 'Immune-mediated mechanisms influencing the efficacy of anticancer therapies.', *Trends Immunol*, 36: 198-216.

Cohen, N, O Shani, Y Raz, Y Sharon, D Hoffman, L Abramovitz, and N Erez. 2017. 'Fibroblasts drive an immunosuppressive and growth-promoting microenvironment in breast cancer via secretion of Chitinase 3-like 1.', *Oncogene*, 36: 4457-68.

Costa, A, Y Kieffer, A Scholer-Dahirel, F Pelon, B Bourachot, M Cardon, P Sirven, I Magagna, L Fuhrmann, C Bernard, C Bonneau, M Kondratova, I Kuperstein, A Zinovyev, AM Givel, MC Parrini, V Soumelis, A Vincent-Salomon, and F Mechta-Grigoriou. 2018. 'Fibroblast Heterogeneity and Immunosuppressive Environment in Human Breast Cancer.', *Cancer Cell*, 33: 463-79.

Cowell, CF, B Weigelt, RA Sakr, CK Ng, J Hicks, TA King, and JS Reis-Filho. 2013. 'Progression from ductal carcinoma in situ to invasive breast cancer: revisited.7', *Mol Oncol*, 7: 859-69.

Curtis, C, SP Shah, SF Chin, G Turashvili, OM Rueda, MJ Dunning, D Speed, AG Lynch, S Samarajiwa, Y Yuan, S Gräf, G Ha, G Haffari, A Bashashati, R Russell, S McKinney, METABRIC Group, A Langerød, A Green, E Provenzano, G Wishart, S Pinder, P Watson, F Markowetz, L Murphy, I Ellis, A Purushotham, AL Børresen-Dale, JD Brenton, S Tavaré, C Caldas, and S Aparicio. 2012. 'The genomic and transcriptomic architecture of 2,000 breast tumours reveals novel subgroups.', *Nature*, 486: 346-52.

Danno, S, K Kubouchi, M Mehruba, M Abe, R Natsume, K Sakimura, S Eguchi, M Oka, M Hirashima, H Yasuda, and H Mukai. 2017. 'PKN2 is essential for mouse embryonic development and proliferation of mouse fibroblasts.', *Genes Cells*, 22: 220-36.

Davies, S. P., H. Reddy, M. Caivano, and P. Cohen. 2000. 'Specificity and mechanism of action of some commonly used protein kinase inhibitors', *Biochem J*, 351: 95-105.

Davis, MI, JP Hunt, S Herrgard, P Ciceri, LM Wodicka, G Pallares, M Hocker, DK Treiber, and PP Zarrinkar. 2011. 'Comprehensive analysis of kinase inhibitor selectivity', *Nat Biotechnol*, 29: 1046-51.

De Laurentiis, M, G Cancello, D D'Agostino, M Giuliano, A Giordano, E Montagna, R Lauria, V Forestieri, A Esposito, L Silvestro, R Pennacchio, C Criscitiello, A Montanino, G Limite, AR Bianco, and S De Placido. 2008. 'Taxane-based combinations as adjuvant chemotherapy of early breast cancer: a meta-analysis of randomized trials', *J Clin Oncol*, 26: 44-53.

De Wever, O, QD Nguyen, L Van Hoorde, M Bracke, E Bruyneel, C Gespach, and M Mareel. 2004. 'Tenascin-C and SF/HGF produced by myofibroblasts in vitro provide convergent pro-invasive signals to human colon cancer cells through RhoA and Rac', *FASEB J*, 18: 1016-8.

Deaton, R. A., C. Su, T. G. Valencia, and S. R. Grant. 2005. 'Transforming growth factor-beta1-induced expression of smooth muscle marker genes involves activation of PKN and p38 MAPK', *J Biol Chem*, 280: 31172-81.

Dekker, TJ, CJ van de Velde, GW van Pelt, JR Kroep, JP Julien, VT Smit, RA Tollenaar, and WE Mesker. 2013. 'Prognostic significance of the tumor-stroma ratio: validation study in node-negative premenopausal breast cancer patients from the EORTC perioperative chemotherapy (POP) trial (10854).', *Breast Cancer Res Treat*, 139: 371-9.

Derynck, R, and XH Feng. 1997. 'TGF-beta receptor signaling.', *Biochim Biophys Acta*, 1333: 105-50.

Derynck, R, and YE Zhang. 2003. 'Smad-dependent and Smad-independent pathways in TGF-beta family signalling', *Nature*, 425: 577-84.

Desmoulière, A, A Geinoz, F Gabbiani, and G Gabbiani. 1993. 'Transforming growth factor-beta 1 induces alpha-smooth muscle actin expression in granulation tissue myofibroblasts and in quiescent and growing cultured fibroblasts', *J Cell Biol*, 122: 103-11.

Dewis, R, and J Gribbin. 2009. 'Breast Cancer: Diagnosis and Treatment: An Assessment of Need', *NICE Clinical Guidelines*, 81.

Dexter, DL, HM Kowalski, BA Blazar, Z Fligiel, R Vogel, and GH Heppner. 1978. 'Heterogeneity of tumor cells from a single mouse mammary tumor.', *Cancer Res*, 38: 3174-81.

Di Mauro, C, R Rosa, V D'Amato, P Ciciola, A Servetto, R Marciano, RC Orsini, L Formisano, S De Falco, V Cicatiello, M Di Bonito, M Cantile, F Collina, A Chambery, BM Veneziani, S De Placido, and R Bianco. 2017. 'Hedgehog signalling pathway orchestrates angiogenesis in triple-negative breast cancers.', *Br J Cancer*, 116: 1425-35.

Dong, LQ, LR Landa, MJ Wick, L Zhu, H Mukai, Y Ono, and F Liu. 2000. 'Phosphorylation of protein kinase N by phosphoinositide-dependent protein kinase-1 mediates insulin signals to the actin cytoskeleton', *Proc Natl Acad Sci U S A*, 97: 5089-94.

Downey, C. L., S. A. Simpkins, J. White, D. L. Holliday, J. L. Jones, L. B. Jordan, J. Kulka, S. Pollock, S. S. Rajan, H. H. Thygesen, A. M. Hanby, and V. Speirs. 2014. 'The prognostic significance of tumour-stroma ratio in oestrogen receptor-positive breast cancer', *Br J Cancer*, 110: 1744-7.

Duda, DG, AM Duyverman, M Kohno, M Snuderl, EJ Steller, D Fukumura, and RK Jain. 2010. 'Malignant cells facilitate lung metastasis by bringing their own soil.', *Proc Natl Acad Sci U S A*, 107: 21677-82.

Dumont, N, B Liu, RA Defilippis, H Chang, JT Rabban, AN Karnezis, JA Tjoe, J Marx, B Parvin, and TD Tlsty. 2013. 'Breast fibroblasts modulate early dissemination, tumorigenesis, and metastasis through alteration of extracellular matrix characteristics', *Neoplasia*, 15: 249-63.

Dupont, S., L. Morsut, M. Aragona, E. Enzo, S. Giulitti, M. Cordenonsi, F. Zanconato, J. Le Digabel, M. Forcato, S. Bicciato, N. Elvassore, and S. Piccolo. 2011. 'Role of YAP/TAZ in mechanotransduction', *Nature*, 474: 179-83.

Eberlein, C, C Rooney, SJ Ross, M Farren, HM Weir, and ST Barry. 2015. 'E-Cadherin and EpCAM expression by NSCLC tumour cells associate with normal fibroblast activation through a pathway initiated by integrin αvβ6 and maintained through TGFβ signalling.', *Oncogene*, 34: 704-16.

Elice, F, and F Rodeghiero. 2012. 'Side effects of anti-angiogenic drugs', *Thromb Res*, 129: S50-3.

Emon, B, J Bauer, Y Jain, B Jung, and T Saif. 2018. 'Biophysics of Tumor Microenvironment and Cancer Metastasis - A Mini Review.', *Comput Struct Biotechnol J*, 16: 279-87.

Falk, M. D., W. Liu, B. Bolanos, K. Unsal-Kacmaz, A. Klippel, S. Grant, A. Brooun, and S. Timofeevski. 2014. 'Enzyme Kinetics and Distinct Modulation of the Protein Kinase N Family of Kinases by Lipid Activators and Small Molecule Inhibitors', *Biosci Rep*.

Farmer, P, H Bonnefoi, P Anderle, D Cameron, P Wirapati, V Becette, S André, M Piccart, M Campone, E Brain, G Macgrogan, T Petit, J Jassem, F Bibeau, E Blot, J Bogaerts, M Aguet, J Bergh, R Iggo, and M Delorenzi. 2009. 'A stroma-related gene signature predicts resistance to neoadjuvant chemotherapy in breast cancer', *Nat Med*, 15: 68-74.

Feng, S, JK Chen, H Yu, JA Simon, and SL Schreiber. 1994. 'Two binding orientations for peptides to the Src SH3 domain: development of a general model for SH3-ligand interactions.', *Science*, 266: 1241-7.

Ferrari-Amorotti, G, C Chiodoni, F Shen, S Cattelani, AR Soliera, G Manzotti, G Grisendi, M Dominici, F Rivasi, MP Colombo, A Fatatis, and B Calabretta. 2014. 'Suppression of invasion and metastasis of triple-negative breast cancer lines by pharmacological or genetic inhibition of slug activity', *Neoplasia*, 16: 1047-58.

Finak, G, N Bertos, F Pepin, S Sadekova, M Souleimanova, H Zhao, H Chen, G Omeroglu, S Meterissian, A Omeroglu, M Hallett, and M Park. 2008. 'Stromal gene expression predicts clinical outcome in breast cancer', *Nat Med*, 14: 518-27.

Fleming, JM, TC Miller, MJ Meyer, E Ginsburg, and BK Vonderhaar. 2010. 'Local regulation of human breast xenograft models.', *J Cell Physiol*, 224: 795-806.

Flynn, P., H. Mellor, R. Palmer, G. Panayotou, and P. J. Parker. 1998. 'Multiple interactions of PRK1 with RhoA. Functional assignment of the Hr1 repeat motif', *J Biol Chem*, 273: 2698-705.

Fraley, C, AE Raftery, TB Murphy, and L Scrucca. 2012. "mclust Version 4 for R: Normal mixture modeling for model]based clustering, classification, and density estimation. ." In *Technical Report*.

Frodin, M., T. L. Antal, B. A. Dummler, C. J. Jensen, M. Deak, S. Gammeltoft, and R. M. Biondi. 2002. 'A phosphoserine/threonine-binding pocket in AGC kinases and PDK1 mediates activation by hydrophobic motif phosphorylation', *EMBO J*, 21: 5396-407.

Gaggioli, C. 2008. 'Collective invasion of carcinoma cells: when the fibroblasts take the lead.', *Cell Adh Migr*, 2: 45-7.

Gaggioli, C, S Hooper, C Hidalgo-Carcedo, R Grosse, JF Marshall, K Harrington, and E Sahai. 2007. 'Fibroblast-led collective invasion of carcinoma cells with differing roles for RhoGTPases in leading and following cells.', *Nat Cell Biol*, 9: 1392-400.

Gao, Y, SP Davies, M Augustin, A Woodward, UA Patel, R Kovelman, and KJ Harvey. 2013. 'A broad activity screen in support of a chemogenomic map for kinase signalling research and drug discovery. ', *Biochem J*, 451: 313-28.

Garin-Chesa, P, LJ Old, and WJ Rettig. 1990. 'Cell surface glycoprotein of reactive stromal fibroblasts as a potential antibody target in human epithelial cancers', *Proc Natl Acad Sci U S A*, 87: 7235-9.

Gesher, A. 1998. 'Analogs of staurosporine: potential anticancer drugs?', *Gen Pharmacol*, 31: 721-8.

Good, DJ, PJ Polverini, F Rastinejad, MM Le Beau, RS Lemons, WA Frazier, and NP Bouck. 1990. 'A tumor suppressor-dependent inhibitor of angiogenesis is immunologically and functionally indistinguishable from a fragment of thrombospondin.', *Proc Natl Acad Sci U S A*, 87: 6624-8.

Grandage, V. L., T. Everington, D. C. Linch, and A. Khwaja. 2006. 'Go6976 is a potent inhibitor of the JAK 2 and FLT3 tyrosine kinases with significant activity in primary acute myeloid leukaemia cells', *BR J Haematol*, 135: 303-16.

Guy, CT1, RD Cardiff, and WJ Muller. 1992a. 'Induction of mammary tumors by expression of polyomavirus middle T oncogene: a transgenic mouse model for metastatic disease.', *Mol Cell Biol*, 12: 954-61.

Guy, CT, RD Cardiff, and WJ Muller. 1992b. 'Induction of mammary tumors by expression of polyomavirus middle T oncogene: a transgenic mouse model for metastatic disease', *Mol Cell Biol*, 12.

Győrffy, B, A Lanczky, AC Eklund, C Denkert, J Budczies, Q Li, and Z Szallasi. 2010. 'An online survival analysis tool to rapidly assess the effect of 22,277 genes on breast cancer prognosis using microarray data of 1,809 patients', *Breast Cancer Res Treat*, 123: 725-31.

Hakem, A, O Sanchez-Sweatman, A You-Ten, G Duncan, A Wakeham, R Khokha, and TW Mak. 2005. 'RhoC is dispensable for embryogenesis and tumor initiation but essential for metastasis.', *Genes Dev*, 19: 1974-9.

Hamaguchi, T., M. Ito, J. Feng, T. Seko, M. Koyama, H. Machida, K. Takase, M. Amano, K. Kaibuchi, D. J. Hartshorne, and T. Nakano. 2000. 'Phosphorylation of CPI-17, an inhibitor of myosin phosphatase, by protein kinase N', *Biochem Biophys Res Commun*, 274: 825-30.

Hamilton, DW. 2008. 'Functional role of periostin in development and wound repair: implications for connective tissue disease.', *J Cell Commun Signal*, 2: 9-17.

Hauge, C., T. L. Antal, D. Hirschberg, U. Doehn, K. Thorup, L. Idrissova, K. Hansen, O. N. Jensen, T. J. Jorgensen, R. M. Biondi, and M. Frodin. 2007. 'Mechanism for activation of the growth factor-activated AGC kinases by turn motif phosphorylation', *EMBO J*, 26: 2251-61.

Heinisch, JJ, A Lorberg, HP Schmitz, and JJ Jacoby. 1999. 'The protein kinase C-mediated MAP kinase pathway involved in the maintenance of cellular integrity in Saccharomyces cerevisiae.', *Mol Microbiol*, 32: 671-80.

Heppner, GH, FR Miller, and PM Shekhar. 2000. 'Nontransgenic models of breast cancer', *Breast Cancer Res*, 2: 331-4.

Herbert, JM, JM Augereau, J Gleye, and JP Maffrand. 1990. 'Chelerythrine is a potent and specific inhibitor of protein kinase C.', *Biochem Biophys Res Commun.*, 172: 993-9.

Hexner, E, G Roboz, R Hoffman, S Luger, J Mascarenhas, M Carroll, R Clementi, D Bensen-Kennedy, and A Moliterno. 2014. 'Open-label study of oral CEP-701 (lestaurtinib) in patients with polycythaemia vera or essential thrombocythaemia with JAK2-V617F mutation', *BR J Haematol*, 164: 83-93.

Hidalgo, M, F Amant, AV Biankin, E Budinská, AT Byrne, C Caldas, RB Clarke, S de Jong, J Jonkers, GM Mælandsmo, S Roman-Roman, J Seoane, L Trusolino, and A Villanueva. 2014. 'Patient-derived xenograft models: an emerging platform for translational cancer research.', *Cancer Discov*, 4: 998-1013.

Hinz, B, G Celetta, JJ Tomasek, G Gabbiani, and C Chaponnier. 2001. 'Alpha-smooth muscle actin expression upregulates fibroblast contractile activity', *Mol Biol Cell*, 12: 2730-41.

Hoffman, RM. 2015. 'Patient-derived orthotopic xenografts: better mimic of metastasis than subcutaneous xenografts.', *Nat Rev Cancer*, 15: 451-2.

Holen, I, V Speirs, B Morrissey, and K Blyth. 2017. 'In vivo models in breast cancer research: progress, challenges and future directions.', *Dis Model Mech*, 10: 359-71.

Holland, R, JL Peterse, RR Millis, V Eusebi, D Faverly, MJ van de Vijver, and B Zafrani. 1994. 'Ductal carcinoma in situ: a proposal for a new classification', *Semin Diagn Pathol*, 11: 167-80.

Hu, M, G Peluffo, H Chen, R Gelman, S Schnitt, and K Polyak. 2009. 'Role of COX-2 in epithelial-stromal cell interactions and progression of ductal carcinoma in situ of the breast.', *Proc Natl Acad Sci U S A*, 106: 3372-7.

Hu, X, YQ Li, QG Li, YL Ma, JJ Peng, and SJ Cai. 2018. 'Osteoglycin (OGN) reverses epithelial to mesenchymal transition and invasiveness in colorectal cancer via EGFR/Akt pathway.', *J Exp Clin Cancer Res*, 37: 41.

Huang, CF, C Lira, K Chu, MA Bilen, YC Lee, X Ye, SM Kim, A Ortiz, FL Wu, CJ Logothetis, LY Yu-Lee, and SH Lin. 2010. 'Cadherin-11 increases migration and invasion of prostate cancer cells and enhances their interaction with osteoblasts.', *Cancer Res*, 70: 4580-9.

Huang, S, L Murphy, and W Xu. 2018 'Genes and functions from breast cancer signatures.', *BMC Cancer*, 18: 473.

Ishizaki, T, M Maekawa, K Fujisawa, K Okawa, A Iwamatsu, A Fujita, N Watanabe, Y Saito, A Kakizuka, N Morii, and S Narumiya. 1996 'The small GTP-binding protein Rho binds to and activates a 160 kDa Ser/Thr protein kinase homologous to myotonic dystrophy kinase.', *EMBO J*, 15: 1885-93.

Jilg, CA, A Ketscher, E Metzger, B Hummel, D Willmann, V Russeler, V Drendel, A Imhof, M Jung, H Franz, S Holz, M Kronig, JM Muller, and R Schule. 2014. 'PRK1/PKN1 controls migration and metastasis of androgen-independent prostate cancer cells', *Oncotarget*.

Johnston, SR. 2011. 'The role of chemotherapy and targeted agents in patients with metastatic breast cancer.', *Eur J Cancer*, 47: S38-47.

Johnstone, CN, YE Smith, Y Cao, AD Burrows, RS Cross, X Ling, RP Redvers, JP Doherty, BL Eckhardt, AL Natoli, CM Restall, E Lucas, HB Pearson, S Deb, KL Britt, A Rizzitelli, J Li, JH Harmey, N Pouliot, and RL Anderson. 2015 'Functional and molecular characterisation of EO771.LMB tumours, a new C57BL/6-mouse-derived model of spontaneously metastatic mammary cancer.', *Dis Model Mech.*, 8: 237-51.

Karagiannis, GS, T Poutahidis, SE Erdman, R Kirsch, RH Riddell, and EP Diamandis. 2012. 'Cancer-associated fibroblasts drive the progression of metastasis through both paracrine and mechanical pressure on cancer tissue.', *Mol Cancer Res*, 10: 1403-18.

Katoh, K, Y Kano, M Amano, H Onishi, K Kaibuchi, and K Fujiwara. 2001. 'Rho-kinase–mediated contraction of isolated stress fibers.', *J Cell Biol*, 153: 569-84.

Kawamata, T., T. Taniguchi, H. Mukai, M. Kitagawa, T. Hashimoto, K. Maeda, Y. Ono, and C. Tanaka. 1998. 'A protein kinase, PKN, accumulates in Alzheimer neurofibrillary tangles and associated endoplasmic reticulum-derived vesicles and phosphorylates tau protein', *J Neurosci*, 18: 7402-10.

Kharaishvili, G, D Simkova, K Bouchalova, M Gachechiladze, N Narsia, and J Bouchal. 2014. 'The role of cancer-associated fibroblasts, solid stress and other microenvironmental factors in tumor progression and therapy resistance', *Cancer Cell Int*, 14: 41.

Kitagawa, M., H. Mukai, H. Shibata, and Y. Ono. 1995. 'Purification and characterization of a fatty acid-activated protein kinase (PKN) from rat testis', *Biochem J*, 310 (Pt 2): 657-64.

Kitagawa, M., H. Shibata, M. Toshimori, H. Mukai, and Y. Ono. 1996. 'The role of the unique motifs in the amino-terminal region of PKN on its enzymatic activity', *Biochem Biophys Res Commun*, 220: 963-8.

Kittaneh, M, AJ Montero, and S Glück. 2013 'Molecular profiling for breast cancer: a comprehensive review.', *Biomark Cancer*, 5: 61-70.

Klemm, F, and JA Joyce. 2015. 'Microenvironmental regulation of therapeutic response in cancer.', *Trends Cell Biol*, 25: 198-213.

Knapper, S, AK Burnett, T Littlewood, WJ Kell, S Agrawal, R Chopra, R Clark, MJ Levis, and D Small. 2006. 'A phase 2 trial of the FLT3 inhibitor lestaurtinib (CEP701) as first-line treatment for older patients with acute myeloid leukemia not considered fit for intensive chemotherapy', *Blood*, 108: 3262-70.

Kobayashi, T, and P Cohen. 1999. 'Activation of serum- and glucocorticoid-regulated protein kinase by agonists that activate phosphatidylinositide 3-kinase is mediated by 3-phosphoinositide-dependent protein kinase-1 (PDK1) and PDK2.', *Biochem J*, 339: 319-28.

Kohler, J., G. Erlenkamp, A. Eberlin, T. Rumpf, I. Slynko, E. Metzger, R. Schule, W. Sippl, and M. Jung. 2012. 'Lestaurtinib inhibits histone phosphorylation and androgen-dependent gene expression in prostate cancer cells', *PLoS One*, 7: e34973.

Kojima, Y, A Acar, EN Eaton, KT Mellody, C Scheel, I Ben-Porath, TT Onder, ZC Wang, AL Richardson, RA Weinberg, and A Orimo. 2010. 'Autocrine TGF-beta and stromal cell-derived factor-1 (SDF-1) signaling drives the evolution of tumor-promoting mammary stromal myofibroblasts', *Proc Natl Acad Sci U S A*, 107: 20009-14.

Kotani, K , K Yonezawa, K Hara, H Ueda, Y Kitamura, H Sakaue, A Ando, A Chavanieu, B Calas, and F Grigorescu. 1994. 'Involvement of phosphoinositide 3-kinase in insulin- or IGF-1-induced membrane ruffling', *EMBO J*, 13: 2313–21.

Lachmann, S., A. Jevons, M. De Rycker, A. Casamassima, S. Radtke, A. Collazos, and P. J. Parker. 2011. 'Regulatory domain selectivity in the cell-type specific PKN-dependence of cell migration', *PLoS One*, 6: e21732.

Lambert, AW, CK Wong, S Ozturk, P Papageorgis, R Raghunathan, Y Alekseyev, AC Gower, BM Reinhard, HM Abdolmaleky, and S Thiagalingam. 2016. 'Tumor Cell-Derived Periostin Regulates Cytokines That Maintain Breast Cancer Stem Cells.', *Mol Cancer Res*, 14: 103-13.

Lattouf, R, R Younes, D Lutomski, N Naaman, G Godeau, K Senni, and S Changotade. 2014. 'Picrosirius red staining: a useful tool to appraise collagen networks in normal and pathological tissues.', *J Histochem Cytochem*, 62: 751-8.

Le Good, J. A., W. H. Ziegler, D. B. Parekh, D. R. Alessi, P. Cohen, and P. J. Parker. 1998. 'Protein kinase C isotypes controlled by phosphoinositide 3-kinase through the protein kinase PDK1', *Science*, 281: 2042-5.

Leenders, F, K Mopert, A Schmiedeknecht, A Santel, F Czauderna, M Aleku, S Penschuck, S Dames, M Sternberger, T Rohl, A Wellmann, W Arnold, K Giese, J Kaufmann, and A Klippel. 2004. 'PKN3 is required for malignant prostate cell growth downstream of activated PI 3-kinase', *EMBO J*, 23: 3303-13.

Lehmann, BD, JA Bauer, X Chen, ME Sanders, AB Chakravarthy, and Pietenpol JA. 2011. 'Identification of human triple-negative breast cancer subtypes and preclinical models for selection of targeted therapies', *J Clin Invest*, 121: 2750-767.

Lehmann, BD, JA Bauer, X Chen, ME Sanders, AB Chakravarthy, Y Shyr, and JA Pietenpol. 2011. 'Identification of human triple-negative breast cancer subtypes and preclinical models for selection of targeted therapies', *J Clin Invest*, 121: 2750-67.

Li, H, P Cherukuri, N Li, V Cowling, M Spinella, M Cole, AK Godwin, W Wells, and J DiRenzo. 2007. 'Nestin is expressed in the basal/myoepithelial layer of the mammary gland and is a selective marker of basal epithelial breast tumors', *Cancer Res*, 67: 815-9.

Li, Q, NJ Birkbak, B Gyorffy, Z Szallasi, and AC Eklund. 2011. 'Jetset: selecting the optimal microarray probe set to represent a gene.', *BMC Bioinformatics*, 12: 474.

Limoge, M, A Safina, A Beattie, L Kapus, AM Truskinovsky, and AV Bakin. 2017. 'Tumor-fibroblast interactions stimulate tumor vascularization by enhancing cytokine-driven production of MMP9 by tumor cells', *Oncotarget*, 8: 35592-608.

Lin, W, J Huang, Z Yuan, S Feng, Y Xie, and W Ma. 2017. 'Protein kinase C inhibitor chelerythrine selectively inhibits proliferation of triple-negative breast cancer cells', *Sci Rep*, 7: 2022.

Linderholm, BK, H Hellborg, U Johansson, G Elmberger, L Skoog, J Lehtiö, and R Lewensohn. 2009. 'Significantly higher levels of vascular endothelial growth factor (VEGF) and shorter survival times for patients with primary operable triple-negative breast cancer.', *Ann Oncol*, 20: 1639-46.

Liu, C, B Chen, J Zhu, R Zhang, F Yao, F Jin, H Xu, and P Lu. 2010. 'Clinical implications for nestin protein expression in breast cancer.', *Cancer Sci*, 101: 815-9.

Liu, X, V Ory, S Chapman, H Yuan, C Albanese, B Kallakury, OA Timofeeva, C Nealon, A Dakic, V Simic, BR Haddad, JS Rhim, A Dritschilo, A Riegel, A McBride, and R Schlegel. 2012. 'ROCK inhibitor and feeder cells induce the conditional reprogramming of epithelial cells.', *Am J Pathol*, 180: 599-607.

Liu, X, Z Zhang, X Yan, H Liu, L Zhang, A Yao, C Guo, X Liu, and T Xu. 2014. 'The Rho kinase inhibitor Y-27632 facilitates the differentiation of bone marrow mesenchymal stem cells', *J Mol Histol*, 45: 707-14.

Loeffler, M, JA Krüger, AG Niethammer, and RA Reisfeld. 2006. 'Targeting tumor-associated fibroblasts improves cancer chemotherapy by increasing intratumoral drug uptake', *J Clin Invest*, 1116: 1955-62.

Lopes, N, D Gregg, S Vasudevan, H Hassanain, P Goldschmidt-Clermont, and H Kovacic. 2003. 'Thrombospondin 2 regulates cell proliferation induced by Rac1 redox-dependent signaling.', *Mol Cell Biol*, 23: 5401-8.

Lovitt, CJ, TB Shelper, and VM Avery. 2018. 'Doxorubicin resistance in breast cancer cells is mediated by extracellular matrix proteins', *BMC Cancer*, 18: 41.

Lu, Y., and J. Settleman. 1999. 'The Drosophila Pkn protein kinase is a Rho/Rac effector target required for dorsal closure during embryogenesis', *Genes Dev*, 13: 1168-80.

Luo, H, G Tu, Z Liu, and M Liu. 2015. 'Cancer-associated fibroblasts: a multifaceted driver of breast cancer progression', *Cancer Lett*, 361: 155-63.

Ma, XJ, R Salunga, JT Tuggle, J Gaudet, E Enright, P McQuary, T Payette, M Pistone, K Stecker, BM Zhang, YX Zhou, H Varnholt, B Smith, M Gadd, E Chatfield, J Kessler, TM Baer, MG Erlander, and DC Sgroi. 2003. 'Gene expression profiles of human breast cancer progression', *Proc Natl Acad Sci U S A*, 100: 5974-9.

Maesaki, R., K. Ihara, T. Shimizu, S. Kuroda, K. Kaibuchi, and T. Hakoshima. 1999. 'The structural basis of Rho effector recognition revealed by the crystal structure of human RhoA complexed with the effector domain of PKN/PRK1', *Mol Cell*, 4: 793-803.

Mao, Y, ET Keller, DH Garfield, K Shen, and J Wang. 2013. 'Stromal cells in tumor microenvironment and breast cancer.', *Cancer Metastasis Rev*, 32: 303-15.

Marini, NJ, E Meldrum, B Buehrer, AV Hubberstey, DE Stone, A Traynor-Kaplan, and SI Reed. 1996. 'A pathway in the yeast cell division cycle linking protein kinase C (Pkc1) to activation of Cdc28 at START', *EMBO J*, 15: 3040-52.

Marshall, J. 2011. 'Transwell(®) invasion assays.', *Methods Mol Biol*, 769: 97-110.

Marshman, E, and CH Streuli. 2002. 'Insulin-like growth factors and insulin-like growth factor binding proteins in mammary gland function', *Breast Cancer Res*, 4: 231-39.

Martin, SS, T Haruta, AJ Morris, A Klippel, LT Williams, and JM Olefsky. 1996. 'Activated phosphatidylinositol 3-kinase is sufficient to mediate actin rearrangement and GLUT4 translocation in 3T3-L1 adipocytes.', *J Biol Chem*, 271: 17605-8.

Martinez-Outschoorn, U. E., A. Goldberg, Z. Lin, Y. H. Ko, N. Flomenberg, C. Wang, S. Pavlides, R. G. Pestell, A. Howell, F. Sotgia, and M. P. Lisanti. 2011. 'Anti-estrogen resistance in breast cancer is induced by the tumor microenvironment and can be

overcome by inhibiting mitochondrial function in epithelial cancer cells', *Cancer Biol Ther*, 12: 924-38.

Matsuzawa, K., H. Kosako, N. Inagaki, H. Shibata, H. Mukai, Y. Ono, M. Amano, K. Kaibuchi, Y. Matsuura, I. Azuma, and M. Inagaki. 1997. 'Domain-specific phosphorylation of vimentin and glial fibrillary acidic protein by PKN', *Biochem Biophys Res Commun*, 234: 621-5.

Mauri, D, N Pavlidis, NP Polyzos, and JP Ioannidis. 2006. 'Survival with aromatase inhibitors and inactivators versus standard hormonal therapy in advanced breast cancer: meta-analysis', *J Natl Cancer Inst*, 98: 1285-91.

McLane, JS, and LA Ligon. 2016. 'Stiffened Extracellular Matrix and Signaling from Stromal Fibroblasts via Osteoprotegerin Regulate Tumor Cell Invasion in a 3-D Tumor in Situ Model', *Cancer Microenviron*, 9: 127-39.

Merchant, A, G Joseph, Q Wang, S Brennan, and W Matsui. 2010. 'Gli1 regulates the proliferation and differentiation of HSCs and myeloid progenitors.', *Blood*, 115: 2391-6.

Metzger, E., J. M. Muller, S. Ferrari, R. Buettner, and R. Schule. 2003. 'A novel inducible transactivation domain in the androgen receptor: implications for PRK in prostate cancer', *EMBO J*, 22: 270-80.

Metzger, E., N. Yin, M. Wissmann, N. Kunowska, K. Fischer, N. Friedrichs, D. Patnaik, J. M. Higgins, N. Potier, K. H. Scheidtmann, R. Buettner, and R. Schule. 2008. 'Phosphorylation of histone H3 at threonine 11 establishes a novel chromatin mark for transcriptional regulation', *Nat Cell Biol*, 10: 53-60.

Misaki, K, H Mukai, C Yoshinaga, K Oishi, T Isagawa, M Takahashi, K Ohsumi, T Kishimoto, and Y Ono. 2001. 'PKN delays mitotic timing by inhibition of Cdc25C: possible involvement of PKN in the regulation of cell division', *Proc Natl Acad Sci USA*, 98: 125-29.

Mishra, PJ, PJ Mishra, R Humeniuk, DJ Medina, G Alexe, JP Mesirov, S Ganesan, JW Glod, and D Banerjee. 2008. 'Carcinoma-associated fibroblast-like differentiation of human mesenchymal stem cells.', *Cancer Res*, 68: 4331-9.

Moffitt, RA, R Marayati, EL Flate, KE Volmar, SG Loeza, KA Hoadley, NU1 Rashid, LA Williams, SC Eaton, AH Chung, JK Smyla, JM Anderson, HJ Kim, DJ Bentrem, MS Talamonti, CA Iacobuzio-Donahue, MA Hollingsworth, and JJ Yeh. 2015. 'Virtual microdissection identifies distinct tumor- and stroma-specific subtypes of pancreatic ductal adenocarcinoma.', *Nat Genet*, 47: 1168-78.

Mohammed, RA, IO Ellis, AM Mahmmod, EC Hawkes, AR Green, EA Rakha, and SG Martin. 2011. 'Lymphatic and blood vessels in basal and triple-negative breast cancers: characteristics and prognostic significance.', *Mod Pathol*, 24: 774-85.

Molyneux, G, FC Geyer, FA Magnay, A McCarthy, H Kendrick, R Natrajan, A Mackay, A Grigoriadis, A Tutt, A Ashworth, JS Reis-Filho, and MJ Smalley. 2010. 'BRCA1 Basal-like Breast Cancers Originate from Luminal Epithelial Progenitors and Not from Basal Stem Cells', *Cell Stem Cell*, 7: 403-17.

Moran, MS, SJ Schnitt, AE Giuliano, JR Harris, SA Khan, J Horton, S Klimberg, M Chavez-MacGregor, G Freedman, N Houssami, PL Johnson, and M Morrow. 2014. 'Society of Surgical Oncology-American Society for Radiation Oncology consensus guideline on margins for breast-conserving surgery with whole-breast irradiation in stages I and II invasive breast cancer.', *J Clin Oncol*, 32: 1507-15.

Mukai, H, M Kitagawa, H Shibata, H Takanaga, K Mori, M Shimakawa, M Miyahara, K Hirao, and Y Ono. 1994. 'Activation of PKN, a novel 120-kDa protein kinase with leucine zipper-like sequences, by unsaturated fatty acids and by limited proteolysis', *Biochem Biophys Res Commun*, 204: 348-56.

Mukai, H, M Miyahara, H Sunakawa, H Shibata, M Toshimori, M Kitagawa, M Shimakawa, H Takanaga, and Y Ono. 1996. 'Translocation of PKN from the cytosol to the nucleus induced by stresses.', *Proceedings of the National Academy of Sciences of the United States of America*, 93: 10195-9.

Mukai, H, A Muramatsu, R Mashud, K Kubouchi, S Tsujimoto, T Hongu, Y Kanaho, M Tsubaki, S Nishida, G Shioi, S Danno, M Mehruba, R Satoh, and R Sugiura. 2016. 'PKN3 is the major regulator of angiogenesis and tumor metastasis in mice', *Sci Rep*, 8: 18979.

Mukai, H, and Y Ono. 1994. 'A Novel Protein Kinase with Leucine Zipper-like Sequences: Its Catalytic Domain Is Highly Homologous to That of Protein Kinase C', *Biochem Biophys Res Commun*, 199: 897-904.

Mukai, H. 2003. 'The structure and function of PKN, a protein kinase having a catalytic domain homologous to that of PKC', *J Biochem*, 133: 17-27.

Mukai, H., M. Toshimori, H. Shibata, M. Kitagawa, M. Shimakawa, M. Miyahara, H. Sunakawa, and Y. Ono. 1996. 'PKN associates and phosphorylates the head-rod domain of neurofilament protein', *J Biol Chem*, 271: 9816-22.

Mukai, H., M. Toshimori, H. Shibata, H. Takanaga, M. Kitagawa, M. Miyahara, M. Shimakawa, and Y. Ono. 1997. 'Interaction of PKN with alpha-actinin', *J Biol Chem*, 272: 4740-6.

Nam, JS, M Terabe, M Mamura, MJ Kang, H Chae, C Stuelten, E Kohn, B Tang, H Sabzevari, MR Anver, S Lawrence, D Danielpour, S Lonning, JA Berzofsky, and LM Wakefield. 2008. 'An anti-transforming growth factor beta antibody suppresses metastasis via cooperative effects on multiple cell compartments.', *Cancer Res*, 68: 3835-43.

Netti, PA, DA Berk, MA Swartz, AJ Grodzinsky, and RK Jain. 2000. 'Role of extracellular matrix assembly in interstitial transport in solid tumors.', *Cancer Res*, 60: 2497-503.

Network, Cancer Genome Atlas. 2012. 'Comprehensive molecular portraits of human breast tumours.', *Nature*, 490: 61-70.

Nusrat, A, M Giry, JR Turner, SP Colgan, CA Parkos, D Carnes, E Lemichez, P Boquet, and JL Madara. 1995. 'Rho protein regulates tight junctions and perijunctional actin organization in polarized epithelia.', *Proc Natl Acad Sci U S A*, 7: 23.

O'Hare, MJ, J Bond, C Clarke, Y Takeuchi, AJ Atherton, C Berry, J Moody, AR Silver, DC Davies, AE Alsop, AM Neville, and PS Jat. 2001. 'Conditional immortalization of freshly isolated human mammary fibroblasts and endothelial cells.', *Proc Natl Acad Sci U S A*, 98: 646-51.

O'Toole, SA, DA Machalek, RF Shearer, EK Millar, R Nair, P Schofield, D McLeod, CL Cooper, CM McNeil, A McFarland, A Nguyen, CJ Ormandy, MR Qiu, B Rabinovich, LG Martelotto, D Vu, GE Hannigan, EA Musgrove, D Christ, RL Sutherland, DN Watkins, and A Swarbrick. 2011. 'Hedgehog overexpression is associated with stromal interactions and predicts for poor outcome in breast cancer.', *Cancer Res*, 71: 4002-14.

Oishi, K., H. Mukai, H. Shibata, M. Takahashi, and Y. Ona. 1999. 'Identification and characterization of PKNbeta, a novel isoform of protein kinase PKN: expression and arachidonic acid dependency are different from those of PKNalpha', *Biochem Biophys Res Commun*, 261: 808-14.

Olsen, CJ, J Moreira, EM Lukanidin, and NS Ambartsumian. 2010. 'Human mammary fibroblasts stimulate invasion of breast cancer cells in a three-dimensional culture and increase stroma development in mouse xenografts.', *BMC Cancer*, 10: 444.

Onichtchouk, D, YG Chen, R Dosch, V Gawantka, H Delius, J Massagué, and C Niehrs. 1999. 'Silencing of TGF-beta signalling by the pseudoreceptor BAMBI.', *Nature*, 401: 480-5.

Orimo, A, PB Gupta, DC Sgroi, F Arenzana-Seisdedos, T Delaunay, R Naeem, VJ Carey, AL Richardson, and RA Weinberg. 2005. 'Stromal fibroblasts present in invasive human breast carcinomas promote tumor growth and angiogenesis through elevated SDF-1/CXCL12 secretion.', *Cell*, 121: 335-48.

Orimo, A., and R. A. Weinberg. 2006. 'Stromal fibroblasts in cancer: a novel tumor-promoting cell type', *Cell Cycle*, 5: 1597-601.

Ostman, A, and M Augsten. 2009. 'Cancer-associated fibroblasts and tumor growth--bystanders turning into key players.', *Curr Opin Genet Dev*, 19: 67-73.

Ostman, A, and CH Heldin. 2007. 'PDGF receptors as targets in tumor treatment', *Adv Cancer Res*, 97: 247-74.

P, De Marco, Lappano R, De Francesco EM, Cirillo F, Pupo M, Avino S, Vivacqua A, Abonante S, Picard D, and Maggiolini M. 2016. 'GPER signalling in both cancer-associated fibroblasts and breast cancer cells mediates a feedforward IL1β/IL1R1 response', *Sci Rep*, 13: 24354.

Paik, S, S Shak, G Tang, C Kim, J Baker, M Cronin, FL Baehner, MG Walker, D Watson, T Park, W Hiller, ER Fisher, DL Wickerham, J Bryant, and N Wolmark. 2004 'A multigene assay to predict recurrence of tamoxifen-treated, node-negative breast cancer.', *N Engl J Med*, 351: 2817-26.

Palmer, R. H., and P. J. Parker. 1995. 'Expression, purification and characterization of the ubiquitous protein kinase C-related kinase 1', *Biochem J*, 309 (Pt 1): 315-20.

Palmer, R. H., J. Ridden, and P. J. Parker. 1995. 'Cloning and expression patterns of two members of a novel protein-kinase-C-related kinase family', *Eur J Biochem*, 227: 344-51.

Palmieri, C, D Roberts-Clark, A Assadi-Sabet, RC Coope, M O'Hare, A Sunters, A Hanby, MJ Slade, JJ Gomm, EW Lam, and RC Coombes. 2003. 'Fibroblast growth factor 7, secreted by breast fibroblasts, is an interleukin-1beta-induced paracrine growth factor for human breast cells.', *J Endocrinol*, 177: 65-81.

Parekh, D. B., W. Ziegler, and P. J. Parker. 2000. 'Multiple pathways control protein kinase C phosphorylation', *EMBO J*, 19: 496-503.

Park, JH, CH Richards, DC McMillan, PG Horgan, and CS Roxburgh. 2014. 'The relationship between tumour stroma percentage, the tumour microenvironment and survival in patients with primary operable colorectal cancer.', *Ann Oncol*, 25: 644-51.

Parker, JS, M Mullins, MC Cheang, S Leung, D Voduc, T Vickery, S Davies, C Fauron, X He, Z Hu, JF Quackenbush, IJ Stijleman, J Palazzo, JS Marron, AB Nobel, E Mardis, TO Nielsen, MJ Ellis, CM Perou, and PS Bernard. 2009. 'Supervised risk predictor of breast cancer based on intrinsic subtypes.', *J Clin Oncol*, 27: 1160-7.

Parry, S, K Savage, C Marchiò, and JS Reis-Filho. 2008. 'Nestin is expressed in basal-like and triple negative breast cancers', *J Clin Pathol*, 61: 1045-50.

Pearce, OMT, RM Delaine-Smith, E Maniati, S Nichols, J Wang, S Böhm, V Rajeeve, D Ullah, P Chakravarty, RR Jones, A Montfort, T Dowe, J Gribben, JL Jones, HM Kocher, JS Serody, BG Vincent, J Connelly, JD Brenton, C Chelala, PR Cutillas, M Lockley, C Bessant, MM Knight, and FR Balkwill. 2018a. 'Deconstruction of a Metastatic Tumor Microenvironment Reveals a Common Matrix Response in Human Cancers.', *Cancer Discov*, 8: 304-19.

Pearce, OMT, RM Delaine-Smith, E Maniati, S Nichols, J Wang, S Böhm, V Rajeeve, D Ullah, P Chakravarty, RR Jones, A Montfort, T Dowe, J Gribben, JL Jones, HM Kocher, JS Serody, BG Vincent, J Connelly, JD Brenton, C Chelala, PR Cutillas, M Lockley, C Bessant, MM Knight, and FR Balkwill. 2018b. 'Deconstruction of a Metastatic Tumor Microenvironment Reveals a Common Matrix Response in Human Cancers', *Cancer Discov*, 8: 304-19.

Perou, CM, T Sørlie, MB Eisen, M van de Rijn, SS Jeffrey, CA Rees, JR Pollack, DT Ross, H Johnsen, LA Akslen, O Fluge, A Pergamenschikov, C Williams, SX Zhu, PE Lønning, AL Børresen-Dale, PO Brown, and D Botstein. 2000. 'Molecular portraits of human breast tumours', *Nature*, 406: 747-52.

Piekny, AJ, and M Glotzer. 2008. 'Anillin is a scaffold protein that links RhoA, actin, and myosin during cytokinesis.', *Curr Biol*, 18: 30-6.

Pinder, SE, and IO Ellis. 2003. 'The diagnosis and management of pre-invasive breast disease: Ductal carcinoma in situ (DCIS) and atypical ductal hyperplasia (ADH) – current definitions and classification', *Breast Cancer Res*, 5: 254-57.

Pontiggia, O, R Sampayo, D Raffo, A Motter, R Xu, MJ Bissell, EB Joffé, and M Simian. 2012. 'The tumor microenvironment modulates tamoxifen resistance in breast cancer: a role for soluble stromal factors and fibronectin through β1 integrin.', *Breast Cancer Res Treat*, 133: 459-71.

Provenzano, P. P., and P. J. Keely. 2011. 'Mechanical signaling through the cytoskeleton regulates cell proliferation by coordinated focal adhesion and Rho GTPase signaling', *J Cell Sci*, 124: 1195-205.

Qadota, H., T. Miyauchi, J. F. Nahabedian, J. N. Stirman, H. Lu, M. Amano, G. M. Benian, and K. Kaibuchi. 2011. 'PKN-1, a homologue of mammalian PKN, is involved in the regulation of muscle contraction and force transmission in C. elegans', *J Mol Biol*, 407: 222-31.

Quétier, I., J. Marshall, B. Spencer-Dene, S. Lachmann, A. Casamassima, C. Franco, S. Escuin, J. T. Worrall, P. Baskaran, V. Rajeeve, M. Howell, Copp. A. J., G. Stamp, I. Rosewell, P. Cutillas, H. Gerhardt, P. J. Parker, and A. J. M. Cameron. 2016. 'Knockout of the PKN family of Rho effector kinases reveals a non-redundant role for PKN2 in developmental mesoderm expansion.', *Cell Reports*, 14: 440-48.

Rajski, M, R Zanetti-Dällenbach, B Vogel, R Herrmann, C Rochlitz, and M Buess. 2010. 'IGF-I induced genes in stromal fibroblasts predict the clinical outcome of breast and lung cancer patients', *BMC Med*, 8: 1.

Roelants, FM, KL Leskoske, MN Martinez Marshall, MN Locke, and J Thorner. 2017. 'The TORC2-Dependent Signaling Network in the Yeast Saccharomyces cerevisiae.', *Biomolecules*, 7: E66.

Rønnov-Jessen, L, OW Petersen, VE Koteliansky, and MJ Bissell. 1995. 'The origin of the myofibroblasts in breast cancer. Recapitulation of tumor environment in culture unravels diversity and implicates converted fibroblasts and recruited smooth muscle cells.', *J Clin Invest*, 95: 859-73.

Sahai, E, and CJ Marshall. 2002. 'ROCK and Dia have opposing effects on adherens junctions downstream of Rho.', *Nat Cell Biol*, 4: 408-15.

Said, SM, DW Visscher, A Nassar, RD Frank, RA Vierkant, MH Frost, K Ghosh, DC Radisky, LC Hartmann, and AC Degnim. 2015. 'Flat epithelial atypia and risk of breast cancer: A Mayo cohort study.', *Cancer*, 121: 1548-55.

Sappino, AP, O Skalli, B Jackson, W Schürch, and G Gabbiani. 1988. 'Smooth-muscle differentiation in stromal cells of malignant and non-malignant breast tissues.', *Int J Cancer*, 41: 707-12.

Scanlan, MJ, BK Raj, B Calvo, P Garin-Chesa, MP Sanz-Moncasi, JH Healey, LJ Old, and WJ Rettig. 1994. 'Molecular cloning of fibroblast activation protein alpha, a member of the serine protease family selectively expressed in stromal fibroblasts of epithelial cancers.', *Proc Natl Acad Sci U S A*, 91: 5657-61.

Schmidt, A., J. Durgan, A. Magalhaes, and A. Hall. 2007. 'Rho GTPases regulate PRK2/PKN2 to control entry into mitosis and exit from cytokinesis', *EMBO J*, 26: 1624-36.

Sewell-Loftin, MK, SVH Bayer, E Crist, T Hughes, SM Joison, GD Longmore, and SC George. 2017. 'Cancer-associated fibroblasts support vascular growth through mechanical force.', *Sci Rep*, 7: 12574.

Shekhar, MP, J Werdell, SJz Santner, RJ Pauley, and L Tait. 2001. 'Breast stroma plays a dominant regulatory role in breast epithelial growth and differentiation: implications for tumor development and progression.', *Cancer Res*, 61: 1320-6.

Shewan, AM, M Maddugoda, A Kraemer, SJ Stehbens, S Verma, EM Kovacs, and AS Yap. 2005. 'Myosin 2 is a key Rho kinase target necessary for the local concentration of E-cadherin at cell-cell contacts.', *Mol Biol Cell*, 16: 4531-42.

Singh, S, SK Srivastava, A Bhardwaj, LB Owen, and AP Singh. 2010. 'CXCL12-CXCR4 signalling axis confers gemcitabine resistance to pancreatic cancer cells: a novel target for therapy.', *Br J Cancer*, 103: 1671-9.

Small, EM. 2012. 'The actin-MRTF-SRF gene regulatory axis and myofibroblast differentiation.', *J Cardiovasc Transl Res*, 5: 794-804.

Smutny, M, HL Cox, JM Leerberg, EM Kovacs, MA Conti, C Ferguson, NA Hamilton, RG Parton, RS Adelstein, and AS Yap. 2010. 'Myosin II isoforms identify distinct functional modules that support integrity of the epithelial zonula adherens', *Nat Cell Biol*, 12: 696-702.

Soon, PS, E Kim, CK Pon, AJ Gill, K Moore, AJ Spillane, DE Benn, and RC Baxter. 2013. 'Breast cancer-associated fibroblasts induce epithelial-to-mesenchymal transition in breast cancer cells.', *Endocr Relat Cancer*, 20: 1-12.

Sørlie, T, CM Perou, R Tibshirani, T Aas, S Geisler, H Johnsen, T Hastie, MB Eisen, M van de Rijn, SS Jeffrey, T Thorsen, H Quist, JC Matese, PO Brown, D Botstein, PE Lønning, and AL Børresen-Dale. 2001. 'Gene expression patterns of breast carcinomas distinguish tumor subclasses with clinical implications', *Proc Natl Acad Sci U S A*, 98: 10869-74.

Sorlie, T, R Tibshirani, J Parker, T Hastie, JS Marron, A Nobel, S Deng, H Johnsen, R Pesich, S Geisler, J Demeter, CM Perou, PE Lønning, PO Brown, AL Børresen-Dale, and D Botstein. 2003. 'Repeated observation of breast tumor subtypes in independent gene expression data sets', *Proc Natl Acad Sci U S A*, 100: 8418-23.

Standaert, M, G Bandyopadhyay, L Galloway, Y Ono, H Mukai, and R Farese. 1998. 'Comparative effects of GTPgammaS and insulin on the activation of Rho, phosphatidylinositol 3-kinase, and protein kinase N in rat adipocytes. Relationship to glucose transport', *J Biol Chem*, 273: 7470-7.

Stapleton, G, CP Nguyen , KA Lease, and MB Hille. 1998. 'Phosphorylation of protein kinase C-related kinase PRK2 during meiotic maturation of starfish oocytes', *Dev Biol*, 193: 36-46.

Statistics, Office for National. 2017. 'Cancer diagnoses and age-standardised incidence rates for all cancer sites by age, sex and region', *Cancer Registration Statistics, England: 2015*.

Stone, RM, SJ Mandrekar, BL Sanford, K Laumann, S Geyer, CD Bloomfield, C Thiede, TW Prior, K Döhner, G Marcucci, F Lo-Coco, RB Klisovic, A Wei, J Sierra, MA Sanz, JM Brandwein, T de Witte, D Niederwieser, FR Appelbaum, BC Medeiros, MS Tallman, J Krauter, RF Schlenk, A Ganser, H Serve, G Ehninger, S Amadori, RA Larson, and H Döhner. 2017. 'Midostaurin plus Chemotherapy for Acute Myeloid Leukemia with a FLT3 Mutation', *N Eng J Med*, 377: 454-64.

Straussman, R, T Morikawa, K Shee, M Barzily-Rokni, ZR Qian, J Du, A Davis, MM Mongare, J Gould, DT Frederick, ZA Cooper, PB Chapman, DB Solit, A Ribas, RS Lo, KT Flaherty, S Ogino, JA Wargo, and TR Golub. 2012. 'Tumour micro-environment elicits innate resistance to RAF inhibitors through HGF secretion', *Nature*, 487: 500-4.

Streit, M, AE Stephen, T Hawighorst, K Matsuda, B Lange-Asschenfeldt, LF Brown, JP Vacanti, and M Detmar. 2002. 'Systemic inhibition of tumor growth and angiogenesis by thrombospondin-2 using cell-based antiangiogenic gene therapy.', *Cancer Res*, 62: 2004-12.

Su, X, AK Esser, SR Amend, J Xiang, Y Xu, MH Ross, GC Fox, T Kobayashi, V Steri, K Roomp, F Fontana, MA Hurchla, BL Knolhoff, MA Meyer, EA Morgan, JC Tomasson, JS Novack, W Zou, R Faccio, DV Novack, SD Robinson, SL Teitelbaum, DG DeNardo, JG Schneider, and KN Weilbaecher. 2016. 'Antagonizing Integrin β3 Increases Immunosuppression in Cancer', *Cancer Res*, 76: 3484-95.

Sugiura, K, and CC Stock. 1952. 'Studies in a tumor spectrum. I. Comparison of the action of methylbis(2-chloroethyl)amine and 3-bis(2-chloroethyl)aminomethyl-4-methoxymethyl-5-hydroxy-6-methylpyridine on the growth of a variety of mouse and rat tumors', *Cancer*, 5: 382–402.

Surowiak, P, D Murawa, V Materna, A Maciejczyk, M Pudelko, S Ciesla, J Breborowicz, P Murawa, M Zabel, M Dietel, and H Lage. 2007. 'Occurence of stromal myofibroblasts in the invasive ductal breast cancer tissue is an unfavourable prognostic factor.', *Anticancer Res*, 27: 2917-24.

Surowiak, P, S Suchocki, B Györffy, T Gansukh, A Wojnar, A Maciejczyk, M Pudełko, and M Zabel. 2006. 'Stromal myofibroblasts in breast cancer: relations between their occurrence, tumor grade and expression of some tumour markers', *Folia Histochem Cytobiol*, 44: 111-16.

Takahashi, M, H Shibata, M Shimakawa, M Miyamoto, H Mukai, and Y Ono. 1999. 'Characterization of a novel giant scaffolding protein, CG-NAP, that anchors multiple signaling enzymes to centrosome and the golgi apparatus', *J Biol Chem*, 274: 17267-74.

Takai, K, AP Drain, DA Lawson, LE Littlepage, M Karpuj, K Kessenbrock, A Le, K Inoue, VM Weaver, and Z Werb. 2018. 'Discoidin domain receptor 1 (DDR1) ablation promotes tissue fibrosis and hypoxia to induce aggressive basal-like breast cancers', *Genes Dev*, 32: 244-57.

Talmage, DA, R Freund, AT Young, J Dahl, CJ Dawe, and TL Benjamin. 1989. 'Phosphorylation of middle T by pp60c-src: a switch for binding of phosphatidylinositol 3-kinase and optimal tumorigenesis.', *Cell*, 59: 55-65.

Tamura, D, T Hiraga, A Myoui, H Yoshikawa, and T Yoneda. 2008. 'Cadherin-11-mediated interactions with bone marrow stromal/osteoblastic cells support selective colonization of breast cancer cells in bone.', *Int J Oncol*, 33: 17-24.

Tang, J, CC Gifford, R Samarakoon, and PJ Higgins. 2018. 'Deregulation of Negative Controls on TGF-β1 Signaling in Tumor Progression.', *Cancers (Basel)*, 10: E159.

Taniguchi, T., T. Kawamata, H. Mukai, H. Hasegawa, T. Isagawa, M. Yasuda, T. Hashimoto, A. Terashima, M. Nakai, H. Mori, Y. Ono, and C. Tanaka. 2001. 'Phosphorylation of tau is regulated by PKN', *J Biol Chem*, 276: 10025-31.

Tao, L, G Huang, H Song, Y Chen, and L Chen. 2017. 'Cancer associated fibroblasts: An essential role in the tumor microenvironment.', *Oncol Lett*, 14: 2611-20.

Tape, CJ, S Ling, M Dimitriadi, KM McMahon, JD Worboys, HS Leong, IC Norrie, CJ Miller, G Poulogiannis, DA Lauffenburger, and C Jørgensen. 2016. 'Oncogenic KRAS Regulates Tumor Cell Signaling via Stromal Reciprocation.', *Cell*, 165: 910-20.

Teicher, BA, TS Herman, SA Holden, YY Wang, MR Pfeffer, JW Crawford, and E 3rd Frei. 1990. 'Tumor resistance to alkylating agents conferred by mechanisms operative only in vivo', *Science*, 247: 1457-61.

Tian, S, P Roepman, LJ Van't Veer, R Bernards, F de Snoo, and AM Glas. 2010. 'Biological functions of the genes in the mammaprint breast cancer profile reflect the hallmarks of cancer.', *Biomark Insights*, 5: 129-38.

Togo, S, UM Polanska, Y Horimoto, and A Orimo. 2013. 'Carcinoma-associated fibroblasts are a promising therapeutic target', *Cancers (Basel)*, 5: 149-69.

Tsuyada, A, A Chow, J Wu, G Somlo, P Chu, S Loera, T Luu, AX Li, X Wu, W Ye, S Chen, W Zhou, Y Yu, YZ Wang, X Ren, H Li, Z Scherle, Y Kuroki, and SE Wang. 2012. 'CCL2 mediates cross-talk between cancer cells and stromal fibroblasts that regulates breast cancer stem cells.', *Cancer Res*, 72: 2768-79.

Turner, N., M. B. Lambros, H. M. Horlings, A. Pearson, R. Sharpe, R. Natrajan, F. C. Geyer, M. van Kouwenhove, B. Kreike, A. Mackay, A. Ashworth, M. J. van de Vijver, and J. S. Reis-Filho. 2010. 'Integrative molecular profiling of triple negative breast cancers identifies amplicon drivers and potential therapeutic targets', *Oncogene*, 29: 2013-23.

Tyan, SW, CH Hsu, KL Peng, CC Chen, WH Kuo, EY Lee, JY Shew, KJ Chang, LJ Juan, and WH Lee. 2012. 'Breast cancer cells induce stromal fibroblasts to secrete ADAMTS1 for cancer invasion through an epigenetic change.', *PLoS One*, 12: e35128.

Uehata, M, T Ishizaki, H Satoh, T Ono, T Kawahara, T Morishita, H Tamakawa, K Yamagami, J Inui, M Maekawa, and S Narumiya. 1997. 'Calcium sensitization of smooth muscle mediated by a Rho-associated protein kinase in hypertension.', *Nature*, 389.

Unsal-Kacmaz, K, S Ragunathan, E Rosfjord, S Dann, E Upeslacis, M Grillo, R Hernandez, F Mack, and A Klippel. 2012. 'The interaction of PKN3 with RhoC promotes malignant growth', *Molecular Oncology*, 6: 284-98.

Vallejos, CS, HL Gómez, WR Cruz, JA Pinto, RR Dyer, R Velarde, JF Suazo, SP Neciosup, M León, MA de la Cruz, and CE Vigil. 2012. 'Role of stromal myofibroblasts in invasive breast cancer: stromal expression of alpha-smooth muscle actin correlates with worse clinical outcome', *Breast Cancer*, 19: 170-6.

Vallejos, CS, HL Gómez, WR Cruz, JA Pinto, RR Dyer, R Velarde, JF Suazo, SP Neciosup, M León, MA de la Cruz, and CE Vigil. 2010. 'Breast cancer classification according to immunohistochemistry markers: subtypes and association with clinicopathologic variables in a peruvian hospital database', *Clin Breast Cancer*, 10.

van 't Veer, LJ, H Dai, MJ van de Vijver, YD He, AA Hart, M Mao, HL Peterse, K van der Kooy, MJ Marton, AT Witteveen, GJ Schreiber, RM Kerkhoven, C Roberts, PS Linsley, R Bernards, and SH Friend. 2002. 'Gene expression profiling predicts clinical outcome of breast cancer.', *Nature*, 415: 530-6.

van Dongen, JA, AC Voogd, IS Fentiman, C Legrand, RJ Sylvester, D Tong, E van der Schueren, PA Helle, K van Zijl, and H Bartelink. 2000. 'Long-term results of a randomized trial comparing breast-conserving therapy with mastectomy: European Organization for Research and Treatment of Cancer 10801 trial', *J Natl Cancer Inst*, 92: 1143-50.

Vincent, S., and J. Settleman. 1997. 'The PRK2 kinase is a potential effector target of both Rho and Rac GTPases and regulates actin cytoskeletal organization', *Mol Cell Biol*, 17: 2247-56.

Vukicevic, S, HK Kleinman, FP Luyten, AB Roberts, NS Roche, and AH Reddi. 1992. 'Identification of multiple active growth factors in basement membrane Matrigel suggests caution in interpretation of cellular activity related to extracellular matrix components.', *Exp Cell Res*, 202: 1-8.

Wallace, SW, A Magalhaes, and A Hall. 2011. 'The Rho target PRK2 regulates apical junction formation in human bronchial epithelial cells', *Mol Cell Biol*, 31: 81-91.

Walsh, SV, AM Hopkins, J Chen, S Narumiya, CA Parkos, and A Nusrat. 2001. 'Rho kinase regulates tight junction function and is necessary for tight junction assembly in polarized intestinal epithelia.', *Gastroenterology*, 121: 566-79.

Wang, K, F Wu, BR Seo, C Fischbach, W Chen, L Hsu, and D Gourdon. 2017. 'Breast cancer cells alter the dynamics of stromal fibronectin-collagen interactions.', *Matrix Biol*, 60: 86-95.

Watson, SS, M Dane, K Chin, Z Tatarova, M Liu, T Liby, W Thompson, R Smith, M Nederlof, E Bucher, D Kilburn, M Whitman, D Sudar, GB Mills, LM Heiser, O Jonas, JW Gray, and JE Korkola. 2018. 'Microenvironment-Mediated Mechanisms of Resistance to HER2 Inhibitors Differ between HER2+ Breast Cancer Subtypes', *Cell Syst*, 6: 329-42.

Weber, CE, AN Kothari, PY Wai, NY Li, J Driver, MA Zapf, CA Franzen, GN Gupta, C Osipo, A Zlobin, WK Syn, J Zhang, PC Kuo, and Z Mi. 2015. 'Osteopontin mediates an MZF1-TGF-β1-dependent transformation of mesenchymal stem cells into cancer-associated fibroblasts in breast cancer.', *Oncogene*, 34: 4821-33.

Weigelt, B, FL Baehner, and JS Reis-Filho. 2010. 'The contribution of gene expression profiling to breast cancer classification, prognostication and prediction: a retrospective of the last decade', *J Pathol*, 220: 263-80.

Weisberg, E., C. Boulton, L. M. Kelly, P. Manley, D. Fabbro, T. Meyer, D. G. Gilliland, and J. D. Griffin. 2002. 'Inhibition of mutant FLT3 receptors in leukemia cells by the small molecule tyrosine kinase inhibitor PKC412', *Cancer Cell*, 1: 433-43.

Wellings, SR, and HM Jensen. 1973. 'On the origin and progression of ductal carcinoma in the human breast', *J Natl Cancer Inst*, 50: 1111-8.

Wennström, S, A Siegbahn, K Yokote, AK Arvidsson, CH Heldin, S Mori, and L Claesson-Welsh. 1994. 'Membrane ruffling and chemotaxis transduced by the PDGF beta-receptor require the binding site for phosphatidylinositol 3' kinase.', *Oncogene*, 9: 651-60.

Winslow, S, K Leandersson, A Edsjö, and C Larsson. 2015. 'Prognostic stromal gene signatures in breast cancer.', *Breast Cancer Res*, 17: 23.

Wodicka, LM, P Ciceri, MI Davis, JP Hunt, M Floyd, S Salerno, XH Hua, JM Ford, RC Armstrong, PP Zarrinkar, and DK Treiber. 2010. 'Activation state-dependent binding of small molecule kinase inhibitors: structural insights from biochemistry', *Chem Biol*, 17: 1241-9.

Wong, PP, N Bodrug, and KM Hodivala-Dilke. 2016. 'Exploring Novel Methods for Modulating Tumor Blood Vessels in Cancer Treatment.', *Curr Biol*, 26: 1161-66.

Xing, F, J Saidou, and K Watabe. 2010. 'Cancer associated fibroblasts (CAFs) in tumor microenvironment.', *Front Biosci (Landmark Ed)*, 15: 166-79.

Yamashita, H, P ten Dijke, P Franzén, K Miyazono, and CH Heldin. 1994. 'Formation of hetero-oligomeric complexes of type I and type II receptors for transforming growth factor-beta', *J Biol Chem*, 269: 20172-8.

Yang, MC, CJ Wang, PC Liao, CJ Yen, and Y Shan. 2014. 'Hepatic stellate cells secretes type I collagen to trigger epithelial mesenchymal transition of hepatoma cells', *Am J Cancer Res*, 4: 751–63.

Yang, Z, W Ni, C Cui, L Fang, and Y Xuan. 2017. 'Tenascin C is a prognostic determinant and potential cancer-associated fibroblasts marker for breast ductal carcinoma.', *Exp Mol Pathol*, 102: 262-67.

Yao, Z, S Fenoglio, DC Gao, M Camiolo, B Stiles, T Lindsted, M Schlederer, C Johns, N Altorki, V Mittal, L Kenner, and R Sordella. 2010. 'TGF-beta IL-6 axis mediates selective and adaptive mechanisms of resistance to molecular targeted therapy in lung cancer.TGF-beta IL-6 axis mediates selective and adaptive mechanisms of resistance to molecular targeted therapy in lung cancer', *Proc Natl Acad Sci U S A*, 107: 15535-40.

Yasui, T., K. Sakakibara-Yada, T. Nishimura, K. Morita, S. Tada, G. Mosialos, E. Kieff, and H. Kikutani. 2012. 'Protein kinase N1, a cell inhibitor of Akt kinase, has a central role

in quality control of germinal center formation', *Proc Natl Acad Sci U S A*, 109: 21022-7.

Yazhou, C, S Wenlv, Z Weidong, and W Licun. 2004. 'Clinicopathological significance of stromal myofibroblasts in invasive ductal carcinoma of the breast.', *Tumour Biol*, 25: 290-5.

Yee, D, S Paik, GS Lebovic, RR Marcus, RE Favoni, KJ Cullen, ME Lippman, and N Rosen. 1989. 'Analysis of insulin-like growth factor I gene expression in malignancy: evidence for a paracrine role in human breast cancer', *Mol Endocrinol*, 3: 509-17.

Yoshida, A, M Ookura, K Zokumasu, and T Ueda. 2014. 'Gö6976, a FLT3 kinase inhibitor, exerts potent cytotoxic activity against acute leukemia via inhibition of survivin and MCL-1', *Biochem Pharmacol*, 90: 16-24.

Yoshinaga, C, H Mukai, M Toshimori, M Miyamoto, and Y Ono. 1999. 'Mutational analysis of the regulatory mechanism of PKN: the regulatory region of PKN contains an arachidonic acid-sensitive autoinhibitory domain', *J Biochem*, 126: 475-84.

Yu, Y, CH Xiao, LD Tan, QS Wang, XQ Li, and YM Feng. 2014. 'Cancer-associated fibroblasts induce epithelial-mesenchymal transition of breast cancer cells through paracrine TGF-β signalling.', *Br J Cancer*, 110: 724-32.

Yu, YP, D Landsittel, L Jing, J Nelson, B Ren, L Liu, C McDonald, R Thomas, Dhir. R, . S Finkelstei, G Michalopoulos, M Becich, and JH Luo. 2004. 'Gene expression alterations in prostate cancer predicting tumor aggression and preceding development of malignancy.', *J Clin Oncol*, 22: 2790-9.

Zeisberg, EM, S Potenta, L Xie, M Zeisberg, and R Kalluri. 2007. 'Discovery of endothelial to mesenchymal transition as a source for carcinoma-associated fibroblasts.', *Cancer Res*, 67: 10123-8.

Zhang, XH, X Jin, S Malladi, Y Zou, YH Wen, E Brogi, M Smid, JA Foekens, and J Massagué. 2013. 'Selection of bone metastasis seeds by mesenchymal signals in the primary tumor stroma.', *Cell*, 154: 1060-73.

zur Nedden, S, R Eith, C Schwarzer, L Zanetti, H Seitter, F Fresser, A Koschak, AJ Cameron, PJ Parker, G Baier, and G Baier-Bitterlich. 2018. 'Protein kinase N1 critically regulates cerebellar development and long-term function', *J Clin Invest*, 128: 2076-88.